

# **Identification of bacterial transporters for hydroxyalkylcysteinyglycines**

Daniel Bawdon

A thesis submitted for the degree of  
Doctor of Philosophy

University of York  
Department of Biology

September 2014

## Abstract

The generation of malodour in the human underarm (axilla) is caused by bacterial biotransformation of specific malodour precursor molecules contained within non-odorous apocrine gland secretions. The dipeptide-conjugated thioalcohol, (S)-(1-(2-hydroxyethyl)-1-methylbutyl)-L-cysteinylglycine (Cys-Gly-3M3SH) is known to be secreted into the axilla and biotransformed into the highly volatile thioalcohol 3-methyl-3-sulfanylhexan-1-ol (3M3SH) by members of the axillary microbiota, consisting principally of the genera *Corynebacterium* and *Staphylococcus*. However, the exact bacterial species that carry out this biotransformation have not been thoroughly characterised. Additionally, the route by which malodour precursor molecules are transported across the bacterial cell membrane to the cytoplasm have not been assessed, and a general disagreement within the literature is evident regarding the intracellular catabolic fate of such molecules.

Here, malodour precursor biotransformation data is presented from a library of skin isolated corynebacteria and staphylococci which identified significant variations in thioalcohol production across individual bacterial species and strains. Three *Staphylococcus* species, *S. hominis*, *S. haemolyticus* and *S. lugdunensis* were the strongest Cys-Gly-3M3SH biotransformers whereas all *Corynebacterium* spp. assessed showed weak or absent catabolism of this substrate. The molecular basis of uptake and biotransformation of dipeptide-conjugated malodour precursor compounds in the model organism *Escherichia coli* K-12 was assessed by creating and characterising peptide transporter deficient strains, which revealed novel phenotypes for several poorly studied peptide transporters in this organism. The relevant *E. coli* strains were then used as a background to overexpress and characterise putative dipeptide-conjugated malodour precursor transporters from a strong malodour producing *S. hominis* isolate. This revealed that a general *S. hominis* peptide transporter mediates Cys-Gly-3M3SH uptake. An *in silico* analysis of putative Cys-Gly-3M3SH catabolic genes revealed a novel cystathionine  $\beta$ -lyase-like gene present only in those *Staphylococcus* species able to biotransform Cys-Gly-3M3SH, strongly suggesting an involvement in Cys-Gly-3M3SH biotransformation.

This work provides major advances in understanding the molecular basis of human axillary malodour.

## List of Contents

Abstract .....	1
List of Contents.....	2
List of Figures .....	7
List of Tables .....	10
Acknowledgements.....	11
Author's declaration .....	12
Chapter 1 - Introduction.....	13
1.1 Skin structure and perspiration.....	14
1.1.1 The eccrine gland .....	14
1.1.2 The apocrine gland .....	16
1.2 The evolutionary origins and historical significance of body odour .....	18
1.3 The origins of axillary mal(odour) .....	20
1.3.1 The microbiota of the human axilla and its correlation with malodour .....	21
1.4 The biochemical basis of axillary malodour and the current unknowns .....	25
1.4.1 Odorous steroids.....	26
1.4.2 Volatile fatty acids (VFAs) .....	29
1.4.3 Thioalcohols.....	33
1.4.3.1 Identification of thioalcohols as components of axillary malodour and characterisation of their precursor conjugates.....	33
1.4.3.2 Molecular biotransformation of Cys-Gly-3M3SH and other thioalcohol-conjugates by axillary-isolated bacteria .....	38
1.5 <i>E. coli</i> as a model organism .....	42
1.5.1 Molecular transport in <i>E. coli</i> .....	43
1.5.2 Peptide transport in <i>E. coli</i> .....	45
1.5.2.1 The ABC peptide transporters of <i>E. coli</i> .....	45
1.5.2.2 The MFS peptide transporters of <i>E. coli</i> .....	49
1.5.2.3 C-S- $\beta$ -lyases of <i>E. coli</i> .....	51

1.6	Aims of this study .....	53
 Chapter 2 – Materials and methods .....		55
2.1	Chemicals and strains .....	55
2.1.1	Chemicals .....	55
2.1.2	Antibiotics .....	55
2.1.3	Malodour precursor substrate molecules .....	55
2.1.4	Bacterial strains and plasmids .....	55
2.1.5	Oligonucleotide primers .....	60
2.1.6	Bacterial growth media and reaction buffers .....	61
2.2	Molecular and biochemical techniques .....	62
2.2.1	Polymerase chain reaction (PCR) with <i>E. coli</i> .....	62
2.2.2	PCR with <i>S. hominis</i> B10 .....	63
2.2.3	Agarose gel electrophoresis .....	64
2.2.4	DNA extraction from agarose gel .....	65
2.2.5	Preparation of chemically competent <i>E. coli</i> cells .....	65
2.2.6	Transformation of chemically competent <i>E. coli</i> with plasmid DNA .....	65
2.2.7	Purification and restriction endonuclease digestion of plasmid DNA .....	66
2.2.8	pCP20-mediated removal of the kanamycin resistance cassette from Keio Collection strains .....	66
2.2.9	pKD46-mediated replacement of wild-type genetic loci with the kanamycin resistance cassette .....	67
2.2.10	Cloning .....	67
2.2.10.1	Purification of cloning vector pBADcLIC2005 and preparation of ‘LIC-ready’ plasmid .....	67
2.2.10.2	Purification and preparation of LIC-ready insert .....	68
2.2.10.3	Ligation-independent cloning of ‘LIC-ready’ plasmid and insert .....	68
2.2.10.4	Confirmation of gene insertion into pBADcLIC2005 .....	68
2.2.11	Malodour precursor biotransformation assays .....	69
2.2.11.1	S-Benzyl-L-cysteine and S-Benzyl-L-cysteinylglycine biotransformation assays using resting cells .....	69

2.2.11.2	(3-(4,5-dimethylthiazol-2-yl)-5-(3-carboxymethoxyphenyl)-2-(4-sulfophenyl)-2H-tetrazolium) (MTS) and phenazine methosulfate (PMS)-mediated chemical labelling of benzyl-mercaptan.....	69
2.2.11.3	Chemical labelling of known concentrations of benzyl-mercaptan and 3-mercaptohexan-1-ol using MTS/PMS.....	70
2.2.11.4	Cys-Gly-3M3SH biotransformation assays using resting cells.....	70
2.2.11.5	5,5'-dithiobis-(2-nitrobenzoic acid) (DTNB)-mediated chemical labelling of 3M3SH.....	71
2.2.11.6	Lysostaphin-mediated cell lysis of staphylococci.....	71
2.2.11.7	S-Benzyl-L-cysteine and Cys-Gly-3M3SH biotransformation by <i>Staphylococcus</i> spp. crude cell lysate.....	71
2.2.11.8	Purified cystathionine $\beta$ -lyase enzyme activity assays.....	72
2.2.11.9	Thin layer chromatography (TLC).....	72
2.3	Microbiological techniques .....	73
2.3.1	Speciation of unidentified axillary isolates using MicroSeq 500 .....	73
2.3.2	Growth phenotype experiments in shake flasks .....	73
2.3.3	Growth phenotype experiments in 96-well microplates.....	74
2.3.4	Agar plate toxic peptide inhibition assays.....	74
2.3.5	Growth of <i>E. coli</i> in spent tryptone broth medium .....	75
2.3.6	End point final growth yield measurement.....	75
2.3.7	Preparation of crude cell lysate from <i>E. coli</i> .....	75
2.4	Bioinformatics .....	76
2.4.1	Construction of Dtp protein phylogenetic tree.....	76
2.4.2	Construction of staphylococcal C-S- lyase protein phylogenetic tree.....	76
2.4.3	Identification of molecular symporters in <i>S. hominis</i> SK119 .....	76

## Chapter 3 – Catabolism of malodour precursor substrates by axillary

bacteria – Introduction and aims .....	78
3.1 Uptake and biotransformation of S-Benzyl-L-cysteinylglycine by corynebacteria and staphylococci .....	80
3.2 Development of a thioalcohol labelling assay to detect physiologically relevant malodour molecules.....	82

3.3	DTNB labelling assay assessment - uptake and biotransformation of Cys-Gly-3M3SH by corynebacteria and staphylococci .....	84
3.4	Cys-Gly-3M3SH biotransformation by <i>S. haemolyticus</i> G431.....	86
3.5	Speciation of unknown axillary isolates by riboprofiling at Unilever Discover, Colworth .....	90
3.6	Uptake and biotransformation of Cys-Gly-3M3SH by skin-isolated corynebacteria and staphylococci .....	92
3.7	Energetics of Cys-Gly-3M3SH uptake by <i>S. hominis</i> and <i>S. haemolyticus</i> .....	96
3.8	Preparation and characterisation of staphylococcal whole cell lysate for malodour precursor biotransformation assays.....	98
3.9	Competitive inhibition of Cys-Gly-3M3SH biotransformation in <i>S. hominis</i> B10 .....	100
3.10	Discussion .....	104

## Chapter 4 – Creation and characterisation of peptide transporter

	deficient strains of <i>E. coli</i> K-12 – Introduction and aims .....	110
4.1	Genome-wide phylogenetic analysis of Dtp-like proteins across the bacterial kingdom.....	112
4.2	Creation of peptide transporter deficient (TD-Pep) strains of <i>E. coli</i> K-12.....	115
4.3	Growth of <i>E. coli</i> TD-Pep strains in L-Alanine-L-Alanine-containing minimal medium.....	117
4.4	Growth of <i>E. coli</i> TD-Pep strains in aromatic residue-containing dipeptide minimal medium.....	119
4.5	Inhibition of growth of <i>E. coli</i> TD-Pep strains by L-leucine-containing dipeptides .....	122
4.6	Inhibition of growth of <i>E. coli</i> TD-Pep strains by L-valine-containing tripeptides .....	124
4.7	Growth of <i>E. coli</i> TD-Pep strains in tryptone broth.....	127
4.8	Late-stage exponential growth of <i>E. coli</i> in tryptone broth is limited by carbon starvation .....	132
4.9	Discussion .....	136

## Chapter 5 – Transport and catabolism of malodour precursor

substrates by <i>E. coli</i> K-12 – Introduction and aims .....	145
5.1 Uptake and biotransformation of S-Benzyl-L-cysteinyglycine by <i>E. coli</i> K-12 .....	147
5.2 The role of C-S- $\beta$ -lyase enzymes in biotransformation of malodour precursor substrates .....	149
5.3 Transport and biotransformation of S-Benzyl-L-cysteinyglycine by TD-Pep <i>E. coli</i> .....	152
5.4 Cloning, overexpression and functional complementation of <i>ntpA</i> , <i>ntpB</i> , <i>ntpC</i> and <i>ntpD</i> .....	154
5.5 Overexpression of DtpB transforms <i>E. coli</i> into an efficient Cys-Gly-3M3SH biotransforming bacterium.....	160
5.6 Discussion .....	162

## Chapter 6 – Identification and characterisation of malodour precursor

catabolic genes in <i>S. hominis</i> – Introduction and aims .....	168
6.1 Bioinformatic analysis of the secondary transporter (symporter) repertoire of <i>S. hominis</i> SK119 and identification of C-S- $\beta$ -lyase.....	170
6.2 Cloning, expression and characterisation of <i>S. hominis</i> B10 peptide transporters .....	174
6.3 Cloning, expression and characterisation of <i>S. hominis</i> B10 C-S- $\beta$ -lyase.....	177
6.4 Bioinformatic-based analysis of malodour precursor catabolic genes in staphylococci .....	179
6.5 Discussion .....	183

Summary and future directions .....	186
-------------------------------------	-----

Abbreviations .....	191
---------------------	-----

References .....	193
------------------	-----

## List of Figures

<b>Figure 1.1</b> The glandular composition of the human axilla.....	17
<b>Figure 1.2</b> Chemical structures of model and physiological thioalcohol malodour precursor molecules .....	37
<b>Figure 1.3</b> Putative process of Cys-Gly-3M3SH biotransformation by axillary bacteria....	41
<b>Figure 1.4</b> The peptide transporter repertoire of <i>E. coli</i> .....	47
<b>Figure 3.1</b> Biotransformation of S-Benzyl-L-cysteinyglycine by corynebacteria and staphylococci .....	81
<b>Figure 3.2</b> Biochemical labelling of benzyl-mercaptan and 3-mercaptohexan-1-ol with MTS/PMS and mechanism of sulfhydryl group labelling by DTNB .....	83
<b>Figure 3.3</b> Biotransformation of Cys-Gly-3M3SH by corynebacteria and staphylococci isolates .....	85
<b>Figure 3.4.1</b> Time-dependent biotransformation of Cys-Gly-3M3SH by <i>S. haemolyticus</i> G431.....	88
<b>Figure 3.4.2</b> Biotransformation of Cys-Gly-3M3SH by <i>S. haemolyticus</i> G431 with decreasing concentrations of bacterial cells and Cys-Gly-3M3SH .....	89
<b>Figure 3.6.1</b> Biotransformation of Cys-Gly-3M3SH by representative isolates of skin-isolated <i>Corynebacterium</i> sp. and <i>Staphylococcus</i> sp .....	94
<b>Figure 3.6.2</b> Time-dependent biotransformation of Cys-Gly-3M3SH by <i>S. hominis</i> B10 ..	95
<b>Figure 3.7</b> Biotransformation of Cys-Gly-3M3SH by <i>S. hominis</i> isolates in the presence or absence of 100 $\mu$ M CCCP or 20 mM $\text{Na}_3\text{VO}_4$ .....	97
<b>Figure 3.8</b> Biotransformation of S-Benzyl-L-cysteine and Cys-Gly-3M3SH by <i>S. hominis</i> B10 (whole cells and crude cell extract) and <i>S. epidermidis</i> G428 crude cell extract .....	99
<b>Figure 3.9.1</b> Biotransformation of Cys-Gly-3M3SH by <i>S. hominis</i> B10 isolate in the presence of 20 mM (10-fold excess) dipeptides and amino acids .....	102
<b>Figure 3.9.2</b> Biotransformation of Cys-Gly-3M3SH by <i>S. hominis</i> B10 isolate in the presence of 20 mM (10-fold excess) tripeptides and other small molecule competitors .	103

<b>Figure 4.1</b> Rooted phylogenetic tree displaying the relationship between POT family Dtp proteins.....	114
<b>Figure 4.2</b> Agarose gel (1%) stained with ethidium bromide showing colony PCR amplification products from single gene deletions at <i>dppC</i> and <i>oppC</i> loci, the double gene deletion strain $\Delta$ DB1 ( $\Delta$ <i>dppC</i> $\Delta$ <i>oppC</i> ) and the quadruple gene deletion strain $\Delta$ DB5 ( $\Delta$ <i>dtpA</i> $\Delta$ <i>dtpB</i> $\Delta$ <i>dtpC</i> $\Delta$ <i>dtpD</i> ) .....	116
<b>Figure 4.3</b> Growth curves of TD Pep strains of <i>E. coli</i> K-12 grown in M9 glucose minimal medium containing, as the sole source of nitrogen; 20 mM L-Alanine-L-Alanine or 20 mM L-Alanine .....	118
<b>Figure 4.4.1</b> Growth curves of TD Pep strains of <i>E. coli</i> K-12 grown in M9 glucose minimal medium containing, as the sole source of nitrogen; 20 mM L-Phenylalanine-L-Alanine or 20 mM L-Tyrosine-L-Alanine.....	120
<b>Figure 4.4.2</b> Growth curves of TD Pep strains of <i>E. coli</i> K-12 grown in M9 glucose minimal medium containing 20 mM L-Alanine-L-Phenylalanine as the sole source of nitrogen .....	121
<b>Figure 4.5</b> Growth curves of TD Pep strains of <i>E. coli</i> K-12 grown in M9 glucose minimal medium containing, as the sole source of nitrogen; 20 mM L-Alanine-L-Leucine or 20 mM L-Leucine-L-Alanine.....	123
<b>Figure 4.6</b> Representative images of TD Pep strains grown on M9 minimal glucose agar plates with toxic peptide supplementation.....	126
<b>Figure 4.7.1</b> Growth curves of peptide symporter deficient strains of <i>E. coli</i> K-12 in 96-well plate format grown in 1% tryptone broth medium.....	129
<b>Figure 4.7.2</b> Growth curves of ABC TD-Pep strains of <i>E. coli</i> K-12 in tryptone broth medium.....	130
<b>Figure 4.7.3</b> Final growth yield (OD <sub>650</sub> nm) of WT and $\Delta$ DB1 <i>E. coli</i> K-12 grown in filter-sterilised, spent tryptone broth growth medium of $\Delta$ DB1 .....	131
<b>Figure 4.8.1</b> Growth curves of wild-type (WT) and $\Delta$ DB1 <i>E. coli</i> K-12 in 1% tryptone broth medium with carbon or nitrogen supplementation .....	133
<b>Figure 4.8.2</b> Growth curves of wild-type (WT) and $\Delta$ DB1 <i>E. coli</i> K-12 in 1% tryptone broth medium with yeast extract supplementation and yeast extract broth.....	134
<b>Figure 4.8.3</b> Growth curves of wild-type (WT) and $\Delta$ DB1 <i>E. coli</i> K-12 in LB medium, yeast extract broth and tryptone broth.....	135

<b>Figure 4.9</b> Multiple sequence alignment of <i>E. coli</i> Dtp proteins and selected prokaryotic homologues .....	137
<b>Figure 5.1</b> Uptake and biotransformation of S-Benzyl-L-cysteinylglycine by <i>E. coli</i> K-12 .....	148
<b>Figure 5.2</b> Biotransformation of S-Benzyl-L-cysteine and S-Benzyl-L-cysteinylglycine by purified C-S- $\beta$ -lyase from <i>C. jeikeium</i> K411 and <i>E. coli</i> C-S- $\beta$ -lyase mutants.....	151
<b>Figure 5.3</b> Biotransformation of S-Benzyl-L-cysteinylglycine by TD-Pep <i>E. coli</i> .....	153
<b>Figure 5.4.1</b> Plasmid map of pBADcLIC2005 and biotransformation of S-Benzyl-L-cysteinylglycine by Dtp protein-overexpressing <i>E. coli</i> .....	157
<b>Figure 5.4.2</b> Biotransformation of S-Benzyl-L-cysteinylglycine by <i>E. coli</i> WT pDtpB with decreasing levels of overnight L-arabinose induction and in the presence of 100 $\mu$ M CCCP .....	158
<b>Figure 5.4.3</b> Biotransformation of S-Benzyl-L-cysteinylglycine by <i>E. coli</i> WT pDtpB and whole cell lysate prepared from WT pDtpB .....	159
<b>Figure 5.5</b> Biotransformation of Cys-Gly-3M3SH by Dtp protein-overexpressing <i>E. coli</i> and by <i>E. coli</i> WT, WT pDtpB, WT pDtpB and $\Delta$ <i>tnaA</i> pDtpB in the presence of 100 $\mu$ M CCCP .....	161
<b>Figure 5.6</b> Proposed model of malodour precursor substrate biotransformation by <i>E. coli</i> K-12.....	163
<b>Figure 6.1</b> Genome context of STAHO0001_1446, STAHO0001_0415 and STAHO0001_2140 .....	173
<b>Figure 6.2</b> Biotransformation of S-Benzyl-L-cysteinylglycine and Cys-Gly-3M3SH by <i>E. coli</i> overexpressing STAHO0001_1446 and STAHO0001_0415.....	176
<b>Figure 6.3</b> Biotransformation of S-Benzyl-L-cysteine and S-Benzyl-L-cysteinylglycine by $\Delta$ <i>tnaA</i> <i>E. coli</i> expressing STAHO0001_2140 .....	178
<b>Figure 6.4.1</b> Rooted phylogenetic tree showing the relationship between C-S- lyase type proteins in staphylococci.....	181
<b>Figure 6.4.2</b> BLAST search using the protein sequence of EEK11697.1 as a query and identification of multiple functional domains .....	182

## List of Tables

<b>Table 1.1</b> The prevalence and density of bacteria within the axillae of male and female subjects .....	22
<b>Table 1.2</b> Major odorous steroid molecules identified in non-sterile axillary secretion.....	28
<b>Table 1.3</b> Selected high-odour impact VFAs isolated from hydrolysed human axillary extracts.....	30
<b>Table 1.4</b> High-odour impact thioalcohols isolated from hydrolysed human axillary extracts .....	35
<b>Table 1.5</b> Properties of PTR-family secondary peptide transporters of <i>E. coli</i> .....	52
<b>Table 2.1</b> Strains of <i>E. coli</i> used in this work .....	56
<b>Table 2.2</b> Strains of corynebacteria used in this work.....	57
<b>Table 2.3</b> Strains of staphylococci used in this work.....	58
<b>Table 2.4</b> Plasmids used in this work.....	59
<b>Table 2.5</b> Oligonucleotide primers used in this work.....	60
<b>Table 2.6</b> Thermocycling parameters used for standard Taq DNA polymerase PCR.....	63
<b>Table 2.7</b> Thermocycling parameters used for standard KOD DNA polymerase PCR .....	63
<b>Table 2.8</b> Thermocycling parameters used to extract crude <i>S. hominis</i> B10 template DNA .....	64
<b>Table 2.9</b> Thermocycling parameters used for standard MyFi DNA polymerase PCR .....	64
<b>Table 3.1</b> Speciation of axillary isolated corynebacteria and staphylococci.....	92
<b>Table 4.6</b> Average zone of inhibition of TD-Pep strains grown on M9 minimal glucose agar plates containing discs saturated with equimolar concentrations of Val-Gly-Gly or Val ..	126
<b>Table 4.9</b> Summary of growth-associated phenotypes for TD-Pep strains of <i>E. coli</i> .....	145
<b>Table 6.1</b> Metabolite symporters of <i>S. hominis</i> SK119 as identified using BioCyc Database Collection.....	173

## **Acknowledgements**

Firstly I would like to express my endless gratitude to my supervisors Dr. Gavin Thomas and Dr. Gordon James for allowing me the opportunity to undertake a PhD under their supervision and for all of their support, enthusiasm and insight over the duration of the project.

Many thanks also go to Diana Cox and Della Hyliands at Unilever Discover, Colworth. Thanks to Diana for her valuable help with initial experimental set up and for hosting me during two extremely enjoyable placements at Unilever, and to Della for her assistance with the riboprofiling work. Many thanks also go to Dr. Malcolm Horsburgh and his lab at the University of Liverpool along with Sally Grimshaw at Unilever R&D, Port Sunlight, for supplying numerous bacterial isolates used for the project.

Special thanks go to my TAP members Dr Daniela Barillà and Dr James Moir for their support and patience, particularly during the first 18 months of the project where I began to find my feet in the fascinating world of molecular microbiology.

A special mention to those who made the last 4 years in York an unbelievable experience, particularly Simon, Adrian, Joe, Wayne and Andrew who never refused the opportunity to grab a pint and discuss the plaudits of the false nine role. Many thanks also go to past and present members of the Thomas lab and everyone on L1 who made the working environment very enjoyable.

My sincere appreciation and love goes to Naomi for pushing me to chase my dreams and for her continued love and support. I would also like to thank Mum, Dad, Jess and all of my extended family for their never-ending encouragement and interest.

... and not forgetting the BBSRC and Unilever for their financial support.

## **Author's declaration**

I declare that all work presented in this thesis submitted by myself for the degree of Doctor of Philosophy is entirely my own original work, except where due reference is made to other authors.

Daniel Bawdon

# **Chapter 1**

## **Introduction**

## **1.1 Skin structure and perspiration**

The skin is the largest organ of the human body, playing a critical role in thermoregulation. Excessive internal body temperatures ( $>40^{\circ}\text{C}$ ) result in protein denaturation, cell death and ultimately multiple organ failure (Wilke *et al.*, 2007). It is the job of the skin to regulate core body temperature under excessive environmental temperature and during physiological stress, particularly during immune system activation in response to invading microbial pathogens. The primary means of regulating core body temperature is by perspiration (sweating). During sweating, thermal energy is released when the water component of sweat evaporates from the surface of the skin in a process known as evaporative cooling (Shelley & Hurley, 1975). This process has the net effect of lowering the temperature of the skin and underlying tissue. Sweating is controlled by the central nervous system, with the hypothalamus being the primary portion of the brain controlling this process by responding to fluctuations in core body temperature, stress, changes in the levels of certain hormones and the concentration of pyrogens present in the bloodstream (Holzle, 2002). The physical act of sweating is performed by sweat glands, which are tubular exocrine glands on the surface of mammalian skin. Most mammals have two types of sweat gland, apocrine and eccrine. A key difference between these sweat glands is that the apocrine gland opens into a hair follicle whereas the eccrine gland opens directly onto the surface of the skin. The apocrine/eccrine classification was devised in the early 1900s by Schiefferdecker (1922) and still stands today. A comprehensive review of apocrine and eccrine glands is provided below. An additional type of skin-associated exocrine gland is the sebaceous gland which is relatively evenly distributed across the skin, with the exception of the palms of the hands and soles of the feet. Sebaceous glands are at particularly high density on the scalp and face, where up to 900 glands per  $\text{cm}^2$  of skin can be present (Folk & Semken, 1991). Sebaceous glands are proposed to lubricate the skin by secreting a waxy substance known as sebum which is thought to provide a physical defence barrier against invading microorganisms (Boutelier, 1959), but sebaceous glands are not involved in sweating.

### **1.1.1 The eccrine gland**

Located at the top, shallow portion of the dermis, the eccrine gland is almost exclusively involved in thermoregulatory sweating. In humans, chimpanzees and gorillas, it is distributed evenly across the entire surface of the skin, with particularly concentrated regions in the palms of the hands and soles of the feet (Robertshaw, 1985). In fact, on the palms of the hand, human skin can contain as many as 2000 eccrine glands per  $\text{cm}^2$ . This

is significantly higher than other areas of the body such as the trunk and limbs which contain up to 10-fold fewer (Weiner & Hellmann, 1959). Estimations of the total number of eccrine glands on the entire surface area of human skin range from 1.6 to  $4.0 \times 10^6$ , which, when averaged out, equates to approximately 80 to 200  $\text{cm}^{-2}$  skin (Kawahata, 1950). As well as providing evaporative cooling, the eccrine gland is occasionally involved in an additional type of sweating termed emotional sweating. Emotional sweating is a specific stress reaction whereby sweat production is increased in response to an environmental stimulus such as pain, fear, mental stress or other physiological stimuli. It is thought to be controlled, at least in part, by the amygdala (Asahina *et al.*, 2003). The few eccrine sweat glands involved in emotional sweating are innervated by cholinergic nerves, that is, they are activated specifically and exclusively by the neurotransmitter acetylcholine. A specific example of this response is the observed heavy sweating on the palms of the hands and soles of the feet as a fight-or-flight response, which is carried out by a concentrated group of eccrine glands in these regions. This process is evident in many mammals, including humans, and serves to increase friction in the hands and feet to reduce slipping and aid in escape from predators (Adelman *et al.*, 1975).

Eccrine sweat consists mainly of water, but is very hypotonic as it contains high concentrations of ionic salts such as  $\text{Na}^+$ ,  $\text{K}^+$  and  $\text{Cl}^-$ . NaCl is said to account for up to 90% of the osmotic activity of sweat (van Heyningen, 1952), but this varies considerably between individuals. In fact, sufferers of pancreatic cystic fibrosis have such altered electrolyte composition that a clinical diagnosis of the condition can be made on this basis alone (Naruse *et al.*, 2004). Eccrine sweat also contains small waste-product molecules such as lactate (Patterson *et al.*, 2000), accounting for the slight acidity of eccrine sweat, of which, the pH varies between approximately 4.0 and 6.0 (Shelley *et al.*, 1953). Along with electrolytes and lactate, eccrine sweat typically contains amino acids such as histidine, lysine and arginine (Hirokawa *et al.*, 2007), oligosaccharides and urea (Mosher, 1933), trace elements of metals such as zinc, copper, nickel and cadmium (Cohn & Emmett, 1978) and even novel antimicrobial peptides such as dermcidin (Schitteck *et al.*, 2001). The total volume of sweat secreted by an individual is reported to be as much as 10 litres per day (Kuno, 1965). Coincidentally, the dissipation of between 6 to 8 litres of sweat per day is equivalent to an evaporative heat loss of approximately  $600 \text{ kcal m}^{-2} \text{ skin hr}^{-1}$ , which is said to be a sufficient amount to allow *Homo sapiens* to carry out a full day's work in a hot, dry, sun-exposed environment without suffering heat exhaustion, conditions similar to those observed in prehistoric equatorial climates (Weiner & Hemmlann, 1959).

### 1.1.2 The apocrine gland

The apocrine gland is distinct from the eccrine gland both morphologically and by the pattern of distribution across the skin and spatial locality within the dermal layers. Apocrine glands are spongy in appearance and located subcutaneously, deep inside the dermis. In contrast to the eccrine gland, apocrine glands are relatively scarcely distributed across human skin, with particular clustering occurring almost exclusively in the armpit (axilla), but also within the nipples and areolae of the breast, ear canal and in the perianal and pubic regions (Kurosumi *et al.*, 1984). The limited and concentrated spatial distribution of the apocrine gland is unique to only a handful of animals such as humans, chimpanzees and gorillas. The skin of most other primates and mammals is almost exclusively covered by apocrine glands. It is argued that the human apocrine gland is an evolutionary relic that was once involved in evaporative cooling but is now only retained by mammals that did not develop an eccrine gland system for thermoregulation (Montagna & Parakkal, 1974). The structure and spatial distribution of glands within the human axilla is shown in Fig. 1.1. In contrast to the eccrine gland, the apocrine gland has evolved solely to respond to emotional stimuli. Whereas the limited numbers of emotionally-responsive eccrine glands are activated exclusively by the neurotransmitter acetylcholine, all apocrine glands are innervated specifically by sympathetic adrenergic nerves, that is, they are activated by adrenaline (Hurley, 1953). This phenomenon was demonstrated empirically in the 1950's in a series of experiments which involved injecting subjects with diluted adrenaline, noradrenaline or acetylcholine and measuring axillary sweat secretions (Shelley *et al.*, 1953). In all subjects tested, specific apocrine sweating was exclusively observed following adrenaline or noradrenaline injection whereas eccrine sweating was specifically observed following injection of acetylcholine. In the same study, subjects were exposed to infra-red heat for a period of 30 min. An absence of apocrine secretion was noted but a significant amount of eccrine sweat was apparent, demonstrating that eccrine glands and not apocrine glands are involved in thermoregulation. The two main emotions that promote apocrine secretion are fear and pain. In an early study on the effect of fear (apprehension) on apocrine sweating, visible apocrine secretions were visible in several individual males immediately prior to minor dermatological surgery (Shelley *et al.*, 1953). In the same study, the effect of pain on apocrine sweating was studied using pregnant women in different stages of labour. It was observed that as the uterine contractions intensified, so did apocrine secretions, directly correlating with an increased level of pain.

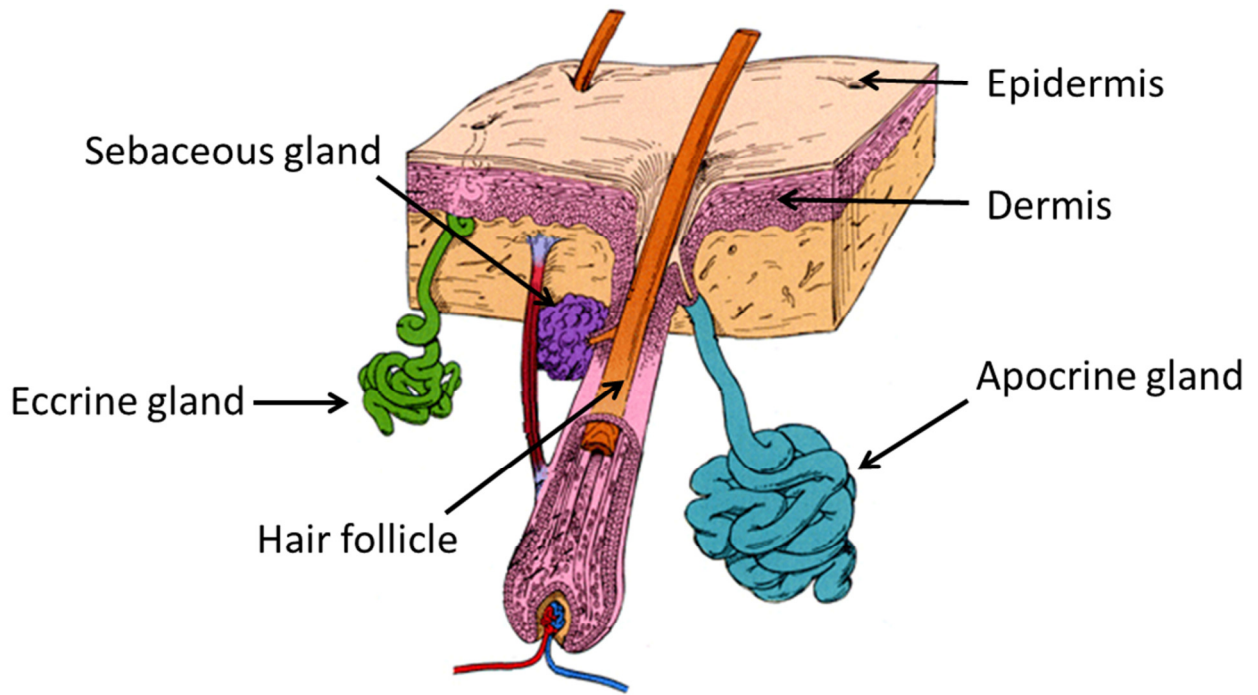


**Figure 1.1.** The glandular composition of the human axilla. Adapted from Gallik (2013).

The chemical composition of apocrine and eccrine sweat is very similar, but apocrine sweat additionally contains a relatively high concentration of lipids (20 mg/ml), most of which are cholesterol or triglyceride (76.2%) or fatty acid (19.2%) (Leyden *et al.*, 1981). Proteins are also a significant component, accounting for approximately 10% of apocrine sweat (Gower, 1988). These specific secretions give apocrine sweat a characteristic milky and viscid appearance that dries with a glue-like consistency (Folk & Semken, 1991). The pH of apocrine sweat ranges from approximately 5.0 to 6.5, making it slightly more alkaline than eccrine sweat due to the apparent absence of lactate (Shelley *et al.*, 1953). Importantly in the context of this work, trace amounts of many other small molecules and compounds that are particularly significant for characteristic human body odour are also secreted in apocrine sweat and will be discussed in detail later.

## **1.2 The evolutionary origins and historical significance of body odour**

The production of body odour is well accepted to be an evolutionary trait, with strong historical associations with ancestral mate selection, sexual attraction and kin recognition. It is well documented that newborn infants can correctly identify their own mothers breast (Russell, 1976) and axillary scent (Cernoch & Porter, 1985) by olfactory signals, presumably provided by the concentrated cluster of apocrine glands in those regions, particularly the axillae. These studies outline the apparent role of body odour in non-verbal communication between mothers and their infants, with particular emphasis on those odours emanating from clusters of apocrine glands.

The role of axillary body odour in sexual attraction has been described since the mid-1800s when anthropologists began to suggest that the function of the human axilla was to produce scent or odour deemed to be attractive to members of the opposite sex. In 1840, Thomas Laycock remarked on human body odour:

“The principal seat of this odour is in the follicles of the axillae, and is not given off before puberty. It is most powerful in individuals who are continent, or with strong sexual powers, and in some it is very pleasant.”

Similarly in 1901, Albert Hagen, stated:

“The axillary scent in man seems to be superior to the scent of the sexual organ or any other part of the body...as had already been described, the apocrine glands in the axillae, to which the axillary scent is essentially due, develop first a few years before the onset of puberty and undergo some cyclic or temporary changes concomitantly with the menstruation or pregnancy. This also supports the existence of sexual significance of the axillary scent.” (Stoddart, 1991)

In human development, the apocrine gland is visible by the third trimester of pregnancy, developing first as a coiled rod of cells (Stoddart, 1991). By age four, the human apocrine gland begins to enlarge. By age seven, the muscle fibres required to expel apocrine secretions begin to develop in the basal cells. Apocrine gland secretion is not observed until puberty but continues from this point throughout life. Further support for the notion of the axillary apocrine gland as a scent organ followed throughout the 20<sup>th</sup> century, with observations that the apocrine gland develops slightly earlier and to a higher density in females than males (Schiefferdecker, 1922). This observation strongly suggested to researchers that the apocrine gland is involved in sexual attraction with odours emanating from the axillary region, particularly in sexually active females, serving as a signal to attract a sexual partner. This opinion has continued to be favourable into the present day. Rikowski & Grammar (1999) demonstrated that males perceive the body odour of facially attractive women as more pleasant than less facially attractive women. However, the historical opinion that ‘attractive’ human body odour is stronger in females during their most fertile periods has been significantly challenged, particularly by Thornhill & Gangestad (1999) who demonstrated that there are no differences between the perceived attractiveness of female body odour at different stages of the menstrual cycle, suggesting that female fertility does not influence body odour profile. An interesting hypothesis has also been proposed by Wedekind *et al.* (1995), who suggest that sexual attractiveness through body odour, though not necessarily axillary odour, is partly controlled by products of the major histocompatibility complex (MHC), a large set of cell-surface molecules controlling a significant part of the immune system. Wedekind demonstrated that subjects rate the relative pleasantness of other individuals’ body odour as more attractive if they have an MHC profile discordant to their own. The reasons for this have not been fully elucidated, but it is hypothesised that selecting a mate with a different MHC profile would promote MHC heterozygosity, in turn serving to increase protection against rapidly evolving pathogens and also, more simply, prevent inbreeding within the population. The ‘inbreeding avoidance hypothesis’ is particularly favoured for mice, where a distinct fitness disadvantage is observed in those populations with severe inbreeding (Meagher *et al.*, 2000). Fittingly, it has also been demonstrated that the MHC profile influences the mate choice of mice, who, just like humans, tend to look for mates with dissimilar MHC

phenotypes (Wedekind & Penn, 2000). Interestingly, Wedekind *et al.* (1995) also described that mice are able to recognise human MHC scents from urine samples and subsequently ascertained that the converse was also true, demonstrating that humans can distinguish between two genetically identical mice differing only in their MHC profile by scent alone.

Clearly therefore, there appears to be strong positive selection for particular body odour profiles to develop in humans. The odour profiles generated, particularly in the axillae, seem to be geared towards enhancing reproductive biology. From studies on kin recognition, the odour profiles appear to be extremely individualistic and it is likely that they are more closely controlled than one would imagine.

### **1.3 The origins of axillary (mal)odour**

The term 'axillary malodour' has crept into existence and everyday use over the past century. It is now generally applied to odour emanating from the axillary region of humans. For this reason, the term axillary malodour will be used henceforth in this context. Despite reports dating back to the 1800's regarding axillary odour, it was not until the 1950's that the biological origins of axillary malodour began to be unravelled. Prior to 1953 there was no knowledge of microbiological involvement in producing odorous compounds directly from human apocrine gland secretions, which is now the generally accepted route to human axillary malodour. It was the pioneering work of Walter B Shelley that first described this in detail. Shelley *et al.* (1953) began by demonstrating that apocrine sweat was a sterile fluid immediately after secretion onto the surface area of the axilla. Multiple vials of sterile and non-sterile apocrine sweat were then prepared, along with several vials of independently isolated eccrine sweat to serve as a control. All vials were incubated at room temperature for 2 weeks and subjective odour measurements taken by two independent panellists at appropriate time intervals. It was observed that only those vials containing non-sterile apocrine sweat produced an odour, which appeared very rapidly following only 6 hours incubation. Vials containing eccrine sweat remained completely odourless. Apocrine-associated odour production could be inhibited, although not completely, by applying an antibacterial wash to the axilla prior to isolating apocrine sweat samples. Shelley concluded that bacterial biotransformation must be responsible for the odour produced in the non-sterile apocrine sweat samples and that specific components of apocrine sweat must serve as primary substrates for production of such odour. A later study by Shehadeh & Kligman (1963) narrowed down the bacteria responsible for this phenotype to Gram-positive organisms. Cultures of the most commonly isolated axillary

bacteria were prepared in rich growth media and transferred to glass capillary tubes. Human-isolated apocrine secretions were subsequently added to the bacterial cultures and incubated for 48 hours, followed by subjective odour analysis. It was observed that Gram-positive bacteria, particularly coagulase negative staphylococci along with diphtheroids (non-pathogenic corynebacteria) produced the most pungent smell characteristic of typical axillary malodour, whereas all Gram-negative bacteria produced little or no characteristic axillary malodour.

### **1.3.1 The microbiota of the human axilla and its correlation with malodour**

Studies through the latter part of the 20<sup>th</sup> century attempted to fully characterise the composition of the axillary microbiota in order to specifically identify which bacteria were responsible for malodour. Aly & Maibach (1977) observed a significant coryneform domination of the axilla when they noted that coryneforms represented, on average (n=66), 96% of the total bacteria in this region. The term coryneform was coined by Cowan (1968) and covers all non-sporulating, pleiomorphic rod-shaped bacteria. Historically, it has been used interchangeably with corynebacteria, despite the observation that only around 60% of skin coryneforms belong to the genus *Corynebacterium* (Pitcher, 1983). Throughout the late 1960's to the 1980's studies confirmed that corynebacteria and the increasingly relevant genus *Staphylococcus* represented the dominant bacterial genera of the axillary microflora. Marples & Williamson (1969) identified that, on average, coagulase-negative cocci (likely consisting mainly of non-pathogenic staphylococci) and lipophilic coryneforms represented 85% of the total axillary flora. Kloos & Musselwhite (1975) found that coryneforms represented approximately 70% of the axillary population. A more refined study by Leyden *et al.* (1981) examined the previously reported corynebacterial domination of the axilla and began to assess, in detail, the axillary microbiota and its relationship with axillary odour. Through culture-based methods, Leyden compiled and averaged data on the prevalence and density of the axillary microbiota in both male (n=128) and female (n=77) subjects. This data is displayed in Table 1.1. In all subjects, members of the Micrococcaceae could be cultured, which, when broken down to the genus level, consisted solely of *Staphylococcus* spp., mainly *S. epidermidis* (51%) and *S. saprophyticus* (29%). It should be noted that this historic misassignment of staphylococci within the Micrococcaceae family has since been rectified. The overall density of these bacteria was approximately three-fold greater in females than in males.

**Table 1.1** The prevalence and density of bacteria within the axillae of male and female subjects.  
Taken from Leyden *et al.*, (1981)

*Prevalence and density of axillary resident bacterial flora*

	Males (N = 128)			Females (N = 77)		
	Prevalence	Density <sup>a</sup>	SEM <sup>b</sup>	%	Density	SEM
Aerobic flora	100	$6.9 \times 10^5$	0.06	100	$8.9 \times 10^5$	0.09
Micrococaceae	100	$1.2 \times 10^5$	0.07	100	$3.6 \times 10^5$	0.11
Lipophilic diphtheroids	85	$2.5 \times 10^5$	0.09	66	$2.3 \times 10^5$	0.14
Large colony diphtheroids	26	$2.7 \times 10^4$	0.21	25	$3.7 \times 10^4$	0.24
Gram negative rods	20	$2.3 \times 10^3$	0.25	19	$2.1 \times 10^3$	0.31
Propionibacteria (total)	70	$5.1 \times 10^3$	0.21	47	$1.7 \times 10^4$	0.30
<i>P. acnes</i>	47	$7.2 \times 10^3$	0.29	30	$1.8 \times 10^4$	0.38
<i>P. avidum</i>	34	$4.2 \times 10^3$	0.22	21	$1.5 \times 10^4$	0.43
<i>P. granulosum</i>	8	$4.1 \times 10^3$	0.32	5	$4.5 \times 10^3$	0.28

<sup>a</sup> Geometric mean per square centimeter.

<sup>b</sup> Standard error of the mean, expressed in logarithms.

When comparing the ratio of staphylococci and corynebacteria, Leyden's data suggested that, on average, approximately 75% of the bacterial load within the axilla consisted of corynebacteria, with staphylococci accounting for the majority of the remaining 25%. Other minor component microbes of the axilla were identified as Gram-negative rods and *Propionibacterium* spp., but these bacteria were present at densities at least two log (base 10)-fold lower than either staphylococci or lipophilic corynebacteria. The presence of corynebacteria in the human axilla was supported by Jackman & Noble (1983) who identified lipophilic diphtheroids (now an obsolete taxonomic term historically applied to mean a microorganism which resembles the diphtheria-causing bacterium, *C. diphtheriae*) and large colony diphtheroids, consisting exclusively of *Corynebacterium* spp., which, when taken together were present, but not always dominant, in almost all individuals assessed. It was also demonstrated that males, on average, are three times more likely to have a coryneform-dominated axilla than females. However, in absolute terms, Jackman & Noble disagreed with Leyden's observation regarding the mean distribution of corynebacteria and staphylococci, and stated that coryneform- or coccal-dominated floras were evenly split between a representative population.

Leyden went on to relate this data to axillary malodour. He observed that individuals described as having apocrine odour, that is "the offensive pungent smell so typical of body odour", reproducibly had a significantly higher density of total bacteria within their axillae ( $1.3 \times 10^5 \text{ cm}^{-2}$  compared to  $4.8 \times 10^4 \text{ cm}^{-2}$ ). These bacteria were principally lipophilic diphtheroids, whereas Micrococcaceae (staphylococci) that were associated with individual axillae did not exhibit typical malodour, but displayed a distinctive non-apocrine odour phenotype. Leyden was one of the first to suggest a correlation between axillary malodour and a high density of corynebacterial commensals within the axilla. Jackman and Noble supported this association, stating that individuals exhibiting strong axillary malodour have a coryneform-dominated axilla, which usually consists of greater than  $1.6 \times 10^5$  total coryneform bacteria  $\text{cm}^{-2}$  skin.

Recent work using more sophisticated culture-based methods was carried out by Taylor *et al.* (2003). The approach of this study was similar to that of Leyden, whereby axillary samples were taken from multiple male and female volunteers and bacteria cultured in both aerobic and anaerobic growth media. The results revealed particular genus-specific differences between individuals, with the axillary region dominated by either staphylococci (52% of subjects) or aerobic coryneforms (34% of subjects). The remaining subjects (14%) had a propionibacteria-dominated axilla. Taylor then assessed the relationship between microbial counts and associated malodour using a malodour scoring system which allows trained assessors to subjectively assess axillary malodour intensity. The

microbial composition of each respective axilla is then correlated with malodour on a 5-point hedonic scale. A significant association between malodour and high microbial counts was observed for total aerobes (aerobic coryneforms, staphylococci, micrococci and *Malassezia* spp., combined), aerobic coryneforms alone and micrococci alone. No significant correlation between malodour and high population densities of staphylococci, propionibacteria or *Malassezia* spp. was observed. In order to identify the most prominent *Corynebacterium* spp. within the axilla, Taylor isolated 16S rDNA from 61 aerobic coryneforms, originally isolated from cultured axillary samples. A significant proportion (67%) was identified with the highest similarity score to *Corynebacterium* G-2 CDC G5840, identified earlier as *C. tuberculostearicum* (Riegel *et al.*, 1995). 7% (4 out of 61 isolates) were identified as *C. mucifaciens* with other species such as *C. afermentans*, *C. amycolatum*, *C. genitalium* and *C. riegelii* each representing less than 4% of the total corynebacterial pool. This data provided further evidence that aerobic bacteria, particularly corynebacteria, were strongly associated with malodour, with *C. tuberculostearicum* being the most likely culprit based on its high prevalence relative to other aerobic coryneforms isolated from the axilla.

Further attempts to characterise the axillary microbiota have adopted culture-independent metagenomic and molecular-based techniques. Callewaert *et al.* (2013) sampled the axillary microbiome of 53 individuals and used high-throughput next-generation DNA sequencing to characterise microbial populations of these samples. Again, similar to Taylor *et al.* (2003), Callewaert observed either a corynebacterial-dominated (39% of subjects) or staphylococcal-dominated axilla (61% of subjects). Species-level discrimination within these samples was not entirely possible, but within the staphylococcal-dominated axilla, *S. epidermidis* appeared to be the most abundant species but with distinct populations of *S. hominis* and an unspiciated *Staphylococcus* sp. also detected. Gender-specific differences were also apparent, with females more likely to have staphylococcal-dominated axillae than males. The staphylococcal-dominated axillae phenotype was echoed by Costello *et al.* (2009) who probed microbial colonisation of various sites on human skin, including the axilla. Egert *et al.* (2011) adopted a slightly different study focus and assessed, in detail, the bacterial population symmetry between the left and right axillae both intra- and inter-personally using a pool of 10 male volunteers. Statistically significant differences were observed between individuals but not between the left and right axillae of the same individual, a phenomenon reaffirmed in a later study (Callewaert *et al.*, 2013). Within Egert's study, species discrimination of axillary-isolated staphylococci and corynebacteria revealed a *Staphylococcus* species bias of *S. epidermidis* and *S. hominis*, whereas the majority of *Corynebacterium* species consisted of either *C. tuberculostearicum* (echoing the findings of Taylor *et al.*, 2003) or *C.*

*kroppenstedtii*. In addition to the two major axillary-colonising genera, several samples of the Gram-positive anaerobic coccus *Anaerococcus* sp. DQ847450 were identified. This represented a novel axillary commensal, as members of this genus are commonly isolated exclusively from clinical samples (Song *et al.*, 2007). These bacteria were presumably not isolated previously due to insufficient anaerobic culturing techniques. It is important to note that Egert's analysis assessed pooled samples from only three individual axillae and therefore cannot be satisfactorily representative of a universal axillary microbiota.

Although over the past decades there appears to have been a gradual switch from the view that the human axilla is completely dominated by corynebacteria to the position that the majority of axillae are marginally dominated by staphylococci, a consensus on the exact microbial make-up of the axilla remains unresolved. Collectively, microbiome studies show huge variation in the abundance of not only species but also genera across the skin microbiome, prohibiting the assertion of a 'typical' axillary carriage of bacteria. Nevertheless, a significant improvement in the ability to isolate and identify bacteria within this environmental niche has emerged, most likely brought about by improvements in bacterial isolation techniques, which, in their infancy, likely inadvertently excluded or prohibited the growth of certain bacteria and promoted the growth of others, leading to inherent bias in the final data. In fact, Leyden *et al.* (1981) remarked that the disparity in bacterial numbers observed in his study and the study of Aly & Maibach (1977) were likely due to environmental, hygiene or sampling differences. The advent of new methods to detect, enumerate and characterise the resident skin microbiota such as high-throughput DNA sequencing has undoubtedly also aided in the position that we are at today and is likely to play a central role in future species and strain discrimination of the axillary microbiota.

#### **1.4 The biochemical basis of axillary malodour**

It is now generally accepted that three classes of odorous molecule are responsible for axillary malodour. These are odorous steroids, volatile fatty acids (VFAs) and thioalcohols, which all exhibit a distinct and characteristic odour, culminating in what modern society would term 'body odour'. The generation of these odorous molecules is, as reported previously (Shelley *et al.*, 1953) dependent upon biotransformation of their constituent non-odorous precursor molecule(s) by members of the resident axillary microbiota. The three classes of odorous molecules are discussed below.

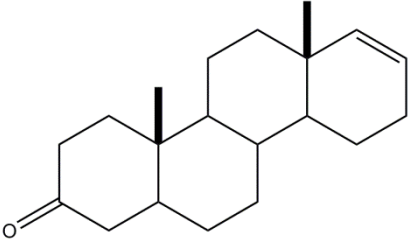
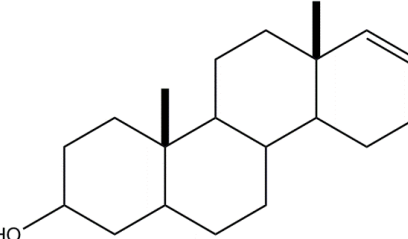
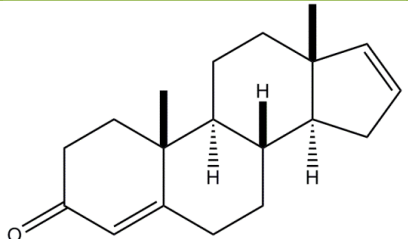
### 1.4.1 Odorous steroids

The first class of malodorous molecules, odorous steroids, were discovered in the 1970's, with 5 $\alpha$ -androst-16-en-3-one (androstenone) being one of the first discovered on human skin (Gower, 1972), closely followed by its respective alcohol, 5 $\alpha$ -androst-16-en-3 $\alpha$ -ol (androstenol) (Brooksbank *et al.*, 1974). 4,16-Androstadien-3-one (androstadienone) is also present at detectable levels (Gower *et al.*, 1994). These molecules are collectively termed 16-androstenes (Table 1.2). Androstenone, an important porcine pheromone, was subsequently isolated directly from the human axilla (Claus & Alsing, 1976), where, at the time, it was thought to be one of the key contributors to axillary malodour. The postulated odourless precursor molecules of 16-androstenes were testosterone, 5 $\alpha$ -dihydrotestosterone (DHT) and pregnenolone, but none of these molecules appeared to be converted to appreciable levels of 16-androstenes by incubation with mixed populations of aerobic corynebacteria (Nixon *et al.*, 1986, Gower *et al.*, 1986). The average olfactory thresholds for the commonly isolated odorous axillary steroids, androsterone and androstenol are 0.18 parts per billion (ppb) and 6.2 ppb, respectively (Amoore *et al.*, 1977). It has been stated that the physiological concentrations of such molecules are in the low pmol cm<sup>-2</sup> axillary skin (Gower *et al.*, 1994). This means that theoretically, odorous steroids are present at a high enough concentration to contribute to axillary malodour. Direct bacterial biotransformation of 16-androstene precursor molecules has been shown by Tue *et al.* (1998) who demonstrated that corynebacteria were able to biotransform testosterone into androstenedione and androstanedione. However, testosterone and other precursors of these odorous steroids are not present at significant concentrations in human axillary secretions. In a later study it was demonstrated that no single *Corynebacterium* spp. was able to perform all of the necessary biochemical reactions required to biotransform a common axillary steroid precursor, 5,16-androstadien-3-ol, into the full complement of odorous steroid products, identifiable by gas chromatography-mass spectrometry (GC-MS) (Austin & Ellis, 2003). Those bacteria that were able to produce detectable levels of odorous molecules did so only after prolonged (48 h) incubation and were found to be present at insignificant levels within the axillary microbiota.

When the field of odorous axillary steroids is assessed as a whole, it becomes apparent that there are no reports linking 16-androstenes to underarm odour when assessing total body odour as a whole, *in vivo*. Zeng *et al.* (1991) undertook an organoleptic evaluation of human axillary odour using GC-MS and asked panellists to identify characteristic body odour-type notes. Despite identifying distinct peaks for 16-androstenes, the panellists did not identify these molecules as being characteristic of axillary malodour. This is possibly

because it has been reported that humans demonstrate a significant qualitative variation in the perceived olfactory odour notes of these molecules, particularly androstenone, which has been described by some panellists as 'sweaty and urinous' and by others as 'floral and sweet'.

**Table 1.2.** Major odorous steroid molecules identified in non-sterile axillary secretions

Molecule	Chemical structure	Reference
<p><b>5<math>\alpha</math>-androst-16-en-3-one</b> (androstenone)</p>		<p>Gower (1972)</p>
<p><b>5<math>\alpha</math>-androst-16-en-3<math>\alpha</math>-ol</b> (androstenol)</p>		<p>Brooksbank <i>et al.</i> (1974)</p>
<p><b>4,16-androstadien-3-one</b> (androstadienone)</p>		<p>Gower <i>et al.</i> (1994)</p>

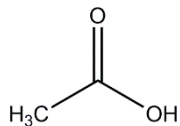
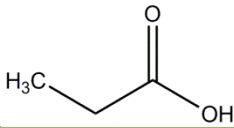
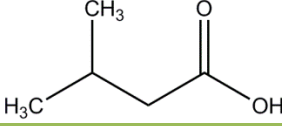
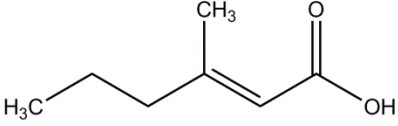
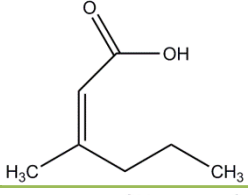
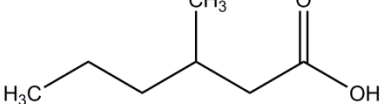
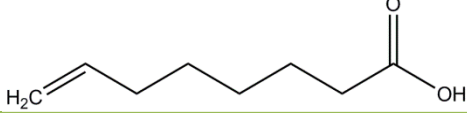
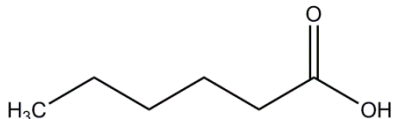
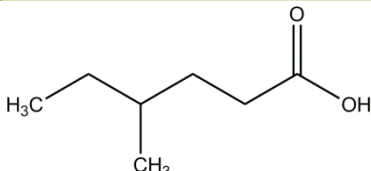
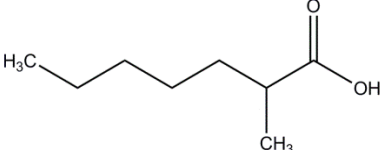
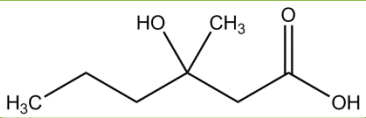
Additionally, it is estimated that up to 50% of individuals are specifically anosmic to androstenone, that is, they have no olfactory perception of this molecule (Amoore *et al.*, 1977). Therefore, odour intensity and descriptors applied to 16-androstenes are likely to be subjective and unique to the individual assessor and may therefore be unimportant in defining the highly characteristic and orthodox smell of axillary malodour. Due to these insights, the notion that odorous steroids are a major contributor to axillary malodour has quickly lost favour and it is now widely accepted that they play a minor or insignificant role (James *et al.*, 2013).

#### **1.4.2 Volatile fatty acids (VFAs)**

Short-to-medium chain (C2-C11) VFAs (Table 1.3) have been routinely isolated from the human axilla and are commonly accepted to be involved in malodour. Short-chain VFA malodorants, commonly defined as acetic (C2) and propionic (C3) acid are thought to be produced via microbial fermentation of glycerol and lactic acid, both naturally present on the surface of the skin. Lactic acid is particularly abundant on skin with a reported concentration of  $2.48 \pm 0.17$  mM (Petersen, 1999). Both glycerol and lactic acid can be broken down efficiently by *Propionibacterium avidum*, a widely isolated skin commensal (Bojar & Holland, 2004) into significant quantities of propionic acid (James *et al.*, 2004). Similarly, branched aliphatic amino acids such as leucine, isoleucine and valine have the potential to be metabolised by commensal bacteria to other short-chain VFAs (C4-C5), including 3-methylbutanoic acid (isovaleric acid). Isovaleric acid is demonstrably produced directly from amino acid catabolism by both propionibacteria (Thierry *et al.*, 2002) and multiple *Staphylococcus* spp. (James *et al.*, 2004, James *et al.*, 2013). However, due to the widespread distribution of short-chain VFA precursor substrates (glycerol, lactic acid and branched-chain amino acids) not only within the axilla, but across the entire surface of the skin, along with the plethora of microorganisms with the inherent ability to metabolise these simple molecules, short-chain VFAs are likely to be a feature of general sweat malodour and not specifically characteristic of underarm malodour.

Medium-chain VFAs have a more prominent role in axillary malodour. Using a GC-MS approach, Zeng *et al.* (1991) identified key axillary malodorants by asking panellists to distinguish typical axillary malodour scents collected from the axillary extracts of six male donors. The molecules responsible for these scents were then identified by isolating the region of the chromatogram where the panellists identified strong characteristic odours.

**Table 1.3.** Selected high-odour impact VFAs isolated from hydrolysed human axillary extracts

Molecule	Chemical structure	Reference
<b>Acetic acid</b>		James <i>et al.</i> (2004)
<b>Propionic acid</b>		James <i>et al.</i> (2004)
<b>3-methylbutanoic acid (Isovaleric acid)</b>		James <i>et al.</i> (2004)
<b>(E)-3-methyl-2-hexenoic acid E-(3M2H)</b>		Zeng <i>et al.</i> (1991) Natsch <i>et al.</i> (2003)
<b>(Z)-3-methyl-2-hexenoic acid Z-(3M2H)</b>		Zeng <i>et al.</i> (1991) Natsch <i>et al.</i> (2003)
<b>3-methylhexanoic acid (3MH)</b>		Zeng <i>et al.</i> (1991)
<b>7-octenoic acid</b>		Zeng <i>et al.</i> (1991)
<b>n-hexanoic acid</b>		Zeng <i>et al.</i> (1991)
<b>4-ethylpentanoic acid</b>		Zeng <i>et al.</i> (1991)
<b>2-methylheptanoic acid</b>		Zeng <i>et al.</i> (1991)
<b>3-hydroxy-3-methylhexanoic acid (HMHA)</b>		Natsch <i>et al.</i> (2003)

Several odorous compounds were identified within the extracts, with the most abundant molecule being 3-methyl-2-hexenoic acid, of which, both the *E*- and *Z*- isomer were identified, but with (*E*)-3-methyl-2-hexenoic acid being the major component (10-fold more abundant). For simplicity, (*E*)-3-methyl-2-hexenoic acid will henceforth be referred to as 3M2H. 3M2H was described by odour assessors as sweaty, burnt, acrid and musty. Other high-impact malodorants were also identified in lower quantities relative to 3M2H, some of which exhibited particularly strong odour properties. Of the molecules identified, those exhibiting unsaturation or branching appeared to have the strongest odour. Some of these molecules are shown in Table 1.3. Exhibiting both unsaturation and branching, 3M2H displays one of the highest odour impacts of all the identified molecules. Historically, 3M2H was described as a characteristic odour of clinical patients suffering from schizophrenia (Smith *et al.*, 1969), but the same group later reported that it was also present in healthy patients (Gordon *et al.*, 1973). Within Zeng's study, four independent odour assessors agreed that characteristic underarm malodour emanated from the acid-fraction of the extracted axillary material and not the steroidal fraction, strongly suggesting that VFAs, particularly 3M2H and not odorous steroids, as previously described, are major contributors to characteristic axillary malodour.

At this time, the biochemical and microbiological route to VFA production was unknown. Given that apocrine secretions are odourless (Shelley *et al.*, 1953) it was postulated that odorous VFAs, specifically 3M2H, would be initially conjugated to a molecule or protein present in apocrine secretions and subsequently metabolised by the axillary microbiota once secreted into the axilla. Originally it was believed that these molecules were non-covalently attached to either of two proteins identified in apocrine sweat, Apocrine Secretion Odor-Binding proteins 1 and 2 (ASOB1 and ASOB2), with the offending 3M2H being liberated by an as yet undefined complement of bacterial proteases (Spielman *et al.*, 1995). Subsequently, Zeng *et al.* (1996), showed that ASOB2 was a homologue of ApoD, a lipocalin protein and part of the  $\alpha_{2u}$ -microglobulin superfamily; a large group of carrier proteins with the capacity to bind small hydrophobic molecules, including lipids (Flower, 1996). This raised the possibility that malodour precursor molecules were transported to the axilla by a similar mechanism to some mammalian odorants. Typically, mammalian odour molecules that play a key role in chemoattraction and chemical signalling are carried to the desired cutaneous location by a subclass of lipocalins, the odourant binding proteins (OBPs) (Tegoni *et al.*, 2000) where they are subsequently liberated by commensal microorganisms in these regions.

This hypothesis was challenged by Natsch *et al.* (2003), who used a sophisticated GC-MS approach to demonstrate that 3M2H, along with a newly-identified and highly abundant

VFA, 3-hydroxy-3-methylhexanoic acid (HMHA), were initially conjugated to an L-glutamine amino acid within sterile apocrine secretions. 3M2H and HMHA were shown to bind to the N<sup>α</sup>-atom of L-glutamine and these VFA malodour precursor molecules were given the functional titles 3M2H-Gln and HMHA-Gln, respectively. From the structure of these molecules, it was predicted that N<sup>α</sup>-acylglutamine aminoacylase activity would be required to release the odorous molecule from its respective precursor. This was indirectly demonstrated when axillary isolated *Corynebacterium* spp., namely *C. jeikeium*, *C. bovis* and *C. striatum* were shown to release appreciable quantities of 3M2H and HMHA from their respective glutamine-conjugated precursor molecules. This activity was not apparent in *S. epidermidis*, *S. capitis* or *Micrococcus luteus*. The putative zinc-dependent N<sup>α</sup>-acylglutamine aminoacylase was subsequently cloned from *C. striatum* axillary isolate 20 (Ax20) and recombinantly expressed in *E. coli*. Pure recombinant enzyme displayed activity towards both 3M2H-Gln and HMHA-Gln but interestingly showed the highest  $V_{max}$  and  $K_m$  towards a synthetic substrate, N<sup>α</sup>-decanoyl-Gln. Nevertheless, this work represented the first direct demonstration that 3M2H and HMHA are released via bacterial N<sup>α</sup>-acylglutamine aminoacylase activity. The involvement of HMHA and 3M2H in axillary malodour was supported by Troccaz *et al.* (2009), who described the minimum olfactory values for these molecules, that is, the lowest detectable levels for the human nose of each molecule in gas phase, averaged across 30 individual odour assessors. The lowest detectable level (pg L<sup>-1</sup> air) of 3M2H was 202.0 and for HMHA, 175.0, which equates to 0.202 and 0.175 parts per trillion, respectively. With reported concentrations of HMHA-Gln averaging 113.5 mg L<sup>-1</sup> sweat (Troccaz *et al.*, 2009), clearly an extremely small percentage of the precursor needs to be biotransformed to release the levels of VFA required to activate the human olfactory system. A plethora of other N<sup>α</sup>-acylglutamine aminoacylase-hydrolysable Gln-conjugated VFAs were subsequently identified in axillary sweat isolated from multiple sweat donors (Natsch *et al.*, 2006). These were present in extremely variable quantities inter-individually, leading to the suggestion that an individuals' unique combination of VFAs made up their body odour 'footprint'.

Despite the isolation of two important VFAs, 3M2H and HMHA and their respective glutamine-conjugated precursors in the human axilla, precursor biotransformation by a physiologically relevant and abundant population of axillary bacteria has yet to be demonstrated. From the limited information available and already discussed, the strong HMHA and 3M2H producing corynebacteria isolated by Natsch, principally *C. jeikeium*, *C. bovis* and *Corynebacterium* sp. Ax20 (initially speciated as *C. striatum* but latterly identified as *C. glaucum* (Natsch & Granier, 2014)) have not been associated with the axillary microbiota (Taylor *et al.*, 2003, Egert *et al.*, 2011). Additionally, those high density *Corynebacterium* spp. identified in the axillary region, namely *C. tuberculostearicum* and

*C. mucifaciens* have never been directly linked to axillary malodour biochemically, suggesting that they do not generate significant quantities of 3M2H or HMHA from their respective Gln-conjugated precursors. These collective observations question how physiological concentrations of VFAs arise in the axilla and hints that the most active VFA producing bacterial species within the axilla have yet to be isolated.

### **1.4.3 Thioalcohols**

#### **1.4.3.1 Identification of thioalcohols as components of axillary malodour and characterisation of their precursor conjugates**

An organic sulphur compound containing a free carbon-bonded sulfhydryl (SH) group is termed a thioalcohol or simply, a thiol. The word derives from an amalgamation of the Greek word 'thion' meaning sulphur and 'alcohol', with a thioalcohol being the sulphur analogue of its respective alcohol. Thioalcohols have previously been implicated in several common odour pathways including cat urine, wherein the amino acid S-(3-hydroxy-1,1-dimethylpropyl)-L-cysteine (felinine) is biotransformed to the thioalcohol 3-methyl-3-sulfanylbutan-1-ol by the action of bacteria present within or in the immediate vicinity of the urine (Westall, 1953). Similar odorous molecules are released during wine fermentation (Tominaga *et al.*, 1998) and also in passion fruit juice, where 3-sulfanylhexasan-1-ol and 3-methyl-3-sulfanbutan-1-ol are released from cysteine-conjugated precursors present in the juice by the action of bacterial enzymes (Tominaga & Dubourdieu, 2000). Thioalcohols also play a role in the flavouring process of many foods and beverages; 3-methyl-2-butene-1-thiol for example, is an important ingredient defining the flavour of coffee. Conversely though, they can be connected to the 'off' flavour of foods and drinks including beer, wherein 3-methyl-2-butene-1-thiol is produced from the metabolism of hop bitter in the presence of light and riboflavin creating a characteristic 'skunky' flavour, explaining why beer is generally brewed and packaged in dark vessels (Vermeulen *et al.*, 2005).

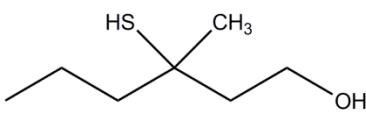
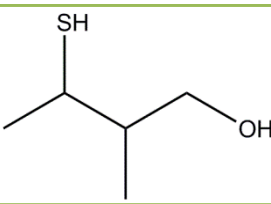
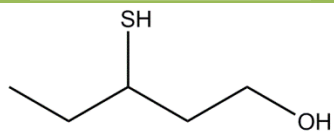
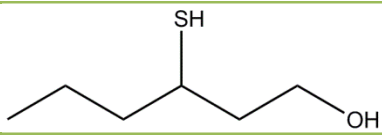
The identification of thioalcohols as a marker of body odour was originally described in a patent application (Lyon *et al.*, 1991), but specific details were vague. The first detailed reports of the presence of thioalcohols in axillary sweat were made independently by three research groups in the same year (Hasegawa *et al.*, 2004, Natsch *et al.*, 2004, Troccaz *et al.*, 2004). Natsch had asked panellists to olfactorily assess hydrolysed axillary secretions and identify key body odour notes. The odorous compounds within these samples were then isolated using GC-MS. Among the offending compounds were the previously isolated

VFAs 3M2H and HMHA along with distinct peaks for a series of as yet unidentified molecules. The most abundant of these (present at approximately 70% abundance compared to HMHA and 3M2H) was subsequently identified as 3-methyl-3-hexan-1-ol (3M3SH). Other thioalcohols present in the sample but at lower concentrations were 2-methyl-butan-1-ol, 3-pentan-1-ol and 3-sulfanhexan-1-ol. The chemical structure of these molecules is displayed in Table 1.4. Subjective descriptors that have since been applied to 3M3SH are oniony, meaty and acrid sweat-like (Troccaz *et al.*, 2004) and the consensus on the olfactory threshold of the molecule has settled between 1-3 pg L<sup>-1</sup> air (Troccaz *et al.*, 2009, Natsch *et al.*, 2004) which equates to 1-3 parts per trillion. These values are approximately 100-fold lower than those of HMHA and 3M2H, confirming that the thioalcohol 3M3SH is much more pungent than the most highly abundant VFAs in the axilla and has been subsequently described as a high-impact, low threshold odorant (Barzantny *et al.*, 2011).

As was suggested in the 1950's, axillary sweat is naturally odourless and it was therefore reasoned that thioalcohols, in a similar manner to VFAs, would be released by the apocrine gland as precursor conjugates. The odorous thioalcohol would then be liberated by the action of bacterial lyase enzymes. In similar biological systems, notably wine fermentation, distinctive sulphurous wine bouquets are produced by bacterial catabolism of S-hydroxyalkyl-L-cysteine-conjugates, naturally present in grapes, to their respective thioalcohols (Tominaga *et al.*, 1998). Natsch *et al.* (2004) therefore postulated that S-hydroxyalkyl-L-cysteine conjugates of axillary thioalcohols were the primary thioalcohol malodour precursor molecules released by the apocrine gland, but failed to provide any direct evidence for this. An alternative hypothesis was suggested by Starckenmann *et al.* (2005), who proposed that thioalcohol malodour precursor compounds would originate in the apocrine gland as glutathione (GSH) adducts. This suggestion was again based on knowledge of thioalcohol production during wine fermentation, whereby certain grapes containing GSH-conjugated thioalcohol compounds are sequentially hydrolysed by the host, first removing the glutamate residue and then the glycine residue to yield cysteine-S-conjugates. These conjugated-intermediates are then further hydrolysed by microorganisms during the fermentation process to yield characteristic wine odours, a process typically performed by microbial carbon-sulphur lyase proteins, specifically cystathionine beta-lyase (C-S-  $\beta$ -lyase) (Grant-Preece *et al.*, 2010).

When a biochemical analysis of axillary sweat was undertaken by Starckenmann, rather than identifying cysteine-S-conjugates in sterile secretions the principal thioalcohol-conjugated precursor molecules isolated were S-hydroxyalkyl-L-cysteinylglycine-conjugates.

**Table 1.4.** High-odour impact thioalcohols isolated from hydrolysed human axillary extracts

Molecule	Chemical structure	Reference
<b>3-methyl-3-sulfanylhexan-1-ol</b> <b>(3M3SH)</b>		Natsch <i>et al.</i> , (2004) Hasegawa <i>et al.</i> , (2004)
<b>2-methyl-butan-1-ol</b>		Natsch <i>et al.</i> , (2004) Hasegawa <i>et al.</i> , (2004)
<b>3-pentan-1-ol</b>		Natsch <i>et al.</i> , (2004) Hasegawa <i>et al.</i> , (2004)
<b>3-methyl-hexan-1-ol</b>		Natsch <i>et al.</i> , (2004) Hasegawa <i>et al.</i> , (2004)

In Starckenmann's study, axillary sweat was fractionated using HPLC coupled to gas chromatography (HPLC/GC) and each fraction biotransformed by bacterial isolates to identify distinct zones of axillary odour. One fraction was shown to produce a strong thioalcohol-associated odour, confirming the presence of thioalcohol precursor molecules in the pre-biotransformed fraction. A non-biotransformed portion of this fraction was then analysed using HPLC to identify the precursor molecules present. A distinct peak subsequently identified as S-[1-(2-hydroxyethyl)-1-methylbutyl]-(L)-cysteinylglycine (Cys-Gly-3M3SH) (Fig. 1.2A) was isolated and confirmed as such when synthetic Cys-Gly-3M3SH firmly matched the major peak identified in the isolated axillary sweat fraction. GSH-conjugated 3M3SH in axillary secretions was not present, suggesting that if it did originate as a GSH-adduct, a host-derived peptidase would be required to cleave the glutamate residue from the precursor prior to secretion by the apocrine gland. Additionally, no evidence was forthcoming for the presence of Cys-3M3SH in axillary sweat, signifying that the previous hypothesis by Natsch that cysteine-S-conjugated thioalcohols were the primary thiol precursor molecules released into the axilla, was incorrect. Further support for Cys-Gly-3M3SH as the principal 3M3SH precursor in axillary sweat was provided by Emter & Natsch (2008), who used a liquid chromatography-mass spectrometry (LC-MS) approach to confirm that the dipeptide conjugate was indeed the major thioalcohol precursor molecule. While they did identify the previously suggested Cys-3M3SH molecule, it was present at an 8-fold lower concentration than Cys-Gly-3M3SH and therefore described as a minor component. A later report suggested that female axillary sweat samples contained, on average, 7-fold more Cys-Gly-3M3SH per ml than male sweat and that the total amount of substrate released into the axilla fell in the  $\mu\text{g}\cdot\text{mg L}^{-1}$  range during excessive sweating (Troccaz *et al.*, 2009).

Given the observed differences in the relative abundance of Cys-Gly-3M3SH between individuals, it has been suggested that there could be a genetic basis for malodour precursor secretion in the human axilla. Historically it has been proposed that axillary odour is more pungent in Europeans and Africans than the Asian population (Matsunaga, 1962), which intriguingly also correlates with an altered earwax phenotype. Accordingly, Martin *et al.* (2009) demonstrated that a single nucleotide polymorphism (SNP) in the human *ABCC11* gene which conferred a G583A base substitution resulted in a clear non-malodour phenotype in those individuals possessing the AA genotype. The ABCC11 protein is an ATP-binding cassette (ABC) transporter and apical efflux protein normally active on the surface of secretory cells of apocrine sweat glands. It commonly acts to load malodour precursor compounds, including HMHA-Gln, 3M2H-Gln and Cys-Gly-3M3SH into vesicles for secretion via the apocrine gland into the axilla.

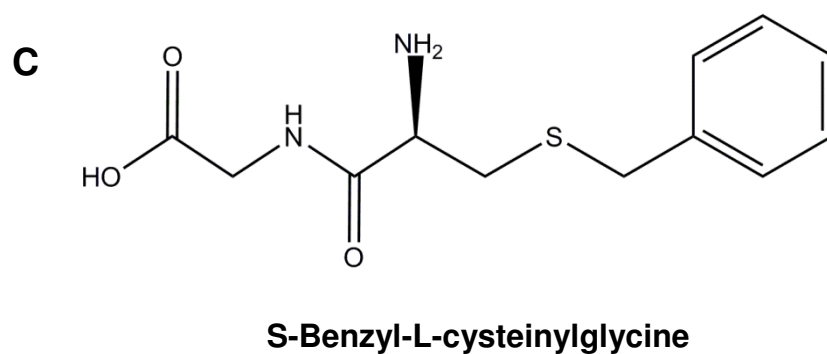
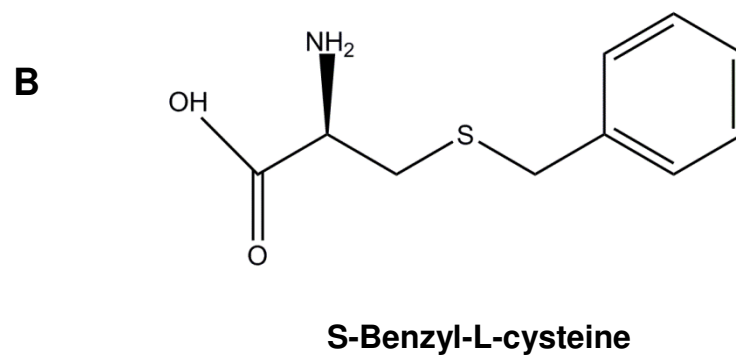
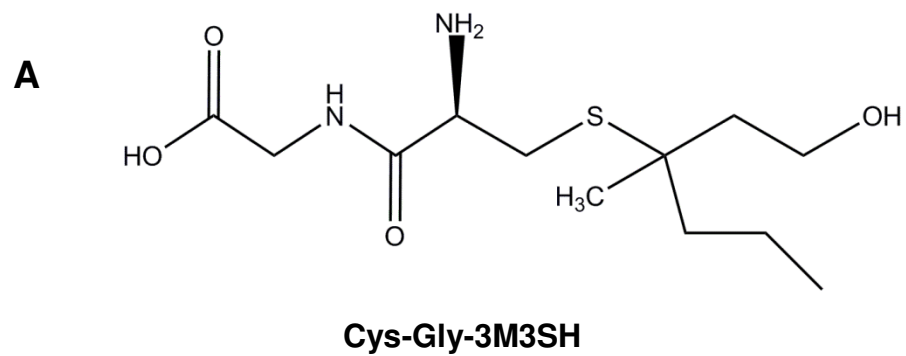


**Figure 1.2.** Chemical structures of model and physiological thioalcohol malodour precursor molecules. **A** – S-Benzyl-L-cysteine, **B** – S-Benzyl-L-cysteinylglycine, **C** – S-[1-(2-hydroxyethyl)-1-methylbutyl]-L-cysteinylglycine (Cys-Gly-3M3SH)

Individuals expressing the mutated form of this protein display a non-malodour phenotype due to malodour precursor compounds failing to reach the axilla. The wild-type *ABCC11* allele is prevalent among Europeans and Africans with the mutated G583A allele widespread mainly in individuals of East Asian descent, particularly Chinese, Korean and Japanese populations. The phenotypic effect of the G583A SNP was verified by Harker *et al.* (2014) who associated a significantly lower axillary odour in individuals homozygous for the mutated gene, which was biochemically connected to an almost complete absence of the malodorants HMHA, 3M2H and 3M3SH. The G583A SNP in *ABCC11* represents the only currently known human SNP responsible for two individual phenotypic characteristics. The selective pressures governing inheritance of this particular gene remain undetermined.

Given the low olfactory threshold for the thioalcohol 3M3SH ( $\text{pg L}^{-1}$ ) and the relative abundance of the Cys-Gly-3M3SH precursor, there is an obvious capacity for thioalcohol production by members of the axillary microbiota and the ability to carry out this process may provide a direct benefit to the bacterium. Beside the waste product 3M3SH, the net molecular gain would be one L-glycine residue and one molecule each of pyruvate and ammonia, giving a favourable reward of both carbon and nitrogen. In order to obtain these products however, the bacterium must also have the molecular capability to carry out the biotransformation process, which is discussed below.

#### **1.4.3.2 Molecular biotransformation of Cys-Gly-3M3SH and other thioalcohol-conjugates by axillary-isolated bacteria**

Analysis of thioalcohol-conjugate biotransformation by axillary bacteria has been largely limited to model malodour precursor substrates. Typically, the model substrate S-Benzyl-L-cysteine (Fig. 1.2B) has been used due to initial, now inaccurate reports, suggesting that S-cysteine conjugates were the principal thioalcohol malodour precursor substrates in the axilla (Natsch *et al.*, 2004). S-Benzyl-L-cysteine is known to be catabolised by many general C-S- $\beta$ -lyase proteins, and therefore this activity was historically deemed to be a sufficient measure of the thioalcohol liberation potential of a bacterial isolate.

James *et al.* (2013) showed that many bacteria were able to biotransform S-Benzyl-L-cysteine into its respective thioalcohol product, benzyl-mercaptan. Activity was strongly associated with corynebacteria, where 67% of strains tested positive compared to only 17% of staphylococci. When broken down to the species level, *C. jeikeium* and more excitingly, *C. tuberculostearicum*, appeared to show the highest activity, hinting that C-S-

$\beta$ -lyase activity was strongest in a highly prevalent axillary species. Subsequently however, activity against this model substrate has been demonstrated for single strains of several *Staphylococcus* spp. including *S. haemolyticus* and *S. hominis*, along with several unspiciated strains of the same genus (Egert *et al.*, 2011).

Despite the prevalence and rigour of this work, studies using model substrates only have limited relevance and the conclusions drawn may not be transferable to the physiological situation, where, in the case of axillary malodour, the most prevalent thioalcohol precursor is Cys-Gly-3M3SH. To date, a detailed analysis of the microbial capacity to biotransform Cys-Gly-3M3SH has not been performed. Of the limited work in this area, early reports consisted of subjective analyses of total axillary secretions that had been biotransformed by several individual species of bacteria. *S. haemolyticus* Ax 4 was determined to produce the most acrid and intense sulphuric odour from these secretions which was subsequently correlated to the production of 3M3SH (Troccaz *et al.*, 2004). The same odour profile was not associated with other axillary isolated bacteria including *C. tuberculostearicum*, *C. minutissimum* or *S. epidermidis*. It was later demonstrated by the same group that *S. haemolyticus* could directly biotransform purified Cys-Gly-3M3SH into 3M3SH, producing a total thioalcohol yield of 75%. *C. xerosis* and *S. epidermidis* both produced a lower 3M3SH yield of 20% and 17% respectively (Starkenmann *et al.*, 2005). Emter & Natsch (2008) later established that bacterial extracts of *Corynebacterium* isolate Ax20 were able to biotransform Cys-Gly-3M3SH relatively efficiently, to a total thioalcohol yield of 65%, whereas extracts of other axillary isolated bacteria such as *C. jeikeium*, *S. epidermidis* and *C. bovis* produced no appreciable levels of 3M3SH.

Two conflicting hypotheses have been proposed regarding the catabolic fate of Cys-Gly-3M3SH. Emter & Natsch (2008) discovered a novel corynebacterial zinc-dependent metallopeptidase in *Corynebacterium* sp. Ax20, subsequently named thiol precursor dipeptidase A (TpdA). TpdA was cloned from this organism, recombinantly expressed in *E. coli* and purified to homogeneity. When TpdA was combined with the C-S-  $\beta$ -lyase from *Corynebacterium* sp. Ax20 (previously implicated in thioalcohol liberation from S-cysteine-conjugates (Grant-Preece *et al.*, 2010)), 3M3SH was liberated from the dipeptide precursor in a sequential manner, i.e. the dipeptidase first cleaved the glycine residue, liberating Cys-3M3SH for catabolism to 3M3SH by C-S-  $\beta$ -lyase. Further characterisation of TpdA showed that the enzyme was active against a wide range of other simple dipeptide molecules along with Cys-Gly-3M3SH and a synthetic, model dipeptide malodour precursor substrate, S-Benzyl-L-cysteinylglycine (Fig. 1.2C), all at physiological concentrations. Interestingly, when the orthologous dipeptidase protein from *C. jeikeium* was cloned, very little activity against Cys-Gly-3M3SH was observed. This suggests that

not all corynebacterial TpdA homologues are adapted to catabolise this substrate. There are no TpdA homologues in staphylococci, which led to the proposal of an alternative Cys-Gly-3M3SH biotransformation hypothesis by Troccaz *et al.* (2008) who had previously shown strong Cys-Gly-3M3SH biotransformation by *S. haemolyticus*. Troccaz suggested that a single enzymatic cleavage step was responsible for liberating 3M3SH from Cys-Gly-3M3SH and postulated that C-S-  $\beta$ -lyase would be the enzyme responsible. Accordingly, SH\_2636, the putative C-S-  $\beta$ -lyase from *S. haemolyticus* was cloned and recombinantly expressed, but showed negligible activity against Cys-Gly-3M3SH despite showing strong activity against its natural substrate, L-cystathionine. Similarly, James *et al.* (2013) cloned and recombinantly expressed the C-S-  $\beta$ -lyase from *C. jeikeium* NCIMB 40928 and demonstrated the enzyme had strong biotransformation activity against the model malodour precursor substrate S-Benzyl-L-cysteine along with a physiologically relevant substrate but minor component of axillary sweat, S-(3-hydroxy-1,2-dimethylpropyl)-L-cysteine. However, activity of this enzyme against the physiologically relevant and abundant malodour substrate Cys-Gly-3M3SH was not assessed.

While Cys-Gly-3M3SH is clearly a major component of axillary sweat, the exact biochemical route of thioalcohol liberation in the axilla remains unclear. Emter & Natsch (2008) showed strong *in vitro* activity of *Corynebacterium* sp. Ax20 and isolated the enzymes responsible, but failed to provide evidence of *in vivo* (whole cell) catabolism. Whereas Starckenmann *et al.* (2005) and Troccaz *et al.* (2009) demonstrated strong *in vivo* activity of *S. haemolyticus* Ax 4 against Cys-Gly-3M3SH, but failed to provide any direct biochemical evidence of the enzymes responsible. Crucially, no study has provided a convincing argument that any of the isolates that are able to biotransform Cys-Gly-3M3SH are present within the axillary microbiota at sufficient cell density to liberate the amount of thioalcohol required to appreciably activate the human olfactory system.

When all studies are taken together, a model for Cys-Gly-3M3SH biotransformation by axillary bacteria can be proposed (Fig. 1.3). It begins with secretion of this molecule by the axillary apocrine gland. There is then a clear requirement for Cys-Gly-3M3SH to be transported into the bacterial cell prior to biotransformation, but this process is not understood in any bacterium. The intracellular catabolism of this molecule is thought to proceed either by a sequential dipeptidase and lyase step as suggested by Emter & Natsch (2008), or directly via a single C-S-  $\beta$ -lyase step as suggested by Troccaz *et al.* (2009).

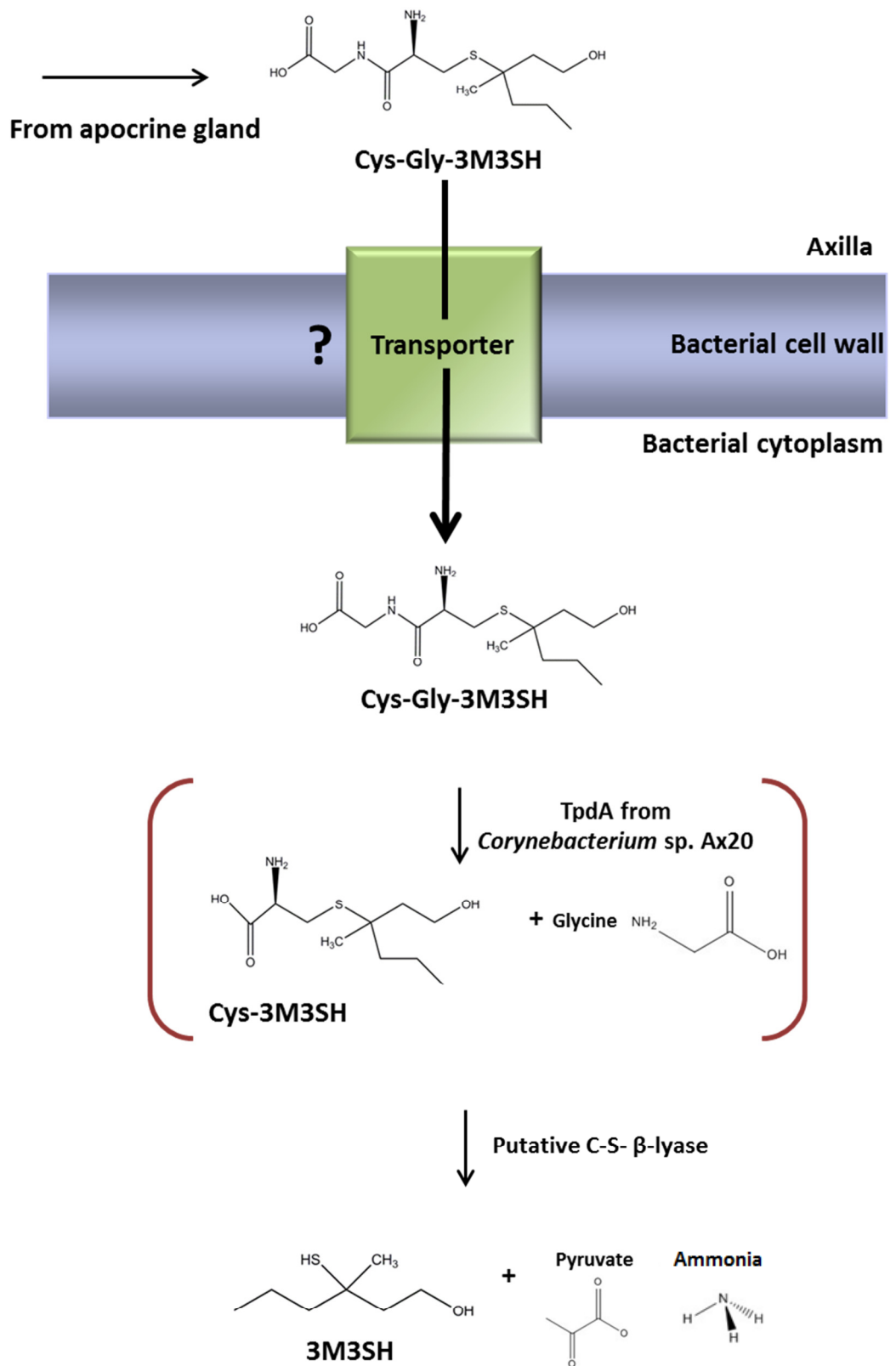


**Figure 1.3.** Putative process of Cys-Gly-3M3SH biotransformation by axillary bacteria.

The complete process generates one molecule each of glycine pyruvate and ammonia per Cys-Gly-3M3SH molecule, which could all be utilised by the bacterium as a source of carbon or nitrogen. The thioalcohol waste product, 3M3SH is presumably transported or diffuses back across the cell wall on to the surface of the axilla where it readily evaporates due to the inherent high volatility of the molecule. Again, the 3M3SH export process is not understood in any bacterium.

In summary, from subjective axillary odour analysis in the early 20<sup>th</sup> century, molecular detection techniques have advanced immeasurably to allow the discovery of malodours compounds and their precursors at pg L<sup>-1</sup> level in the human axilla. It is now commonly accepted that Cys-Gly-3M3SH is one of the most prevalent malodour precursor molecules secreted by the apocrine gland. This molecule is microbially biotransformed to its highly pungent thioalcohol product, 3M3SH which is heavily implicated in characteristic human body odour. The exact microorganisms responsible for this process are not well characterised, although there is a general subjective association between axillary malodour and corynebacteria. There is clearly an important requirement to identify which bacteria are responsible for Cys-Gly-3M3SH biotransformation and understand not only the intracellular biotransformation process but also the mechanism of uptake of the precursor molecule in the relevant bacteria.

## **1.5            *E. coli* as a model organism**

*Escherichia coli* (*E. coli*) is a Gram-negative bacterium belonging to the family Enterobacteriaceae. Environmentally, it thrives in the lower intestine of warm-blooded animals, including humans where it is commonly found as a commensal bacterium of the gut microbiota. *E. coli* is the most widely studied and characterised bacterium and is typically used for laboratory studies and genetic engineering. It can be grown on a wide-variety of complex and minimal media with an approximate doubling time of 20 min when grown aerobically in rich media at 37°C (Tritz, 1987). The strain K-12 was originally isolated in 1922 (Riley *et al.*, 2006) and quickly became the most widely used laboratory strain when the processes of conjugation and transduction were discovered (Lederberg & Tatum, 1946). *E. coli* K-12 was one of the first bacteria to be fully genome sequenced (Blattner *et al.*, 1997) and the library of single, non-essential gene deletion mutants, the Keio Collection (Baba *et al.*, 2006), has greatly aided the comprehensive genetic characterisation of this bacterium.

An alternative, widely-used model organism is *Bacillus subtilis*. Like *E. coli*, *B. subtilis* is genetically and biochemically well-characterised and has a highly annotated genome (Mader *et al.*, 2011). *B. subtilis* is a Gram-positive bacterium and therefore more closely related to the majority of axillary isolates than *E. coli*. It is therefore important to be aware that although *E. coli* will be used in this instance, *B. subtilis* may also be an appropriate model organism in which to study malodour production.

The direct application of *E. coli* as a model organism to study malodour production, specifically the molecular mechanism behind Cys-Gly-3M3SH biotransformation, has not been attempted before. It is clear that transport into the bacterium and enzymatic hydrolysis of the substrate are essential steps leading to 3M3SH liberation and subsequent volatilisation into the atmosphere. Structurally, Cys-Gly-3M3SH is a dipeptide analogue consisting of a cysteinylglycine backbone conjugated to a hydroxyalkyl moiety (Fig. 1.2A). Therefore, uptake is likely to occur via a specific peptide transporter with the ability to transport dipeptide analogues. Thus, a comprehensive review of peptide transport in *E. coli* is provided.

### **1.5.1 Molecular transport in *E. coli***

In general terms, molecular transport is a vital bacterial process, facilitating import of essential molecules into the cytoplasm providing nutrients for the growing cell. Transport proteins are categorised into 5 distinct classes based on the energetics of substrate translocation and further subdivided into superfamilies based on their specific transport mechanism (Busch & Saier, 2002). The most abundant superfamily of bacterial transport proteins are the ATP-binding cassette (ABC) transporters with approximately 5% of the entire genome of *E. coli* encoding for these transport systems (Linton & Higgins, 1998). ABC transporters are found in both prokaryotes and eukaryotes and have a hugely diverse substrate specificity allowing for uptake of large, small, charged, uncharged, hydrophobic and hydrophilic molecules ranging from inorganic ions to complex polysaccharides, all of which need to cross the cellular membrane (Higgins, 2001). ABC transporters belong to the primary active transporter class, as defined by Busch & Saier, and move substrates across the membrane against the concentration gradient, with energy provided by the hydrolysis of ATP.

Structurally, bacterial ABC transporters are multi-subunit proteins usually consisting of two transmembrane domains (TMDs), two adenosine triphosphatase (ATPase) domains and a single substrate-binding protein (SBP) (Higgins *et al.*, 1986), although subtle variations of

this domain architecture are known to exist. In Gram-negative bacteria, the SBP is typically not membrane bound but freely patrols the periplasm, binding to a specific substrate and delivering it to the TMDs. In Gram-positive bacteria which lack a periplasm, the SBP is usually anchored to the outer surface of the cell membrane by attachment to membrane-bound lipids (Perego *et al.*, 1991). This architecture is not true for all ABC transporters from Gram-positive bacteria however, as in the case of the glycine-betaine transporter from *Lactococcus lactis*, the SBP, OpuA, is directly fused to the TMDs (Bouvier *et al.*, 2000). SBPs are highly specific for their cognate substrate(s) and typically bind with high affinity, in some cases at a substrate concentration lower than 1  $\mu\text{M}$  (Madigan & Martinko, 2006). The TMDs are hydrophobic and contain multiple membrane spanning  $\alpha$ -helices which form an internal pore through which the substrate passes. The substrate binding sites within the internal pore determine the substrate specificity of the transporter. Upon binding of the SBP-substrate complex to the TMDs, a conformational change is induced which subsequently initiates the hydrophilic ATPase domains, which are physically associated with the TMDs on the cytoplasmic side of the membrane, to hydrolyse adenosine triphosphate (ATP) to adenosine diphosphate (ADP) and phosphate ( $\text{P}_i$ ) (Higgins, 2001). This process drives substrate translocation across the membrane, resulting in uptake of one molecule of substrate for a total of two ATP molecules hydrolysed (one per ATPase).

Another notable superfamily of transport proteins is the Major Facilitator Superfamily (MFS). These proteins belong to the electrochemical or proton driven transporters, a class also referred to as secondary transporters and are the largest known class of secondary transporters (Pao *et al.*, 1998). Like ABC transporters, MFS transporters are ubiquitous in all classifications of living organisms (Pao *et al.*, 1998). Specifically within the genomes of microorganisms, the combined number of MFS and ABC transporters account for almost 50% of all known solute transporters (Paulsen & Skurray, 1994). Structurally, they consist of a single membrane-imbedded polypeptide that utilises an electrochemical gradient such as  $\text{H}^+$  or  $\text{Na}^+$  to drive substrate translocation across the membrane against its concentration gradient (Saier, 2000a). MFS transporters can function to translocate a substrate into or out of the cell depending on the ionic concentration gradient (Saier, 2000b), but individual transporters typically display directionality. A specific example of a well characterised bacterial MFS transporter is the lactose permease of *E. coli*, LacY, which co-transport an extracellular proton with lactose to facilitate substrate import into the cytoplasm of the cell (Abramson *et al.*, 2003).

## 1.5.2 Peptide transport in *E. coli*

Peptides are molecules consisting of amino acid monomers connected by peptide (amide) bonds. The smallest peptide is a dipeptide, consisting of two amide-bonded amino acids. Peptides can be distinguished from proteins based on the number of amino acid residues that form the molecule. A molecule containing 2-50 amino acids is said to be a peptide, whereas a molecule containing >50 amino acids is typically referred to as a protein (Sato *et al.*, 2006). Peptide transport occurs in all organisms from microbes to man and is a vital route to supply amino acids for nutritional purposes. Uptake of peptides is an energetically favourable process as multiple amino acids can be transported at the same time without the energy cost of transporting them individually. Such amino acids can then fulfil the nutritional requirements of the cell or be used as building blocks to make proteins. There is also growing evidence that peptides are involved in intracellular signalling and metabolic adaptation (Detmers *et al.*, 2001).

Peptide transport in *E. coli* is relatively well characterised, with the two classes of transporters described in section 1.5.1 primarily involved uptake of these molecules. High affinity peptide transport is primarily achieved through two ABC peptide transporters; the dipeptide (Dpp) and oligopeptide (Opp) permeases. Lower affinity, high capacity peptide transport is achieved by MFS secondary transporter of the PTR-family, as discussed below. A graphical representation of these specific classes of *E. coli* peptide transporters is shown in Fig. 1.4.

### 1.5.2.1 The ABC peptide transporters of *E. coli*

The Dpp dipeptide transporter is encoded by five individual genes, *dppABCDF* which are arranged in an operon. *dppA* encodes the SBP, *dppB* and *dppC* encode the TMDs and *dppD* and *dppE* encode the ATPase domains (Fig. 1.4). The X-ray crystal structure of the SBP has been solved both unbound (Dunten *et al.*, 1993) and with Gly-Leu bound in the substrate binding pocket (Dunten & Mowbray, 1995), revealing that the SBP recognises the peptide backbone allowing for accommodation of a structurally diverse range of side chains within the binding pocket. Multiple studies have reported individual substrate specificities for Dpp, including Olson *et al.* (1991) who demonstrated that a proline auxotrophic *dppA* mutant was unable to utilise Pro-Gly as the sole source of proline and Payne *et al.* (1984), who showed that a *dpp* mutant and leucine auxotroph was unable to utilise several leucine-containing dipeptides as the sole source of leucine. De Felice *et al.* (1973) established that Gly-Val, Leu-Val, Val-Leu and Gly-Gly were also substrates for

Dpp. The substrate specificity of *E. coli* DppA was comprehensively substantiated by Smith *et al.* (1999) who concluded that the protein was promiscuous in dipeptide specificity and could also transport a limited range of L-Ala-containing tripeptides, although dipeptides were clearly the preferred substrate. Specific structural requirements of a Dpp-transported peptide are the presence of an unsubstituted  $\alpha$ -amino group Payne (1971) and all residues to be in their L-isoform (Smith *et al.*, 1999).

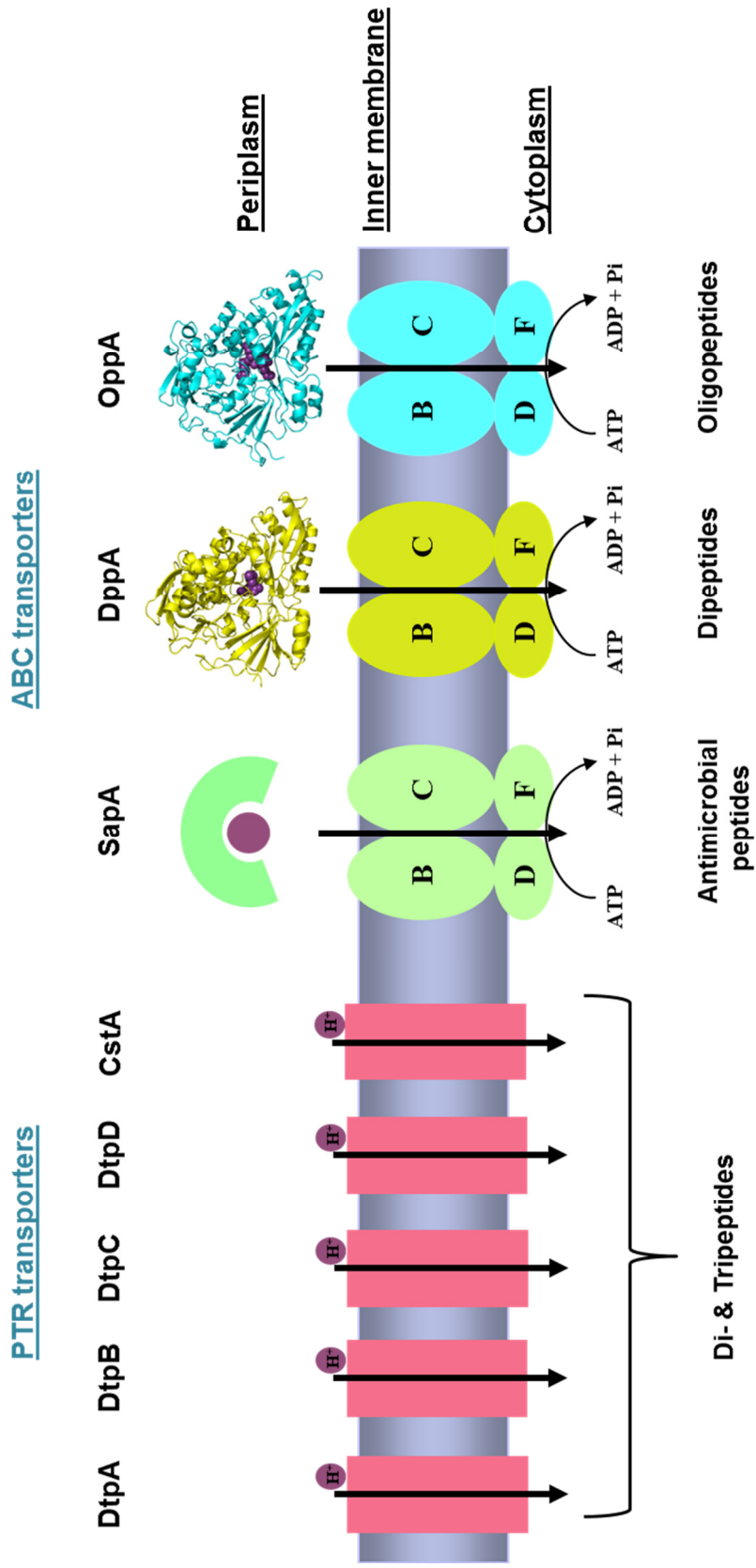


**Figure 1.4.** The peptide transporter repertoire of *E. coli*. Adapted from Maqbool *et al.* (2011)

The genomic layout of the *opp* oligopeptide transporter is identical to *dpp*, with five individual genes, *oppA oppBC* and *oppDF* encoding the SBP, two TMDs and two ATPase domains, respectively (Fig. 1.4).

The Opp system of *E. coli* has not been comprehensively analysed but the orthologous system in *Salmonella enterica* subspecies Typhimurium (*S. typhimurium*) has been extensively studied. The crystal structure of *S. typhimurium* OppA has been solved with Lys-Lys-Lys bound in the substrate binding pocket (Glover *et al.*, 1995). This protein was able to bind peptides ranging from two to five amino acids in length with a structurally diverse range of side chains. Using Ala-Phe-[<sup>3</sup>H]Gly as a reporter substrate Guyer *et al.* (1986) demonstrated that OppA preferentially binds tripeptides, with sequentially decreasing affinity for tetra- and pentapeptides and no affinity for single amino acids or the limited range of dipeptides tested. It was subsequently shown that all five *opp* genes are required for Opp function, with insertion mutations in individual genes leading to disruption of peptide transport (Hiles *et al.*, 1987). Similar to DppA, *E. coli* OppA has little side chain preference with a wide range of glycine-containing tripeptides sufficient to alleviate the effects of the toxic tripeptide triornithine (Naider & Becker, 1975).

The sensitive to antimicrobial peptide (Sap) ABC transporter is an additional *E. coli* peptide transporter sharing an identical gene layout to *opp* and *dpp*. *E. coli* Sap remains uncharacterised but the orthologous multigene operon in *S. typhimurium* has been partially studied. In this organism, Sap is required for resistance to the antimicrobial peptides melittin and protamine, acting as an important virulence factor (Parra-Lopez *et al.*, 1993). The Sap transport system allows these antimicrobials to be transported directly into the cytoplasm of the bacterium where they can be rapidly degraded by intracellular peptidases, rather than localise on the inner membrane where they act to disrupt the structural integrity of the cell.

In the 1970s and 1980s, much attention was focussed on creating novel antimicrobial compounds that would be rapidly and efficiently transported into the bacterial cell. It was proposed that by attaching an antimicrobial compound to a peptide, the drug could be effectively smuggled into the bacterium through the high affinity ABC peptide transporters Dpp and Opp, in a Trojan horse-like manner. A proof-of-principle study was conducted by Ames *et al.* (1973) who demonstrated that histidinol-phosphate ester (HOLP) could be fused to Gly-Gly to create HOLP-Gly-Gly, which was transported into *S. typhimurium* by the Opp system. Similarly, a series of cytotoxic compounds attached to peptides of varying length were also transported by Opp, with the strongest level of transport

observed for tripeptide-conjugated antimicrobials. A similar study was successful in *E. coli* where it was demonstrated that two tripeptide-based antimicrobials were transported by Opp (Diddens *et al.*, 1976). The natural tripeptide antibiotic, phaseolotoxin, is also transported by Opp in both *E. coli* and *S. typhimurium* (Staskawicz & Panopoulos, 1980), but publications on this novel antimicrobial delivery route quickly ceased in subsequent decades, possibly due to difficulties in bringing these compounds to market.

### 1.5.2.2 The MFS peptide transporters of *E. coli*

The MFS peptide transporters of *E. coli* belong to the proton-dependant oligopeptide transporter (POT) classification, which was originally described by Paulsen & Skurray (1994). The POT family was later renamed the Peptide Transporter (PTR) family (Steiner *et al.*, 1995), as it was unclear whether all members of this group used co-transport of a proton to drive substrate translocation across the membrane. However, both POT and PTR nomenclature have been used interchangeably in subsequent literature and PTR family transporters are also more generally referred to as peptide symporters. PTR family proteins are characterised by the presence of a PTR2 (COG3104) domain. One of the first bacterial PTR family peptide transporters to be biochemically characterised was DtpT from *Lactococcus lactis* (Hagting *et al.*, 1994, Hagting *et al.*, 1997) but biochemical characterisation of the four *E. coli* PTR genes encoding the single subunit transporters DtpA, DtpB, DtpC and DtpD (Fig. 1.4) did not begin until the last decade.

DtpA (historically called YdgR and more recently TppB), was originally characterised in *S. typhimurium* (Gibson *et al.*, 1984). Previously, Barak & Gilbarg (1975) had isolated an *E. coli oppABCDF* mutant that was resistant to a toxic tripeptide which normally inhibits growth of this strain, suggesting uptake of the inhibitor by an alternative tripeptide transporter, now strongly hypothesised to be *dtpA*. They demonstrated that Thr-Thr-Thr can support the growth of a threonine auxotroph even in an *opp* mutant background, which can be antagonised by Leu-Leu-Leu and Met-Met-Met, suggesting that these three tripeptides are substrates for DtpA. Similarly, other L-Met-containing tripeptides were shown to support methionine auxotrophy in an *opp* mutant background (Naider & Becker, 1975). There is also indirect evidence that modified tripeptide antimicrobials are transported by DtpA, as an *opp* mutant is resistant to the toxic tripeptide analogue Ala-Ala-NH-Ala which contains a modified peptide linkage (Morley *et al.*, 1983). The dipeptide analogue alafosfalin is also transported by DtpA (Smith & Payne, 1990). Of all four *E. coli* PTR family transporters, DtpA shares the strongest sequence similarity (24%) with the human PTR protein PepT1, suggesting partial functional similarity. PepT1 is found at the

brush border membrane of intestinal tissue and has an extremely broad ranging substrate specificity, which has been empirically validated and collated by Biegel *et al.* (2006) and plays an important role in general peptide uptake from the diet. The substrate specificity of DtpA has since been characterised in detail using an *E. coli* strain overexpressing the transporter. Using radiolabelled glycylsarcosine as a reporter substrate, Harder *et al.* (2008) observed strong specificity for the peptides Ala-Ala (99%), Ala-Ala-Ala (99%), D-Ala-L-Ala (95%), Lys-Gly (98%), Gly-Asp (74%) along with the peptide-based antimicrobials Cephradine (71%), Cefalexin (65%) and Cefadroxil (81%). Weak uptake of alanine and Ala-Ala-Ala-Ala was observed, confirming that DtpA preferentially transports di- and tripeptides. Weitz *et al.* (2007) argue that DtpA shows a preference towards N-terminally positively charged peptides such as Lys-Gly and Lys-Ala rather than C-terminally positively charged peptides such as Gly-Lys. Overall, the substrate range of DtpA is relatively diverse, with simple di- and tripeptides being transported along with certain D-isoform peptides, some peptidomimetic compounds and other structural peptide analogues.

DtpB of *E. coli* (previously named YhiP) is the least characterised member of the PTR family of peptide transporters, with the only single in-depth study carried out by Harder *et al.* (2008). Using an identical method to that used to characterise the substrate specificity of DtpA, radiolabelled glycylsarcosine was used as a reporter molecule to assess the substrate specificity of DtpB. Strong affinity was observed for Ala-Ala (83%), Ala-Ala-Ala (83%), Gly-Asp (83%) and Lys-Gly (43%), but weaker affinity was observed for the majority of other L- and D-isoform peptides, peptide analogues and peptidomimetic compounds, suggesting that DtpB has a more limited substrate range than DtpA. From the study it was concluded that DtpB has a C-terminal negative charge preference.

DtpC (previously named YjdL) was first characterised by Ernst *et al.* (2009) who cloned and overexpressed the *ntpC* gene and used a fluorescent reporter molecule to assess substrate specificity of the transporter in a whole cell-based system. It was observed that DtpC could transport Ala-Ala but not Ala-Ala-Ala or Ala-Ala-Ala-Ala even at 500-fold excess. This was later supported by Prabhala *et al.* (2013). A similar phenomenon was seen with other tripeptides leading to the conclusion that DtpC has a preference for transporting dipeptides. Uptake of D-Ala containing dipeptides, the negatively charged dipeptides Ala-Asp and Asp-Ala and a dipeptide with a positively charged N-terminus, Lys-Ala, was not observed, but Ala-Lys, with a positively charged C-terminus, was transported. A general consensus has been reached which suggests that dipeptides possessing a positively charged C-terminus are excellent substrates for DtpC whereas negatively charged dipeptides are not transported.

A similar series of experiments have been carried out to understand the biochemical basis for peptide transport by DtpD (previously named YbgH), although a full analysis of the substrate specificity of this transport has yet to be carried out. Casagrande *et al.* (2009) concluded that DtpD has a definite preference for C-terminally charged dipeptides such as Ala-Lys and if the charge is reversed, for example in Lys-Ala then the dipeptide will not be transported by this protein. Jensen *et al.* (2012) argued that, like DtpC, DtpD has a preference for dipeptides rather than tripeptides. Jensen also used site-directed mutagenesis to demonstrate that Glu388, an invariant residue in all PTR transporters, is essential to facilitate peptide binding to DtpD, as the E388Q form of the protein could no longer bind Ala-Lys. A summary of the proposed properties of DtpA, DtpB, DtpC and DtpD is provided in Table 1.5.

An additional secondary peptide transporter is encoded in the genome of *E. coli*, the carbon starvation gene, *cstA*. *cstA* encodes a peptide transporter which is part of the CsrA regulon and expressed under carbon-limited conditions (Dubey *et al.*, 2003). When grown in peptide-containing media, *cstA oppABCDF* double mutants were shown to have a slower growth rate than wild-type or either single mutant strain alone (Schultz & Matin, 1991), suggesting a cumulative effect of mutating both the high affinity ABC oligopeptide transporter (*oppABCDF*) and *cstA*. This suggests that CstA and Opp have overlapping substrate specificities and that CstA, like Opp, is able to transport a diverse range of oligopeptides. Unlike the Dtp transporters of *E. coli*, CstA is not a member of the PTR family, but part of its own superfamily, the CstA superfamily, of which full characterisation has yet to be carried out.

### 1.5.3 Cystathionine- $\beta$ -lyases of *E. coli*

As discussed earlier (see section 1.4.3.2), it has been proposed that C-S-  $\beta$ -lyase, and in particular cystathionine  $\beta$ -lyase activity is required to biotransform conjugated thioalcohol malodour precursors. Therefore, if *E. coli* is to be used as a model system to study this process, an understanding of the C-S-  $\beta$ -lyase proteins of this organism is required. *E. coli* possesses two annotated and well characterised C-S-  $\beta$ -lyase proteins, MalY and MetC. MalY is a bi-functional protein with PLP-dependent aminotransferase activity and the ability to act as a negative regulator of the maltose regulon (Clausen *et al.*, 2000). MalY has also been shown to catalyse carbon-sulphur bond cleavage of cystathionine (Zdych *et al.*, 1995). These two functionalities are independent of each other; C-S-  $\beta$ -lyase enzyme activity is not required for the protein to fulfil its regulatory role.

**Table 1.5.** Properties of PTR-family secondary peptide transporters of *E. coli*

Transporter	Peptide transport properties	Strong substrates (empirically verified)	References
<b>DtpA</b>	<p>Preference towards peptide with an N-terminal positive charge such as Lys-Gly and Lys-Ala.</p> <p>Transports a diverse range of di- and tripeptides and also some D-isoform peptides, peptidomimetic compounds and other structural peptide analogues.</p>	<p>Ala-Ala Ala-Ala-Ala D-Ala-L-Ala Lys-Ala Lys-Gly Gly-Asp Gly-Gln Cefadroxil Alafosfalin</p>	<p>Weitz &amp; Harder (2007)</p> <p>Harder <i>et al.</i> (2008)</p>
<b>DtpB</b>	<p>Preference towards dipeptides with a C-terminal negative charge.</p> <p>More limited substrate specificity compared to DtpA, no evidence for tripeptide transport.</p>	<p>Ala-Ala Ala-Ala-Ala Gly-Asp</p>	<p>Harder <i>et al.</i> (2008)</p>
<b>DtpC</b>	<p>Preference towards dipeptides possessing a positively charged C-terminus.</p> <p>Does not transport negatively charged dipeptides.</p> <p>No evidence for tripeptide transport.</p>	<p>Ala-Lys Ala-Gln Tyr-Ala Lys-Ala</p>	<p>Ernst <i>et al.</i> (2009)</p> <p>Prabhala <i>et al.</i> (2013)</p> <p>Jensen <i>et al.</i> (2012)</p>
<b>DtpD</b>	<p>Preference for C-terminally charged dipeptides</p> <p>Does not transport N-terminally charged dipeptides</p> <p>No evidence for tripeptide transport</p>	<p>Ala-Lys Lys-Lys Gly-Lys Gly-Arg</p>	<p>Jensen <i>et al.</i> (2012)</p> <p>Casagrande <i>et al.</i> (2009)</p>

The other annotated cystathionine  $\beta$ -lyase of *E. coli* is MetC, which is also a PLP-dependent aminotransferase playing an important biological role in methionine biosynthesis but also catalysing carbon-sulphur bond cleavage of cystathionine via C-S- $\beta$ -lyase activity (Awano *et al.*, 2003). The MalY/MetC classification of C-S- $\beta$ -lyases originated in *E. coli* and newly characterised C-S- $\beta$ -lyases proteins are now usually assigned into either the MalY or MetC subgroup (James *et al.*, 2013).

## **1.6 Aims of this study**

The physiologically relevant bacteria (at both genus and species level) involved in biotransformation of the conjugated thioalcohol malodour precursor Cys-Gly-3M3SH will be characterised using a library of axillary isolated bacteria. This will aid in identifying the most active Cys-Gly-3M3SH biotransforming species and strains within the human axilla.

Peptide transporter deficient and C-S- $\beta$ -lyase deficient strains of *E. coli* will be created and fully characterised in order to assess the suitability of *E. coli* as a model organism to study thioalcohol precursor biotransformation.

Putative malodour precursor transporters and catabolic enzymes will be identified in the relevant organisms via *in silico* analysis. These genes will then be cloned and expressed in a strain of *E. coli* redundant for thioalcohol malodour precursor biotransformation in order to identify the molecular and biochemical basis behind this process within axillary-isolated bacteria.

# **Chapter 2**

# **Materials and methods**

## **2.1 Chemicals and strains**

### **2.1.1 Chemicals**

All chemicals were reagent grade unless otherwise specified and purchased from Sigma Aldrich (Sigma) unless otherwise stated.

### **2.1.2 Antibiotics**

Antibiotics were either from Melford (ampicillin sodium salt) or Gibco (kanamycin sulfate). All stock concentrations of antibiotics were dissolved in distilled water (dH<sub>2</sub>O) at 1000 X concentration (ampicillin 100 mg/ml and kanamycin 50 mg/ml), filter sterilised using a 0.22 µm syringe filter and stored at 4°C for no longer than 1 week (ampicillin) or 4 weeks (kanamycin). The working concentrations were 100 µg/ml for ampicillin and 50 µg/ml for kanamycin.

### **2.1.3 Malodour precursor substrate molecules**

2.67 mM stock solutions of the model malodour precursor molecules S-Benzyl-L-cysteine (Sigma) and S-Benzyl-L-cysteinylglycine (Bachem, Switzerland) were prepared in either 1 X M9 salt buffer or Minimal Recovery Medium (MRM), depending on the particular assay. The physiological malodour precursor molecule Cys-Gly-3M3SH was chemically synthesised by Peakdale Molecular and routinely prepared at a stock concentration of 2.67 mM in 1 X M9 salt buffer. All malodour precursor molecules were filter sterilised using a 0.22 µm syringe filter and stored at 4°C until use.

### **2.1.4 Bacterial strains and plasmids**

All species and strains of bacteria used in this work are listed in Tables 2.1, 2.2 and 2.3. Table 2.4 details all plasmids used in this work.

**Table 2.1.** Strains of *E. coli* used in this work

Strain	Genotype	Source or Reference
<b><i>Escherichia coli</i></b>		
BW25113	F-, $\Delta(\text{araD-araB})567$ , $\Delta\text{lacZ4787}>::\text{rrnB-3}$ , lambda-, rph-1, $\Delta(\text{rhaD-rhaB})568$ , <i>hsdR514</i>	Baba <i>et al.</i> (2006)
JW1237	BW25113 <i>oppC::Kan</i>	Baba <i>et al.</i> (2006)
JW3511	BW25113 <i>dppC::Kan</i>	Baba <i>et al.</i> (2006)
JW1626	BW25113 <i>dtpA::Kan</i>	Baba <i>et al.</i> (2006)
JW3463	BW25113 <i>dtpB::Kan</i>	Baba <i>et al.</i> (2006)
JW4091	BW25113 <i>dtpC::Kan</i>	Baba <i>et al.</i> (2006)
JW0699	BW25113 <i>dtpD::Kan</i>	Baba <i>et al.</i> (2006)
JW3686	BW25113 <i>tnaA::Kan</i>	Baba <i>et al.</i> (2006)
JW2975	BW25113 <i>metC::Kan</i>	Baba <i>et al.</i> (2006)
JW1614	BW25113 <i>malY::Kan</i>	Baba <i>et al.</i> (2006)
JW1285	BW25113 <i>sapC::Kan</i>	Baba <i>et al.</i> (2006)
JW0590	BW25113 <i>cstA::Kan</i>	Baba <i>et al.</i> (2006)
$\Delta\text{oppC}$	BW25113 $\Delta\text{oppC}$	This work
$\Delta\text{dppC}$	BW25113 $\Delta\text{dppC}$	This work
$\Delta\text{dtpA}$	BW25113 $\Delta\text{dtpA}$	This work
$\Delta\text{dtpB}$	BW25113 $\Delta\text{dtpB}$	This work
$\Delta\text{dtpC}$	BW25113 $\Delta\text{dtpC}$	This work
$\Delta\text{dtpD}$	BW25113 $\Delta\text{dtpD}$	This work
$\Delta\text{tnaA}$	BW25113 $\Delta\text{tnaA}$	This work
$\Delta\text{DB1}$	BW25113 $\Delta\text{oppC} \Delta\text{dppC}$	This work
$\Delta\text{DB5}$	BW25113 $\Delta\text{dtpA} \Delta\text{dtpB} \Delta\text{dtpC} \Delta\text{dtpD}$	This work

**Table 2.2.** Strains of corynebacteria used in this work

Strain	Genotype	Source or Reference
<b><i>Corynebacterium</i> spp.</b>		
<i>Corynebacterium</i> sp. Ax20	Wild-type	Natsch <i>et al.</i> (2003)
<i>C. afermentans</i> G434	Wild-type	Unilever library
<i>C. afermentans</i> G441	Wild-type	Unilever library
<i>C. amycolatum</i> G500	Wild-type	Unilever library
<i>C. amycolatum</i> G501	Wild-type	Unilever library
<i>C. amycolatum</i> G502	Wild-type	Unilever library
<i>C. amycolatum</i> G503	Wild-type	Unilever library
<i>C. amycolatum</i> G511	Wild-type	Unilever library
<i>C. amycolatum</i> G515	Wild-type	Unilever library
<i>C. amycolatum</i> G516	Wild-type	Unilever library
<i>C. amycolatum</i> G517	Wild-type	Unilever library
<i>C. appendicis</i> G465	Wild-type	Unilever library
<i>C. glutamicum</i> NCIMB 10025	Wild-type	Kalinowski <i>et al.</i> (2003)
<i>C. jeikeium</i> K411	Wild-type	Tauch <i>et al.</i> (2005)
<i>C. mucifaciens</i> G435	Wild-type	Unilever library
<i>C. mucifaciens</i> G462	Wild-type	Unilever library
<i>C. mucifaciens</i> G463	Wild-type	Unilever library
<i>C. pseudogenitalium</i> ATCC 33035	Wild-type	Furness <i>et al.</i> (1979)
<i>C. pseudotuberculosis</i> NCTC 3450	Wild-type	Cummins (1962)
<i>C. striatum</i> NCTC 764	Wild-type	Pitcher (1983)
<i>C. suicordis</i> G460	Wild-type	Unilever library
<i>C. tuberculostearicum</i> ATCC 35692	Wild-type	Feurer <i>et al.</i> (2004)
<i>C. tuberculostearicum</i> G438	Wild-type	Unilever library
<i>C. tuberculostearicum</i> G439	Wild-type	Unilever library
<i>C. tuberculostearicum</i> G440	Wild-type	Unilever library
<i>C. tuberculostearicum</i> G459	Wild-type	Unilever library
<i>C. tuberculostearicum</i> G464	Wild-type	Unilever library
<i>C. tuberculostearicum</i> G484	Wild-type	Unilever library
<i>C. tuberculostearicum</i> G485	Wild-type	Unilever library
<i>C. tuberculostearicum</i> A06	Wild-type	Unilever library
<i>C. ulcerans</i> NCTC 7910	Wild-type	Riegel <i>et al.</i> (1995)

**Table 2.3.** Strains of staphylococci used in this work

Strain	Genotype	Source or Reference
<b><i>Staphylococcus</i> spp.</b>		
<i>S. capitis/caprae</i> C07	Wild-type	Unilever library
<i>S. capitis/caprae</i> C15	Wild-type	Unilever library
<i>S. cohnii</i> A01	Wild-type	Unilever library
<i>S. cohnii</i> W17	Wild-type	Unilever library
<i>S. epidermidis</i> B01	Wild-type	Unilever library
<i>S. epidermidis</i> G427	Wild-type	Unilever library
<i>S. epidermidis</i> G428	Wild-type	Unilever library
<i>S. epidermidis</i> G429	Wild-type	Unilever library
<i>S. epidermidis</i> G430	Wild-type	Unilever library
<i>S. epidermidis</i> G467	Wild-type	Unilever library
<i>S. epidermidis</i> G468	Wild-type	Unilever library
<i>S. epidermidis</i> G469	Wild-type	Unilever library
<i>S. epidermidis</i> G470	Wild-type	Unilever library
<i>S. epidermidis</i> G471	Wild-type	Unilever library
<i>S. epidermidis</i> G473	Wild-type	Unilever library
<i>S. epidermidis</i> G474	Wild-type	Unilever library
<i>S. epidermidis</i> G475	Wild-type	Unilever library
<i>S. epidermidis</i> G476	Wild-type	Unilever library
<i>S. haemolyticus</i> G431	Wild-type	Unilever library
<i>S. haemolyticus</i> W19	Wild-type	Unilever library
<i>S. epidermidis</i> G467	Wild-type	Unilever library
<i>S. hominis</i> B10	Wild-type	Kelly (2013)
<i>S. hominis</i> G20	Wild-type	Unilever library
<i>S. hominis</i> I4	Wild-type	Kelly (2013)
<i>S. hominis</i> J6	Wild-type	Kelly (2013)
<i>S. hominis</i> J11	Wild-type	Kelly (2013)
<i>S. hominis</i> J23	Wild-type	Kelly (2013)
<i>S. hominis</i> J27	Wild-type	Kelly (2013)
<i>S. lugdunensis</i> G310	Wild-type	Unilever library
<i>S. saprophyticus</i> B13	Wild-type	Unilever library
<i>S. saprophyticus</i> C06C	Wild-type	Unilever library
<i>S. saprophyticus</i> W14	Wild-type	Unilever library

**Table 2.4.** Plasmids used in this work

<b>Plasmid</b>	<b>Plasmid backbone</b>	<b>Size (Kb)</b>	<b>Antibiotic resistance</b>	<b>Source or reference</b>
pCP20	N/A	9.40	Amp/Cam	Cherepanov & Wackernagel (1995)
pKD46	N/A	6.33	Amp	Datsenko & Wanner (2000)
pBADcLIC2005	N/A	4.14	Amp	Geertsma & Poolman (2007)
pDtpA	pBADcLIC2005	5.64	Amp	This work
pDtpB	pBADcLIC2005	5.61	Amp	This work
pDtpC	pBADcLIC2005	5.60	Amp	This work
pDtpD	pBADcLIC2005	5.62	Amp	This work
pSH0415	pBADcLIC2005	5.33	Amp	This work
pSH1446	pBADcLIC2005	5.65	Amp	This work
pSH2140	pBADcLIC2005	5.32	Amp	This work

## 2.1.5 Oligonucleotide primers

All oligonucleotide primers used in this study are listed in Table 2.5. All primers were supplied by either Eurofins MWG Operon or Sigma. The supplied material was reconstituted in sterile dH<sub>2</sub>O to a stock concentration of 10 µM and stored at -20°C.

**Table 2.5.** Oligonucleotide primers used in this work

Primer name	Sequence (5' – 3')
dppC F	TGCTAATCGACACCGC
dppC R	TGGCGATCATCACGCG
oppC F	GCTGGCGTTATTGCCG
oppC R	CGCATCGAGCATCCGC
dtpA F	GACCTACAAAACATTACACTGGC
dtpA R	TAACGGCAAAGTAATCGTCACCG
dtpB F	AGCGTAAACACCTTATCTGGC
dtpB R	TGATATCTATGCAGGTACGCC
dtpC F	GTGTGAAATCGGCGCTCACTATCCG
dtpC R	TAGCGTAGATAAAGAGACAGATCGG
dtpD F	CTCGCCAGTTCGTGATAGCC
dtpD R	GCGTGAACGCCTTATCCAGCC
tnaA F	TTACTTGTTTTAGTAAATGATGG
tnaA R	TCAGCTTGATCAGTGATGATGCC
dtpA pBADcLIC-F	ATGGGTGGTGGATTTGCTGTGTCCACTGCAAACC
dtpA pBADcLIC-R	TTGGAAGTATAAATTTCCGCTACGGCTGCTTTC
dtpB pBADcLIC-F	ATGGGTGGTGGATTTGCTATGAATACAACAACACCCATGGGG
dtpB pBADcLIC-R	TTGGAAGTATAAATTTTCATGGCTTTCCGGCGTCG
dtpC pBADcLIC-F	ATGGGTGGTGGATTTGCTATGAAAACACCCTCACAGCC
dtpC pBADcLIC-R	TTGGAAGTATAAATTTTCATCGTTGCTCTCCTGTATC
dtpD pBADcLIC-F	ATGGGTGGTGGATTTGCTATGAATAAACACGCATCACAGCCG
dtpD pBADcLIC-R	TTGGAAGTATAAATTTTCAGACTCCAGCGCCAGC
0415 pBADcLIC-F	ATGGGTGGTGGATTTGCTATGAAGAAGCACAGTAAAGATTAC
0415 pBADcLIC-R	TTGGAAGTATAAATTTTCATTTTTAATTGCTGTTTTAAAATATAAACC
1446 pBADcLIC-F	ATGGGTGGTGGATTTGCTATGGCAACAATAACTCCCAT
1446 pBADcLIC-R	TTGGAAGTATAAATTTTCGTGAATACCTTTCATAGCTTTTCGT
2140 pBADcLIC-F	ATGGGTGGTGGATTTGCTATGAGCTTATCTAAAGAAAC
2140 pBADcLIC-R	TTGGAAGTATAAATTTTCGCTACTAAAACGTTGTTCTTC

## 2.1.6 Bacterial growth media and reaction buffers

Liquid and solid media were prepared by dissolving appropriate quantities of powdered constituents in dH<sub>2</sub>O and autoclaving at 121°C, 15 Psi for 15 min. For agar plates, approximately 20 ml of molten agar-containing medium was poured into each Petri dish and allowed to solidify at room temperature. Plates were subsequently dried in a class II microbiology safety cabinet and stored at 4°C until use.

**Luria-Bertani (LB) medium** contained (per litre dH<sub>2</sub>O): 10 g tryptone (Melford), 5 g yeast extract (ForMedium) and 10 g NaCl (Fisher Scientific). For LB agar plates, agar technical number 3 (Oxoid) was added to a final concentration of 1.5%. The pH was adjusted to 7.0 by the addition of NaOH.

**Super Optimal Broth with Catabolite Repression (SOC) medium** contained (per litre dH<sub>2</sub>O): 20 g tryptone, 5 g yeast extract, 0.584 g NaCl, 0.186 g KCl (Fisher Scientific) and 0.024 g MgSO<sub>4</sub> (Fisher Scientific). The pH was adjusted to 7.5 by the addition of NaOH. D-glucose (Fisher Scientific) was dissolved in dH<sub>2</sub>O to a stock concentration of 20%, filter sterilised through a 0.22 µm syringe filter and stored at room temperature. D-glucose was supplemented to the autoclaved SOC medium at a concentration of 20 mM.

**Tryptone Broth** contained (per litre dH<sub>2</sub>O): 10 g tryptone and 10 g NaCl. The pH was adjusted to 7.0 by the addition of NaOH.

**Yeast Extract Broth** contained (per litre dH<sub>2</sub>O): 10 g yeast extract and 10 g NaCl. The pH was adjusted to 7.0 by the addition of NaOH.

**Tryptone Soy Broth with Tween (TSBT)** contained (per litre dH<sub>2</sub>O): 30 g tryptone soy broth (Fluka), 10 g yeast extract and 1 g Tween 80 (Fisher Scientific). The pH was adjusted to 7.0 by the addition of NaOH. For TSBT agar plates (TSAT), agar technical number 3 (Oxoid) was added to a final concentration of 1.5%.

**M9 glucose minimal medium** contained (per litre dH<sub>2</sub>O): 6 g Na<sub>2</sub>HPO<sub>4</sub>, 3 g KH<sub>2</sub>PO<sub>4</sub> (Fisher Scientific), 1 g NH<sub>4</sub>Cl (Fisher Scientific) and 0.5 g NaCl. Filter-sterilised D-glucose was supplemented at 20 mM following autoclaving of the basal M9 medium. The pH was adjusted to 7.0 by the addition of NaOH.

Where peptides or amino acids served as the sole source of nitrogen,  $\text{NH}_4\text{Cl}$  was omitted from the basal medium and filter-sterilised amino acids or peptides were supplemented to the autoclaved basal M9 medium at the appropriate concentration.

**Minimal recovery medium** contained (per litre  $\text{dH}_2\text{O}$ ): 3.95 g  $\text{Na}_2\text{HPO}_4$ , 1.35 g  $\text{KH}_2\text{PO}_4$ , 0.5 g casamino acids (MP Biomedicals) and 0.5 g  $\text{MgSO}_4$ . The pH was adjusted to 7.2 by the addition of  $\text{NaOH}$ .

**1 X M9 minimal salt buffer** contained (per litre  $\text{dH}_2\text{O}$ ): 6 g  $\text{Na}_2\text{HPO}_4$ , 3 g  $\text{KH}_2\text{PO}_4$  and 0.5 g  $\text{NaCl}$ . The pH was adjusted to 7.0 by the addition of  $\text{NaOH}$ .

## **2.2 Molecular and biochemical techniques**

### **2.2.1 Polymerase Chain Reaction (PCR) with *E. coli***

PCR was performed as described by (Mullins *et al.*, 1986). Oligonucleotide primers were prepared as described in section 2.1.5. Template DNA consisted of a single, freshly streaked colony of the appropriate bacterial strain. A dNTP stock solution was prepared to a final concentration of 10 mM in  $\text{dH}_2\text{O}$  (2.5 mM each dATP, dCTP, dGTP and dTTP). For analytical PCR, Taq DNA Polymerase (NEB) was used. In this instance, a 50  $\mu\text{l}$  PCR reaction mixture was prepared by adding the following to a 0.5 ml Eppendorf tube, on ice: 32.5  $\mu\text{l}$   $\text{dH}_2\text{O}$ , 5  $\mu\text{l}$  10x ThermoPol Buffer (NEB), 4  $\mu\text{l}$  10 mM dNTPs (final concentration 0.2 mM), 5  $\mu\text{l}$  each forward and reverse primers (final concentration 1  $\mu\text{M}$  each), 1  $\mu\text{l}$  Taq DNA Polymerase and a single bacterial colony as template DNA. The reaction was mixed by pipetting.

Where high-fidelity PCR was required, KOD Hot Start DNA Polymerase (Novagen) was used. For KOD Hot Start Polymerase PCR, a 50  $\mu\text{l}$  reaction mixture was prepared by adding the following to a 0.5 ml Eppendorf, on ice: 32  $\mu\text{l}$   $\text{dH}_2\text{O}$ , 5  $\mu\text{l}$  10x KOD Buffer (Novagen), 5  $\mu\text{l}$  2 mM dNTPs (Novagen) (final conc. 0.2 mM), 4  $\mu\text{l}$  25 mM  $\text{MgSO}_4$  (Novagen) (final conc. 2 mM) 1.5  $\mu\text{l}$  each forward and reverse primers (final conc. 0.3  $\mu\text{M}$  each), 1  $\mu\text{l}$  KOD Hot Start DNA Polymerase and a single bacterial colony as template DNA.

All PCRs were performed using a Techne Techgene thermocycler. For Taq DNA Polymerase PCRs, the following cycling parameters were used:

**Table 2.6.** Thermocycling parameters used for standard Taq DNA polymerase PCR

<b>Initial denaturation</b>	<b>95°C</b>	<b>5'</b>	} X 30 cycles
<b>Denaturation</b>	<b>95°C</b>	<b>45''</b>	
<b>Annealing</b>	<b>45°C - 60°C</b>	<b>45''</b>	
<b>Extension</b>	<b>72°C</b>	<b>1' 20''</b>	
<b>Final Extension</b>	<b>72°C</b>	<b>5'</b>	
<b>Hold</b>	<b>4°C</b>	<b>HOLD</b>	

For KOD DNA Polymerase PCRs, the following cycling parameters were used:

**Table 2.7.** Thermocycling parameters used for standard KOD DNA polymerase PCR

<b>Initial denaturation</b>	<b>95°C</b>	<b>5'</b>	} X 32 cycles
<b>Denaturation</b>	<b>95°C</b>	<b>20''</b>	
<b>Annealing</b>	<b>45°C - 60°C</b>	<b>30''</b>	
<b>Extension</b>	<b>70°C</b>	<b>30''</b>	
<b>Final Extension</b>	<b>70°C</b>	<b>5'</b>	
<b>Hold</b>	<b>4°C</b>	<b>HOLD</b>	

### 2.2.2 PCR with *S. hominis* B10

To amplify the desired genes from *S. hominis* B10, degenerate primers were manually designed based on the nucleotide sequence of the orthologous genes in *S. hominis* SK119. PCR was performed using high fidelity MyFi DNA Polymerase (Bioline). A crude sample of *S. hominis* B10 DNA to be used as a DNA template was prepared by a preceding DNA extraction thermocycle reaction (Table 2.8) using a single freshly streaked bacterial colony resuspended in 20 µl dH<sub>2</sub>O. A 50 µl PCR reaction mixture was prepared by adding the following to a 0.5 ml Eppendorf: 35 µl dH<sub>2</sub>O, 10 µl 5x MyFi Buffer (containing 2 mM dNTPs), 2 µl each 10 µM forward and reverse primers (final concentration 0.3 µM each) and 1 µl MyFi DNA Polymerase. The PCR reaction parameters used are shown in Table 2.9.

**Table 2.8.** Thermocycling parameters used to extract crude *S. hominis* B10 template DNA

<b>65°C</b>	<b>30"</b>
<b>8°C</b>	<b>30"</b>
<b>65°C</b>	<b>90"</b>
<b>97°C</b>	<b>180"</b>
<b>8°C</b>	<b>60"</b>
<b>65°C</b>	<b>180"</b>
<b>97°C</b>	<b>60"</b>
<b>65°C</b>	<b>60"</b>
<b>4°C</b>	<b>HOLD</b>

**Table 2.9.** Thermocycling parameters used for standard MyFi DNA polymerase PCR

<b>Initial denaturation</b>	<b>95°C</b>	<b>2'</b>	} X 35 cycles
<b>Denaturation</b>	<b>95°C</b>	<b>15"</b>	
<b>Annealing</b>	<b>45°C - 55°C</b>	<b>15"</b>	
<b>Extension</b>	<b>72°C</b>	<b>45"</b>	
<b>Final Extension</b>	<b>72°C</b>	<b>5'</b>	
<b>Hold</b>	<b>4°C</b>	<b>HOLD</b>	

### 2.2.3 Agarose gel electrophoresis

1% (w/v) agarose gels were made by melting 0.5 g agarose (Melford, electrophoresis grade) in 50 ml 1X TBE buffer (10.8 g Tris HCl, 5.5 g Boric acid, 0.75 g EDTA, per litre dH<sub>2</sub>O). Following the addition of 5 µl of 10 mg/ml ethidium bromide, the molten agarose was poured into a pre-cast DNA electrophoresis gel tank. A comb was inserted to create appropriately sized wells and the gel was allowed to solidify at room temperature for approximately 30 min. For sample preparation, appropriate volumes of 5X DNA loading dye (containing 62.5 ml 30% glycerol, 31.25 ml dH<sub>2</sub>O, 6.25 ml 10% SDS, 0.125 g bromophenol blue and 0.125 g xylene cyanol, per 100 ml dH<sub>2</sub>O) were added to the PCR samples. The samples were loaded into the wells of the gel and then electrophoresed at 70 V for 60 min. Gels were visualised under the transilluminator of a Syngene GeneGenius Gel BioImaging Unit using Syngene GeneSnap software.

#### **2.2.4 DNA extraction from agarose gel**

The agarose gel was visualised under low-intensity UV transilluminator and the appropriate band of DNA excised using a clean scalpel and placed inside a 1.5 ml Eppendorf tube. DNA extraction was performed using the Macherey-Nagel NucleoSpin Extract II kit following the manufacturers recommended protocol and eluted in 20-30  $\mu$ l sterile dH<sub>2</sub>O. The quantity and quality of DNA in the sample was determined using a Nanodrop (ND-1000) spectrophotometer. DNA samples were stored at -20°C until use.

#### **2.2.5 Preparation of chemically competent *E. coli* cells**

A 5 ml overnight culture of the desired strain was grown overnight at 37°C in LB with the appropriate antibiotic selection. The following day, 100  $\mu$ l of the culture was added to 10 ml of LB (containing the appropriate antibiotic) and incubated aerobically at 37°C until the OD<sub>650</sub> nm reached 0.3 – 0.4. The cells were pelleted by centrifugation at 3500 rpm for 8 min at 4°C. The cells were resuspend in 1 ml of 0.1 M ice cold sterile CaCl<sub>2</sub> and incubated on ice for 30 min. The cells were pelleted by centrifugation at 3500 rpm for 8 min at 4°C and resuspend in 300  $\mu$ l of ice cold 0.1 M CaCl<sub>2</sub>. 100  $\mu$ l aliquots of cells were prepared and either used immediately or stored at -80°C until future use.

#### **2.2.6 Transformation of chemically competent *E. coli* with plasmid DNA**

100  $\mu$ l aliquots of chemically competent cells were either made fresh or thawed on ice from -80°C stock. 100 ng of plasmid DNA was added to an aliquot of cells and incubated on ice for 30 min. The cells were heat-shocked at 42°C for 90 sec. 900  $\mu$ l pre-warmed (42°C) SOC medium was immediately added and the cells were incubated at the appropriate recovery temperature (30°C or 37°C) for 1 h. 200  $\mu$ l of cells were spread onto LB agar plates supplemented with the appropriate antibiotic and incubated overnight at either 30°C or 37°C. A negative control with no added plasmid DNA added was always included.

### **2.2.7 Purification and restriction endonuclease digestion of plasmid DNA**

A 5 ml overnight culture of *E. coli* harbouring the desired plasmid was grown overnight in LB supplemented with the appropriate antibiotic. Plasmid DNA was extracted using either Macherey-Nagel NucleoSpin Plasmid miniprep kit or Wizard *Plus* SV Minipreps DNA Purification System (Promega) following the manufacturers recommended protocol. The amount of plasmid DNA extracted was quantified using a Nanodrop (ND-1000) spectrophotometer. To confirm extraction of the correct plasmid, or to confirm gene insertion in a particular plasmid, restriction enzyme digestion was carried out. In a 0.5 ml Eppendorf tube, the following components were combined: 2 µl 10 X restriction enzyme buffer (different depending on the restriction enzyme used), 300 ng plasmid DNA, 0.5 µl restriction enzyme (NEB or Promega) and sterile dH<sub>2</sub>O to adjust the volume to 20 µl. The reaction was incubated at the optimum temperature for the particular restriction enzyme for at least 1 h but no more than 2.5 h. The DNA was then separated on a 1% agarose gel, as detailed in section 2.6.3.

### **2.2.8 pCP20-mediated removal of the kanamycin resistance cassette from Keio Collection strains**

Keio Collection strains (Baba *et al.*, 2006) were accessed from an in-house library. To remove the kanamycin resistance cassette from the desired strain in order to create a clean chromosomal deletion, the strain was transformed with pCP20 (Datsenko & Wanner, 2000) following the protocol detailed in section 2.2.6. Three independent colonies were then subcultured in 5 ml LB with no antibiotic supplement and incubated aerobically overnight at 43°C to cure pCP20. A loopful of each culture was plated on LB agar and 10 subsequent colonies from each plate subcultured onto three individual plates consisting of: 1) LB agar, 2) LB agar + 50 µg/ml kanamycin and 3) LB agar + 100 µg/ml ampicillin. Colonies which had lost kanamycin resistance were screened by PCR to confirm removal of the kanamycin resistance cassette. Sensitivity to ampicillin confirmed loss of pCP20.

## **2.2.9 pKD46-mediated replacement of wild-type genetic loci with the kanamycin resistance cassette**

A 5 ml overnight culture of the desired strain harbouring pKD46 (Datsenko & Wanner, 2000) was incubated overnight in LB at 30 °C with 100 µg/ml ampicillin. The following day, 100 µl of the culture was added to 10 ml of LB supplemented with 100 µg/ml ampicillin and 20 mM L-arabinose and incubated aerobically at 30 °C until the OD<sub>650</sub> reached 0.3 – 0.4. The cells were pelleted by centrifugation at 3500 rpm for 8 min at 4 °C. The cells were washed three times in 2 ml ice-cold sterile 10% glycerol and finally resuspended in 200 µl ice-cold sterile 10% glycerol. 50 µl aliquots were prepared and added to pre-cooled 0.2 cm gap sterile electroporation cuvettes (Bio-Rad). 200 – 400 ng purified kanamycin resistance cassette DNA (amplified by KOD polymerase PCR with appropriate flanking homology to the selected gene to be removed) was added to the cuvette. Electroporation was performed using a Bio-Rad Micropulser on the pre-programmed Ec2 setting (V = 2.50 kV, time constant = 5.5 ms). Immediately following electroporation, 950 µl SOC medium, pre-warmed to 42 °C and supplemented with 20 mM L-arabinose was added to the cuvette and mixed by pipetting. The mixture was transferred to a 1.5 ml Eppendorf and incubated horizontally at 30 °C for 1 h. Cells were pelleted in a benchtop microfuge at 3500 rpm for 3 min, resuspended in 200 µl LB and spread onto LB agar plates supplemented with 30 µg/ml kanamycin and incubated overnight at 30 °C. At least 5 resulting colonies were checked for integration of the kanamycin resistance cassette at the appropriate locus by Taq DNA polymerase PCR. pKD46 was subsequently cured from the strain by growing a single bacterial colony in 5 ml LB with no antibiotic selection, aerobically at 43 °C, overnight. Loss of pKD46 from the strain was confirmed by sensitivity to ampicillin.

## **2.2.10 Cloning**

### **2.2.10.1 Purification of cloning vector pBADcLIC2005 and preparation of 'LIC-ready' plasmid**

pBADcLIC2005 (Geertsma & Poolman, 2007) was purified from *E. coli* MG1655 harbouring the plasmid. To create LIC-ready pBADcLIC2005, 400 ng was digested with Swal (NEB) for 2 h at 37 °C. The plasmid was gel extracted and purified. The following components were then added to a 0.5 ml Eppendorf: 400 ng Swal digested pBADcLIC2005, 1.5 µl 25 mM dCTP, 1.5 µl 10 X buffer, 1 µl T4 DNA polymerase and sterile dH<sub>2</sub>O to adjust the volume to 15 µl. The reaction was incubated for 30 min at 37 °C

and the enzyme subsequently heat inactivated by incubating at 70°C for 20 min. LIC-ready plasmid was stored at -20°C for up to 6 months.

#### **2.2.10.2 Purification and preparation of LIC-ready insert**

The *E. coli* or *S. hominis* B10 gene to be cloned into pBADcLIC2005 was amplified by PCR using KOD Hot Start DNA polymerase as detailed in Table 2.7 (for *E. coli*) or MyFi DNA polymerase as detailed in Table 2.9 (for *S. hominis* B10). The PCR products were then separated by electrophoresis on a 1% agarose gel. The DNA was then gel extracted and purified as detailed in section 2.2.7. To make the insert product LIC-ready, the following components were added to a 1.5 ml Eppendorf: 400 ng DNA, 1.5 µl 25 mM dGTP, 1.5 µl 10 X buffer, 1 µl T4 DNA polymerase and sterile dH<sub>2</sub>O to adjust the volume to 15 µl. The reaction was incubated for 30 min at 37°C and the enzyme subsequently heat inactivated by incubating at 70°C for 20 min. LIC-ready insert was stored at -20°C for up to 6 months.

#### **2.2.10.3 Ligation independent cloning of ‘LIC-ready’ plasmid and insert**

To ligate insert and plasmid, the following were added to a 0.5 ml Eppendorf: 50 ng LIC-ready pBADcLIC2005, a 6 X or 10 X molar excess of LIC-ready insert DNA and sterile dH<sub>2</sub>O to adjust the volume to 10 µl. The reaction was incubated at room temperature for 8 min. 3 µl was transformed in to Strategene SoloPack Gold Supercompetent *E. coli* cells (Agilent) using the manufacturers recommended protocol. The cells were plated on LB agar plates supplemented with 100 µg/ml ampicillin. A negative control was always included which consisted of 50 ng Swal digested pBADcLIC2005 vector in the absence of insert DNA.

#### **2.2.10.4 Confirmation of gene insertion into pBADcLIC2005**

10 resulting colonies from cloning of individual genes into pBADcLIC2005 were grown overnight in LB supplemented with 100 µg/ml ampicillin. Plasmid DNA was extracted from each individual culture and digested using restriction endonuclease digestion as detailed in section 2.2.7 using a single restriction endonuclease that cuts at the same site in both pBADcLIC2005 and the gene insert. The digested DNA was then separated by agarose gel electrophoresis and the pattern of restriction compared to that of pBADcLIC2005 plasmid alone, digested with the same restriction enzyme. Correct gene insertion was confirmed by

Sanger sequencing of putative correct constructs using the LIGHTrun service provided by GATC-biotech Ltd.

## **2.2.11 Malodour precursor biotransformation assays**

### **2.2.11.1 S-Benzyl-L-cysteine and S-Benzyl-L-cysteinyglycine biotransformation assays using resting cells**

5 to 20 ml of the appropriate bacterial strain grown overnight in LB (*E. coli*) or TSBT (corynebacteria and staphylococci) was centrifuged at 3500 rpm for 10-15 min and resuspended in 2 ml sterile minimal recovery medium (corynebacteria and staphylococci) or 1 X M9 salts (*E. coli*). Where appropriate, *E. coli* strains harbouring inducible genes on the pBADcLIC2005 plasmid were pre-induced during overnight growth with 0.0001% L-arabinose. To a sterile glass vial (8 ml volume capacity), the following were added: 2 mM substrate (S-Benzyl-L-cysteine or S-Benzyl-L-cysteinyglycine), cells to an OD<sub>650</sub> of 5 (for *E. coli*) or an OD<sub>590</sub> of 5 (for corynebacteria and staphylococci) and appropriate buffer to adjust the volume to 4 ml. All components of the reaction were dissolved or resuspended in either 1 X M9 salt buffer or MRM, depending on the particular assay. Where appropriate, carbonyl cyanide m-chlorophenyl hydrazone (CCCP) was added at a concentration of 50 µM. For reactions where competitive inhibitors were added, a 100 mM stock solution of competitor molecule was made in 1 X M9 salts, filter sterilised and supplemented to the reaction at a final concentration of 20 mM. Cell only (no added substrate) and substrate only (no added cells) reactions were also included in every individual experiment. The reactions were incubated at 37°C for up to 48 h with samples taken at appropriate time points. Subsequent isolation and quantification of released benzyl-mercaptan thioalcohol was carried out as detailed below.

### **2.2.11.2 (3-(4,5-dimethylthiazol-2-yl)-5-(3-carboxymethoxyphenyl)-2-(4-sulfophenyl)-2H-tetrazolium) (MTS) and phenazine methosulfate (PMS)-mediated chemical labelling of benzyl-mercaptan**

To isolate released benzyl-mercaptan thioalcohol, a 500 µl volume from each reaction (isolated as described in section 2.2.11.1) was taken at the appropriate time point and centrifuged at 13000 rpm for 2 min.

To chemically label benzyl-mercaptan, 50  $\mu$ l of labelling reagent, consisting of MTS 4.09 mM MTS (Promega) and 0.2 mM PMS (Sigma) (Goodwin *et al.*, 1995), dissolved in dH<sub>2</sub>O, was aliquotted into either a 96 well microplate or 0.5 ml Eppendorf tubes.

For reactions using a 96 well microplate, 200  $\mu$ l reaction supernatant was added to the pre-aliquotted 50  $\mu$ l MTS/PMS. The plate was sealed with a semi-permable film lid, incubated at room temperature for 50 min and the A<sub>492</sub> was recorded on a Biotek PowerWave XS microplate spectrophotometer. The data was captured by KC junior and exported to Microsoft Excel. For reactions in Eppendorf tubes, 20  $\mu$ l to 50  $\mu$ l reaction supernatant was added to 50  $\mu$ l MTS/PMS. The reaction was incubated at room temperature for 50 min. 20  $\mu$ l was subsequently removed and diluted in 980  $\mu$ l dH<sub>2</sub>O in a 1.5 ml disposable plastic cuvette. The A<sub>492</sub> was recorded.

### **2.2.11.3 Chemical labelling of known concentrations of benzyl-mercaptan and 3-mercaptohexan-1-ol using MTS/PMS**

1  $\mu$ M stock concentrations of benzyl-mercaptan (Sigma) and 3-mercaptohexan-1-ol (Sigma) were prepared in a final volume of 2 ml in a sterile, 8 ml capacity glass vial. 200  $\mu$ l of thioalcohol (diluted to the appropriate concentration using MRM) was added to 50  $\mu$ l MTS/PMS in a 96-well plate. Labelling of the thioalcohol proceeded as detailed in section 2.2.11.2.

### **2.2.11.4 Cys-Gly-3M3SH biotransformation assays using resting cells**

5 to 20 ml of the appropriate bacterial strain grown overnight in LB (*E. coli*) or TSBT (corynebacteria and staphylococci) was centrifuged at 3500 rpm for 10 - 15 min and resuspended in 2 ml sterile 1 X M9 minimal salts. Where appropriate, *E. coli* strains harbouring inducible genes on the pBADcLIC2005 plasmid were pre-induced during overnight growth with 0.0001% L-arabinose. To a sterile glass vial (8 ml volume capacity), the following were added: 2 mM Cys-Gly-3M3SH substrate (dissolved in 1 X M9 salts), cells to an OD<sub>650</sub> of 5 (for *E. coli*) or to an OD<sub>590</sub> of 5 (for corynebacteria and staphylococci) and 1 X M9 minimal salts to adjust the volume to 1 ml. Where appropriate, 100  $\mu$ M CCCP or 20 mM sodium orthovanadate were added. For reactions where competitive inhibitors were added, a 100 mM stock solution of competitor molecule was made in 1 X M9 salts, filter sterilised and supplemented to the reaction at a final concentration of 20 mM. Cell only (no added substrate) and substrate only (no added cells) reactions were also included in every individual experiment but are not always shown in each individual figure.

The reactions were incubated at 37°C for up to 48 h with samples taken at appropriate time points. Subsequent isolation and quantification of released 3M3SH thioalcohol was carried out as detailed below.

#### **2.2.11.5 5,5'-dithiobis-(2-nitrobenzoic acid) (DTNB)-mediated chemical labelling of 3M3SH**

To quantify free 3M3SH, a 75 µl volume from each reaction (isolated as described in section 2.2.11.4) was taken at the appropriate time point and centrifuged at 13000 rpm for 2 min.

950 µl labelling solution, consisting of: 800 µl dH<sub>2</sub>O, 100 µl UltraPure Tris (pH 8.0) and 50 µl DTNB (Ellman, 1958) stock solution (50 mM sodium acetate, 2 mM DTNB, dissolved in dH<sub>2</sub>O) was added to a 1.5 ml disposable cuvette. 50 µl reaction supernatant was added to the cuvette, mixed by pipetting and incubated at room temperature for 5 min. The A<sub>412</sub> was recorded (Van Horn, 2003).

#### **2.2.11.6 Lysostaphin-mediated cell lysis of staphylococci**

50 ml overnight cultures of *S. hominis* B10 and *S. epidermidis* G428 were centrifuged at 3500 rpm for 15 min at 4°C. The pellet was resuspended in 3 ml 1 X M9 minimal salts and the OD<sub>590</sub> was recorded. 50 µg lysostaphin (dissolved in 50 µl 1 X M9 salts) was added to the bacterial suspension along with an appropriate volume of 1 X bacterial protease inhibitor cocktail (Sigma), where required. The culture was incubated at 37°C for up to 5 h until visible clearing of the culture was seen. Following incubation, crude cell lysate was obtained by centrifugation of the material at 13000 rpm for 20 min at 4°C. Crude cell lysate was divided into 300 µl aliquots and stored at -20°C until use.

#### **2.2.11.7 S-Benzyl-L-cysteine and Cys-Gly-3M3SH biotransformation by *Staphylococcus* spp. crude cell lysate**

The protocol for S-Benzyl-L-cysteine and Cys-Gly-3M3SH biotransformation assays by staphylococcal crude cell lysate was comparable to that described in section 2.2.11.1 and 2.2.11.4, respectively. However, resting cells were substituted for crude cell lysate. The volume of crude cell lysate added to each reaction was calculated from the OD<sub>590</sub> of the bacterial suspension prior to lysostaphin-mediated cell lysis (for which, 100% bacterial

lysis and protein recovery was assumed). Labelling of released benzyl-mercaptan and 3M3SH was performed using MTS/PMS (section 2.2.11.2) and DTNB (section 2.2.11.5), respectively.

### **2.2.11.8 Purified cystathionine $\beta$ -lyase enzyme activity assays**

Purified recombinant cystathionine  $\beta$ -lyase from *C. jeikeium* K411 (James *et al.*, 2013) was provided by Unilever. For S-Benzyl-L-cysteine, S-Benzyl-L-cysteinyglycine and Cys-Gly-3M3SH biotransformation assays, a 1:2000 dilution from stock was prepared and substrate biotransformation assays performed as detailed in section 2.2.11.1 - 2.2.11.2 (for benzyl-substrates) and 2.2.11.4 - 2.2.11.5 (for Cys-Gly-3M3SH).

### **2.2.11.9 Thin layer chromatography (TLC)**

7.5  $\mu$ l samples of reaction supernatant (as prepared in section 2.2.11.1) were loaded at 1.5 cm intervals on a cellulose F thin layer chromatography glass plate (Merck Millipore) and allowed to dry at room temperature for 15 min. A 2.5 cm gap was left between the bottom edge of the plate and sample load position. The internal surfaces of a glass TLC tank were lined with technical/qualitative filter paper (Sartorius) and the running solvent 1-butanol:dH<sub>2</sub>O:glacial acetic acid in a 4:1:1 ratio (Emter & Natsch, 2008) was poured to a depth of 1.5 cm at the bottom of the tank and allowed to saturate the filter paper for at least 1 h. The TLC plate was placed, samples at the bottom, into the tank at an angle of approximately 70°. The solvent front was allowed to proceed for a minimum of 7 h until it reached 2-3 cm from the top of the plate. The plate was then removed from the tank and the solvent was allowed to evaporate in a chemical fume hood for 15 min. The plate was then stained by applying a liberal amount of aerosolised 2% ninhydrin (dissolved in 1-butanol:glacial acetic acid in a 97:3 ratio) to the surface of the TLC plate. The plate was subsequently heated to 55 °C for at least 30 min. The plate was incubated overnight at room temperature and then visualised under upper white light in a Syngene GeneGenius Gel BioImaging Unit using Syngene GeneSnap software.

## **2.3 Microbiological techniques**

### **2.3.1 Speciation of unidentified axillary isolates using MicroSeq 500**

An individual colony of each strain was diluted in 100 µl PrepMan Ultra sample preparation buffer (Applied Biosystems) and heated to 100 °C for 10 min to crudely extract genomic DNA. 8 µl of this preparation was diluted in 395 µl sterile, nuclease free dH<sub>2</sub>O and stored at 4 °C until use. The MicroSeq 500 16S rDNA bacterial identification PCR kit (PN 4348229) (Applied Biosystems) contains a PCR master mix required to amplify the first 500 base pairs of the 16S rDNA region of any bacterial chromosome. The manufacturers recommended protocol and reaction set up was followed and PCR was carried out using a GeneAmp PCR System 2700 using the previously isolated DNA as a template. Resulting PCR products were stored at -20 °C until use. Forward and reverse cycle sequencing reactions were prepared by adding 3 µl volumes of each purified PCR product, 4 µl of dH<sub>2</sub>O (supplied in the kit) and 13 µl aliquots of either the forward or reverse sequencing mixes into appropriate PCR tubes. PCR reactions were again performed on a GeneAmp PCR System 2700 and amplicons were purified and dried in a vacuum centrifuge for 15 min. Electrophoretic sequencing was carried out using an Applied Biosystems 3100X Genetic Analyzer instrument. Treatment of the samples was as recommended by Applied Biosystems for the BigDye Terminator Version 2 chemistry. The sequencing data was analysed using MicroSeq ID Analysis Software and confirmed by taking the raw sequence data and searching using the Ribosomal Database Project (<http://rdp.cme.msu.edu/>) for the closest DNA match.

### **2.3.2 Growth phenotype experiments in shake flasks**

Shake flask growth experiments were typically conducted in 100 ml shake flasks using 20 ml growth medium. Cells were routinely pre-grown overnight in M9 glucose medium and directly inoculated into fresh medium the following day to a starting OD<sub>650</sub> nm of 0.1. The cultures were incubated aerobically at 37 °C at 180 rpm for the duration of the experiment. Where supplements were made during bacterial growth, they were aseptically added at the appropriate time point. For sampling, a 1 ml sample (or appropriate dilution thereof) was taken from each shake flask on an hourly basis and the OD<sub>650</sub> recorded using a Jenway 6305 spectrophotometer.

### **2.3.3 Growth phenotype experiments in 96-well microplates**

Growth experiments in a 96-well microplate were performed on a Tecan Infinite M200 Pro microplate reader. For pre-growth of bacterial cultures, strains were inoculated from a single colony into 2.5 ml M9 glucose medium and incubated aerobically overnight at 37°C.

For tryptone broth, LB and yeast extract broth growth assays, 150 µl medium was aliquotted into the internal wells of a 96-well microplate (Corning Costar 3595). The perimeter wells of the microplate were filled with 150 µl of sterile dH<sub>2</sub>O to prevent evaporation from the internal wells. For minimal medium assays, 150 µl of filter sterilised M9 glucose medium with the appropriate concentration of dipeptide or amino acid as the sole source of nitrogen was aliquotted into the internal wells of the microplate.

To inoculate the medium, the OD<sub>650</sub> of each overnight culture was measured and adjusted to 1.0 by addition of 1X M9 salts. 1.5 µl of this bacterial cell suspension was added to the appropriate well and mixed by pipetting to give a starting OD<sub>650</sub> of 0.01. The Tecan Infinite M200 Pro was set to monitor OD<sub>650</sub> every 30 min for 24 to 48 h and maintain a constant temperature of 37°C. Data was exported to Magellan data analysis software for analysis.

For data analysis, the average of three uninoculated growth medium only control wells was taken at every 30 min time point and the experimental data was normalised by subtracting this value from the OD<sub>650</sub> reading for all cultures at the respective time point to eliminate background OD values.

### **2.3.4 Agar plate toxic tripeptide inhibition assays**

M9 agar plates were made by pre-warming 2X concentrated sterile M9 minimal salts to 50°C and adding this to an equivolume of sterile 2% agar, melted and cooled to 50°C. 0.4% (v/v) D-glucose, 18.7 mM NH<sub>4</sub>Cl and 1 mM MgSO<sub>4</sub> were then supplemented. Plates were poured, allowed to set and dried in a class II microbiology safety cabinet and stored at 4°C until use.

For the toxic tripeptide inhibition assays, 400 µl of a saturated culture of the appropriate strain of *E. coli*, grown in M9 glucose, was spread onto the surface of an M9 agar plate and allowed to dry for at least 20 min. Sterile 5 mm filter paper discs were aseptically placed onto the surface of the dried bacterial culture and saturated with equimolar

concentrations of L-valine, L-valylglycylglycine (Val-Gly-Gly) or sterile dH<sub>2</sub>O. Specifically, in a final volume of 10 µl, 5.45 µl of 5 µg/µl L-valine, 5.65 µl of 10 µg/µl Val-Gly-Gly or 10 µl sterile dH<sub>2</sub>O were used. The solutions were allowed to saturate the filter paper discs and dry. Plates were incubated overnight at 37 °C. Zones of inhibition were calculated as the distance of bacterial clearance from the centre of the filter paper disc.

### **2.3.5 Growth of *E. coli* in spent tryptone broth medium**

Spent tryptone broth was prepared from a saturated culture of the appropriate *E. coli* strain following 24 h growth in tryptone broth. The bacterial cultures were centrifuged at 13000 rpm for 20 min. The medium was then filter sterilised twice through a 0.22 µm filter and stored at room temperature. 5 ml aliquots were prepared and bacteria, grown overnight in M9 glucose medium, was added to a starting OD<sub>650</sub> of 0.1. The cultures were incubated overnight at 37 °C and the final growth yield (OD<sub>650</sub> following 24 h incubation) was recorded.

### **2.3.6 End point final growth yield measurement**

Final yield growth experiments were conducted in 5 ml growth medium. Bacteria were pre-grown overnight in M9 glucose medium and added to the fresh medium the following day to a starting OD<sub>650</sub> of 0.1. The cultures were incubated overnight at 37 °C and the final growth yield (OD<sub>650</sub> following 24 h incubation) was recorded.

### **2.3.7 Preparation of crude cell lysate from *E. coli***

4 X 50 ml saturated overnight cultures of *E. coli* K-12 were centrifuged at 3500 rpm for 20 min at 4 °C. Each pellet was resuspended in 5 ml 1X M9 minimal salts and the cells pooled in to a single 50 ml Falcon tube. 10 ml 1 X M9 salts was added to adjust the total volume to 35 ml. The OD<sub>650</sub> was recorded. To obtain cell lysate, the cells were disrupted using a Misonix Sonicator 3000 Ultrasonic Cell Disruptor. The sample was placed (lid off) inside a 500ml plastic beaker filled with ice. The probe was inserted into the sample and the cells were sonicated for a total of 60 pulses of 3 sec, with 7 sec intervals between pulses. Following sonication, cell debris was removed by centrifuging of the sample at 13000 rpm for 20 min at 4 °C. Crude cell lysate was divided into 600 µl aliquots and stored at -20 °C until use.

## **2.4 Bioinformatics**

### **2.4.1 Construction of Dtp protein phylogenetic tree**

The amino acid sequence of each Dtp protein of *E. coli* K-12 was taken from the *E. coli* genetic database EcoCyc (<http://www.ecocyc.org>). Each protein was used as a BLAST query to search for orthologous proteins in other organisms. Orthologues of each Dtp protein were identified based on sequence homology with DtpA, DtpB, DtpC or DtpD. Each independently identified Dtp orthologue was subsequently used as a reciprocal BLAST query against all four *E. coli* Dtp proteins to confirm true orthology to the original protein. The amino acid sequences were compiled in FASTA format using unique identifiers and a multiple sequence alignment was performed using ClustalX2. A phylogenetic tree was constructed in ClustalX2 using the neighbour joining method, employing 1000 bootstrap trials. The phylogenetic tree was viewed and annotated using FigTree v1.4.0 ([http://www. http://tree.bio.ed.ac.uk/software/figtree/](http://www.tree.bio.ed.ac.uk/software/figtree/)).

### **2.4.2 Construction of staphylococcal C-S- lyase protein phylogenetic tree**

The amino acid sequence of the characterised C-S-  $\beta$ -lyase from *C. jeikeium* K411 (NCBI ref: YP\_250369.1) was used as a BLAST query to search for homologous proteins in staphylococci. Each independently identified homologue was subsequently used as a reciprocal BLAST query against YP\_250369.1 to confirm true homology to the original protein. The amino acid sequences were compiled in FASTA format using unique identifiers and a multiple sequence alignment was performed using ClustalX2. A phylogenetic tree was constructed in ClustalX2 using the neighbour joining method, employing 1000 bootstrap trials. The phylogenetic tree was viewed and annotated using FigTree v1.4.0.

### **2.4.3 Identification of molecular symporters in *S. hominis* SK119**

The genome of *S. hominis* SK119 was analysed through the BioCyc Database Collection (<http://biocyc.org/organism-summary?object=SHOM629742-HMP>). The search query terms 'transporter' and 'permease' were used to search the genome of *S. hominis* SK119 for proteins with annotated transport function. Any transporter that was clearly part of a multi-gene ABC transporter operon was excluded from the analysis. The unique

identification references from both BioCyc and NCBI were collated for each protein and compiled into a table.

# **Chapter 3**

## **Catabolism of malodour precursor substrates by axillary bacteria**

## Introduction and aims

A strong qualitative link between malodour intensity and a high population density of corynebacteria within the axilla has been demonstrated (Taylor *et al.*, 2003). It has also been demonstrated that corynebacteria, particularly the model organism *C. jeikeium* K411 and type strain *C. tuberculostearicum* SK141, were strong biotransformers of the model malodour precursor substrate S-Benzyl-L-cysteine (Fig. 1.2B) (James *et al.*, 2013). These assertions have formed a long-standing hypothesis that *Corynebacterium* is the dominant malodour forming bacterial genus residing within the human axilla. In order to test this hypothesis, a library of skin-isolated staphylococci and corynebacteria will be screened for malodour precursor biotransformation using both model and physiologically-relevant precursor substrates. The most active malodour producing bacteria will be identified and malodour precursor uptake in these organisms will be rigorously characterised.

## Specific aims

- To assess the biotransformation ability of culture collection and skin-isolated corynebacteria and staphylococci using both the model (S-Benzyl-L-cysteinyglycine) and physiological (Cys-Gly-3M3SH) malodour precursor substrates
- To assess the range of malodour precursor substrate concentration and concentration of bacterial cells required to generate malodour
- To speciate unspciated isolates used in the substrate biotransformation assays
- To assess the energetic requirements of Cys-Gly-3M3SH uptake in the relevant bacteria
- To assess a range of Cys-Gly-3M3SH mimetic substrates for inhibition of malodour production

### 3.1 Uptake and biotransformation of S-Benzyl-L-cysteinylglycine by corynebacteria and staphylococci

S-Benzyl-L-cysteine has been used routinely by Unilever in thioalcohol production assays for several years. It is broken down intracellularly by C-S-  $\beta$ -lyase to the thioalcohol benzyl-mercaptan, pyruvate and ammonia. By directly measuring benzyl-mercaptan release in a whole-cell assay, the relative malodour precursor biotransformation ability of individual bacterial isolates can be assessed. To determine the malodour precursor biotransformation ability of corynebacteria and staphylococci, a screen of several isolates was carried out using the model dipeptide-conjugated malodour precursor substrate S-Benzyl-L-cysteinylglycine (Fig. 1.2C), a molecule sharing greater structural similarity to the physiological malodour precursor molecule Cys-Gly-3M3SH than S-Benzyl-L-cysteine. The thioalcohol production assay developed by Unilever and applied here is detailed in section 2.2.11.1. Briefly, substrate (final concentration 2 mM) and resting bacterial cells (final OD<sub>590</sub> of 5) were mixed in a sterile glass vial and the final volume was adjusted to 4 ml with reaction buffer. The vials were incubated with shaking at 37°C for 24 h. A sample of cell suspension was taken following 24 h incubation, centrifuged, and 200  $\mu$ l supernatant was combined with the thioalcohol labelling reagent MTS/PMS in order to quantify benzyl-mercaptan yield.

High thioalcohol yield ( $A_{492} > 3$ ) was observed in *Corynebacterium* sp. Ax20, *C. tuberculostearicum* G459 and *C. striatum* (Fig. 3.1) Moderate thioalcohol yield ( $A_{492}$  1.5 - 3) was observed in *C. glutamicum*, *C. tuberculostearicum* G438, *C. jeikeium* K411 and *S. haemolyticus* G431. Low thioalcohol yield ( $A_{492} < 1.5$ ) was observed for all other *Corynebacterium* and *Staphylococcus* isolates. High, moderate and low yield classifications are a relative assignment based on the yield of any given isolate relative to the strongest thioalcohol producer, *C. tuberculostearicum* G459. The data suggest that, in general, corynebacteria are strong biotransformers of S-Benzyl-L-cysteinylglycine. This correlates with previous reports suggesting a qualitative link between corynebacteria and malodour intensity (Taylor *et al.*, 2003).

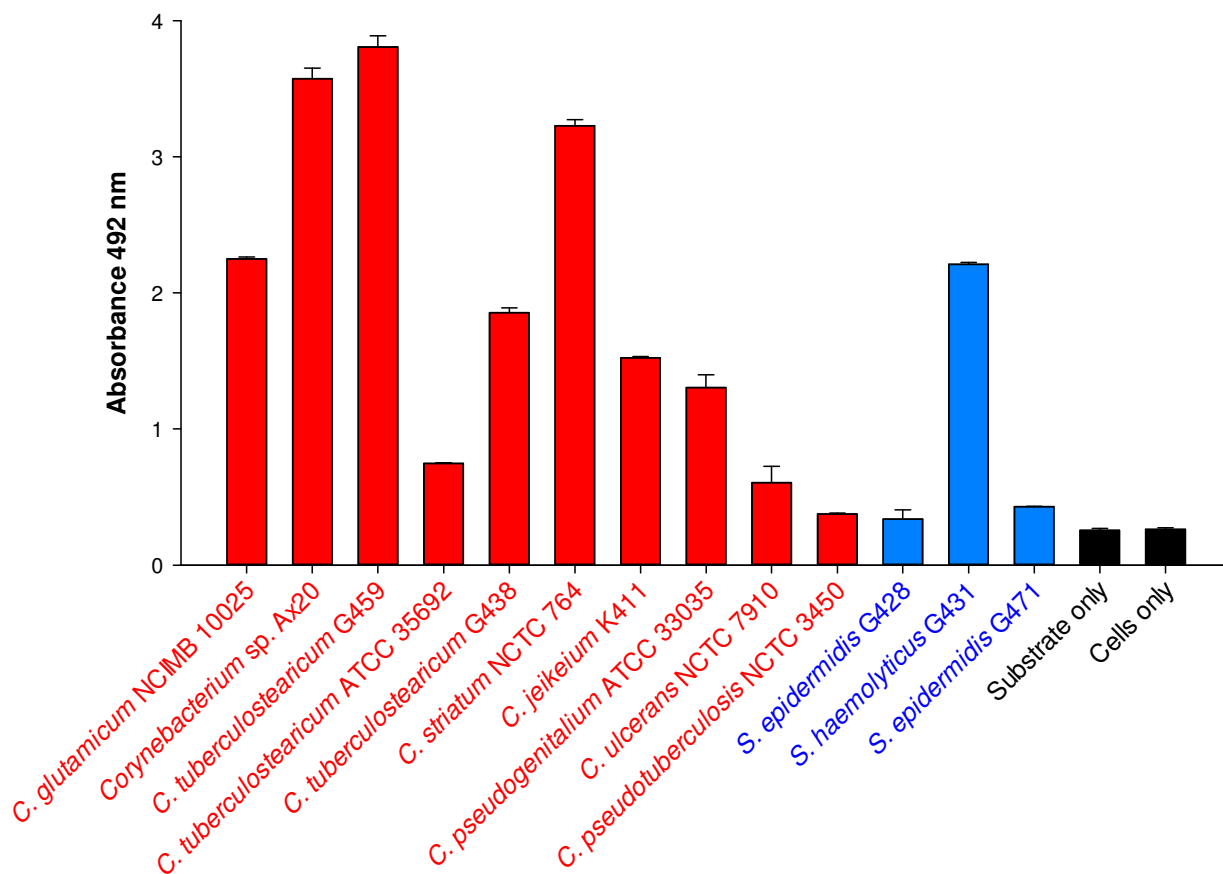


**Figure 3.1.** Biotransformation of S-Benzyl-L-cysteinyglycine by corynebacteria and staphylococci. Thioalcohol yield ( $A_{492}$ ) was quantified for each isolate using MTS/PMS after 24 h incubation. 'Substrate only' and 'cells only (*C. tuberculostearicum* G459)' refer to reactions incubated in the absence of S-Benzyl-L-cysteinyglycine or bacterial cells respectively. Error bars represent standard deviation of two biological replicates. Corynebacteria are coloured red, staphylococci are blue and controls are black.

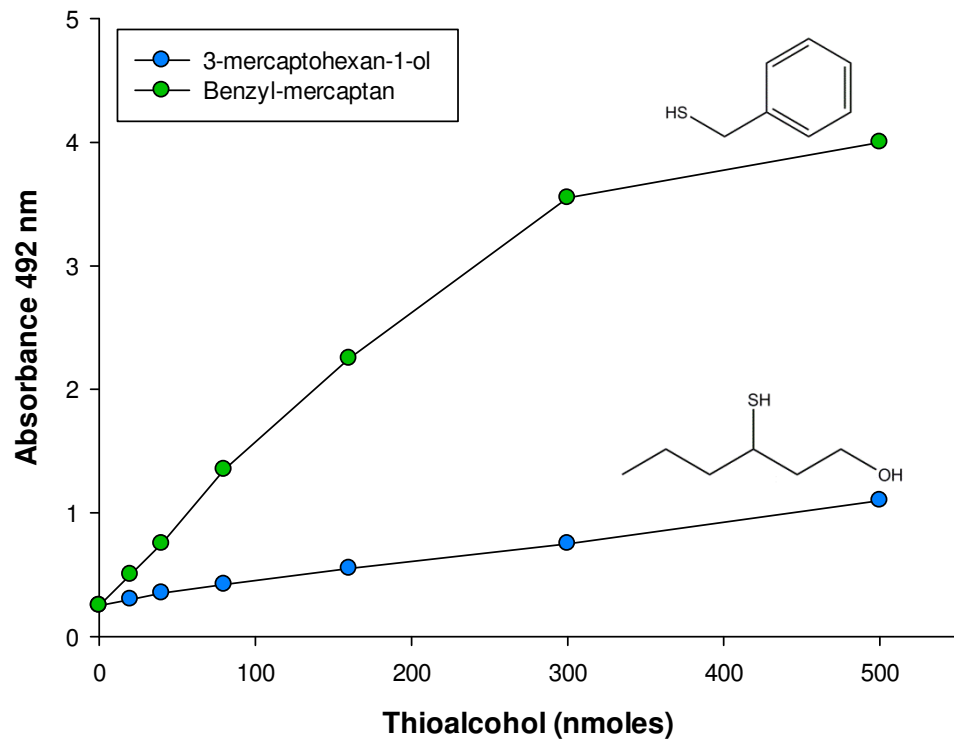
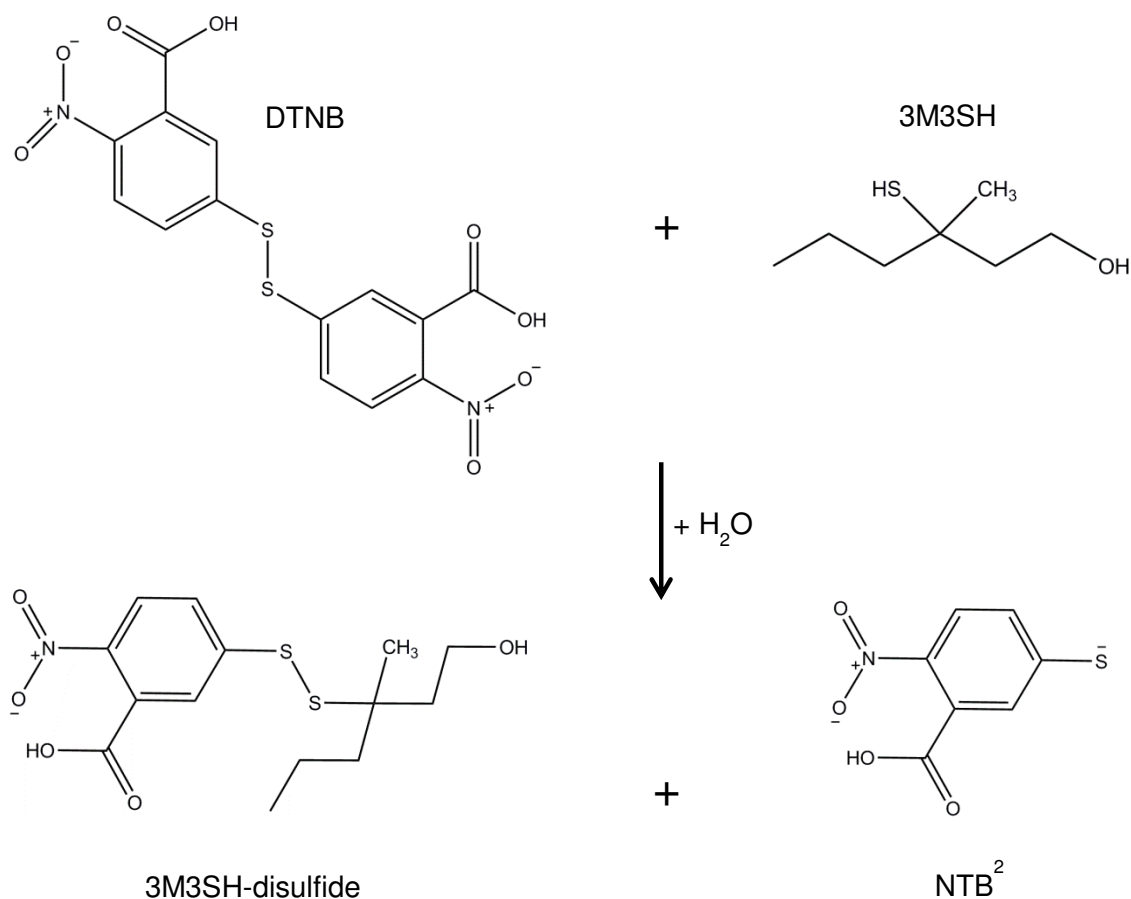
### **3.2 Development of a thioalcohol labelling assay to detect physiologically relevant malodour molecules**

To gain insight into the dynamics of malodour production in the human axilla, there is a clear need to move away from model malodour precursor substrates and assess bacterial biotransformation of the physiologically relevant malodour precursor, Cys-Gly-3M3SH (Fig. 1.2A). As described in chapter 1, Cys-Gly-3M3SH represents one of the most abundant malodour precursor molecules in apocrine gland secretions. It is proposed to be broken down intracellularly by either a single step (Starkenmann *et al.*, 2005) or dual catabolic process (Emter & Natsch, 2008) into glycine, pyruvate, ammonia and the highly odorous thioalcohol 3M3SH. By directly measuring 3M3SH release, the relative ability of individual bacterial isolates to biotransform Cys-Gly-3M3SH can be assessed.

To quantify 3M3SH release, an alternative thioalcohol labelling assay was developed. This was necessary as the pre-existing MTS/PMS labelling reagent showed poor chemical labelling of 3-mercaptohexan-1-ol (Fig. 3.2A), a thioalcohol structurally related to 3M3SH. It was envisaged that MTS/PMS-mediated labelling of 3M3SH would be equally poor.

An alternative approach was sought and the sulfhydryl group labelling molecule, 5,5'-dithiobis-(2-nitrobenzoic acid) (Ellman's reagent or DTNB) was integrated into the pre-existing assay. The mechanism of action of DTNB is summarised in Fig. 3.2B. Essentially, a sulfhydryl group-containing molecule, for example, 3M3SH, forms a disulfide with DTNB, displacing 2-nitro-5-thiobenzoate (NTB<sup>-</sup>). In water, at neutral or alkaline pH, NTB<sup>-</sup> ionises to NTB<sup>2-</sup> with 1:1 stoichiometry (Dal Prá *et al.*, 2013). NTB<sup>2-</sup> is bright yellow in solution and has an absorbance maximum at 412 nm (Ellman, 1958). The amount of released 3M3SH (or other thioalcohol product) is thus directly quantifiable.

This assay allows direct quantification of physiologically relevant malodorants and represents a novel method to screening bacteria for malodour precursor biotransformation using physiological substrates.

**A****B**

**Figure 3.2. (A)** Biochemical labelling of benzyl-mercaptan (filled green circles) and 3-mercaptohexan-1-ol (filled blue circles) with MTS/PMS. For absorbance readings  $>0.7$ , samples were diluted appropriately prior to measurement. **(B)** Mechanism of sulfhydryl group labelling by DTNB.

### **3.3 DTNB labelling assay assessment - uptake and biotransformation of Cys-Gly-3M3SH by corynebacteria and staphylococci**

To assess how efficiently the DTNB labelling method works with 3M3SH, substrate biotransformation assays were repeated as in section 3.1 using the physiologically relevant malodour precursor molecule, Cys-Gly-3M3SH as the substrate. The 3M3SH labelling method is detailed in 2.2.11.5.

Following 24 h incubation, high 3M3SH yield ( $A_{412} > 0.2$ ) was observed in only one bacterial isolate, *S. haemolyticus* G431 (Fig. 3.3). Moderate 3M3SH yield ( $A_{412}$  0.07 - 0.2) was observed for *Corynebacterium* sp. Ax20. All other corynebacteria and staphylococci displayed low or negligible 3M3SH yield ( $A_{412} < 0.07$ ). With the exception of *C. tuberculostearicum* G438 and *C. tuberculostearicum* G459, all *Corynebacterium* isolates used here were type or culture collection strains. All three *Staphylococcus* isolates were obtained from Unilever's library of skin-isolated bacteria.

There is a surprising discordance between the ability of a bacterial isolate to biotransform Cys-Gly-3M3SH (Fig. 3.3) and the ability to biotransform the model malodour precursor S-Benzyl-L-cysteinylglycine (Fig. 3.1). In a physiological setting, biotransformation of Cys-Gly-3M3SH is clearly more relevant and important. This data questions the relative contribution of corynebacteria and staphylococci to thioalcohol generation, as all of the *Corynebacterium* isolates tested show weak 3M3SH generation, whereas *S. haemolyticus* G431 is clearly an efficient biotransformer of this substrate. A more detailed assessment of corynebacterial and staphylococcal (particularly *S. haemolyticus* G431) Cys-Gly-3M3SH biotransformation is evidently required in order to define the most efficient thioalcohol generating bacterial genus (and species) within the axilla.

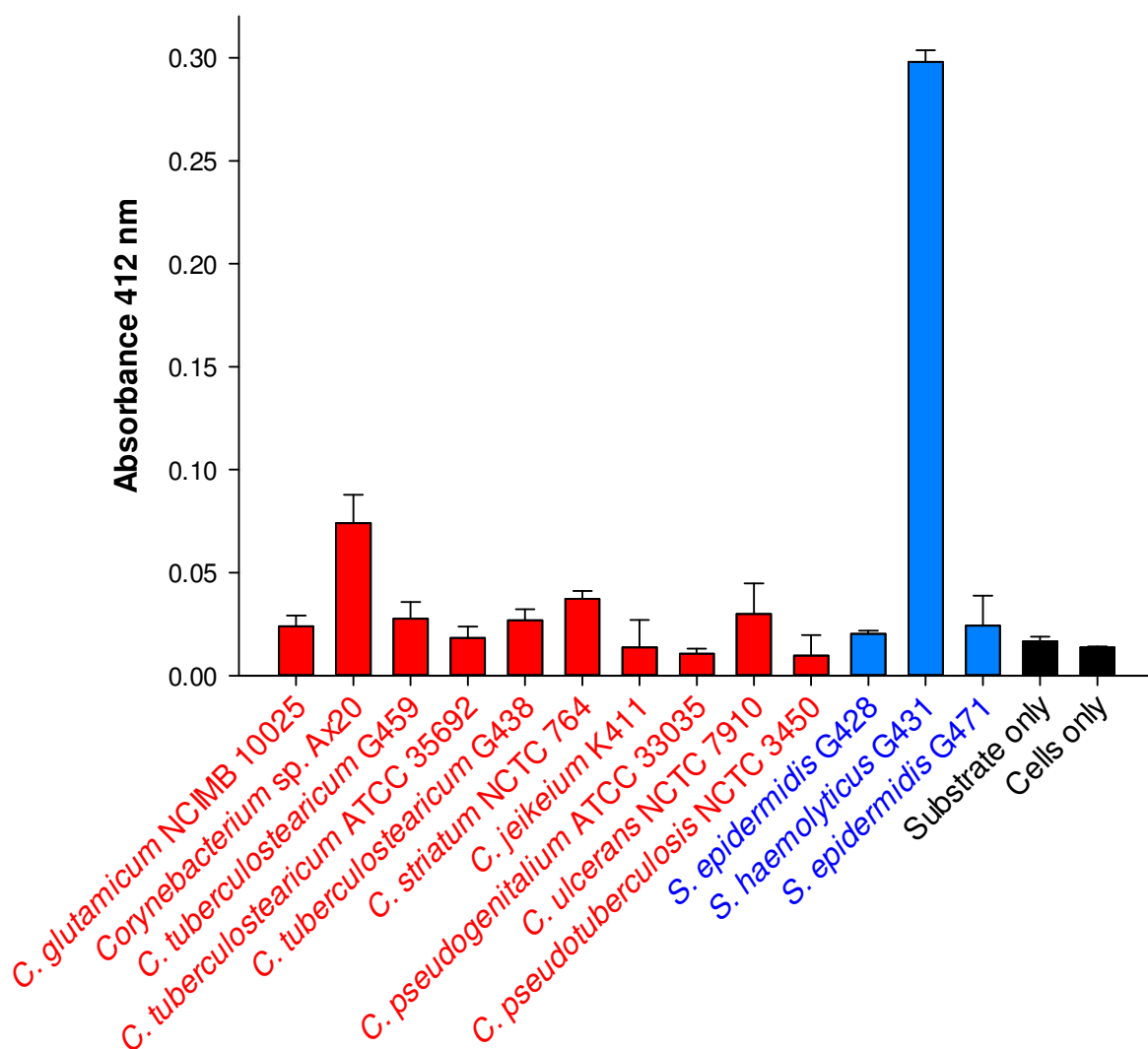


**Figure 3.3.** Biotransformation of Cys-Gly-3M3SH by corynebacteria and staphylococci isolates. Thioalcohol yield ( $A_{412}$ ) was quantified for each isolate using DTNB after 24 h incubation. 'Substrate only' and 'cells only (*S. haemolyticus* G431)' refer to reactions incubated in the absence of Cys-Gly-3M3SH or bacterial cells respectively. Error bars represent standard deviation of three biological replicates. Corynebacteria are coloured red, staphylococci are blue and controls are black.

### 3.4 Cys-Gly-3M3SH biotransformation by *S. haemolyticus* G431

*S. haemolyticus* G431 was identified as a strong 3M3SH generating isolate. For that reason, a detailed analysis of Cys-Gly-3M3SH biotransformation by *S. haemolyticus* G431 was undertaken. To determine how quickly Cys-Gly-3M3SH is biotransformed by *S. haemolyticus* G431, a time course of 3M3SH generation was performed. Maximum 3M3SH yield was achieved following only 3 h incubation with Cys-Gly-3M3SH (Fig. 3.4.1). The concentration of 3M3SH in the reaction remained constant over 24 h, suggesting that there is no loss of thioalcohol signal during the course of the assay. The data suggest that Cys-Gly-3M3SH biotransformation by *S. haemolyticus* G431 is relatively efficient and requires no supplemented enzymatic co-factor.

In order to determine whether 3M3SH yield correlates with the starting concentration of bacterial cells and substrate, Cys-Gly-3M3SH biotransformation assays were performed with decreasing concentrations of bacterial cells (*S. haemolyticus* G431) and Cys-Gly-3M3SH, respectively.

Standard Cys-Gly-3M3SH biotransformation assays use a high concentration of bacterial cells ( $OD_{590} = 5.0$ ). It was observed that decreasing the cell density to  $OD_{590} = 2.5$  had no effect on final 3M3SH yield (Fig. 3.4.2A). However, step-wise decreases in cell density ( $OD_{590} = 1.25$  and  $OD_{590} = 0.625$ ), led to step-wise reductions in 3M3SH yield after 24 h. This suggests that the minimum cell density required to efficiently biotransform 2 mM Cys-Gly-3M3SH is an  $OD_{590}$  of between 1.25 and 2.5. An increase in cell density above  $OD_{590} = 2.5$  does not correlate with an increase in thioalcohol yield, suggesting that at these cell densities, either all substrate has been biotransformed after 24 h or 3M3SH is inhibitory when produced at relatively high concentrations.

A similar pattern of 3M3SH generation was observed when the starting concentration of Cys-Gly-3M3SH was reduced in a step-wise manner. Standard Cys-Gly-3M3SH biotransformation assays use 2 mM substrate. Interestingly, no increase in thioalcohol yield was observed when the concentration of Cys-Gly-3M3SH was doubled from 2 mM to 4 mM (Fig. 3.4.2B). This suggests that at substrate concentrations above 2 mM, either the substrate or product is inhibitory to further Cys-Gly-3M3SH biotransformation. It was observed, as expected, that single-fold serial reductions in Cys-Gly-3M3SH concentration (from 2 mM down to 0.1 mM) lead to a step-wise decrease in 3M3SH yield. At 0.1 mM Cys-Gly-3M3SH it becomes unfeasible to distinguish between signal (3M3SH yield) and background noise. This suggests that at Cys-Gly-3M3SH concentrations below 2 mM, the

majority of substrate is biotransformed as there is a progressive reduction in thioalcohol yield as initial substrate concentration decreases. An alternative explanation is that the Cys-Gly-3M3SH transporter is relatively low affinity and transport of Cys-Gly-3M3SH is inefficient at concentrations below 2 mM.

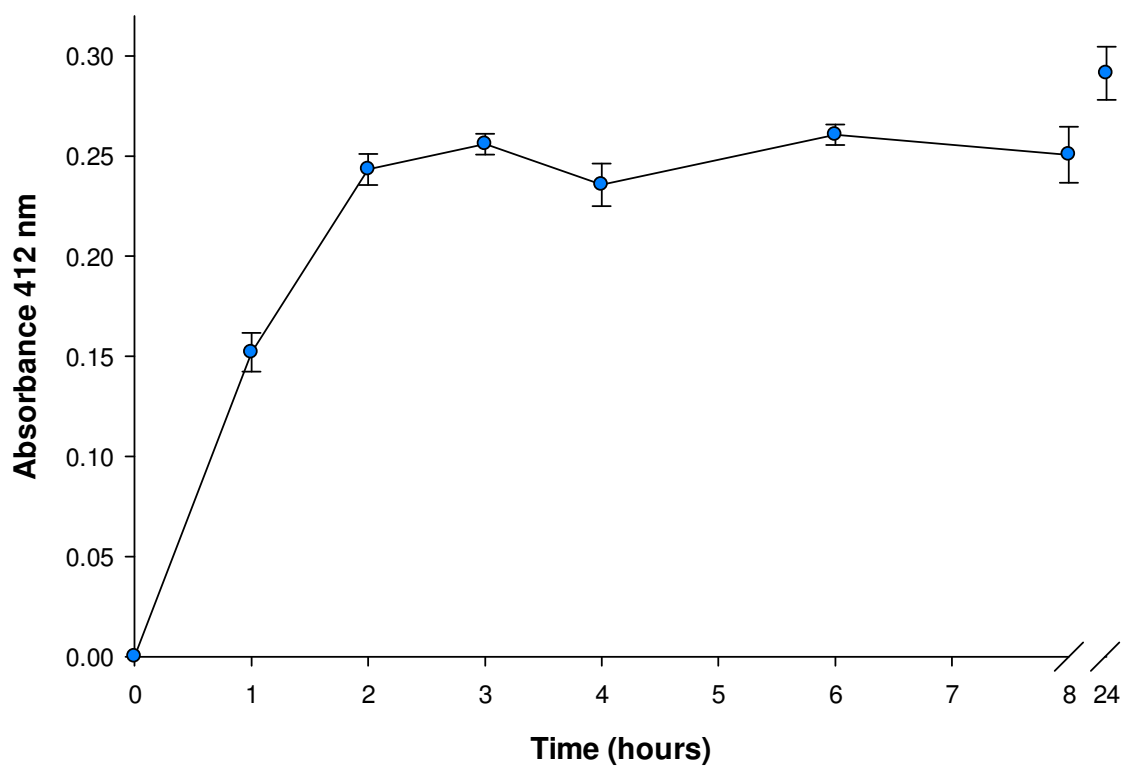


**Figure 3.4.1.** Time-dependent biotransformation of Cys-Gly-3M3SH by *S. haemolyticus* G431. At each time point, thioalcohol yield ( $A_{412}$ ) was quantified using DTNB. Isolated data point represents thioalcohol yield following 24 h incubation. Error bars represent standard deviation of three biological replicates.

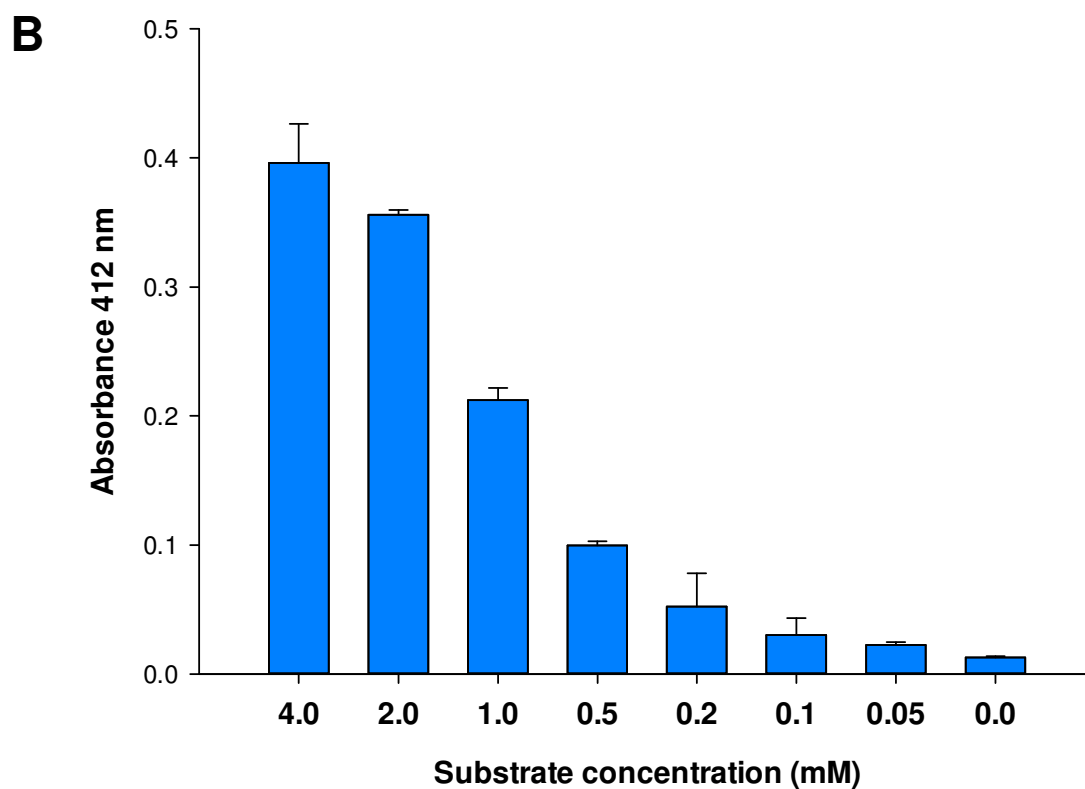
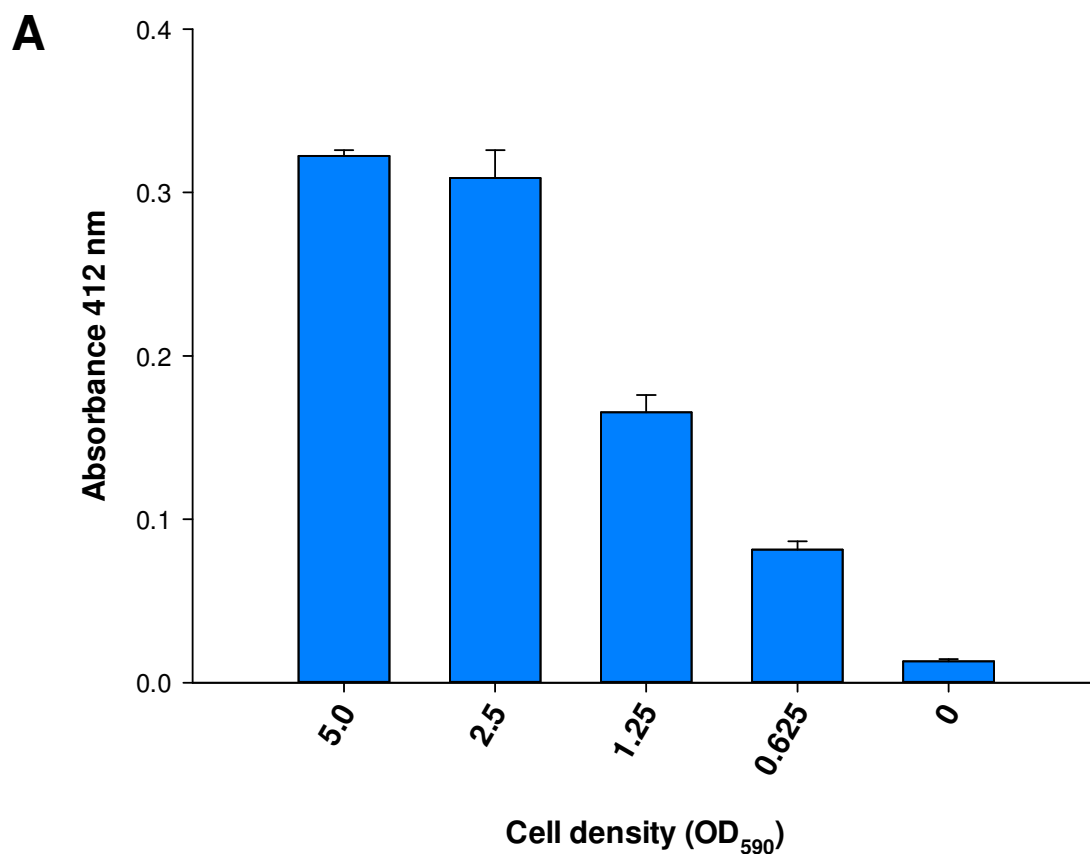


**Figure 3.4.2.** Biotransformation of Cys-Gly-3M3SH by *S. haemolyticus* G431 with decreasing concentrations of **(A)** bacterial cells (substrate concentration = 2 mM) and **(B)** Cys-Gly-3M3SH (cell OD<sub>590</sub> = 5.0). Thioalcohol yield (A<sub>412</sub>) was quantified using DTNB after 24 h incubation period. Error bars represent standard deviation of three biological replicates.

### **3.5 Speciation of unknown axillary isolates by riboprofiling at Unilever Discover, Colworth**

A large library of axillary isolated bacteria has been collected and partially speciated at Unilever Discover, Colworth. Some unspciated isolates were to be included in subsequent screening assays and it was therefore necessary to speciate these unidentified isolates. Accordingly, 16S rDNA amplification followed by DNA sequence analysis was performed.

A detailed protocol can be found in section 2.3.1. Briefly, DNA was extracted from a single bacterial colony and used as a template to amplify a section of the 16S rDNA. The purified products were sequenced using an Applied Biosystems 3100X Genetic Analyzer. The read length of good quality sequencing data varied per sample from 400 to 500 nucleotides. A continuous read of at least 300 nucleotides of good quality sequence data (defined by a strong, defined peak) was used as a BLAST query against the pre-existing rDNA database. The highest matching BLAST hit for each individual bacterial isolate is displayed in Table 3.1. All top BLAST hits were unambiguous, meaning that the 16S rDNA nucleotide sequence matched the identified species more closely than any other species.

All unspciated corynebacteria (G501, G503, G511, G515, G516 and G517) were identified as *Corynebacterium amycolatum*. This correlates with the physical morphology of other *C. amycolatum* strains, which, when suspended in liquid, exhibit a non-homogenous clumping phenotype. This clumping phenotype appears to be unique to the *C. amycolatum* species of *Corynebacterium*, as all other species tested suspend homogenously in liquid medium.

Single species of *S. cohnii* (A01), *S. haemolyticus* (G431) and *S. hominis* (G323) were also identified.

**Table 3.1.** Speciation of axillary isolated corynebacteria and staphylococci identified via 16S rDNA sequence analysis. All top NCBI hits were unambiguous.

<b>Isolate</b>	<b>Consensus sequence length (nt)</b>	<b>Top NCBI hit</b>	<b>% identity</b>
G501	465	<i>Corynebacterium amycolatum</i> CIP103452	100
G503	465	<i>Corynebacterium amycolatum</i> CIP103452	100
G511	466	<i>Corynebacterium amycolatum</i> CIP103452	100
G515	465	<i>Corynebacterium amycolatum</i> CIP103452	100
G516	426	<i>Corynebacterium amycolatum</i> CIP103452	100
G517	402	<i>Corynebacterium amycolatum</i> CIP103452	100
A01	480	<i>Staphylococcus cohnii</i> subsp. <i>urealyticus</i> CK27	100
G323	445	<i>Staphylococcus hominis</i> subsp. <i>hominis</i> DM122	99
G431	476	<i>Staphylococcus haemolyticus</i> JCSC1435	99

### 3.6 Uptake and biotransformation of Cys-Gly-3M3SH by skin-isolated corynebacteria and staphylococci

Biotransformation of Cys-Gly-3M3SH by skin-isolated bacteria has never been investigated in detail, with the majority of studies using this substrate being limited to a handful of bacterial isolates (Starkenmann *et al.*, 2005, Emter & Natsch, 2008). With the relative contribution of corynebacteria and staphylococci to 3M3SH-based malodour under question (section 3.3), a comprehensive screen of multiple skin isolated bacteria is required to reveal active and non-active Cys-Gly-3M3SH biotransforming species. Accordingly, the Unilever-based library of skin-isolated bacteria was screened for Cys-Gly-3M3SH biotransformation ability, in a species-dependant manner.

Fig. 3.6.1A illustrates Cys-Gly-3M3SH biotransformation ability of multiple axilla-isolated *Corynebacterium* species. All individual species that were assessed are shown, and where multiple isolates of the same species were screened, a representative isolate of that species is displayed. Negligible 3M3SH generation ( $A_{412} < 0.075$ ) was observed for all *Corynebacterium* species with the exception of *C. amycolatum* G502, which displayed moderate 3M3SH yield ( $A_{412} = 0.1-0.2$ ). In total, negligible 3M3SH generation ( $A_{412} < 0.075$ ) was observed for 8 out of 8 isolates of *C. tuberculostearicum* (G438, G439, G440, G459, G464, G484, G485 and A06), 3 out of 3 isolates of *C. mucifaciens* (G435, G462 and G463), 2 out of 2 isolates of *C. afermentans* (G434 and G441), 1 out of 1 isolate of *C. appendicis* (G465) and 1 out of 1 isolate of *C. suicordis* (G460), following 24 h incubation (data not shown). Moderate 3M3SH yield ( $A_{412} = 0.1-0.2$ ) was observed for 7 out of 8 strains of *C. amycolatum* (G500, G501, G502, G503, G515, G516 and G517) and low 3M3SH yield was observed for *C. amycolatum* G511, following 24 h incubation.

Fig. 3.6.1B illustrates Cys-Gly-3M3SH biotransformation ability of multiple skin-isolated *Staphylococcus* species. All individual species that were assessed are shown, and where multiple isolates of the same species were screened, a representative isolate is displayed. In total, high 3M3SH generation ( $A_{412} > 0.2$ ) was observed for 9 out of 10 isolates of *S. hominis* (B10, G20, I4, J6, J11, J23, J27, J31 and W12), all of which are volar forearm isolates (Kelly, 2013), 2 out of 2 isolates of *S. haemolyticus* (G431 and W19) and 1 out of 1 isolates of *S. lugdunensis* (G310) following 24 h incubation. In most cases, high 3M3SH yield was observed following only 5 h incubation, suggesting efficient substrate biotransformation in these strains.

Moderate 3M3SH yield was observed for *S. cohnii* A01, whereas *S. cohnii* W17 displayed negligible 3M3SH yield. Similarly, negligible 3M3SH yield was observed for 13 out of 13 isolates of *S. epidermidis* (B01, G427, G428, G429, G430, G467, G468, G469, G470, G473, G474, G475 and G476), 3 out of 3 isolates of *S. saprophyticus* (B13, C06C and W14), and 2 out of 2 isolates of *S. capitis/S. caprae* (C07 and C15) (species discrimination not possible by previous riboprofiling analysis) following 24 h incubation.

In order to determine the kinetics of 3M3SH generation, a time-course of 3M3SH generation was performed with *S. hominis* B10. This isolate was chosen as it displays efficient Cys-Gly-3M3SH biotransformation. *S. hominis* B10 reaches maximum 3M3SH yield after approximately 4.5 h incubation (Fig. 3.6.2).

To confirm that the number of cells added to each reaction is not significantly different between corynebacteria and staphylococci, CFU counts were performed using bacteria at a starting OD<sub>590</sub> of 1.0. Average CFU counts for *S. hominis* B10 were  $9.03 \times 10^7$  CFU ml<sup>-1</sup> and for *C. jeikeium* K411 were  $6.44 \times 10^7$  CFU ml<sup>-1</sup>. This confirms that an OD<sub>590</sub> of 5 (added at the start of each reaction) represented approximately 25% more staphylococcal cells than corynebacteria. Although this slightly skews direct inter-genus comparison of thioalcohol yield, the all-or-nothing phenotype observed for the majority of strains would remain unaffected by this small difference in absolute number of cells in the assay.

At this point, analysis of staphylococci was switched from *S. haemolyticus* G431 to *S. hominis* B10. This was because, unlike *S. haemolyticus*, *S. hominis* represents a relatively prevalent species of *Staphylococcus* in the human axilla (Callewaert *et al.*, 2013). Characterisation of malodour production in *S. hominis* is therefore more closely associated to a physiological situation and subsequently collected data is more informative of the *in vivo* state.

Taken together, these data suggest that *S. hominis*, *S. haemolyticus*, and *S. lugdunensis* are the most efficient biotransformers of Cys-Gly-3M3SH, as they reach high 3M3SH yield after only 5 h incubation. Although *C. amycolatum* is able to partially biotransform Cys-Gly-3M3SH, it takes over 5 h to reach even a moderate yield, suggesting it is inefficient and likely insignificant in thioalcohol-based malodour relative to certain *Staphylococcus* species. The efficient Cys-Gly-3M3SH biotransformation ability and relatively high abundance of *S. hominis* in the human axilla (Callewaert *et al.*, 2013) makes it an appealing target for further biochemical characterisation of thioalcohol generation.

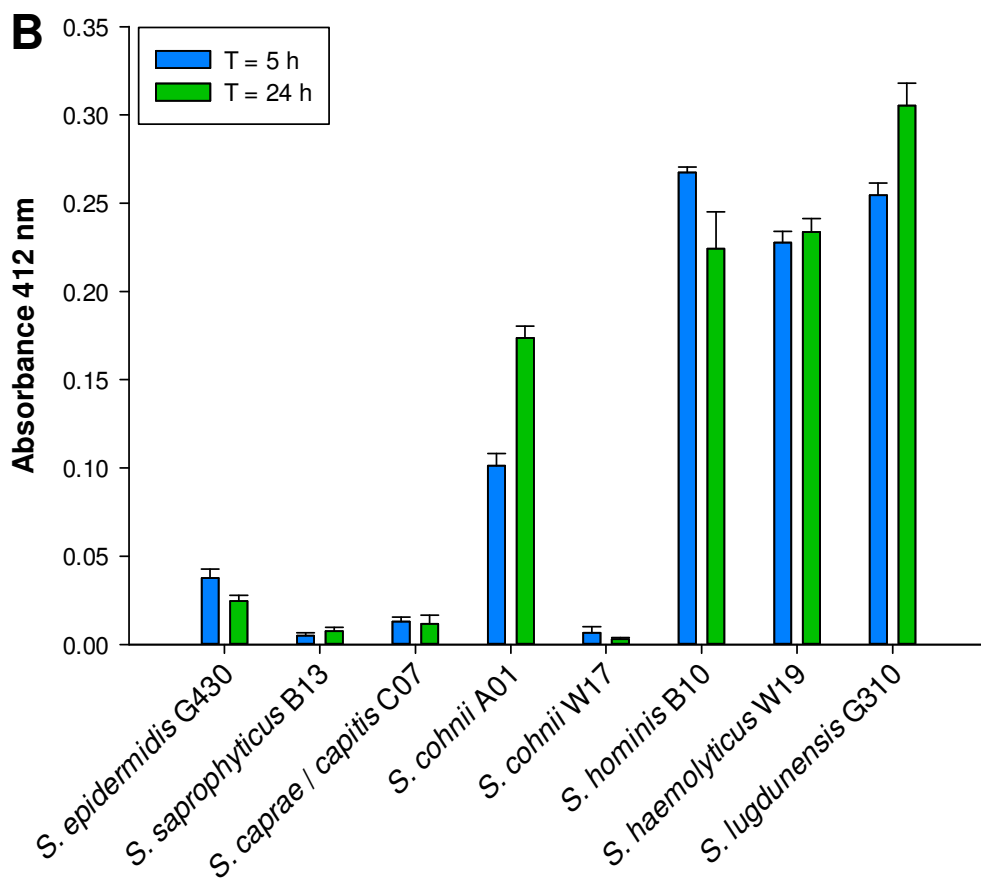
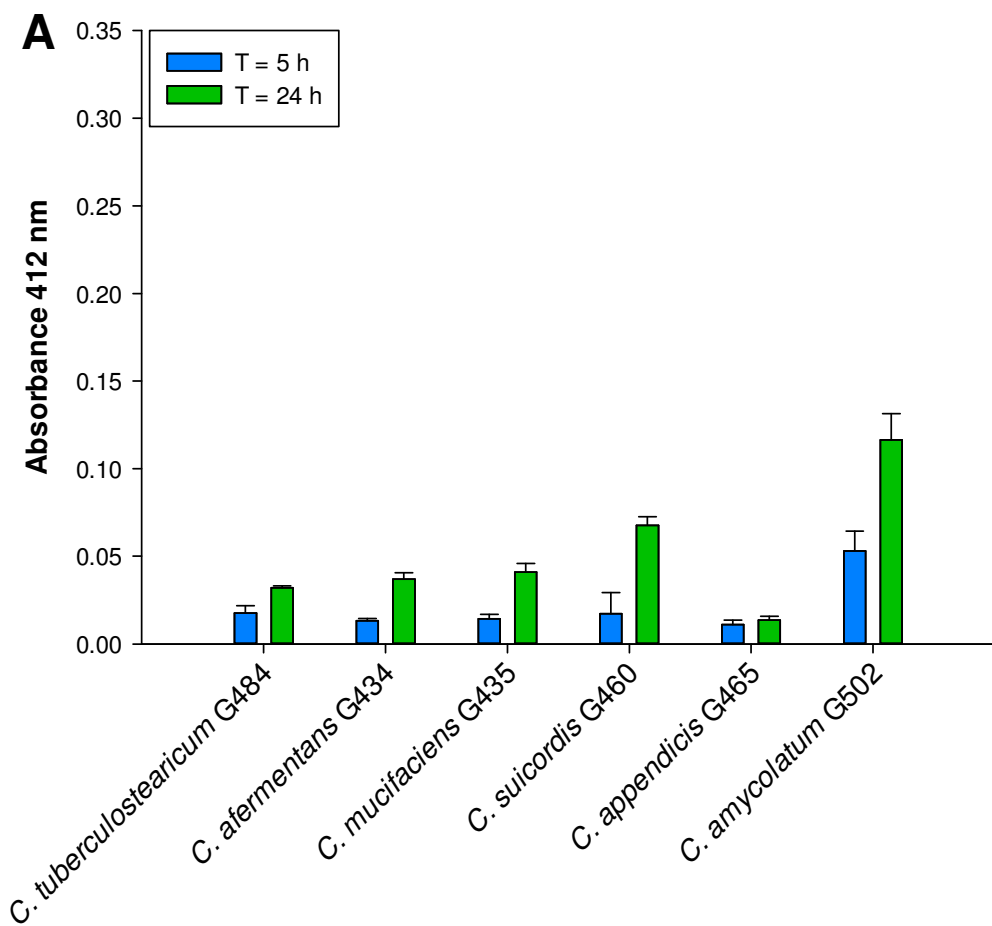


**Figure 3.6.1.** Biotransformation of Cys-Gly-3M3SH by representative isolates of **(A)** skin-isolated *Corynebacterium* spp. and **(B)** skin-isolated *Staphylococcus* spp. Thioalcohol yield ( $A_{412}$ ) was quantified for each isolate using DTNB after 5 h (blue bars) and 24 h (green bars) incubation periods. Error bars represent standard deviation of three biological replicates.

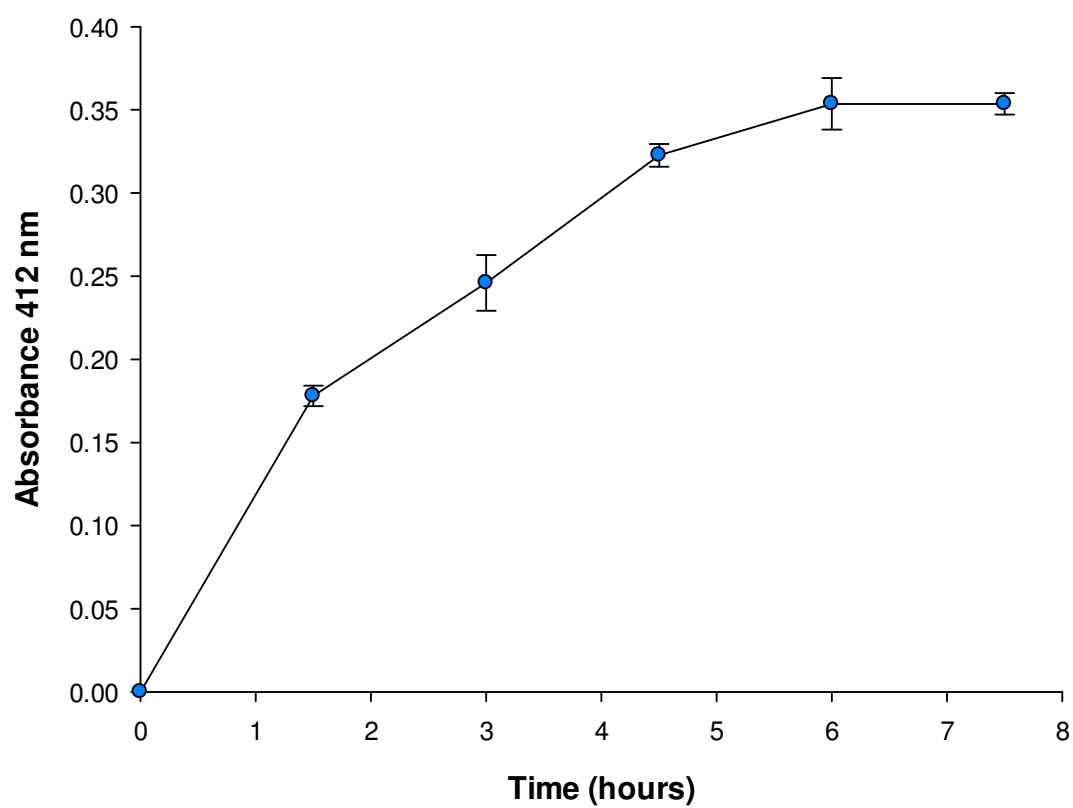


**Figure 3.6.2.** Time-dependent biotransformation of Cys-Gly-3M3SH by *S. hominis* B10. At each time point, thioalcohol yield ( $A_{412}$ ) was quantified using DTNB. Error bars represent standard deviation of three biological replicates.

### 3.7 Energetics of Cys-Gly-3M3SH uptake by *S. hominis* and *S. haemolyticus*

In order to characterise Cys-Gly-3M3SH uptake by *S. hominis* more comprehensively, an assessment of the energetic requirements of substrate uptake was performed. Based on the size of the molecule, it was hypothesised that Cys-Gly-3M3SH would be transported through a dedicated transport system, rather than passively diffuse across the bacterial cell membrane. To determine whether uptake of Cys-Gly-3M3SH is energy-dependent, the ability of several *S. hominis* isolates to biotransform the substrate in an energy-independent manner was assessed. Firstly, Cys-Gly-3M3SH biotransformation assays were carried out in the presence of the protonophore, carbonyl cyanide m-chlorophenyl hydrazone (CCCP). CCCP disrupts the proton motive force, effectively preventing symport of molecules across the membrane (Kaback *et al.*, 1974). In the presence of 100  $\mu\text{M}$  CCCP, 3M3SH generation was inhibited in all 9 *S. hominis* isolates along with *S. haemolyticus* isolate G431 (Fig. 3.7A). This suggests that Cys-Gly-3M3SH is transported through a secondary transport system, requiring the co-transport of a proton to facilitate substrate translocation into the cell.

Secondly, Cys-Gly-3M3SH biotransformation assays were repeated for several isolates in the presence of the ATPase inhibitor, sodium orthovanadate ( $\text{Na}_3\text{VO}_4$ ).  $\text{Na}_3\text{VO}_4$  was able to inhibit 3M3SH generation in 3 out of 3 *S. hominis* isolates along with *S. haemolyticus* G431 (Fig. 3.7B). Initially, this result contradicted the work carried out using CCCP and suggested that Cys-Gly-3M3SH may be taken up via an ABC transporter, which relies on ATP hydrolysis to drive substrate translocation across the membrane (Higgins, 2001). However,  $\text{Na}_3\text{VO}_4$  is also a strong inhibitor of pyridoxal phosphate (PLP)-dependent enzymes and may therefore act to inhibit intracellular catabolism of Cys-Gly-3M3SH via the proposed carbon-sulphur-lyase route. It is also possible that  $\text{Na}_3\text{VO}_4$  acted pleiotropically to disrupt other ATPase-dependent cellular processes, ultimately leading to inhibition of substrate biotransformation. A combination of these factors could explain why both CCCP and  $\text{Na}_3\text{VO}_4$  prevent 3M3SH generation in all strains tested.

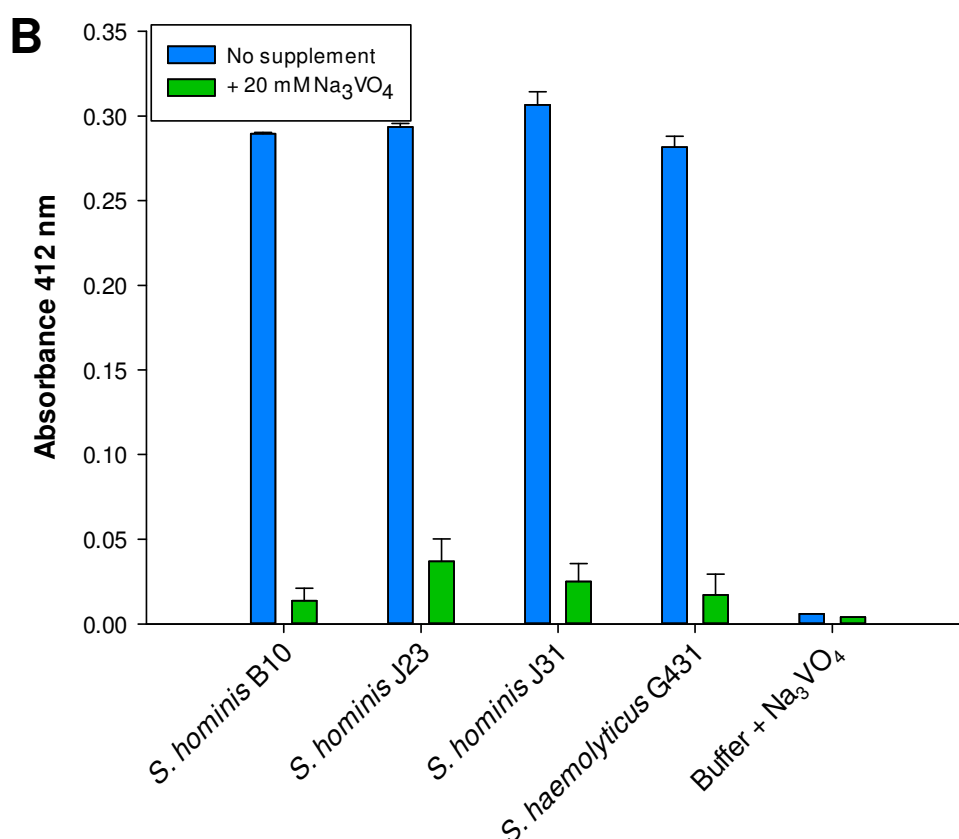
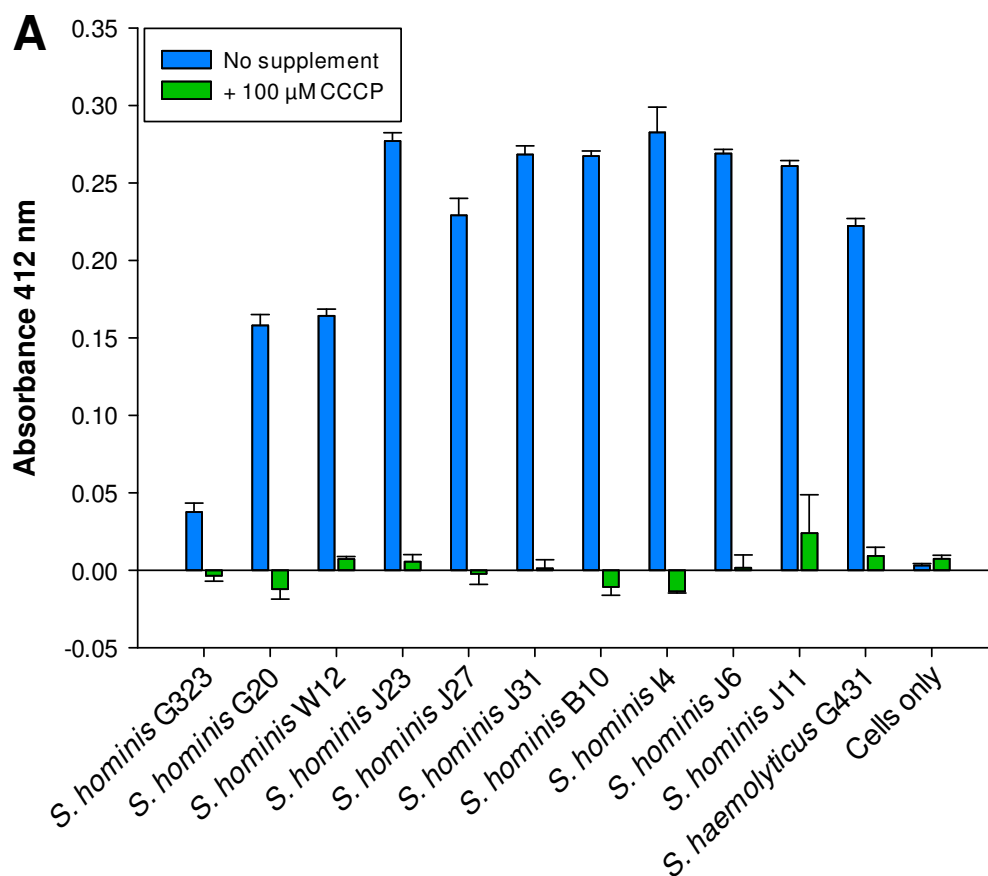


**Figure 3.7.** Biotransformation of Cys-Gly-3M3SH by *S. hominis* isolates in the presence (green bars) or absence (blue bars) of (A) 100  $\mu$ M CCCP or (B) 20 mM  $\text{Na}_3\text{VO}_4$ . Thioalcohol yield ( $A_{412}$ ) was quantified using DTNB after 5 h (for CCCP) or 24 h (for  $\text{Na}_3\text{VO}_4$ ). For CCCP data,  $A_{412}$  values were normalised against an incubated reaction containing 2 mM substrate, 100  $\mu$ M CCCP and reaction buffer to account for intrinsic absorbance of CCCP at 412nm. Error bars represent standard deviation of three biological replicates.

### 3.8 Preparation and characterisation of staphylococcal whole cell lysate for malodour precursor biotransformation assays

To determine whether non-Cys-Gly-3M3SH biotransforming bacteria have the enzyme(s) required to biotransform Cys-Gly-3M3SH, whole cell bacterial lysate was prepared from two isolates. It was hypothesised that within the crude cell extract, the enzymes required to biotransform Cys-Gly-3M3SH would be present. If crude cell extract from non-3M3SH generating bacteria was able to biotransform Cys-Gly-3M3SH then the defect in substrate biotransformation ability of these strains must be at the level of substrate uptake.

Accordingly, soluble crude cell extract was generated from *S. hominis* B10 and *S. epidermidis* G428 using lysostaphin-mediated cell lysis (for protocol see section 2.2.11.6). Lysostaphin is a glycyl-glycyl metalloendopeptidase capable of cleaving glycine-crosslinks in the cell wall of staphylococci (Schroeder *et al.*, 2009) and has been routinely used to generate staphylococcal crude cell lysate for DNA and RNA extraction.

Cys-Gly-3M3SH and S-Benzyl-L-cysteine biotransformation assays were performed using either whole bacterial cells (final concentration  $OD_{590} = 5.0$ ) or crude cell extract (normalised to an equivalent of whole cell  $OD_{590} = 5.0$ ). S-Benzyl-L-cysteine biotransformation assays were carried out as it has been demonstrated that purified C-S- $\beta$ -lyase (a soluble cytoplasmic protein) from *C. jeikeium* K411 is sufficient to biotransform S-Benzyl-L-cysteine into its cognate thioalcohol, benzyl-mercaptan (James *et al.*, 2013). S-Benzyl-L-cysteine biotransformation assays were therefore expected to act as a positive control for cell lysate activity.

Soluble cell extract from both *S. hominis* B10 and *S. epidermidis* G428 was unable to biotransform S-Benzyl-L-cysteine (Fig. 3.8A). Similarly, no activity against Cys-Gly-3M3SH was observed (Fig. 3.8B). The addition of protease inhibitors during cell lysate preparation had no impact on substrate biotransformation activity (data not shown).

Taken together, these data demonstrate that there is no intrinsic activity of soluble cell extract from *S. hominis* B10 or *S. epidermidis* G428 against S-Benzyl-L-cysteine or Cys-Gly-3M3SH. By lysing the cells, the ability to intracellularly concentrate the substrate is removed, which could be an important factor that prevents substrate biotransformation. Alternatively, the concentration of enzyme(s) within the cell extract required to biotransform these substrates may be insufficient due to normalisation of lysate volume against a cellular optical density rather than against total protein concentration.

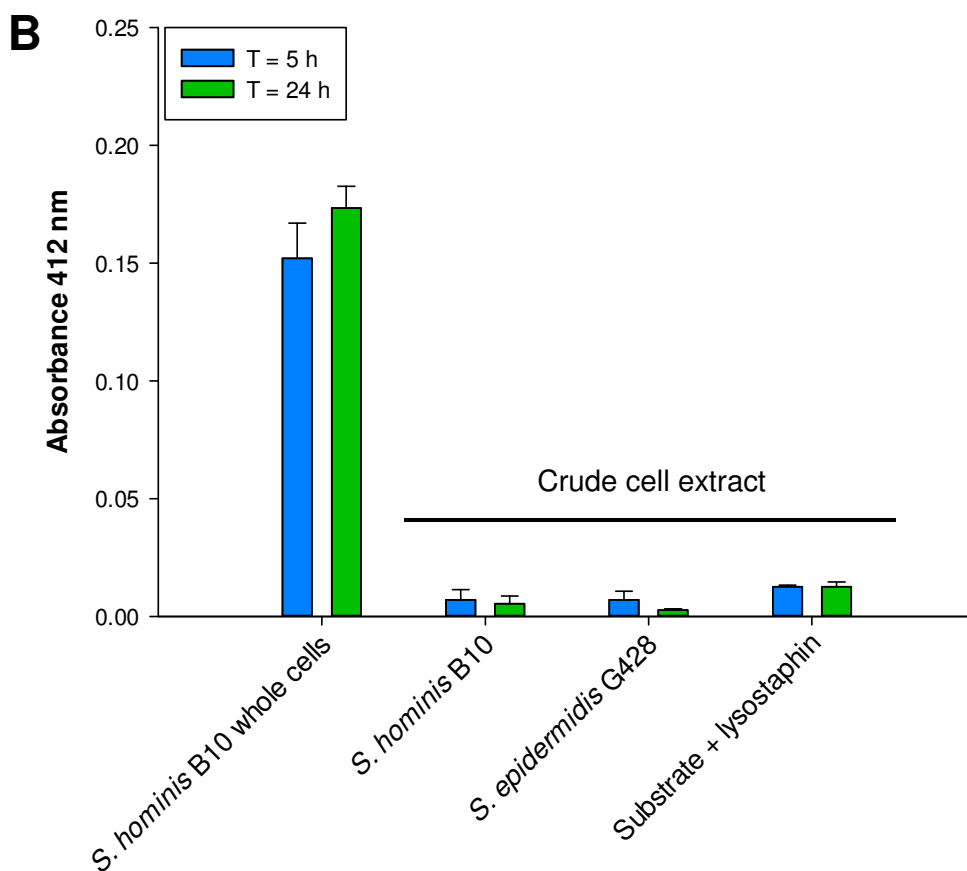
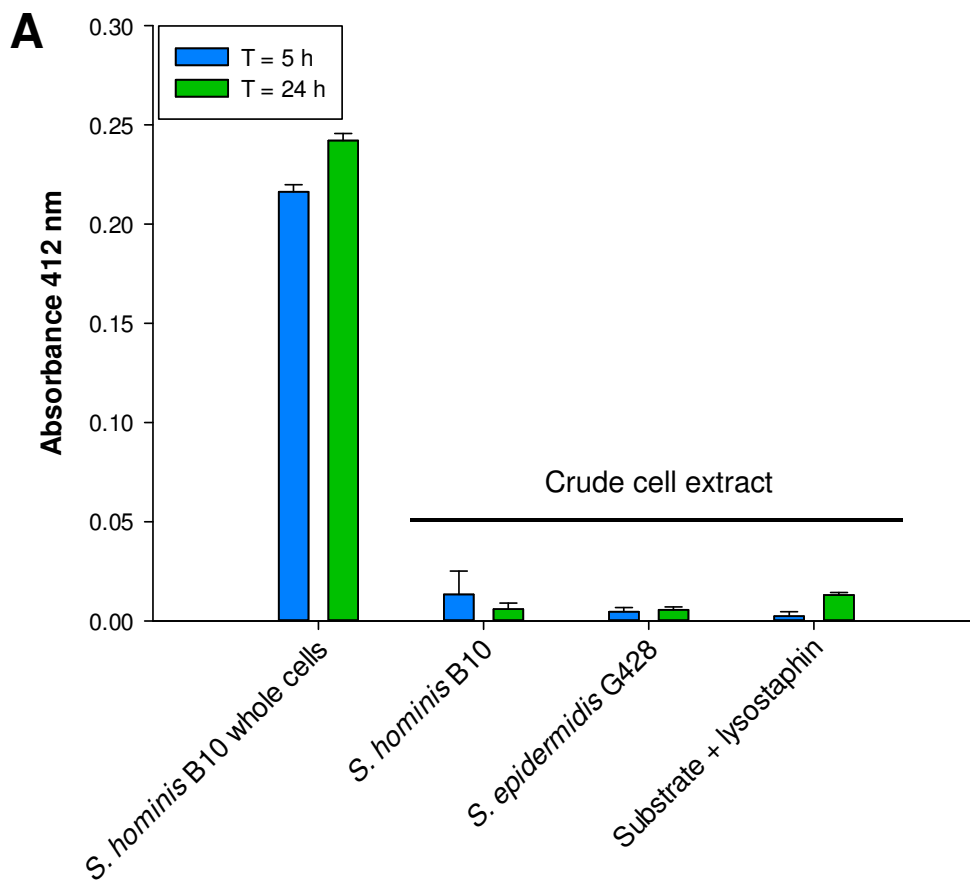


**Figure 3.8.** Biotransformation of **(A)** S-Benzyl-L-cysteine and **(B)** Cys-Gly-3M3SH by *S. hominis* B10 (whole cells and crude cell extract) and *S. epidermidis* G428 crude cell extract. Thioalcohol yield ( $A_{412}$ ) was quantified using DTNB after 5 h and 24 h incubation. Error bars represent standard deviation of three biological replicates.

### 3.9 Competitive inhibition of Cys-Gly-3M3SH biotransformation in *S. hominis* B10

Active transport of Cys-Gly-3M3SH was demonstrated in section 3.7 and it was hypothesised that Cys-Gly-3M3SH would be transported in *S. hominis* (and other Cys-Gly-3M3SH biotransforming bacteria) by a peptide transporter. Additionally, the intracellular catabolic enzyme(s) would also likely recognise the peptide backbone of the substrate. Small di- and tripeptides could therefore potentially inhibit Cys-Gly-3M3SH biotransformation, either by blocking substrate uptake or by preventing intracellular substrate catabolism.

Accordingly, several small peptide-based molecules and their respective single amino acid building blocks were screened for ability to prevent 3M3SH generation in *S. hominis* B10. All competitor molecules were added at 20 mM, representing a 10-fold excess of competitor to substrate.

Several dipeptides including Phe-Ala, Ala-Phe, Ala-Tyr-Tyr-Ala, Leu-Ala, Ala-Leu, Gly-Phe and Ala-Ala were able to completely inhibit 3M3SH generation in *S. hominis* B10 (Fig. 3.9.1A). Gly-Gly and Gly-His also inhibited 3M3SH generation by  $62\% \pm 3\%$  and  $76\% \pm 2\%$  respectively, following 5 h incubation. Gly-Ser slightly increased 3M3SH yield. The single amino acid constituents of these dipeptides, L-Phe, L-Ala, L-Leu and Gly had little observable effect on 3M3SH generation (Fig. 3.9.1B). L-Met inhibited 3M3SH generation by  $77\% \pm 2\%$ . L-Tyr and L-His could not be included due to solubility issues.

Several L-Lys-containing tripeptides were also strong inhibitors of 3M3SH generation in *S. hominis* following 5 h incubation. The most effective tripeptide, Lys-Lys-Met completely inhibited 3M3SH generation (Fig. 3.9.2A). Strong inhibition was also observed for Lys-Phe-Lys ( $76\% \pm 2\%$ ), Lys-Lys-Tyr ( $61\% \pm 2\%$ ), Lys-Lys-Ala ( $60\% \pm 7\%$ ) and Gly-Gly-Gly ( $57\% \pm 3\%$ ). Moderate inhibition was observed for Lys-Pro-Lys ( $39\% \pm 6\%$ ). No significant inhibition was observed for Lys-Arg-Lys.

Other compounds tested for inhibition of Cys-Gly-3M3SH biotransformation that had no observable effect on 3M3SH generation following 5 h incubation included D-glucose, S-methylglutathione, S-methyl-L-cysteine and biotin (Fig. 3.9.2B). As expected, N-lauroylsarcosine, an ionic surfactant, completely inhibited 3M3SH generation. Interestingly, 4-aminomethylbenzoic acid (AMBA), a known inhibitor of peptide symporters (Meredith *et al.*, 1998), reduced 3M3SH generation by ( $47\% \pm 3\%$ ) following

5 h incubation. This data supports the notion that in staphylococci, uptake of Cys-Gly-3M3SH may be mediated by a general peptide symporter.

For the majority of molecular inhibitors, the level of inhibition remained constant over the 24 h time period. This suggests that either the inhibitor compound is not metabolised by the bacteria, or, more likely, given the diverse range of effective small peptide inhibitors, that the concentration of inhibitor compound in the reaction remains sufficiently high regardless of continuous turnover by bacterial metabolism.

It is a realistic assumption that small peptides could inhibit either the putative Cys-Gly-3M3SH transporter or the intracellular enzymatic machinery required for biotransformation of the substrate but unfortunately it is not possible to distinguish the precise inhibitory targets of these molecules using this assay.

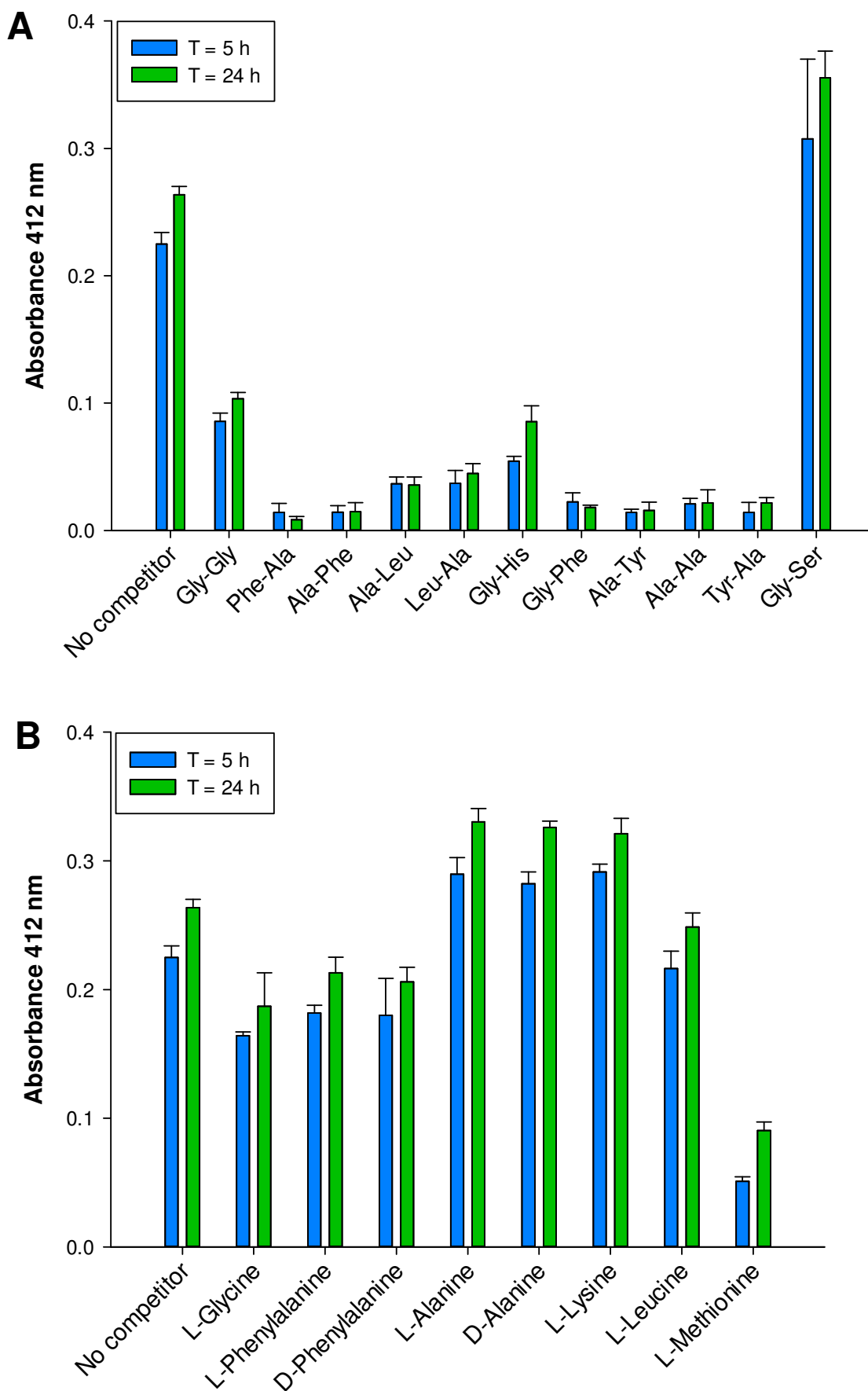


**Figure 3.9.1.** Biotransformation of Cys-Gly-3M3SH by *S. hominis* B10 isolate in the presence of 20 mM (10-fold excess) (A) dipeptides and (B) amino acids. Unless stated, all amino acids and peptides used were the L- isoform. Thioalcohol yield ( $A_{412}$ ) was quantified using DTNB after 5 h and 24 h incubation. Error bars represent standard deviation of three biological replicates.

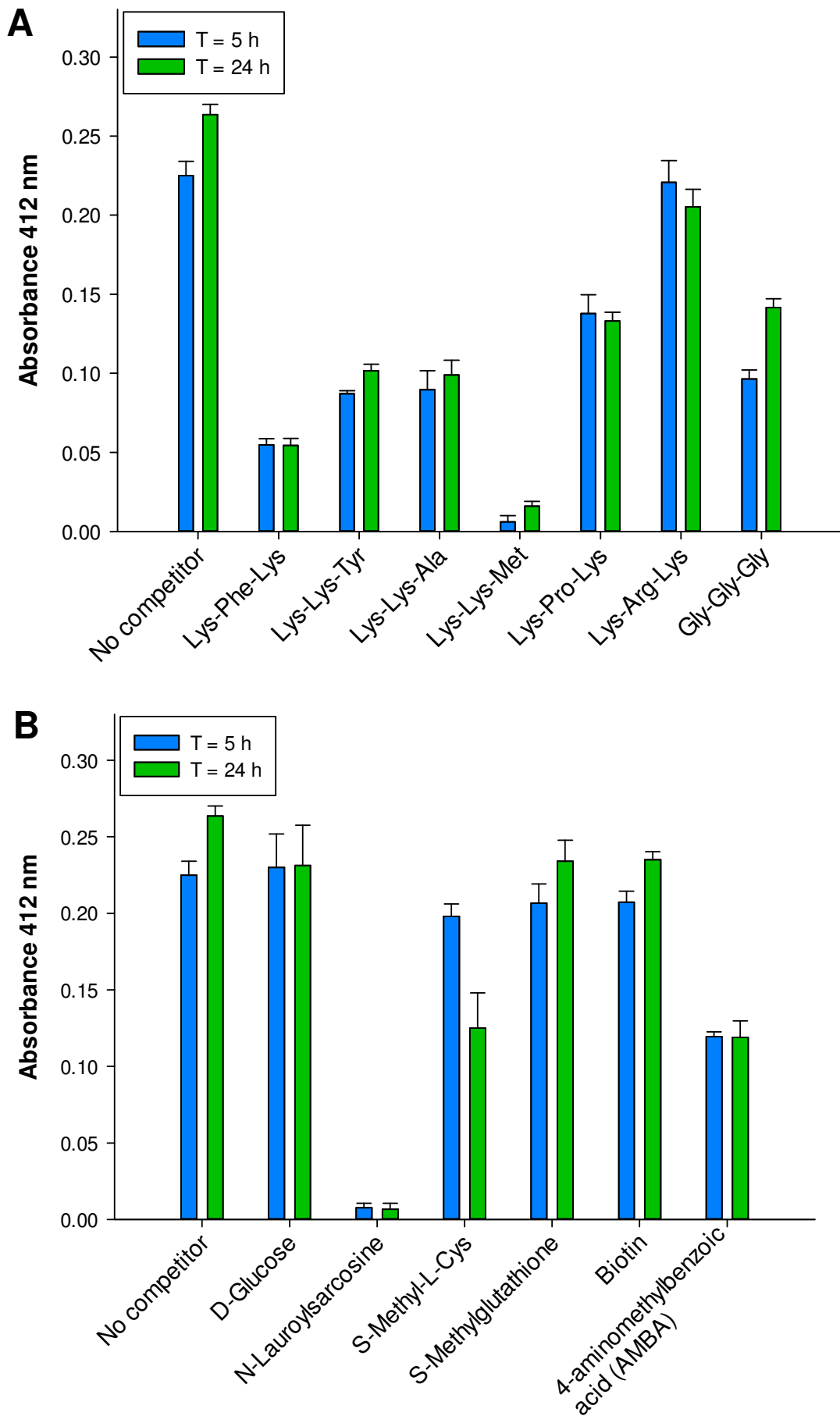


**Figure 3.9.2.** Biotransformation of Cys-Gly-3M3SH by *S. hominis* B10 isolate in the presence of 20 mM (10-fold excess) **(A)** tripeptides and **(B)** other small molecule competitors. All peptides used were the L- isoform. Thioalcohol yield ( $A_{412}$ ) was quantified using DTNB after 5 h and 24 h incubation. Error bars represent standard deviation of three biological replicates.

### 3.10 Discussion

In this chapter, the C-S-  $\beta$ -lyase activity of several bacterial species was confirmed using a pre-existing Unilever assay to measure released benzyl-mercaptan from the model dipeptide malodour precursor substrate S-Benzyl-L-cysteinylglycine. The analysis revealed that the majority of corynebacteria (both axillary-isolated and type/culture collection strains) were able to biotransform S-Benzyl-L-cysteinylglycine relatively efficiently. This is in general agreement with previous studies that assessed biotransformation of a similar model malodour precursor substrate, S-Benzyl-L-cysteine. For example, it was demonstrated by Natsch *et al.* (2004), that biotransformation of S-Benzyl-L-cysteine is carried out by multiple *Corynebacterium* isolates and release of benzyl-mercaptan is attributable to cystathionine  $\beta$ -lyase in this genus. Purified C-S-  $\beta$ -lyase from *Corynebacterium* isolate Ax20 was shown to cleave S-Benzyl-L-cysteine even more efficiently than its natural substrate cystathionine, demonstrating the important role of this enzyme in thioalcohol generation from model malodour precursor substrates. This observation was corroborated by James *et al.* (2013), who demonstrated that of 28 individual *Corynebacterium* isolates, 67% were C-S-  $\beta$ -lyase positive, whereas only 3 out of 17 *Staphylococcus* strains (17%) isolated from the same environmental niche, displayed the same activity. These collective observations strongly implicated corynebacteria in thioalcohol-based malodour until, in this study, a biochemical assay was developed to detect 3M3SH, the thioalcohol product of the physiological malodour precursor molecule, Cys-Gly-3M3SH. Using this assay, Unilever's library of axillary isolates was screened for Cys-Gly-3M3SH biotransformation activity. The expectation was that strong Cys-Gly-3M3SH biotransformation by axillary isolated bacteria would be attributable to *Corynebacterium* spp., based on the general association of this genus with malodour. This assumption proved to be inaccurate, as, generally speaking, all *Corynebacterium* isolates tested displayed weak to moderate Cys-Gly-3M3SH biotransformation. This raises important considerations regarding the use of model substrates in analysis of biochemical processes, as the pattern of biotransformation of model (S-Benzyl-L-cysteine and S-Benzyl-L-cysteinylglycine) versus physiological (Cys-Gly-3M3SH) malodour precursor substrates was completely different in this instance.

Although this was the first example of a large-scale screen of Cys-Gly-3M3SH biotransformation by bacteria, weak Cys-Gly-3M3SH biotransformation by corynebacteria is not completely unprecedented. It was demonstrated by Emter & Natsch (2008) that crude cell lysate prepared from three discrete axillary-isolated strains of *C. jeikeium* and a single *C. bovis* isolate was unable to biotransform Cys-Gly-3M3SH to a significant yield. In contrast, however, the same report illustrated that crude cell lysate of *Corynebacterium*

isolate Ax20 was able to generate >60% 3M3SH yield from biotransformation of Cys-Gly-3M3SH, suggesting that Ax20 is involved in Cys-Gly-3M3SH biotransformation in the human axilla. Despite this observation, in the whole cell Cys-Gly-3M3SH biotransformation assay presented here (Fig. 3.3), Ax20 produced <30% 3M3SH yield compared to an efficient Cys-Gly-3M3SH biotransformer, *S. hominis* B10. Interestingly, however, whole cell lysate from *S. hominis* B10 was completely unable to biotransform Cys-Gly-3M3SH (Fig. 3.8B). These collective observations imply two things. Firstly, that *S. hominis* and *Corynebacterium* sp. Ax20 may employ different enzymes to catabolise this substrate. This hypothesis is based on the observation that the intracellular enzyme(s) utilised by *S. hominis* to biotransform Cys-Gly-3M3SH were not recovered during cell lysate preparation, or were inactive during the assay, whereas the necessary enzymes from Ax20 were clearly recovered by Emter & Natsch (2008) using a similar cell lysate recovery procedure. No attempt was made here to recapitulate the results of Emter and Natsch by preparing whole cell extract from Ax20 due to the general difficulty in working with this strain *in vivo*, along with the consideration that Ax20 does not represent a highly prevalent axillary isolate. Secondly, given that whole cell lysate but not whole cells of Ax20 is able to biotransform Cys-Gly-3M3SH, it is likely that Ax20 is unable to transport Cys-Gly-3M3SH into the cytoplasm, a process which is clearly not required in the crude cell lysate assay but which is necessary *in vivo* and also in the physiological environment of the bacterium. Therefore, despite the report by Emter & Natsch that *Corynebacterium* isolate Ax20 possesses a set of enzymes necessary to biotransform Cys-Gly-3M3SH, in a physiological setting, Ax20 is unlikely to be a significant contributor to 3M3SH generation.

The general inability of corynebacteria to biotransform Cys-Gly-3M3SH is surprising, given the overall prevalence of this genus in the human axilla. It was reported by Taylor *et al.* (2003) that aerobic coryneforms were present in the axilla of >90% of individuals (n=61) and were the dominant bacterial genus in 35% of these axillae. Taylor also proposed that unlike staphylococci, corynebacteria have a high general association with malodour intensity, particularly at high population densities, as determined by an axillary malodour scoring system. As discussed in chapter 1, the biochemical basis for this remains undetermined.

The species-wide analysis of Cys-Gly-3M3SH biotransformation presented here revealed three species of bacteria which were able to actively transport and efficiently biotransform this substrate: *S. haemolyticus*, *S. hominis* and *S. lugdunensis*. Starkenmann *et al.* (2005) previously reported that an axillary-isolated strain of *S. haemolyticus* was able to efficiently biotransform synthetic Cys-Gly-3M3SH with a final 3M3SH yield of 75%. This is in agreement with the high Cys-Gly-3M3SH biotransformation activity of *S. haemolyticus*

G431 observed in this study. The ability of *S. lugdunensis* to biotransform Cys-Gly-3M3SH has not been previously reported, nor has the prevalence of this species on human skin. Interestingly, *S. lugdunensis* was not described as a taxon until 1988. The most phenotypically related species to *S. lugdunensis* is *S. hominis*, suggesting that in bacterial identification studies prior to 1988, *S. lugdunensis* may have been grouped with *S. hominis*. This could explain why there are no early reports of *S. lugdunensis* as an axillary commensal or as an active malodour producer. In contrast, *S. hominis* has been known as a major skin commensal since the mid-1970's (Kloos and Schleifer, 1975). A report by Kloos & Musselwhite (1975) that assessed the relative distribution of bacteria on human skin concluded that of all species of staphylococci present in the axilla, generally speaking, the population density of *S. hominis* is second only to that of *S. epidermidis*. Reports of malodour precursor biotransformation by *S. hominis* are not widespread in the literature, with the only notable report by Egert *et al.* (2013) identifying a putative *S. hominis* isolate as the most efficient staphylococcal biotransformer of the model malodour precursor substrate, S-Benzyl-L-cysteine. Given that 90% of *S. hominis* strains tested here were strong biotransformers of Cys-Gly-3M3SH (Fig. 3.7A), coupled with their high population density in the human axilla, it is reasonable to suggest that *S. hominis* represents an important microbial species in terms of thioalcohol-based malodour.

It was interesting to note that of the two isolates of *S. cohnii* assessed, isolate A01 was a strong biotransformer of Cys-Gly-3M3SH whereas isolate W17 was weak. Little is known about the axillary malodour potential of *S. cohnii*, as this organism has not been routinely studied. It is weakly associated with a common foot malodour pathway, converting small amounts (16.2% mol:mol) of L-leucine to isovaleric acid (James *et al.*, 2012) but not as strongly as other staphylococci such as *S. capitis*, which displayed an 80% mol:mol yield under the same conditions. The discordance of Cys-Gly-3M3SH biotransformation between *S. cohnii* A01 and W17 and the all-or-nothing phenotype suggests that A01 possesses a gene which is essential for Cys-Gly-3M3SH biotransformation and which is absent from isolate W17. In order to characterise Cys-Gly-3M3SH biotransformation in *S. cohnii* in more detail, both strains could be genome sequenced and compared for the presence or absence of putative Cys-Gly-3M3SH biotransformation genes, or single nucleotide polymorphisms (SNPs). However, given that *S. cohnii* appears to be a minor axillary commensal species (Kloos and Musselwhite, 1975) it is unlikely to be a major contributory organism to thioalcohol-based malodour in the axilla.

All strains of *S. epidermidis* tested here (13 out of 13) were negative for Cys-Gly-3M3SH biotransformation. This observation does not support the report by Starkenmann *et al.* (2005) which demonstrated that an axillary isolated *S. epidermidis* was able to

biotransform Cys-Gly-3M3SH to a final yield of 17%. Although 3M3SH yield was relatively low, a final yield of 17% would still be recognised as biotransformation activity in this study. This discordance likely results from isolation of non-clonal *S. epidermidis* isolates by Starkenmann and Unilever, respectively, but the negligible Cys-Gly-3M3SH biotransformation by multiple *S. epidermidis* isolates assessed here suggests that even moderate Cys-Gly-3M3SH biotransforming *S. epidermidis* are the exception rather than the rule. This conclusion is also supported by Emter & Natsch (2008) who demonstrated that whole cell extracts from various staphylococci, including that of an axillary isolated strain of *S. epidermidis* were unable to biotransform Cys-Gly-3M3SH. This phenotype is notable given the domineering prevalence of *S. epidermidis* over other *Staphylococcus* species in the human axilla (Kloos & Musselwhite, 1975). The high microbial density of *S. epidermidis* over other staphylococci in the axilla, coupled with the evident inability of this species to biotransform Cys-Gly-3M3SH is an attractive basis for a unique area of research; deodorant probiotics. This area has received little to no attention in the literature, perhaps due to the arrival of a United States patent by Banowski *et al.* (2007). Banowski proposed a method for promoting growth of non-malodorous bacterial species in the axilla using a variety of naturally occurring compounds extracted from a variety of plants including grapes (*Vitis viticola*), white tea (*Camellia sinensis*) and myrrh (*Commiphora myrrh*). The group claim that such compounds promote the growth or physiological activity of non-odour producing bacteria while at the same time reducing or at least not promoting the growth of odour-producing bacteria. The fundamental basis of this innovation is to allow non-odour producing bacteria to thrive and ultimately out-compete their odour-forming counterparts. Despite the novelty and originality of the proposal, to this date, no mainstream probiotic deodorants have entered the market.

Overall, it seems that *S. haemolyticus*, *S. hominis* and *S. lugdunensis* have specifically evolved the Cys-Gly-3M3SH biotransformation trait, rather than it being a biological side effect of another, more important biochemical process common to all staphylococci. This conclusion is based on the evidence provided here that this functionality is only present in a small group of phylogenetically related staphylococci and is not widespread within the genus as a whole, although the entire staphylococcal species diversity was not screened in this study. The most parsimonious explanation for a bacterium to evolve Cys-Gly-3M3SH biotransformation ability is that it allows the organism to utilise the molecule as a nutrient supplement by providing a unique carbon and nitrogen source. The ability to transport and biotransform Cys-Gly-3M3SH is likely to present the bacterium with a fitness advantage by providing an exclusive substrate for growth within the human axilla.

Further studies on the representative *S. hominis* isolate B10 revealed that 3M3SH production could be prevented by a range of di- and tripeptides (Fig. 3.9.1 & 3.9.2). As it is known that a transport step and at least one intracellular catabolism step is required to liberate 3M3SH from Cys-Gly-3M3SH the exact site of action of the peptide inhibitors is unknown. Gram-negative bacteria such as *E. coli* encode a plethora of peptidases which are able to cleave cysteinylglycine (Suzuki *et al.*, 2001) along with a diverse range of other peptide substrates (Miller and Schwartz, 1978). Therefore, peptide competitor molecules could feasibly prevent 3M3SH production by inhibiting broad substrate specificity staphylococcal peptidases or other enzymes involved in intracellular Cys-Gly-3M3SH biotransformation. However, there is also indirect evidence that peptide transporter(s) of *S. aureus* have broad substrate specificity. This conclusion was drawn when it was noted that uptake of the peptide antibiotic bacilysin is inhibited by a wide range of di- and tripeptide competitor molecules (Perry & Abraham, 1979). It is therefore attractive to hypothesise that peptide competitor molecules, rather than inhibit intracellular substrate catabolism, directly interact with the binding site of the specific Cys-Gly-3M3SH transporter, preventing uptake of the malodour precursor molecule into the cell. Given that transport occurs before intracellular substrate catabolism, competitive inhibition of Cys-Gly-3M3SH uptake by blocking access to the transport protein is the preferred postulate.

It was also interesting to note that L-methionine inhibited Cys-Gly-3M3SH biotransformation in *S. hominis* B10 by 75% (Fig. 3.9.1B). Since all staphylococcal cystathionine  $\beta$ -lyases belong to the MetC sub-group (James *et al.*, 2013), this observation indirectly suggests a role for this C-S-  $\beta$ -lyase in malodour precursor biotransformation in *S. hominis*. This hypothesis is supported by the fact that MetC is involved in cellular methionine biosynthesis (Awano *et al.*, 2003) and expression of *metC* (in *E. coli*) is repressed by L-methionine (Rowbury & Woods, 1964). The strong inhibition of Cys-Gly-3M3SH biotransformation by L-methionine observed here therefore provides indirect evidence that MetC of *S. hominis* B10, or a similar enzyme whose expression is also repressed by L-methionine, is involved in malodour precursor biotransformation.

The discovery of *S. hominis* as a strong thioalcohol producer means that this organism now becomes the focus for identification of the staphylococcal Cys-Gly-3M3SH transporter. Unfortunately, there are few biological tools available for genetic manipulation in *S. hominis* and more importantly no easily accessible gene deletion protocol. Since Cys-Gly-3M3SH is likely transported by a peptide transporter owing to the dipeptide backbone of the molecule, understanding the biological basis of peptide transport in the model organism *E. coli* K-12 is an appropriate starting point to gain insight into

fundamental peptide (and subsequently Cys-Gly-3M3SH) transport in the relevant bacteria.

# **Chapter 4**

## **Creation and characterisation of peptide transporter deficient strains of *E. coli* K-12**

## Introduction and aims

The direct application of *E. coli* as a model organism to study malodour production, specifically the molecular mechanism behind dipeptide-malodour precursor uptake and biotransformation, has not been attempted before. As uptake is likely to occur via a specific peptide transporter with the ability to transport dipeptide analogues, it is important to firstly understand fundamental peptide transport in this organism. *E. coli* expresses both ABC peptide transporters (Dpp and Opp) and several peptide symporters including DtpA, DtpB, DtpC and DtpD (section 1.5.2). Accordingly, individual and multiple peptide transporter-specific genes will be deleted, including the ABC transporters *opp* and *dpp*, along with the aforementioned Dtp peptide symporters. These peptide transporter-deficient (TD-Pep) strains of *E. coli* K-12 will then be characterised in terms of their ability to transport specific peptide molecules. This will aid in providing a comprehensive overview of peptide transporter biology in this well-studied bacterium, particularly for the less well-characterised Dtp transporters.

## Specific aims

- To assess the phylogenetic relationship between *E. coli* Dtp peptide symporters and PTR-family homologues in both prokaryotes and eukaryotes.
- To create individual chromosomal deletions in the following genes of *E. coli* K-12: *oppC*, *dppC*, *dtpA*, *dtpB*, *dtpC* and *dtpD*.
- To create multiple chromosomal deletions in the ABC- and peptide symporter systems of *E. coli* K-12, specifically a double mutant  $\Delta oppC \Delta dppC$  and a quadruple mutant  $\Delta dtpA \Delta dtpB \Delta dtpC \Delta dtpD$ .
- To characterise these mutants in terms of their ability to grow in minimal medium supplemented with specific dipeptides as a sole nutrient source.
- To characterise these mutants in terms of their ability to grow in a complex media consisting of mixed di- and oligopeptides as the sole nutrient source.

#### 4.1 Genome-wide phylogenetic analysis of Dtp-like proteins across the bacterial kingdom

Although high affinity peptide transport via the Opp and Dpp peptide transport systems in *E. coli* has been investigated in detail (see section 1.5.2.1), only a limited number of studies have examined the role of the MFS superfamily peptide transporters in this organism. *E. coli* possesses multiple MFS peptide transporters, of which four, DtpA, DtpB, DtpC and DtpD, are members of the PTR family (see section 1.5.2.2). The phylogenetic relationship between Dtp proteins from *E. coli* and other selected bacteria was assessed. Each *E. coli* Dtp protein was used as a Basic Local Alignment Search Tool (BLAST) query to identify the closest homologues in other bacteria. The inclusion of an individual organism in the final analysis was dependent upon that bacterium having at least one orthologue of an *E. coli* K-12 Dtp protein. An orthologue was defined as a protein identified in the original BLAST search that corresponded to the original query (DtpA, DtpB, DtpC or DtpD) when a reciprocal BLAST search was performed. Although Gammaproteobacteria represented the principal bacterial class in this analysis, representative organisms from diverse classes and phyla were also included, along with representatives with known structure such as the peptide transporter PepT<sub>SO</sub> from *Shewanella oneidensis* (Newstead *et al.*, 2011) and the human intestinal peptide transporter hPEPT1, which, when sequence aligned with bacterial Dtp proteins, shows the strongest identity to DtpA (24% identity at the amino acid level).

Fig. 4.1 shows the phylogenetic relationship between bacterial Dtp transport proteins. Where an organism is present in one clade but absent from another, there is no clear orthologue of that respective Dtp protein in that bacterium. The majority of Gammaproteobacteria have at least one orthologue of a Dtp transport protein, but the precise number of Dtp proteins varies between 1 (for example *Vibrio cholera* HE-09 and *Yersinia pestis* strain Angola) to 5 (for example *Klebsiella oxytoca* KCTC 1686 and *Klebsiella pneumoniae* KCTC2242). Each Dtp protein falls into a specific clade, with DtpA and DtpB forming a sub-clade and DtpC and DtpD likewise. DtpC and DtpD are clearly a more recent duplication than DtpA and DtpB. The presence of multiple Dtp proteins is almost exclusive to Gammaproteobacteria, with only a single example of a Dtp protein in representative Epsilonproteobacteria (*Campylobacter jejuni jejuni* PT14 and *Helicobacter mustelae* 12198), Alphaproteobacteria (*Acetobacter tropicalis* NBRC 101654), Betaproteobacteria (*Burkholderia terrae* BS001 and *Chromobacterium violaceum* ATCC 12472) and Deltaproteobacteria (*Desulfovibrio salexigens* DSM 2638 and *Lawsonia intracellularis* MN1-00). Of the non-Gammaproteobacteria, only *C. violaceum* has an orthologue of DtpA. All representative Proteobacteria with the exception of the

Epsilonproteobacteria have an orthologue of DtpB. The DtpC and DtpD expansion appears to be unique to the Gammaproteobacteria, although not all Gammaproteobacteria have a DtpC protein, *S. boydii* is a notable example.

The DtpE clade appears to be a further expansion of the Dtp proteins in the Gammaproteobacteria, particularly the Enterobacteriaceae, but there is a notable absence of a DtpE-like protein in *E. coli* K-12. Within the Gammaproteobacteria, *E. coli* K-12 and *Salmonella enterica* subsp. *enterica* serovar Typhimurium strain LT2 (abbreviated as *S. Typhimurium* LT2) share the same repertoire of Dtp proteins (DtpA, DtpB, DtpC and DtpD), which would be expected given the genetic relatedness of these bacteria. Within *Yersinia*, *Y. pestis* strain Angola has only a single Dtp protein, DtpA, whereas *Y. kristensenii* ATCC 33638 has both a DtpA and a DtpE orthologue. Both DtpA and DtpE are present in the majority of *Yersinia* spp. but notably absent in all *Y. pestis* and *Y. pseudotuberculosis* strains.

It is interesting that Dtp proteins are present in both prokaryotes and eukaryotes, with clear examples in humans (*Homo sapiens* PepT1 and PepT2) and yeast (*Saccharomyces cerevisiae* 2S288c), suggesting that the role of the Dtp proteins is important enough for the ancestral genes to have been maintained across all domains of life. A sequence comparison of Dtp and Dtp-like proteins is provided in Fig. 4.9.

While there is a clear expansion of Dtp proteins in Gammaproteobacteria, the reasons behind this remain undetermined and the relative role of ABC- versus Dtp-peptide transporters in *E. coli* has not been established. For this reason, functional characterisation of peptide transport in *E. coli* was undertaken.

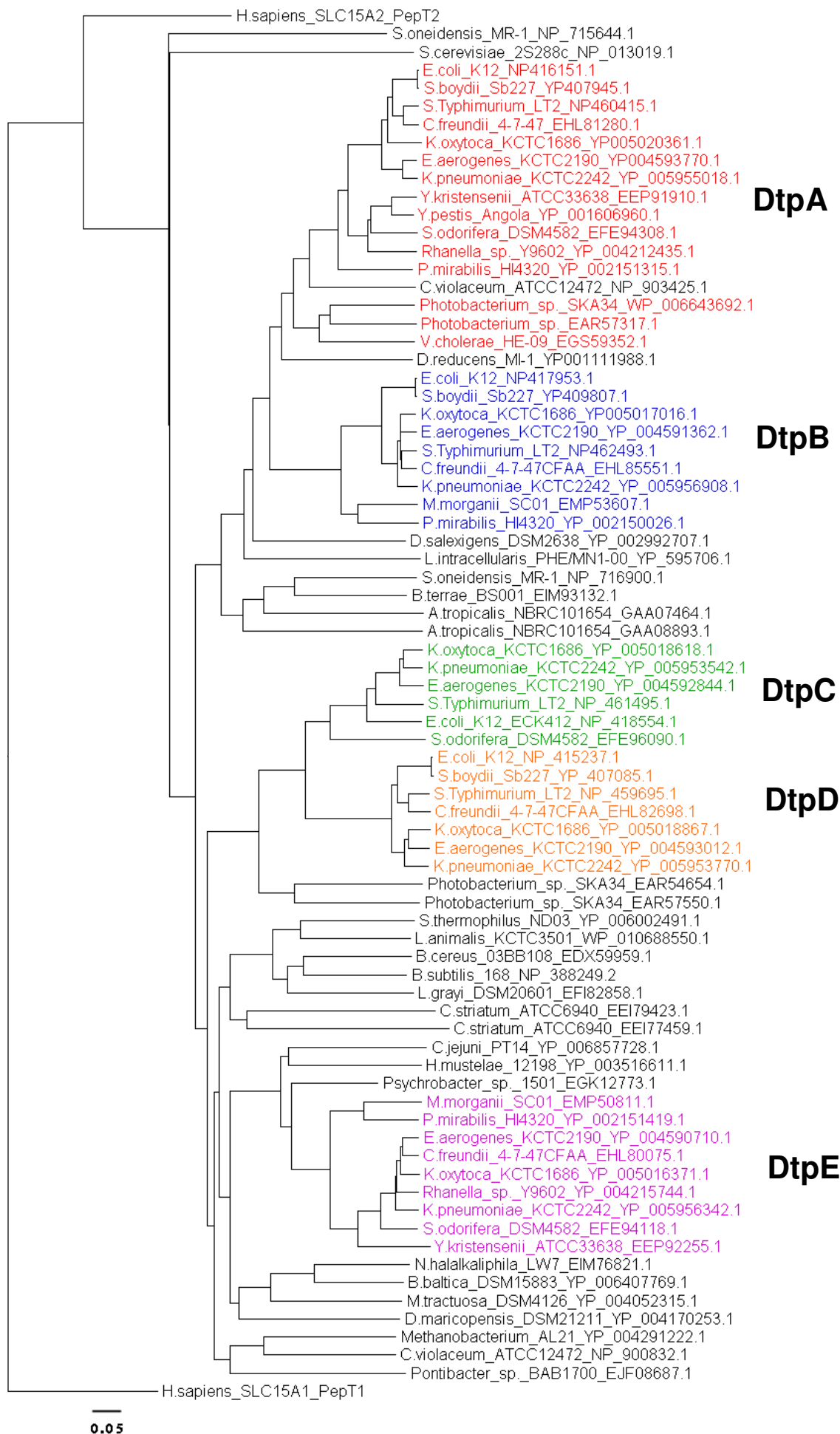


**Figure 4.1.** Rooted phylogenetic tree displaying the relationship between PTR family Dtp proteins. Colour coding is based on each Dtp protein family within the Gammaproteobacteria: DtpA – Red, DtpB – Blue, DtpC – Green, DtpD – Orange, DtpE – Pink. Multiple sequence alignment and phylogenetic tree building was carried out using ClustalX2.

## 4.2 Creation of peptide transporter deficient (TD-Pep) strains of *E. coli* K-12

To create the strains required to characterise the relative role of ABC- and Dtp-mediated peptide transport in *E. coli* K-12, clean genetic deletions of peptide transporters were constructed using Keio Collection strains. The original Keio Collection strains were constructed by the Mori group (Baba *et al.*, 2006) following the gene replacement method developed by Datsenko & Wanner (2000). Following construction, each respective strain was checked via colony PCR to confirm pCP20-mediated gene deletion at the respective locus. Oligonucleotide primers were designed to amplify from within the chromosomal regions immediately upstream and downstream of the deleted gene which resulted in different sized amplicons at individual loci. Where multiple genes were deleted in the same strain, pKD46-mediated homologous recombination (section 2.2.9) followed by pCP20-mediated gene deletion (section 2.2.8) was used to sequentially remove the chosen genes.

The ABC-peptide transporters Dpp and Opp are each encoded by a five gene operon. To delete *dpp* and *opp*, a deletion of a single transmembrane subunit gene of each transporter was created. These strains were designated  $\Delta dppC$  and  $\Delta oppC$ , respectively. Agarose gel images of colony PCR (using primers detailed in Table 2.5) to confirm construction of  $\Delta dppC$ ,  $\Delta oppC$  and the double mutant  $\Delta dppC \Delta oppC$  ( $\Delta DB1$ ) are shown in Fig. 4.2. The amplicon size of the kanamycin gene replacement Keio collection strain is larger than wild-type (WT) in both cases. Successful deletion mutants resulted in a clean deletion of the kanamycin resistance gene in the respective strain. The amplicons for the strains harbouring deleted genes relate to the upstream and downstream regions of the chromosome that are amplified by the respective primers, and are consistently smaller than the respective wild-type gene and the kanamycin gene replaced Keio collection strain.

The *dtpA*, *dtpB*, *dtpC* and *dtpD* genes encode single gene peptide transporters as detailed in section 4.1. Strains  $\Delta dtpA$ ,  $\Delta dtpB$ ,  $\Delta dtpC$  and  $\Delta dtpD$  were created to represent deletion mutants of the PTR family peptide transporters of *E. coli*. The quadruple deletion mutant  $\Delta dtpA \Delta dtpB \Delta dtpC \Delta dtpD$  ( $\Delta DB5$ ) was also created. Agarose gel images to confirm the creation of  $\Delta DB5$  are shown in Fig. 4.2. A decision was taken at this point not to make all possible double and triple deletion combinations of the Dtp transporters in order to allow a consistent collection of strains to be used for phenotypic characterisation.

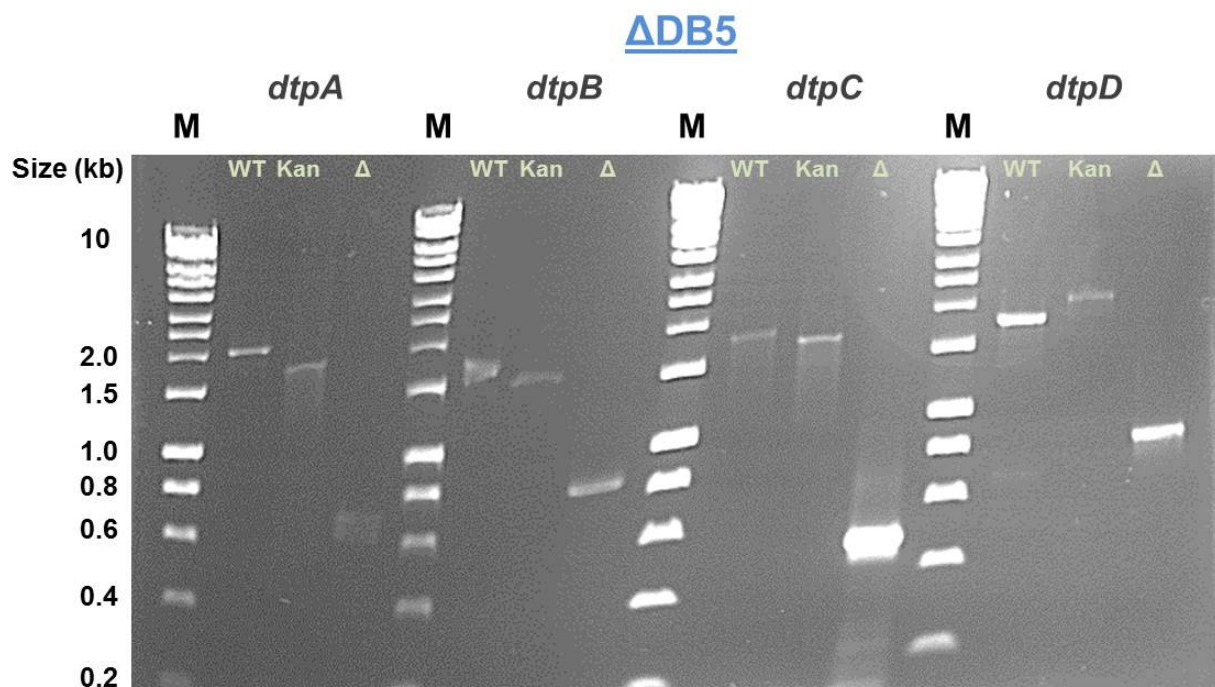
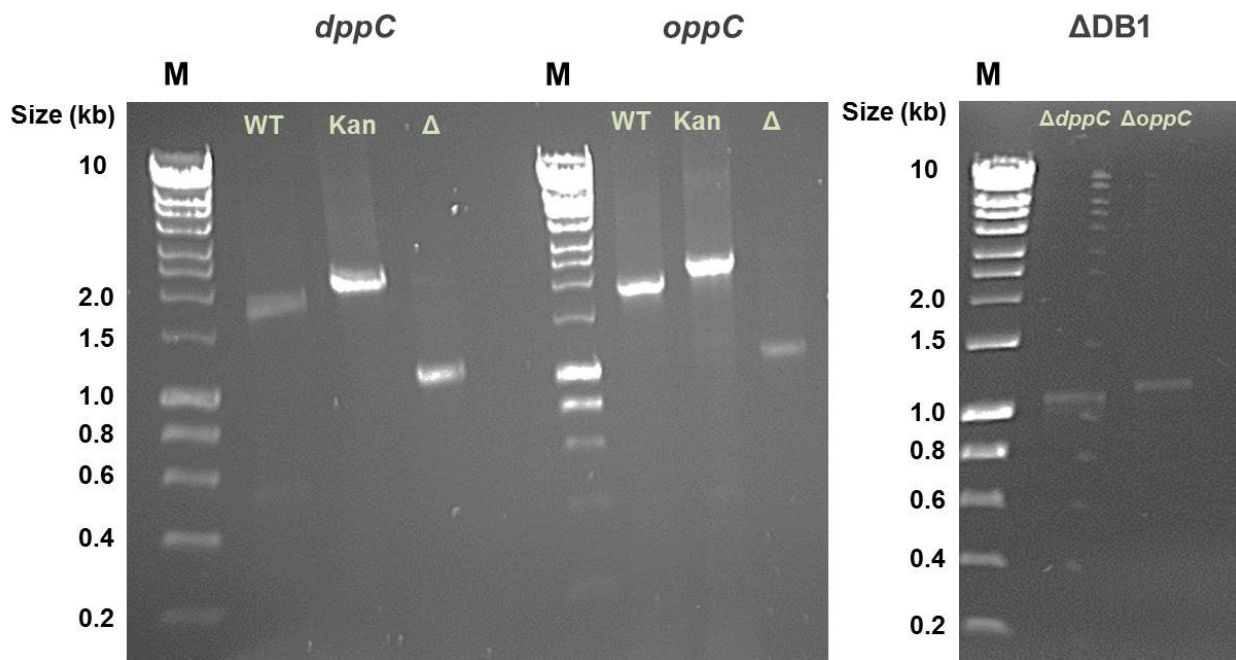


**Figure 4.2.** Agarose gel (1%) stained with ethidium bromide showing colony PCR amplification products from single gene deletions at *dppC* and *oppC* loci (top left panel), the double gene deletion strain  $\Delta$ DB1 ( $\Delta$ *dppC*  $\Delta$ *oppC*) (top right panel) and the quadruple gene deletion strain  $\Delta$ DB5 ( $\Delta$ *dtpA*  $\Delta$ *dtpB*  $\Delta$ *dtpC*  $\Delta$ *dtpD*) (bottom panel). Lane 'M' denotes DNA size marker. All other lanes are labelled accordingly. WT – wild type gene amplified from BW25113, Kan – kanamycin gene replacement amplified from respective Keio collection strain,  $\Delta$  – clean genetic deletion at respective locus. Expected amplicons sizes (bp): ***dppC*** WT: 1885 Kan: 2239  $\Delta$ : 1052 ***oppC*** WT: 1969 Kan: 2317  $\Delta$ : 1130 ***dtpA*** WT: 2098 Kan: 1852  $\Delta$ : 689 ***dtpB*** WT: 1786 Kan: 1573  $\Delta$ : 810 ***dtpC*** WT: 1835 Kan: 1634  $\Delta$ : 447 ***dtpD*** WT: 1815 Kan: 1981  $\Delta$ : 804

### 4.3 Growth of *E. coli* TD-Pep strains in L-Alanine-L-Alanine-containing minimal medium

In order to characterise the effect of deleting peptide transporters in *E. coli*, a series of growth-based assays were performed using peptides as the sole nitrogen source. Firstly, TD-Pep strains were grown in M9 minimal glucose medium containing L-Alanine-L-Alanine (Ala-Ala) as the sole source of nitrogen. Ala-Ala was chosen as it represents a simple dipeptide. The high affinity dipeptide ABC-transporter mutant  $\Delta dppC$  showed no growth phenotype relative to wild-type (Fig. 4.3A). There was no clear growth defect for the oligopeptide ABC-transporter mutant  $\Delta oppC$  or the double deletion mutant,  $\Delta dppC \Delta oppC$  ( $\Delta DB1$ ). This suggests that neither Dpp nor Opp are significantly involved in Ala-Ala uptake in *E. coli*. Similarly, there was no growth defect for any single symporter deletion mutant  $\Delta dtpA$ ,  $\Delta dtpB$ ,  $\Delta dtpC$  or  $\Delta dtpD$ . In contrast, a strong growth defect was observed for the multiple peptide symporter deletion mutant,  $\Delta DB5$ , which failed to grow following 24 h incubation. This suggests that there is redundancy between these transporters and that multiple Dtp proteins can transport Ala-Ala. As a control, growth of wild-type,  $\Delta DB1$  and  $\Delta DB5$  was assessed on M9 minimal glucose medium containing L-Alanine as the sole source of nitrogen. Both mutant strains grew comparatively well compared to wild-type (Fig. 4.3B), confirming that the observed phenotype relates specifically to using the dipeptide Ala-Ala as the sole source of nitrogen.

Overall, the significant growth defect of  $\Delta DB5$  compared to any other strain suggests that the primary route for Ala-Ala uptake in *E. coli* is via a combination of Dtp peptide transporters and not high affinity ABC-peptide transport systems.

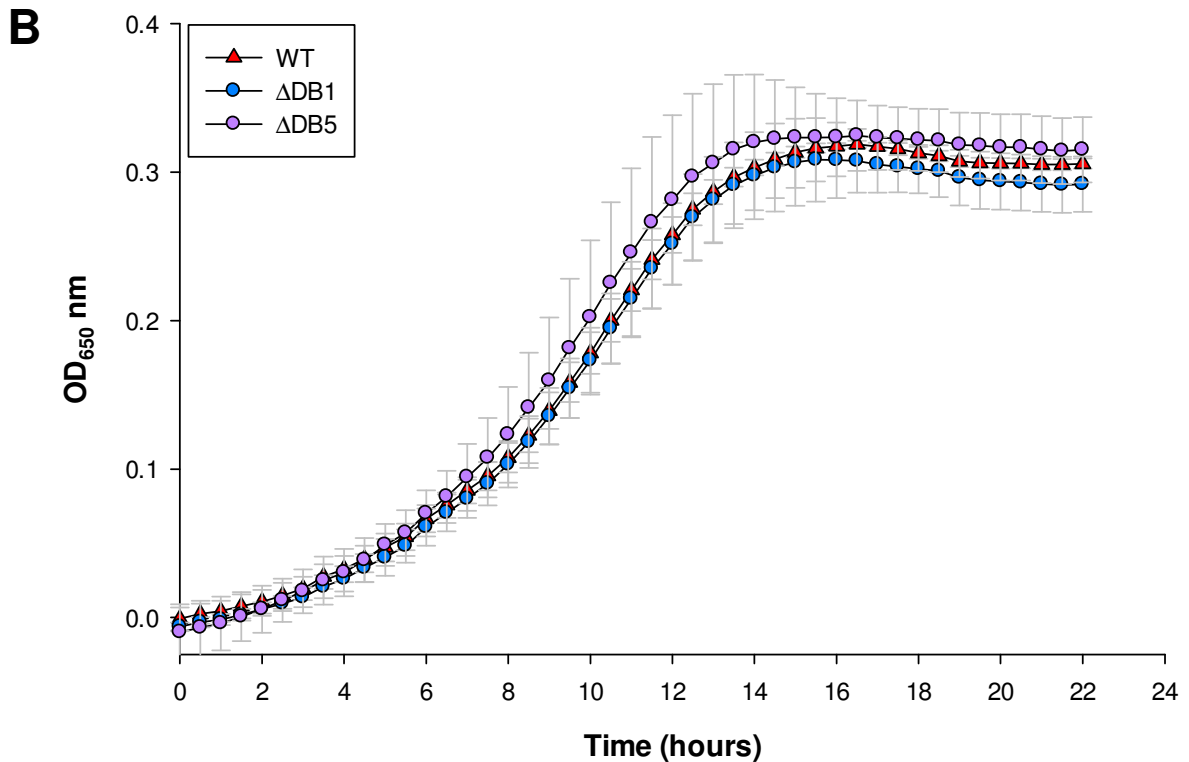
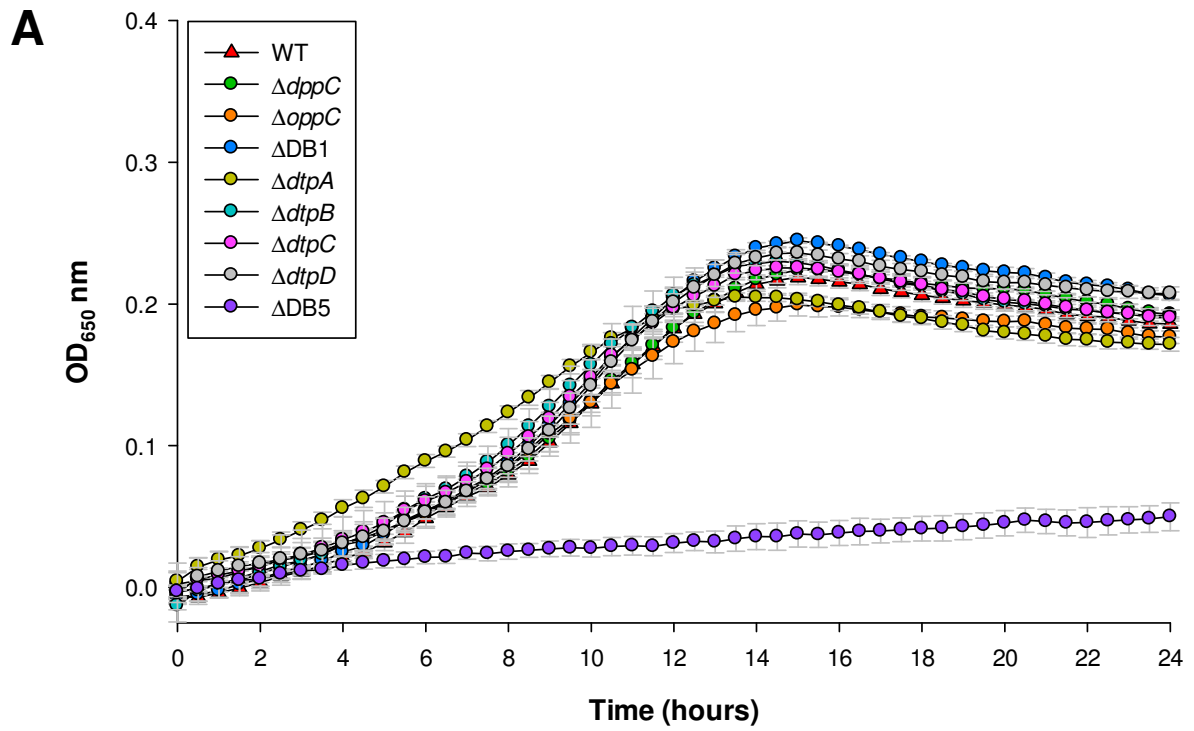


**Figure 4.3.** Growth curves of TD-Pep strains of *E. coli* K-12 grown in M9 glucose minimal medium containing, as the sole source of nitrogen; **(A)** 20 mM L-Alanine-L-Alanine or **(B)** 20 mM L-Alanine. Cultures were grown under aerobic conditions at 37°C. Error bars represent standard deviation of four (part A) or three (part B) biological replicates.

#### 4.4 Growth of *E. coli* TD-Pep strains in aromatic residue-containing dipeptide minimal medium

To assess the impact of bulky aromatic residues on dipeptide uptake in *E. coli*, TD-Pep strains were grown in M9 minimal glucose medium containing L-Alanine-L-Phenylalanine (Ala-Phe), L-Phenylalanine-L-Alanine (Phe-Ala), or L-Tyrosine-L-Alanine (Tyr-Ala) as the sole source of nitrogen. These dipeptides were chosen as representative N-terminal small, C-terminal bulky/aromatic dipeptides (Ala-Phe) and N-terminal bulky/aromatic, C-terminal small dipeptides (Phe-Ala and Tyr-Ala).

When grown on Phe-Ala as the sole source of nitrogen, there was no growth phenotype for  $\Delta dtpB$ ,  $\Delta dtpC$  or  $\Delta dtpD$  (Fig. 4.4.1A) and little observable growth phenotypes for  $\Delta dppC$ ,  $\Delta oppC$ ,  $\Delta DB1$  and  $\Delta dtpA$ . However, the multiple peptide symporter deletion mutant  $\Delta DB5$  displayed a strong growth defect, which is similar but not as severe as the phenotype observed when grown on Ala-Ala (Fig. 4.3A). Overall, this data suggest that the peptide symporters have a greater role in Phe-Ala uptake than Dpp or Opp. When TD-Pep strains were grown in minimal medium containing Tyr-Ala as the sole source of nitrogen, small growth defects were observed for strains  $\Delta DB1$  and  $\Delta DB5$  (Fig. 4.4.1B). Both  $\Delta DB1$  and  $\Delta DB5$  appear to grow at a slower rate than wild-type but reached similar final growth yields. This suggests that Tyr-Ala uptake in *E. coli* can be mediated by a multiplicity of peptide transporters and cannot be attributed to a single peptide transport system.

Growth of TD-Pep strains was then assessed in M9 minimal glucose medium containing Ala-Phe as the sole source of nitrogen. In this medium, the most impaired growth was observed for  $\Delta DB1$ , but clear growth defects were also seen for  $\Delta dppC$  and  $\Delta oppC$  (Fig. 4.4.2). There was no apparent phenotype for any single peptide symporter deletion and a negligible growth defect was observed for  $\Delta DB5$ . This suggests that Dpp and Opp are predominantly responsible for Ala-Phe uptake in *E. coli*.

Overall, it appears that ABC peptide transporters are the primary means of transporting Ala-Phe, whereas N-terminal bulky/aromatic, C-terminal small dipeptide uptake (Phe-Ala and Tyr-Ala) appears to be mediated either peptide symporters or ABC peptide transporters. Across the limited substrate range assessed, there appears to be an additive effect of deleting multiple peptide transporters in terms of ability to grow on peptides, with  $\Delta DB1$  and  $\Delta DB5$  consistently displaying stronger growth defects than individual deletion mutants.

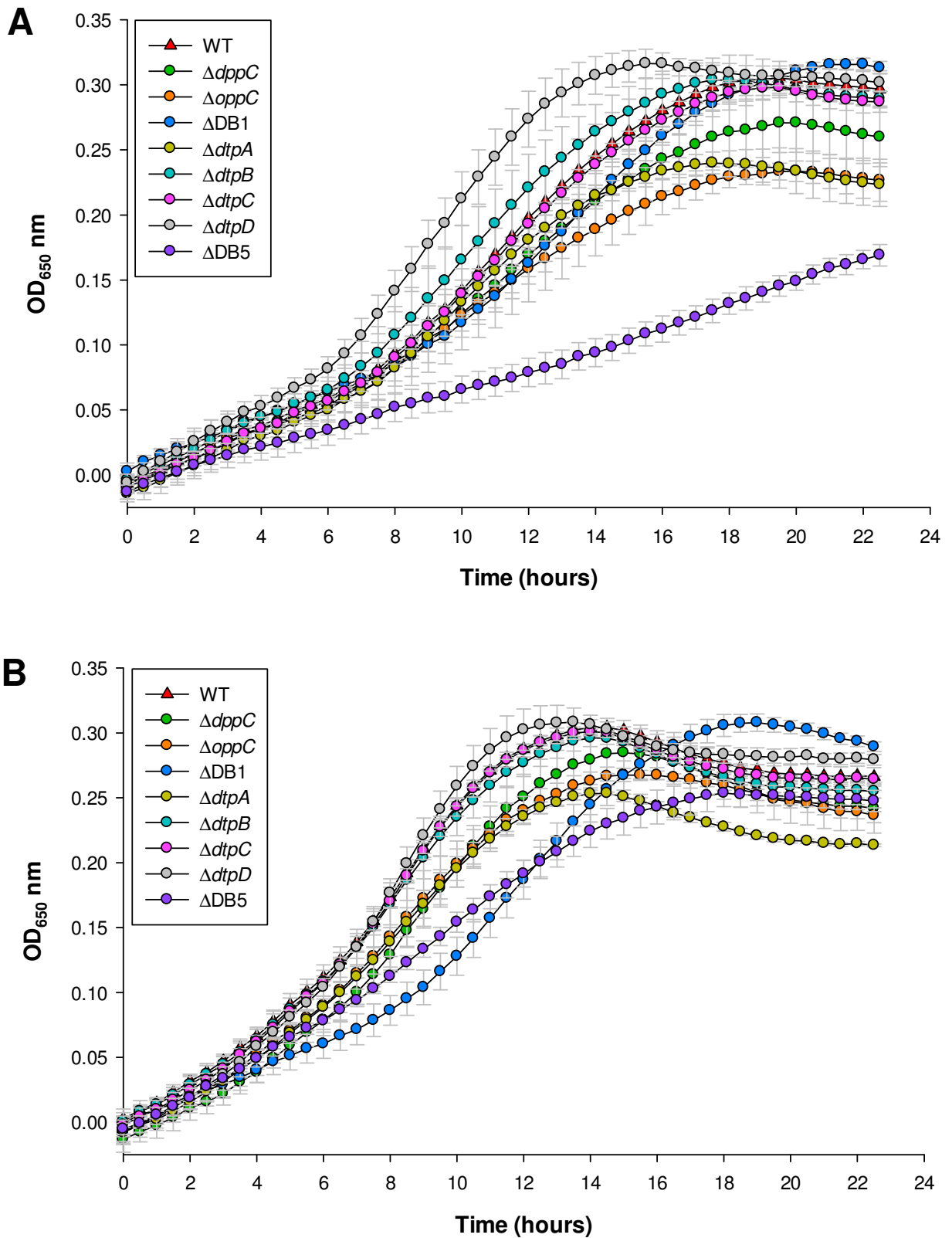


**Figure 4.4.1.** Growth curves of TD-Pep strains of *E. coli* K-12 grown in M9 glucose minimal medium containing, as the sole source of nitrogen; **(A)** 20 mM L-Phenylalanine-L-Alanine or **(B)** 20 mM L-Tyrosine-L-Alanine. Cultures were grown under aerobic conditions at 37°C. Error bars represent standard deviation of three biological replicates.

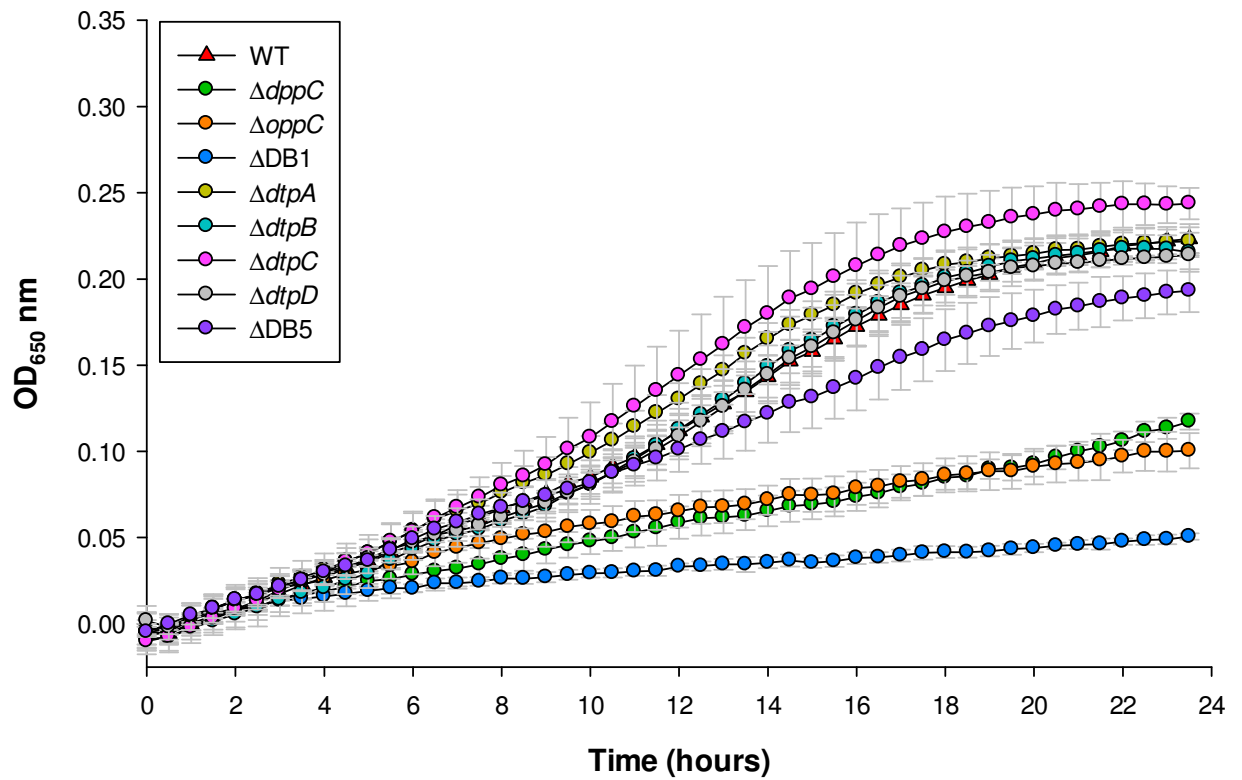


**Figure 4.4.2.** Growth curves of TD-Pep strains of *E. coli* K-12 grown in M9 glucose minimal medium containing 20 mM L-Alanine-L-Phenylalanine as the sole source of nitrogen. Cultures were grown under aerobic conditions at 37°C. Error bars represent standard deviation of three biological replicates.

#### 4.5 Inhibition of growth of *E. coli* TD-Pep strains by L-leucine-containing dipeptides

The growth inhibitory effects of L-leucine (Leu)-containing dipeptides on *E. coli* K-12 is thought to arise from a direct interaction between a Leu-containing dipeptide and threonine deaminase (IlvA), which is responsible for the first step in L-isoleucine (Ile) biosynthesis. The dipeptide is thought to directly bind to the Ile binding site on IlvA, leading to Ile limitation in the absence of an exogenous source of Ile (Vonder Haar & Umbarger, 1972). As Leu-containing dipeptide is catabolised by the cell, the inhibitory effects subside and the growth rate increases. This phenomenon can be exploited to assess the route of Leu-containing peptide uptake in *E. coli*.

If Leu-containing peptides are taken up at inhibitory concentrations by *E. coli*, growth will be inhibited. However, if Leu-containing peptide transport is disrupted, a lower (non-inhibitory) concentration of intracellular Leu-dipeptide will be maintained, allowing for stronger growth. To define the transport system(s) used to take up Leu-containing dipeptides, TD-Pep strains of *E. coli* were grown in M9 minimal glucose medium supplemented with either L-Alanine-L-Leucine (Ala-Leu) or L-Leucine-L-Alanine (Leu-Ala) as the sole nitrogen source.

When grown in minimal medium containing either 20 mM Ala-Leu (Fig. 4.5A) or 20 mM Leu-Ala (Fig. 4.5B) as the sole nitrogen source, negligible growth phenotypes were observed for all mutants assessed with the exception of  $\Delta$ DB5, although the final optical density reached in these experiments were approximately 2-fold lower using Ala-Leu or Leu-Ala compared to other, non-inhibitory Ala-containing dipeptides. Although a modest phenotype, these data suggest that deletion of multiple Dtp peptide transporters leads to slower uptake of Ala-Leu or Leu-Ala, conceivably allowing this strain to overcome the toxic effects of the dipeptide by maintaining sub-inhibitory intracellular concentrations of Leu, ultimately enabling slow but sustained growth. This implies Ala-Leu and Leu-Ala are substrates for Dtp- rather than ABC peptide transporters.

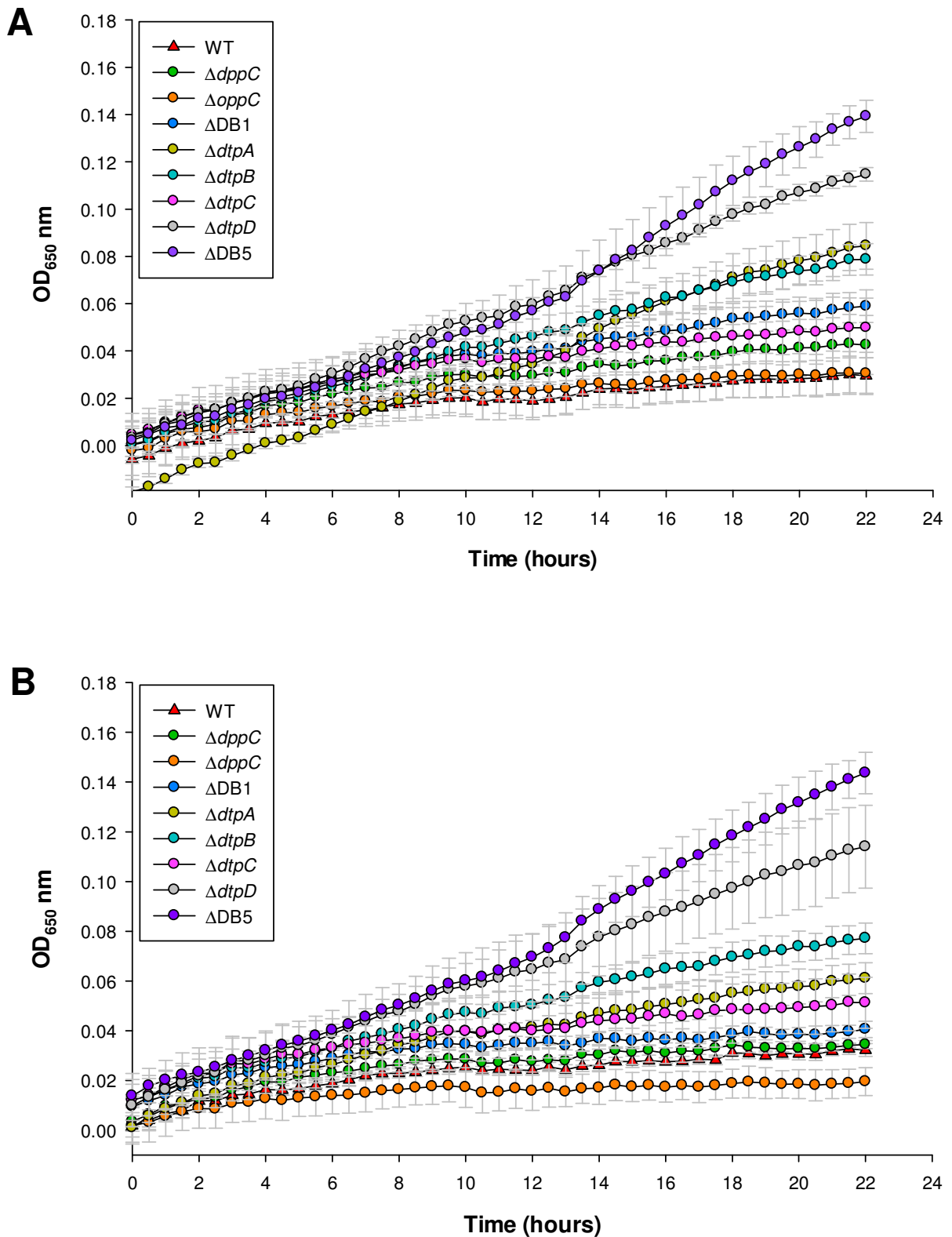


**Figure 4.5.** Growth curves of TD-Pep strains of *E. coli* K-12 grown in M9 glucose minimal medium containing, as the sole source of nitrogen; **(A)** 20 mM L-Alanine-L-Leucine or **(B)** 20 mM L-Leucine-L-Alanine. Cultures were grown under aerobic conditions at 37°C. Error bars represent standard deviation of three biological replicates.

#### 4.6 Inhibition of growth of *E. coli* TD-Pep strains by L-valine-containing tripeptides

In *E. coli*, branched-chain amino acid biosynthesis begins with any one of three isozymes of acetohydroxy acid synthase (AHAS). Expression of AHAS I (encoded by *ilvB* and *ilvN*) and AHAS III (encoded by *ilvH* and *ilvI*), which are both involved in L-isoleucine (Ile) and L-valine (Val) biosynthesis is repressed when Val is in excess (Leavitt and Umbarger, 1962) However, if not exogenously supplied, the bacterium still requires *de novo* synthesis of Ile, which normally proceeds via AHAS II (encoded by *ilvG* and *ilvM*). *E. coli* K-12 has a frameshift mutation in *ilvG* meaning that AHAS II is non-functional. Consequently, when AHAS I and III are repressed by Val in *E. coli* K-12, Ile biosynthesis is completely turned off. Fundamentally, when Val is added to a culture of *E. coli* K-12 at millimolar concentrations, the cells become starved for L-isoleucine and growth is inhibited. This phenomenon can be exploited to assess the route of Val-containing peptide uptake. If Val-containing peptides are taken up by *E. coli*, they will be intracellularly metabolised to free Val and accumulate to inhibitory concentrations, leading to inhibition of growth. However, if Val-containing peptide transport is disrupted, a non-inhibitory concentration of intracellular Val will be maintained, allowing the cells to grow.

To establish the transport route of L-valine-L-glycine-L-glycine (Val-Gly-Gly) in *E. coli* K-12, an agar plate growth inhibition assay was performed. A lawn of each TD-Pep strain was spread onto the surface of an M9 minimal glucose agar plate and allowed to dry. Filter paper discs were placed onto the surface of the plate and saturated with equimolar concentrations of Val or Val-Gly-Gly and, as a control, H<sub>2</sub>O. Zones of inhibition around the toxic substrates for each strain were measured following overnight incubation. The average zones of inhibition for all strains are shown in Table 4.6 and a representative image of growth inhibition of each strain is shown in Fig. 4.6. Small zones of inhibition signify a weak inhibitory effect of Val-Gly-Gly, meaning that the peptide transporter mutation in that given strain prevents Val-Gly-Gly uptake.  $\Delta dtpA$  and  $\Delta DB5$  both displayed a small average zone of inhibition ( $5.3 \text{ mm} \pm 0.67$  and  $4.7 \text{ mm} \pm 0.33$ , respectively). The phenotype of  $\Delta DB5$  was almost exclusively attributable to the *dtpA* mutation in this strain, as neither  $\Delta dtpB$ ,  $\Delta dtpC$  nor  $\Delta dtpD$  were able to overcome the toxic effects of Val-Gly-Gly.  $\Delta DB1$  displayed a zone of inhibition of  $8.7 \text{ mm} \pm 0.33$ , which was primarily the result of the *oppC* deletion;  $\Delta oppC$  alone had an average zone of inhibition of  $9.7 \text{ mm} \pm 0.33$ . All strains displayed similar growth inhibition when Val was supplemented, confirming that the difference in inhibitory effect of Val-Gly-Gly is attributable to differences in peptide uptake between strains. It was concluded that Val-Gly-Gly uptake in *E. coli* is primarily carried out by DtpA.

**Table 4.6.** Average zone of inhibition (three biological replicates) of TD-Pep strains grown on M9 minimal glucose agar plates containing discs saturated with equimolar concentrations of Val-Gly-Gly or Val. Zones of inhibition were measured from the centre of the disc.

Strain	Average zone of inhibition (mm) $\pm$ SEM	
	Val-Gly-Gly	Val
Wild-type	11 $\pm$ 0.0	13.7 $\pm$ 0.33
$\Delta dppC$	12 $\pm$ 0.57	13.3 $\pm$ 0.33
$\Delta oppC$	9.7 $\pm$ 0.33	14 $\pm$ 0.0
$\Delta DB1$	8.7 $\pm$ 0.33	13.3 $\pm$ 0.33
$\Delta dtpA$	5.3 $\pm$ 0.67	13.3 $\pm$ 0.88
$\Delta dtpB$	13.3 $\pm$ 0.88	13.3 $\pm$ 1.2
$\Delta dtpC$	12.7 $\pm$ 0.88	14 $\pm$ 0.0
$\Delta dtpD$	11 $\pm$ 0.57	14 $\pm$ 0.58
$\Delta DB5$	4.7 $\pm$ 0.33	13.3 $\pm$ 0.33

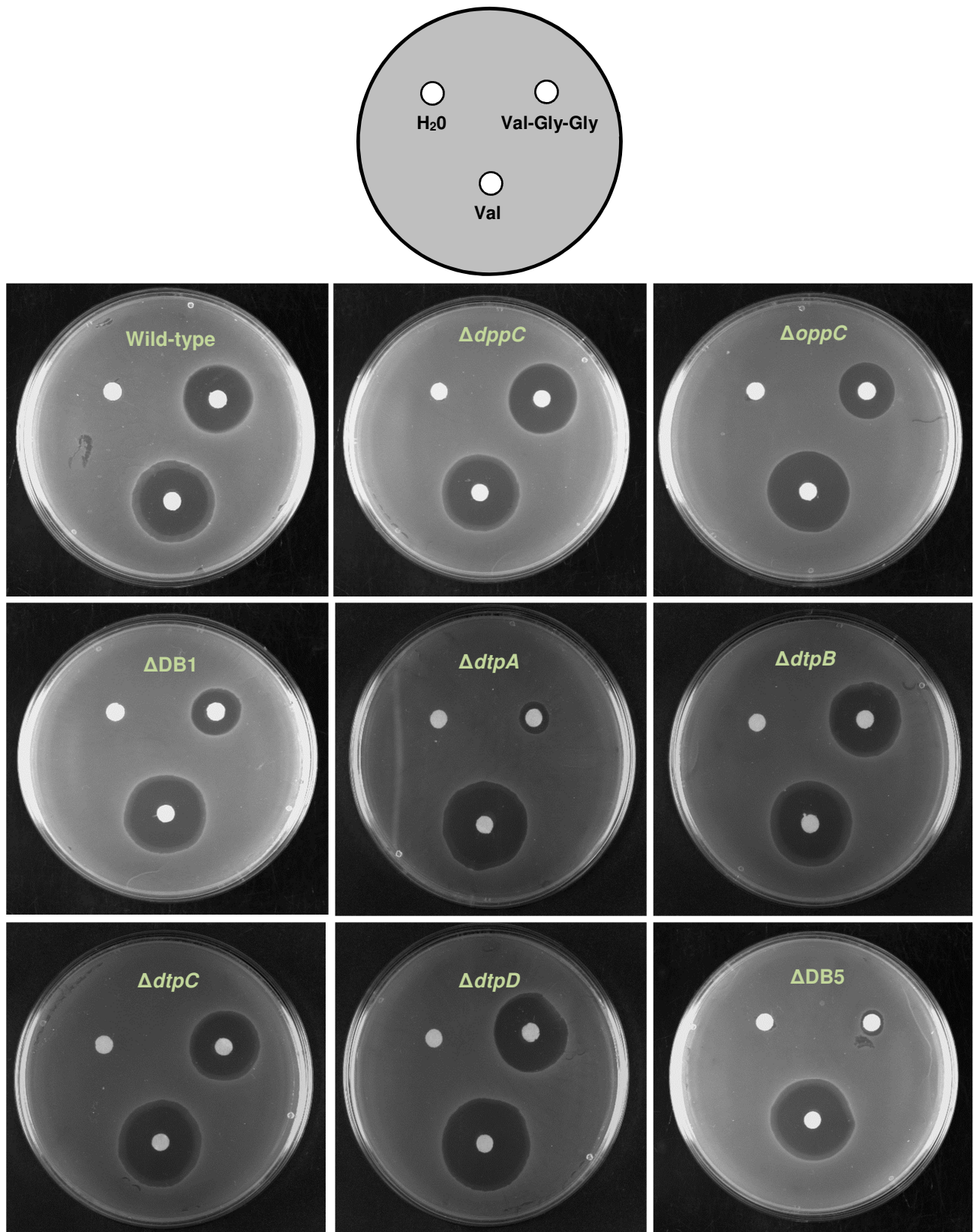


**Figure 4.6.** Representative images of TD-Pep strains grown on M9 minimal glucose agar plates with toxic peptide supplementation. A lawn of bacteria was spread onto each plate, allowed to dry and filter paper discs added and saturated with the given compound. Top panel shows layout of filter discs on each plate. Discs were saturated with equimolar concentrations of Val-Gly-Gly, L-Valine or H<sub>2</sub>O.

## 4.7 Growth of *E. coli* TD-Pep strains on tryptone broth

The TD-Pep strains were assessed for their ability to grow in medium consisting of 1% tryptone and 1% NaCl (tryptone broth). Tryptone is a trypsin-digest of the milk protein casein and while the exact composition of commercially available tryptone has not been characterised, the bulk of the material is likely comprised of a complex mixture of amino acids and small peptides. This experiment was carried out to assess the relative involvement of each peptide transporter when a complex peptide mixture is supplied as the sole source of both carbon and nitrogen.

When the peptide symporter deletion mutants were grown in tryptone broth, it was observed that both  $\Delta dtpB$  and  $\Delta dtpC$  grew at the same rate and reached similar growth yields compared to wild-type (Fig. 4.7.1). However, growth of  $\Delta dtpD$  began to visibly slow following 5 h incubation. A similar phenotype was observed for  $\Delta dtpA$  which displayed a slower growth rate than wild-type and reached a lower final growth yield.

Given that a growth defect is observed for  $\Delta dtpA$  and  $\Delta dtpD$ , we can conclude that these two peptide symporters play a role in peptide uptake in *E. coli* and likely participate in general peptide uptake. As no growth defect was observed for  $\Delta dtpB$  or  $\Delta dtpC$ , this suggests that the substrate specificity of these transporters may be more defined.

When the ABC-peptide transporter deletion mutants were grown in tryptone broth, it was observed that  $\Delta dppC$ ,  $\Delta oppC$  and  $\Delta DB1$  grew at a similar rate to wild-type during the initial 3 h of growth (Fig. 4.7.2A), suggesting that during this time, *E. coli* is using a non-peptide based nutrient source for growth, specifically, amino acids. Following 4 h incubation, a strong and immediate cessation of growth was observed for  $\Delta oppC$  and  $\Delta DB1$ .  $\Delta dppC$  continued to grow at a similar rate to wild-type until approximately 5 h, when the growth rate began to decrease.  $\Delta oppC$  and  $\Delta DB1$  reached a final growth yield of approximately 40% compared to wild-type. In contrast, while  $\Delta dppC$  continued to grow at a slower rate than wild-type, it reached a comparable final yield following 24 h incubation. This pattern of growth was strongly reproducible when the strains were grown under the same conditions in 100 ml shake flasks (Fig. 4.7.2B).

The point at which growth halts in  $\Delta oppC$  and  $\Delta DB1$  implies that all utilisable growth substrates, assumed to be amino acids and dipeptides, had been exhausted. Without a functional Opp transport system, these strains were unable to access the large pool of oligopeptides that remained in the medium. The similarity in growth rate and yield

between wild-type and  $\Delta dppC$  suggests that the Dpp peptide transport system is not involved in general peptide uptake in tryptone broth. Equally, given that a strong growth defect is observed for  $\Delta oppC$  and  $\Delta DB1$  but not  $\Delta dppC$ , these data suggest that the major component nutrient source in tryptone is oligopeptides. Further support for this hypothesis is observed when wild-type and  $\Delta DB1$  strains were grown on tryptone broth medium taken from an overnight culture of  $\Delta DB1$ . Within this 'spent' medium, there were predicted to be a pool of oligopeptides that  $\Delta DB1$  failed to utilise for growth. Bacteria from the spent medium were removed by centrifugation and the medium was filter sterilised. Wild-type and  $\Delta DB1$  were inoculated into the spent medium and grown for 24 h. Wild-type grew to a final yield 5-fold higher than  $\Delta DB1$  (Fig. 4.7.3), suggesting that wild-type is able to access the pool of peptides in the spent medium that  $\Delta DB1$  cannot. Both wild-type and  $\Delta DB1$  grew to similar final growth yields when D-glucose was supplemented, confirming that the inability of  $\Delta DB1$  to grow on spent medium was not due to cell death.

Taken together, it can be concluded that Opp, DtpA and DtpD participate in general oligopeptide uptake in *E. coli*, with Dpp playing a minor role. It appears that under normal growth on a mixed amino acid and peptide medium (tryptone broth), *E. coli* preferentially transports and utilises the non-peptide-based nutrient source (presumably amino acids) as a growth substrate.

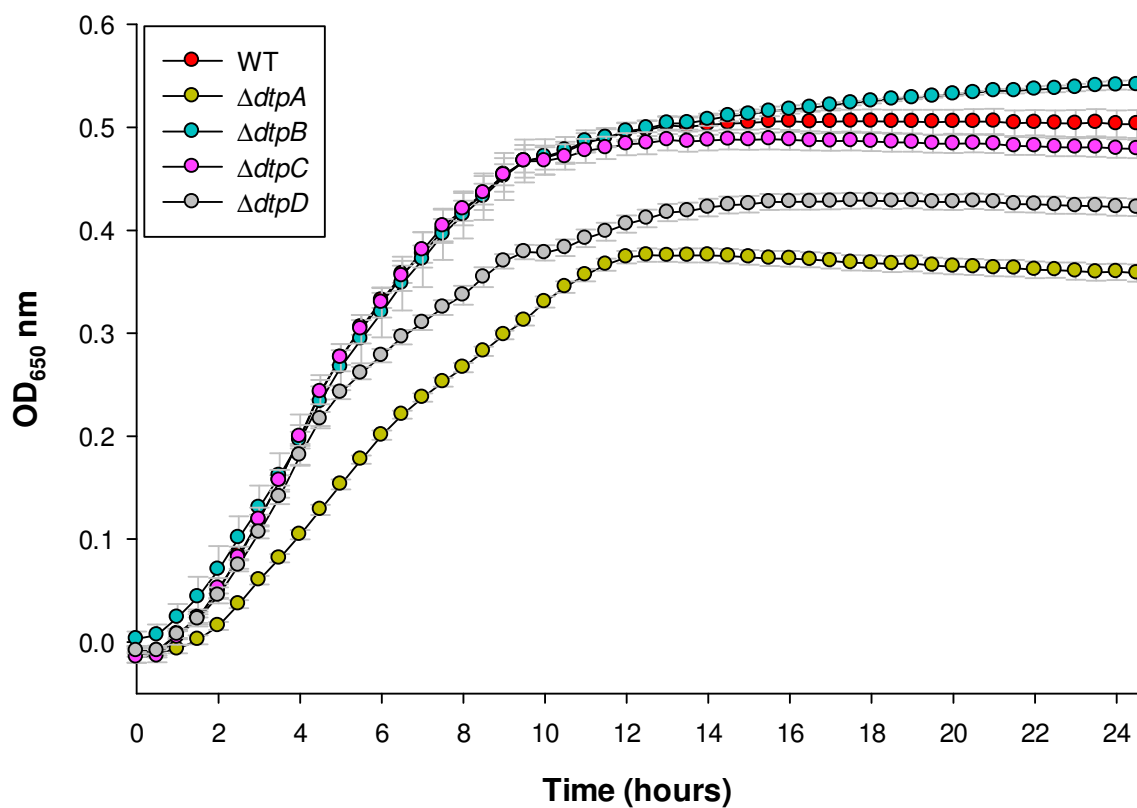


**Figure 4.7.1.** Growth curves of peptide symporter deficient strains of *E. coli* K-12 in 96-well plate format grown in 1% tryptone broth medium. Cultures were grown under aerobic conditions at 37°C. Error bars represent standard deviation of three biological replicates.

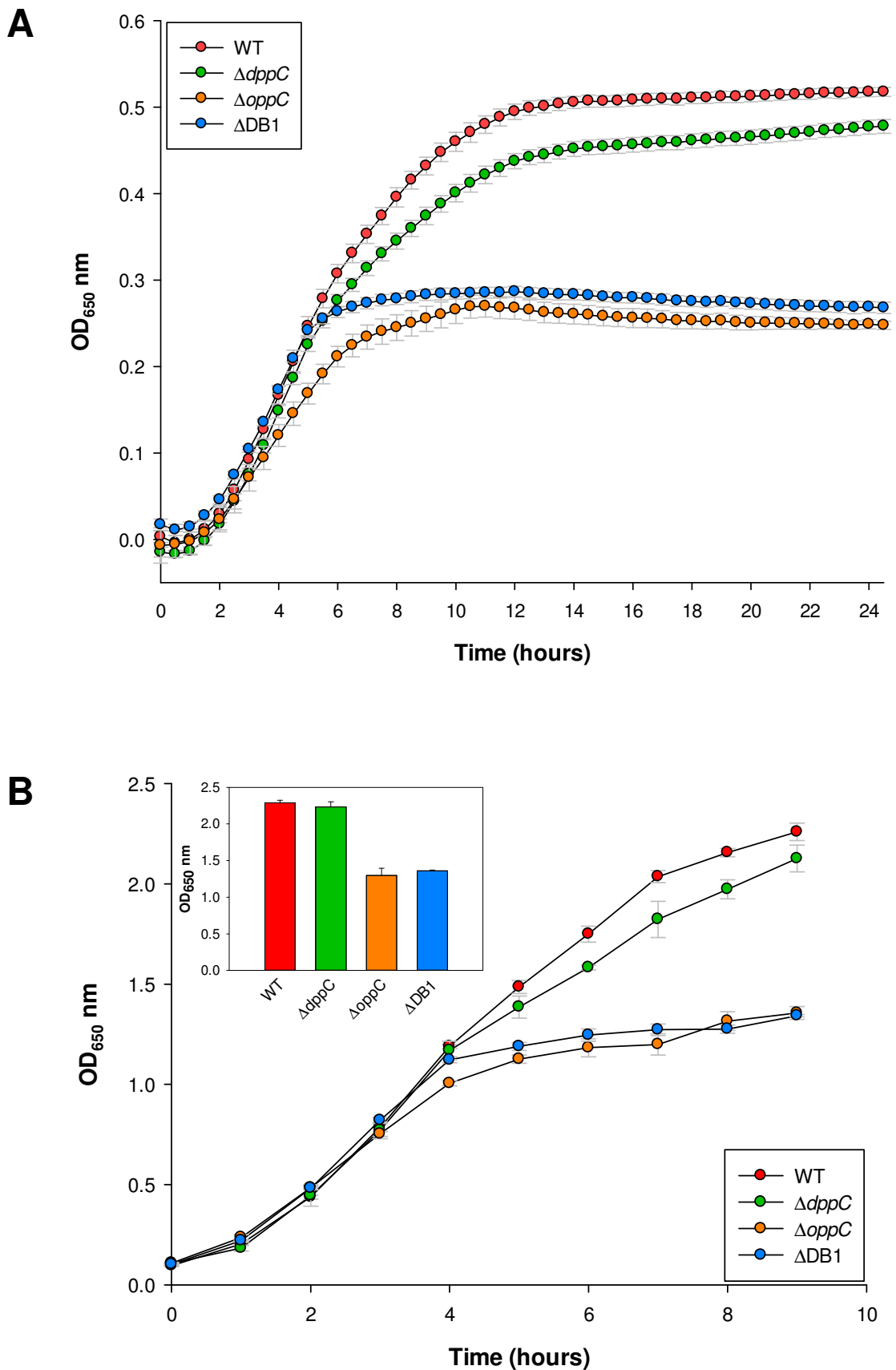


**Figure 4.7.2.** Growth curves of ABC TD-Pep strains of *E. coli* K-12 in tryptone broth medium. **(A)** 96-well plate format and **(B)** 100 ml shake flasks. Inset (in panel B) shows final growth yield of all cultures following 24 h incubation. For  $OD_{650}$  measurements over 0.8, appropriate dilutions were made. Cultures were grown under aerobic conditions at 37°C. Error bars represent standard deviation of four (96-well plate) or three (shake flasks) biological replicates.

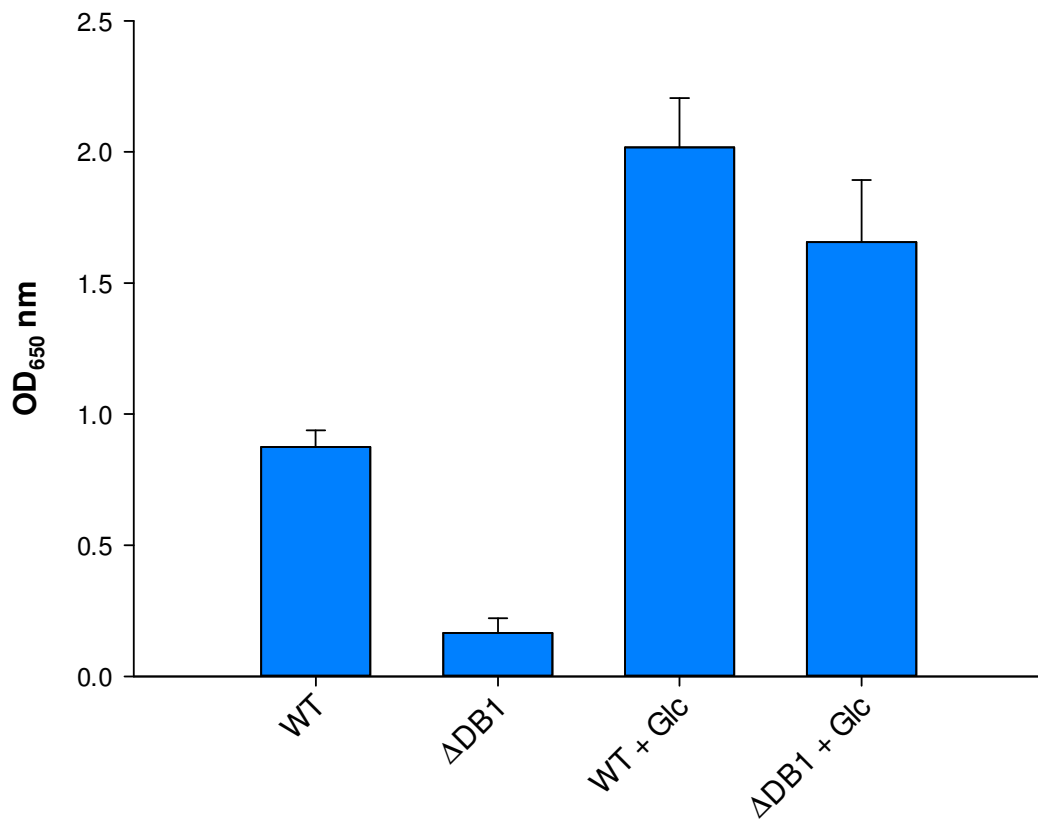


**Figure 4.7.3.** Final growth yield (OD<sub>650</sub> nm) of WT and ΔDB1 *E. coli* K-12 grown in filter-sterilised, spent tryptone broth growth medium of ΔDB1. As a control, 20 mM D-glucose (Glc) was supplemented where appropriate. Error bars represent standard deviation of six biological replicates.

#### **4.8 Late-stage exponential growth of *E. coli* on tryptone broth is limited by carbon starvation**

The immediate cessation of exponential growth of  $\Delta$ DB1 following 5 h incubation in tryptone broth was predicted to be caused by either carbon or nitrogen starvation. To assess this, 20 mM D-glucose or 18.7 mM ammonium chloride were added to cultures of wild-type and  $\Delta$ DB1 cultures of *E. coli* following 5 h growth in tryptone broth.

It was observed that following addition of D-glucose, both strains re-established exponential growth for at least 1 h (Fig. 4.8.1A). In contrast, the growth rate of both strains was unaltered following addition of ammonium chloride (Fig. 4.8.1B). This suggests that at late-stage exponential growth in tryptone broth, *E. coli* is carbon, not nitrogen starved. Similarly, supplementation of 1% yeast extract also led to a re-establishment of exponential growth in both strains, which lasted longer in wild-type than  $\Delta$ DB1 (Fig. 4.8.2A). This suggests that the composition of commercially available yeast extract has some peptide content which wild-type *E. coli* is able to use as a carbon source, but  $\Delta$ DB1 cannot. This conclusion was refuted however when wild-type and  $\Delta$ DB1 were grown in 1% yeast extract broth. No visible growth rate or final yield defect was observed for  $\Delta$ DB1 compared to wild-type (Fig. 4.8.2B), suggesting that peptides do not make up a significant proportion of the utilisable nutrient source in commercially available yeast extract. Similarly, no growth defect was observed during early to mid-exponential growth when both strains were grown in LB medium (Fig. 4.8.3A). There was however a small growth defect for  $\Delta$ DB1 during late exponential growth, suggesting that peptides may be utilised during this time. No significant differences were observed in the final yield of  $\Delta$ DB5 compared to wild-type when grown on tryptone broth, yeast extract broth or LB (Fig. 4.8.3B), suggesting that peptide symporters are not preferentially used over ABC-peptide transporters to transport undefined mixed peptides.

Overall, it was concluded that, during growth on amino acid- and peptide-based medium, *E. coli* is exhausted for carbon before nitrogen. Given that neither  $\Delta$ DB1 nor  $\Delta$ DB5 show significant growth defects when grown on LB or components thereof, it may be that both ABC-peptide transporters and peptide symporters can compensate for each other and play a dual role in peptide uptake on undefined media. In order to see a significant growth defect, a  $\Delta$ DB1/ $\Delta$ DB5 combination strain may be required.

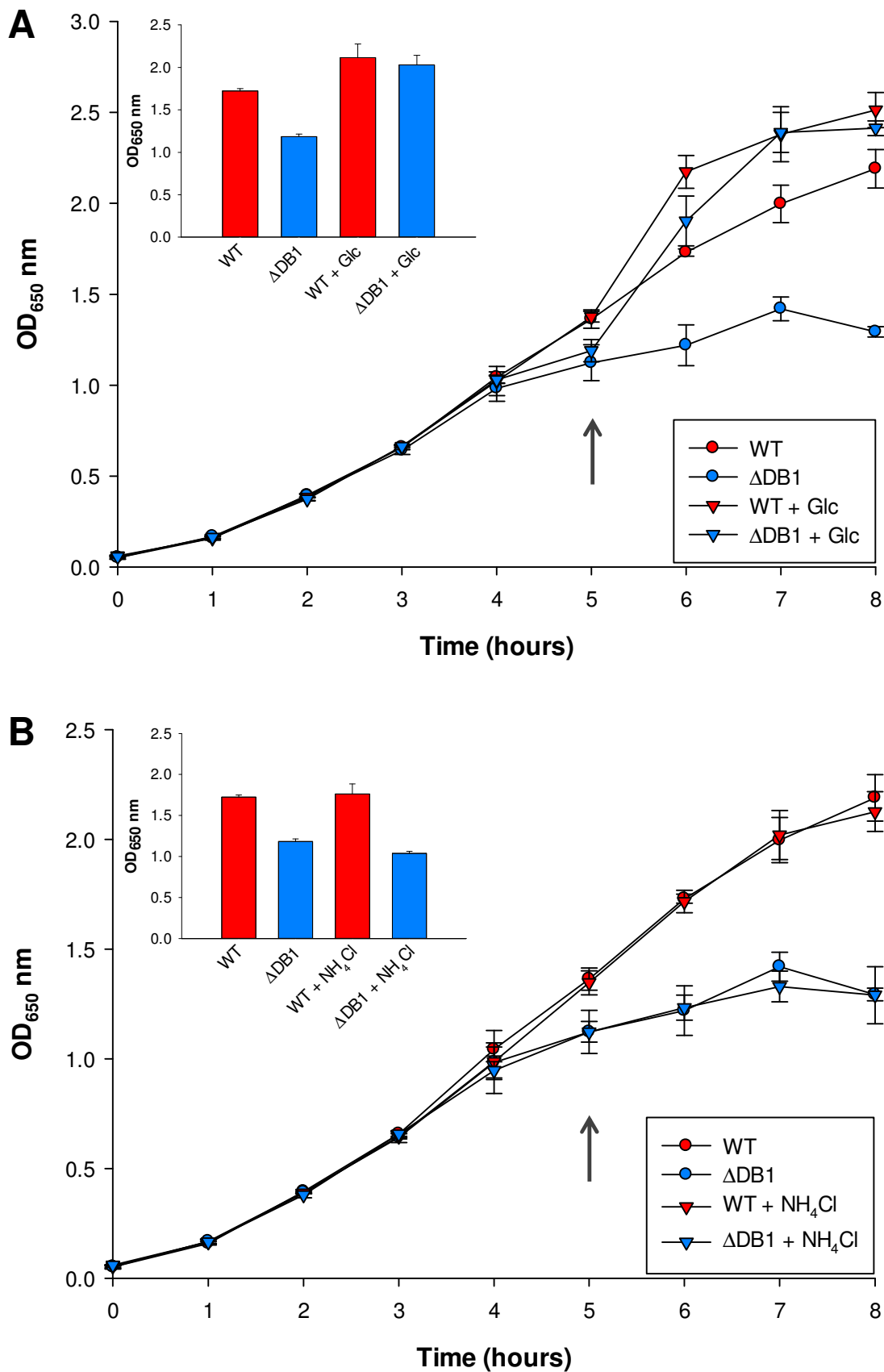


**Figure 4.8.1.** Growth curves of wild-type (WT) and  $\Delta$ DB1 *E. coli* K-12 in 1% tryptone broth medium with carbon or nitrogen supplementation. Black arrow designates addition of **(A)** 20 mM D-glucose or **(B)** 18.7 mM ammonium chloride (NH<sub>4</sub>Cl). Inset shows final growth yield of all cultures following 24 h incubation. Cultures were grown under aerobic conditions at 37°C. Error bars represent standard deviation of three biological replicates.

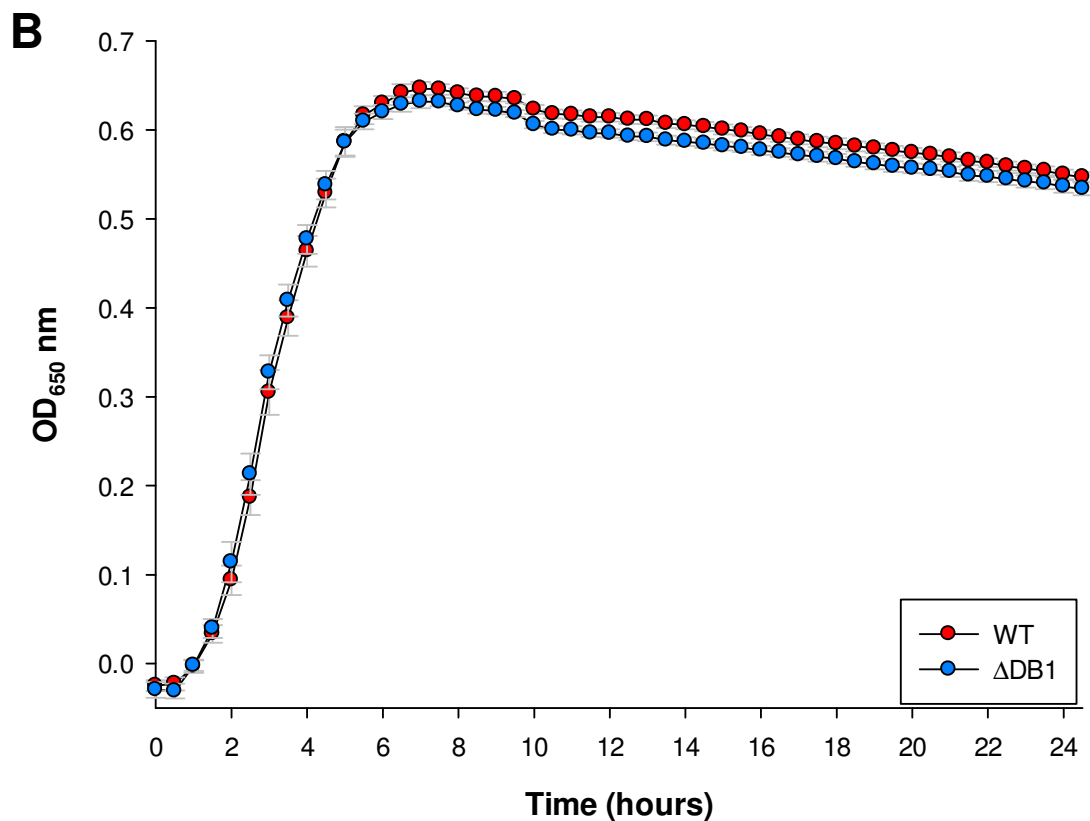
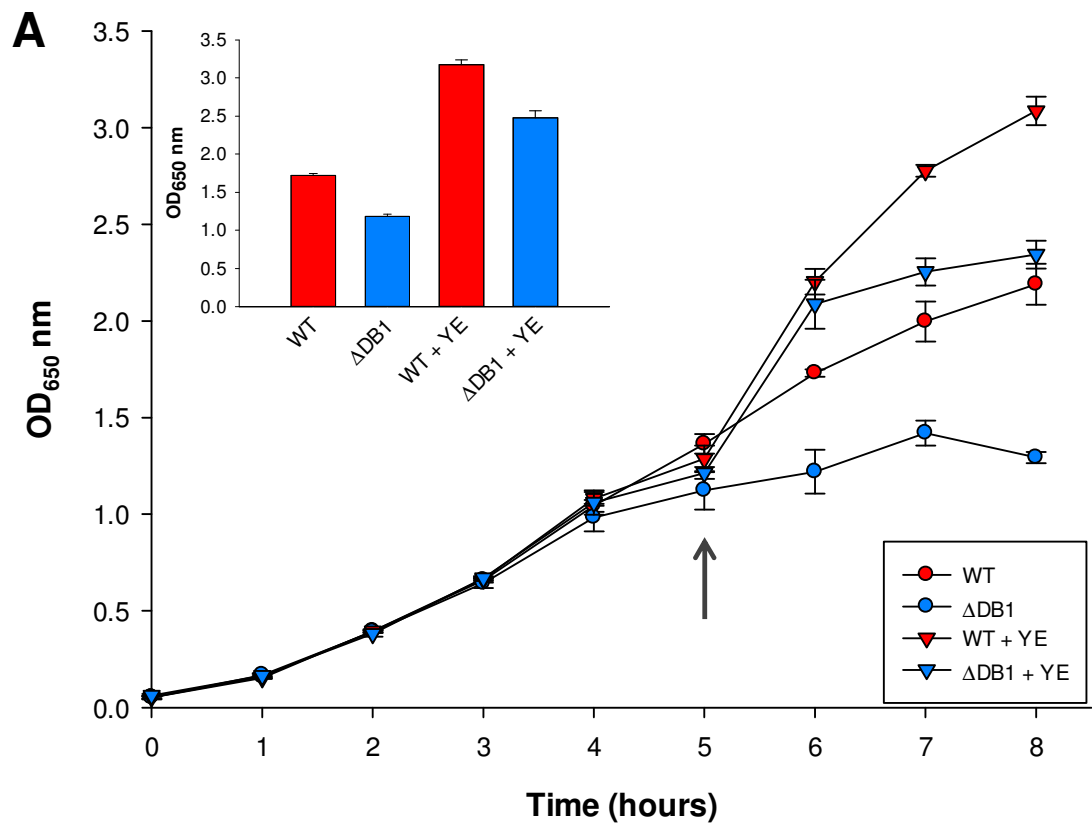


**Figure 4.8.2. (A)** Growth curves of wild-type (WT) and  $\Delta$ DB1 *E. coli* K-12 in 1% tryptone broth medium with yeast extract supplementation (+YE). Black arrow designates addition of 1% yeast extract. Inset shows final growth yield of all cultures following 24 h incubation. **(B)** Growth curves of wild-type (WT) and  $\Delta$ DB1 *E. coli* K-12 in 1% yeast extract broth medium. All cultures were grown under aerobic conditions at 37°C. Error bars represent standard deviation of three biological replicates.

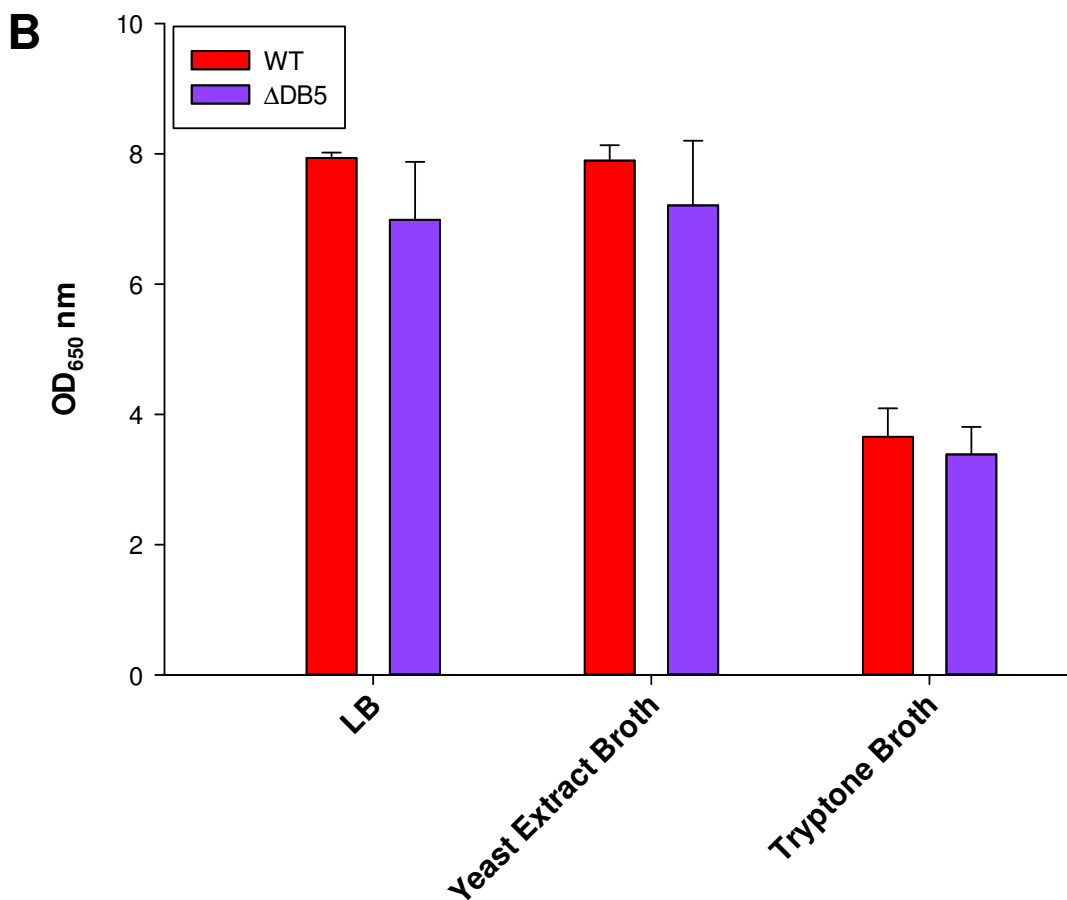
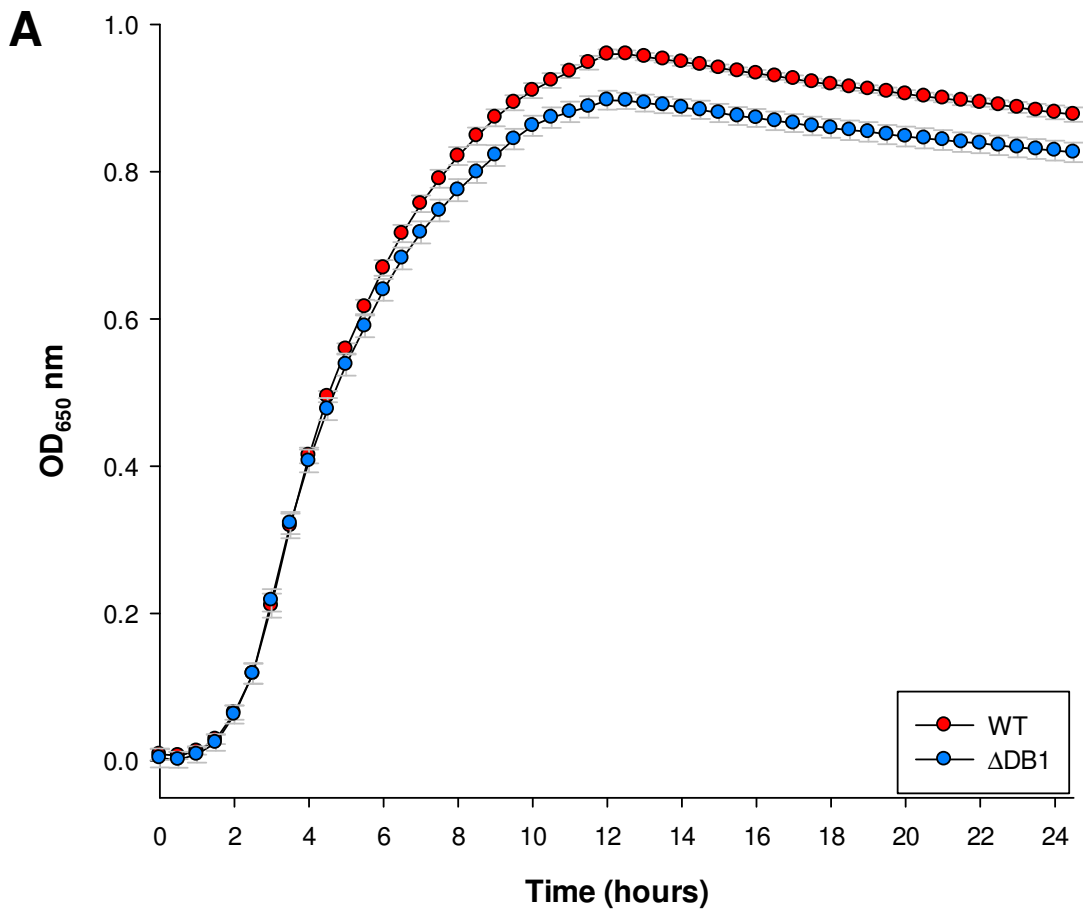


**Figure 4.8.3. (A)** Growth curves of wild-type (WT) and  $\Delta$ DB1 *E. coli* K-12 in LB medium. **(B)** Final growth yield (OD<sub>650</sub> nm) of wild-type (WT) and  $\Delta$ DB5 *E. coli* K-12 grown in LB, 1% yeast extract broth and 1% tryptone broth. All cultures were grown under aerobic conditions at 37°C. Error bars represent standard deviation of three biological replicates.

## 4.9 Discussion

The presence or absence of Dtp transport proteins across the bacterial kingdom has been characterised, with particular attention paid to the Proteobacteria, where there is a clear expansion of Dtp transporters within the Gammaproteobacteria, particularly the Enterobacteriaceae. Although the reasons for this expansion remain unclear, it could be suggested that the environmental niche of enteric Gammaproteobacteria that have a disproportionately large number of Dtp transporters such as *K. oxytoca*, *K. pneumoniae*, *E. aerogenes* and *C. freundii* (a total of 5 Dtp proteins each) necessitates an increased requirement for peptide transport due to high availability of peptides within the human intestinal tract (Adibi, 1971), particularly after their host has consumed a protein-rich meal. The presence of an array of Dtp transporters, all with differing substrate specificities may serve to increase the probability that any given peptide will be transported, maximising the variety and total number of di- and oligopeptides that are taken up by the bacterium to be used as a nutrient source. It could be envisaged that a fitness advantage may be gained from being able to uptake peptides that other bacteria within the environmental niche are unable access. Generally speaking, non-enteric bacteria may have a reduced requirement for peptide transport due to lower environmental peptide availability; it may be energetically unfavourable and disadvantageous to overall fitness to encode and express multiple peptide transporters if peptides do not make up a significant portion of available growth substrates. This would be reflected in the limited number of Dtp transporters typically found in the genome of non-Enterobacteriaceae as described in section 4.1, although a comprehensive analysis of the peptide transporter repertoire of non-enteric bacteria was not carried out in this study.

While the exact substrate specificity of individual prokaryotic PTR2 family transporters differs (as discussed later), they clearly share a general related functionality in terms of ability to transport peptides. This is substantiated by the observation that the majority of residues deemed to be important for catalytic activity and substrate positioning within the binding pocket of PTR2 family proteins are conserved between structurally characterised members and *E. coli* Dtp proteins, although there are some notable exceptions, as discussed below. A multiple sequence alignment of all *E. coli* Dtp proteins, DtpE from *K. pneumoniae*, along with examples of structurally characterised prokaryotic homologues, PepT<sub>So</sub> (Newstead *et al.*, 2011), PepT<sub>So2</sub> (Guettou *et al.*, 2013), PepT<sub>St</sub> (Solcan *et al.*, 2012) and GkPOT (Doki *et al.*, 2013), is shown in Fig. 4.9.

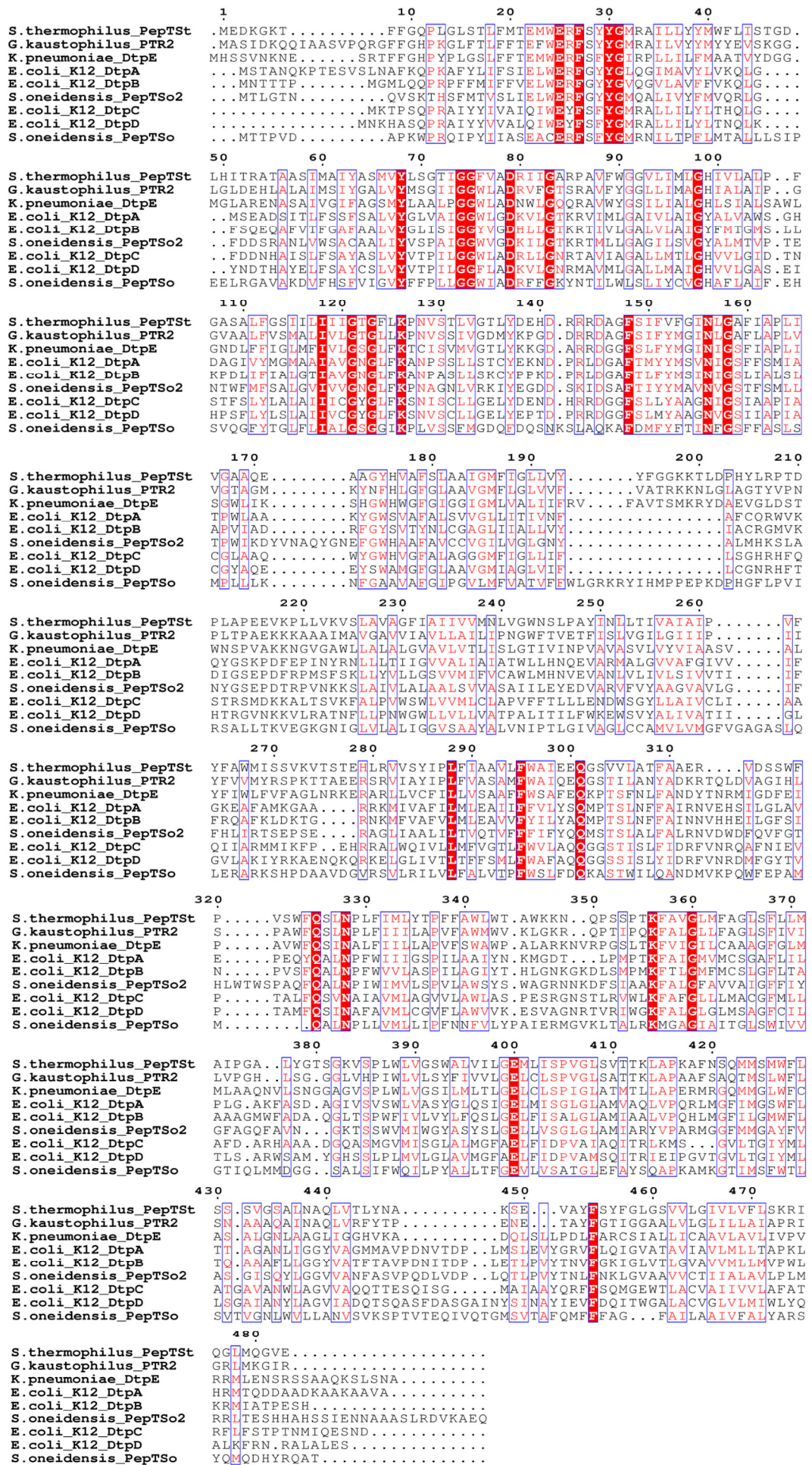


**Figure 4.9.** Multiple sequence alignment of *E. coli* Dtp proteins and selected prokaryotic homologues. Alignment was carried out in Clustal X2. ESPript 3.0 (<http://esprict.ibcp.fr/ESPript/cgi-bin/ESPript.cgi>) multiple sequence alignment graphic software was used to visualise the alignment.

Histidine residue 57 (His57) of *H. sapiens* PTR2 family peptide transporter, PepT1, which is essential for catalytic function (Fei *et al.*, 1997) and was later reported to be the possible proton binding site of the transporter (Uchiyama *et al.*, 2003) is conserved only in PepT1 (not shown) and PepT<sub>So</sub>, demonstrating that the equivalent His57 residue in *E. coli* is not essential for catalytic function. In a similar vein, all PTR2 family proteins have been reported to contain a conserved sequence motif in transmembrane helix 1, ExxERFxYY (Newstead, 2014, in press). Interestingly, this motif does not show absolute conservation across all *E. coli* Dtp transporters with differences arising in DtpC and DtpD, where the first Glu residue in the motif, Glu21 in PepT<sub>So</sub>, has been replaced with Gln. More notably, just upstream of this motif, a conserved Arg residue (at position 32 in PepT<sub>So</sub>) has been replaced with a Gln in DtpA, (Gln41), DtpB (Gln34) and, as previously reported by Newstead, PepT<sub>So2</sub> (Gln32). In structurally characterised PTR2 proteins, Arg32 is proposed to form a salt bridge with the C-terminus of a peptide substrate, aiding in its coordination within the binding pocket (Newstead, 2014, in press). The Arg32Gln substitution observed in DtpA, DtpB and PepT<sub>So2</sub> means that the peptide substrate is now coordinated slightly differently within the binding pocket, as it has to now form a salt bridge with an alternative arginine residue, Arg25 in PepT<sub>So2</sub>. This may imply that PTR2 family members with Arg32Gln substitutions exhibit different substrate specificity to their more ancestral counterparts, allowing bacteria with examples of both protein types to transport a wider range of peptide substrates. Arg25 itself is relatively well conserved among PTR2 family proteins, with a mutation of this residue to His in human PepT2 completely inactivating transport (Terada *et al.*, 2004). This raises questions relating to the role of this non-conservative mutation in DtpC and DtpD, again, suggesting that these transporters are able to recognise different peptide-based substrates to DtpA and DtpB.

Furthermore, the FYxxINxG sequence motif, attributed to show absolute conservation between PTR2 peptide transporters from bacteria to mammals (Daniel *et al.*, 2006) is not conserved among *E. coli* Dtp transporters, or in PepT<sub>St</sub>. This suggests that PTR2 family proteins are not as well conserved as historically suggested and residue substitutions within these regions are likely important for the overall function of the protein.

The *H. sapiens* PTR2 family member and DtpA homologue, PepT1, is found at the brush border membrane of intestinal tissue and has an extremely broad ranging substrate specificity, which has been empirically validated (Biegel *et al.*, 2006), indicating an important role in general peptide uptake from diet. PepT1 shares homology of between 17% to 24% with individual *E. coli* K-12 Dtp proteins, suggesting a partial functional similarity. The fact that the range of enteric bacteria analysed here generally encode multiple *dtp* homologues in their genome supports the notion that in the human intestine,

these transporters play a role in scavenging nutrients from the human diet. It could be hypothesised that because out of all four Dtp proteins of *E. coli*, *H. sapiens* PepT1 shares the most sequence identity with DtpA (24%), that DtpA and PepT1 have some level of parallel substrate specificity; both could be broad-specificity, general transporters of di- and tripeptides. This notion is supported by the observation that a  $\Delta dtpA$  strain of *E. coli* K-12 exhibited a significant growth phenotype when required to uptake 5 out of the 7 individual di- or tripeptides assessed in this work (Phe-Ala, Tyr-Ala, Val-Gly-Gly, Leu-Ala and Ala-Leu), along with the complex peptide mixture, tryptone. This observation largely supports the conclusions drawn in other studies of *E. coli* DtpA which together demonstrate that purified DtpA is able to transport a wide range of structurally unrelated peptides containing both L- and D- amino acid isoforms, along with a plethora of peptidomimetic drugs (Harder *et al.*, 2008, Weitz *et al.*, 2007, Prabhala *et al.*, 2014).

While it is clear that DtpA has broad substrate specificity, the same is not true for the other three *E. coli* Dtp transporters, DtpB, DtpC and DtpD. During this work, no significant phenotype was observed for individual mutants of either *dtpB* or *dtpC* when required to uptake any of the 7 individual di- or tripeptides, or the complex peptide mixture, tryptone. Very little published work has been carried out on the substrate specificity of DtpB. The single in-depth study concluded that DtpB has a strong C-terminal negative charge preference (Harder *et al.*, 2008), which may explain why DtpB is not implicated in transport of any peptide substrate assessed here. Conversely, DtpC has been shown to transport C-terminal positively charged peptides (Ernst *et al.*, 2009), but, again, due to limited availability of certain peptides, none of the dipeptides assessed here have those chemical properties, possibly explaining why no growth phenotype was observed for  $\Delta dtpC$ . A limited number of previous attempts to functionally characterise DtpD revealed that the transporter has a preference for L-lysine containing dipeptides (Jensen *et al.*, 2012), a strong C-terminal charge preference and no affinity for N-terminally charged peptides (Casagrande *et al.*, 2009). Based on the toxic dipeptide growth assays, DtpD also appears to transport amino acids with a hydrophobic residue at either the N- or C-terminus (Leu-Ala or Ala-Leu, respectively) and may also play a role in general peptide uptake, suggested by the growth rate and final yield defect exhibited by  $\Delta dtpD$  when grown in tryptone broth. It is difficult to distinguish why DtpA and DtpD would share common peptide transport features when phylogenetically, bacterial DtpA proteins cluster more closely to DtpB than DtpD. It may be that the nature of the peptide binding site of DtpA and DtpD is naturally more promiscuous, being able to accept a wider range of peptide substrates, meaning that the effect of deleting these transporters has a more pronounced effect than deleting either DtpB and DtpC, which may have a more specialised substrate specificity.

Although unique phenotypes have been observed for at least two Dtp transporter mutants of *E. coli*, it is pertinent to assume that these transporters have a degree of overlapping substrate specificity, given that they all belong to the same family. This proposal is strengthened by the observation that when *E. coli* is required to uptake Ala-Ala as the sole source of nitrogen, growth is almost completely abolished only when multiple Dtp transporters are mutated, meaning that at least two transporters play a role in Ala-Ala uptake. The capacity to transport Ala-Ala has been demonstrated for DtpA (Weitz *et al.*, 2007), DtpB (Harder *et al.*, 2008) and DtpC (Ernst *et al.*, 2009), all of which supports the observation that single *dtp* deletions have little effect on Ala-Ala uptake. It was surprising to note that the high affinity ABC peptide transporters of *E. coli* (Dpp and Opp) appear not to transport Ala-Ala *in vivo*, given that previously published work suggests that Ala-Ala is a good substrate for the substrate binding protein of Dpp, DppA (Smith *et al.*, 1999). While this work does not directly contradict the observation of Smith, it brings into question the relative role of Dpp in relation to Ala-Ala transport *in vivo* and proposes that in a biological system, Ala-Ala is preferentially transported by a combination of Dtp transporters and not by Dpp. It is not unprecedented that a substrate of Dpp is also a substrate for other peptide transporters, such as Opp or DtpA (Smith and Payne, 1990), which partly explains why no growth phenotype is observed for  $\Delta dppC$  or  $\Delta DB1$  when Ala-Ala is supplied as the sole source of nitrogen.

It is clear from the work described above that *E. coli* does not rely exclusively on Dpp and Opp for uptake of every individual di- or tripeptide. However, it was concluded that these high affinity peptide transporters play a role in general peptide uptake in undefined peptide-based medium. This conclusion was based on the observation that a  $\Delta dppC$   $\Delta oppC$  double mutant ( $\Delta DB1$ ) displayed strong growth rate and final yield phenotypic defects compared to wild type when grown in tryptone broth, which was almost solely attributable to the mutation in *oppC*. It should also be noted that  $\Delta dtpA$  also displayed a growth rate and yield defect when grown in tryptone broth, although the phenotype was not as severe as observed for  $\Delta DB1$  or  $\Delta oppC$ . This suggested that during late exponential and stationary phase growth, strains with a functional *oppC* were able to access a pool of oligopeptides within the growth medium that  $\Delta DB1$  ( $\Delta oppC$ ) could not, confirming that Opp is primarily responsible for uptake of the major nutrient peptide source in tryptone broth, oligopeptides. This conclusion largely supports previous literature that suggests *E. coli* has at least two oligopeptide transporters (later identified as Opp and DtpA) that have a combination of diverse and overlapping substrate specificities (Naider & Becker, 1975, Barak & Gilbarg, 1975).

While *E. coli* undoubtedly uses peptides as a growth substrate during the latter stages of growth, all TD-Pep strains exhibited almost identical growth rates during lag and early exponential phase when grown in tryptone broth and the differential growth rate and final yield phenotype between wild-type *E. coli* and  $\Delta$ DB1 was almost completely abolished when strains were grown in LB. This suggests that during early growth in tryptone broth and until late exponential/early stationary phase growth in LB, *E. coli* preferentially utilises non-peptide based growth substrates before switching to peptide metabolism. These observations are in agreement with relative expression of the *dpp* and *opp* operons in *E. coli*, which are maximally expressed during late exponential and stationary phase during growth in LB medium (Baev *et al.*, 2006a) suggesting a reliance on peptides as a nutrient source only during later phases of growth. This also contradicts anecdotal claims that when growing in LB, *E. coli* is growing solely on peptides. It is likely that during non-peptide metabolising growth in tryptone broth and LB, *E. coli* utilises either amino acids or sugars as the primary growth substrate. However, the relative amount of these nutrients present in commercially available tryptone has not been disclosed nor empirically verified. Baev *et al.* (2006b) demonstrated that the relative expression of genes involved in catabolism of D-maltose, D-galactose, L-fuculose, D-mannose and D-mannitol fluctuate according to the specific growth rate of *E. coli* when grown in LB and further stated that, according to the Difco manual (a commercial supplier of tryptone), the carbohydrate content of tryptone is 7.7% and in yeast extract is 17.5%. Extrapolating this to calculate the total carbohydrate concentration of typical LB medium, which contains twice as much tryptone as yeast extract, a value of 0.16% is obtained  $((7.7*2)+17.5)/2$ . This is equivalent to an approximate mixed carbohydrate concentration of 8 mM, if normalised based on the molecular weight of D-glucose. If accurate, this concentration of sugar would be sufficient to support initial bacterial growth for several hours, with the saccharide component of the medium preferentially used over the peptide component. However, the sugar content of commercially available yeast extract is extremely inconsistent, with a notable report by Zhang *et al.*, (2003), demonstrating that the trehalose content of yeast extract can range from <2 to >17% between individual lots, emphasising the significant variation in the total amount of individual growth substrates present in separate batches undefined, complex bacterial growth media. If sugars are used as the primary growth substrate in 1% tryptone broth, the approximate sugar concentration is 3.85 mM, based on a 7.7% carbohydrate content of Difco branded tryptone, as suggested by Baev. This would be sufficient to support bacterial growth for several hours before becoming limiting, forcing the bacteria to switch metabolism to the only remaining nutrient source, peptides. However, this would likely be observed during bacterial growth in the form of a diauxic shift from sugar-based to peptide-based metabolism, which was not apparent. Thus, the initial growth substrate used by *E. coli* in tryptone broth is unlikely to be sugar-based.

A conflicting report by Sezenov *et al.* (2007) indirectly calculated the sugar content of LB as less than 100  $\mu\text{M}$ , based on absence of growth of an *E. coli* strain that required fermentable sugars to support growth. Sezenov also calculated the total amino acid concentration of LB by hydrolysing all peptide bonds to release the entire pool of free amino acids. The total amino acid concentration was calculated to be in the range of 80 mM – 100 mM, an ample amount to support bacterial growth in the absence of any sugar component within the medium. Therefore, in the absence of a diauxic growth shift, the almost identical growth rate of all TD-Pep strains during early exponential phase in tryptone broth supports the claims of Sezenov, where *E. coli* grows sequentially on free amino acids and then peptides. This pattern of growth is unlikely to be diauxic as the bacteria will already be expressing a plethora of peptidases (Miller & Schwartz, 1978), the necessary amino acid-catabolising enzymes and a basal level of *dpp* and *opp* (Baev *et al.*, 2006a) required to make a seamless transition from amino acid to peptide uptake and catabolism (note that the relative expression levels of *dtpA* and *dtpD* during growth of *E. coli* in any media are unknown).

The pattern of growth observed for TD-Pep *E. coli* in tryptone broth with no diauxie (Fig. 4.7.1 and 4.7.2) supports the hypothesis that the sugar content of tryptone is relatively low. This implies that lag and early exponential phase bacterial growth is sustained by amino acid catabolism. However, this conclusion cannot be drawn when *E. coli* is grown in LB, as the molecular composition of the added yeast extract component, while extremely inconsistent, is reported to contain non-amino acid based growth substrates including sugars which were observed to drastically reduce the differential phenotype between wild-type *E. coli* and  $\Delta\text{DB1}$ . This confirms that when grown in LB, the requirement of *E. coli* to catabolise peptides is reduced. Overall, this highlights the requirement for a comprehensive, direct analysis of commercially available tryptone and yeast extract to reach a consensus regarding the composition of nutrients available to bacteria during growth in tryptone broth and LB.

Data presented here also suggested that when grown in tryptone broth, *E. coli* becomes starved for carbon before nitrogen, as the addition of either D-glucose or 1% yeast extract following entry into stationary phase allowed *E. coli* to re-establish exponential growth. This phenotype was not observed following addition of the nitrogen source ammonium chloride. This phenomenon has been reported previously by Sezenov *et al.* (2007), who observed that addition of a carbon source (D-glucose) to exhausted LB medium allowed *E. coli* to re-establish growth to a final yield proportional to the amount of D-glucose added. This brings into question the importance of the nitrogen starvation response (the Ntr regulon), in relation to peptide transporter expression when *E. coli* is growing in LB

and challenges previous reports which have demonstrated that both *dpp* and *opp* are part of the Ntr regulon and expression is upregulated during nitrogen starvation (Zimmer *et al.*, 2000). The observation that *E. coli* is not nitrogen limited during stationary phase coupled with the report that expression of *dpp* and *opp* increase during exponential growth LB (Baev *et al.*, 2006a) suggests that *opp* and *dpp* are also upregulated by carbon limitation. This is a realistic hypothesis as it has been reported that expression of *dpp* and *opp* is also regulated by several other factors including the amino acids L-leucine and L-alanine (Andrews *et al.*, 1986), a small untranslated RNA, GcvB (Urbanowski *et al.*, 2000) and phosphate limitation (Smith and Payne, 1992). Therefore, under the conditions tested, expression of *dpp* and *opp* is likely to be controlled by factors other than nitrogen limitation.

In summary, Opp, DtpA, DtpD and to a certain extent Dpp, appear to be involved in general, high flux peptide transport. This likely masks the true substrate specificity of DtpB, DtpC and DtpD, as individual mutants of these strains still retain DtpA, Dpp and Opp. If a more detailed analysis of the substrate specificities of these transporters is sought, an *E. coli* K-12 strain with the genotype  $\Delta dppC$ ,  $\Delta oppC$   $\Delta dtpA$  should be used as the parental strain, in which, sequential individual mutations of *dtpB*, *dtpC* and *dtpD* should be made in order to assess the relative involvement of these more poorly characterised transporters in peptide uptake. Generally speaking, the observation that the Dtp peptide transporters are crucial for growth of *E. coli* in certain peptide-containing media brings into question the reliance on the ABC peptide transporters Dpp and Opp for primary peptide uptake in this organism. Under physiological conditions it would be prudent to suggest that both ABC and peptide symporters work in tandem to facilitate peptide transport into the cell.

A summary of the growth-associated phenotypes of all TD-Pep strains is displayed in table 4.9.

**Table 4.9.** Summary of growth-associated phenotypes for TD-Pep strains of *E. coli*. Phenotypes are described as either strong (+++), moderate (++), weak (+) or absent (-) for each peptide substrate assessed. ND = Not determined.

Strain	Ala-Ala	Phe-Ala	Tyr-Ala	Ala-Phe	Leu-Ala	Ala-Leu	Val-Gly-Gly	Tryptone	Yeast extract
$\Delta dtpA$	-	+	-	-	-	-	+++	+	ND
$\Delta dtpB$	-	-	-	-	-	-	-	-	ND
$\Delta dtpC$	-	-	-	-	-	-	-	-	ND
$\Delta dtpD$	-	-	-	-	+	+	-	+	ND
$\Delta DB5$	+++	++	+	+	+	+	+++	ND	-
$\Delta dppC$	-	-	-	++	-	-	-	-	ND
$\Delta oppC$	-	+	-	++	-	-	+	++	ND
$\Delta DB1$	-	-	+	+++	-	-	+	++	-

# Chapter 5

## Transport and catabolism of malodour precursor substrates by *E. coli* K-12

## Introduction and aims

Following characterisation of *E. coli* TD-Pep strains detailed in chapter 4, analysis of malodour precursor uptake in these strains can be investigated. There is an absence of knowledge regarding malodour precursor uptake and biotransformation in *E. coli* as this bacterium has never been used as a model organism for this purpose. It is envisaged that understanding malodour precursor uptake and biotransformation in *E. coli* will provide insight into malodour precursor uptake and biotransformation in the relevant axillary bacteria.

Uptake of dipeptide-conjugated malodour precursor molecules is likely to occur via a specific peptide transporter with the ability to transport dipeptide analogues. If *E. coli* is to be used as a model organism to study this process, it is essential that the specific peptide transporter(s) that transports malodour precursors is identified. Additionally, it is important to understand the biochemical and molecular mechanisms that lead to intracellular catabolism of malodour precursor substrates. This will subsequently allow putative Cys-Gly-3M3SH transporters and intracellular catabolic enzymes from *S. hominis* to be cloned and expressed in the relevant mutant strains of *E. coli*.

### Specific aims

- To assess the ability of *E. coli* K-12 to metabolise dipeptide-conjugated malodour precursor substrates using substrate depletion and thioalcohol labelling assays.
- To identify the genes involved in both transport and intracellular catabolism of the substrate using TD-Pep mutants generated and characterised in chapter 4.
- To clone and express these genes in *E. coli* in order to functionally complement TD-Pep mutants for malodour precursor biotransformation activity.
- To assess the effect of dipeptide competitor molecules on malodour precursor biotransformation in *E. coli*.

## 5.1 Uptake and biotransformation of S-Benzyl-L-cysteinyglycine by *E. coli* K-12

Firstly, it was shown that *E. coli* is able to metabolise S-Benzyl-L-cysteinyglycine in a time-dependant manner by following a time-course of benzyl-mercaptan production. In a standard S-Benzyl-L-cysteinyglycine biotransformation assay, benzyl-mercaptan production increased linearly until approximately 4.5 h, at which point, production levelled off (Fig. 5.1A). The benzyl-mercaptan yield for *E. coli* K-12 wild-type ( $A_{492} = 6.82 \pm 0.11$  at  $t = 6.5$  h) was 3-fold higher than the high thioalcohol producer *S. haemolyticus* G431 ( $2.24 \pm 0.03$ ), confirming that *E. coli* is an efficient S-Benzyl-L-cysteinyglycine biotransformer.

Biotransformation of S-Benzyl-L-cysteinyglycine was inhibited by carbonyl cyanide m-chlorophenyl hydrazone (CCCP) (Fig. 5.1A, inset). CCCP is a protonophore, which disrupts the proton-motive force across the bacterial cell membrane. Uptake processes that are inhibited by CCCP generally use protons to drive substrate translocation across the membrane. This suggests that S-Benzyl-L-cysteinyglycine may be transported by *E. coli* using a molecular symporter, rather than an ABC transporter.

S-Benzyl-L-cysteinyglycine depletion by resting *E. coli* cells was also followed semi-quantitatively using a Thin-Layer Chromatography (TLC) assay. The TLC protocol is detailed in section 2.2.11.9. Substrate (S-Benzyl-L-cysteinyglycine) could be visualised by staining with the amine-specific stain, ninhydrin (Santiago *et al.*, 2006). Removal of substrate from the buffer by resting cells was followed over time and almost complete removal was observed following 3 h incubation (Fig. 5.1B). When S-Benzyl-L-cysteinyglycine was incubated in the absence of cells, it could still be detected following 5 h incubation, confirming that bacterial cells are required to remove the substrate from the buffer.

Together, these data demonstrate that *E. coli* actively transports and metabolises the model malodour precursor substrate S-Benzyl-L-cysteinyglycine in an efficient and time-dependent manner.

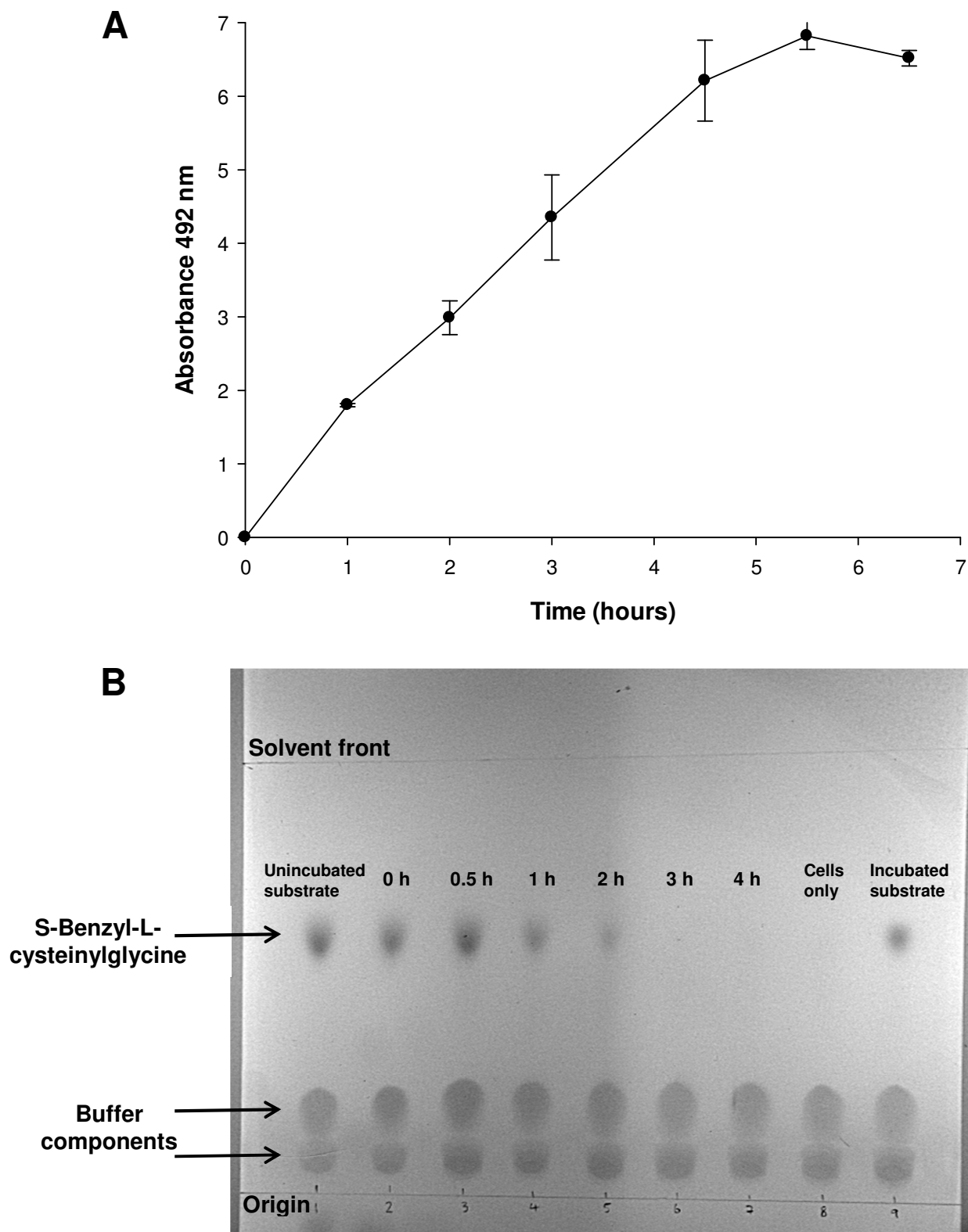


**Figure 5.1.** Uptake and biotransformation of S-Benzyl-L-cysteinylglycine by *E. coli* K-12. **(A)** Time dependent biotransformation of S-Benzyl-L-cysteinylglycine. Inset shows thioalcohol yield of S-Benzyl-L-cysteinylglycine biotransformation by *E. coli* K-12 in the absence and presence of 50  $\mu$ M CCCP. Thioalcohol yield ( $A_{492}$ ) was quantified for using MTS/PMS at the respective time point. Error bars represent standard deviation of three biological replicates. **(B)** TLC analysis of S-Benzyl-L-cysteinylglycine uptake by *E. coli* K-12. Lanes are labelled accordingly. Time points refer to incubation time. 'Unincubated' and 'incubated' substrate refers to S-Benzyl-L-cysteinylglycine incubated in the absence of bacterial cells at 37°C and room temperature, respectively. Substrate only samples were taken following 5 h incubation. 'Cells only' refers to bacterial cells incubated in the absence of substrate.

## 5.2 The role of C-S- $\beta$ -lyase enzymes in biotransformation of malodour precursor substrates

Previous work within Unilever had ascertained that model malodour precursor biotransformation (S-Benzyl-L-cysteine) was dependent on the cytoplasmic enzyme cystathionine  $\beta$ -lyase in the model organism *C. jeikeium* K411 (James *et al.*, 2013). This work was corroborated here in malodour precursor biotransformation assays using a purified recombinant preparation of this C-S-  $\beta$ -lyase (NCBI accession: YP\_250369.1) from *C. jeikeium* K411 (supplied by Unilever). It was observed that S-Benzyl-L-cysteine was efficiently biotransformed by K411 C-S-  $\beta$ -lyase and maximum benzyl-mercaptan yield was reached following 3 h incubation (Fig. 5.2A). In contrast, K411 C-S-  $\beta$ -lyase was unable to generate benzyl-mercaptan from the model dipeptide malodour precursor substrate, S-Benzyl-L-cysteinylglycine, or biotransform the physiological malodour precursor dipeptide substrate Cys-Gly-3M3SH. This strongly suggests that a dipeptidase-like enzyme is required to liberate L-cysteine-malodour precursors from their respective dipeptide counterparts, which would then be biotransformed into thioalcohol by cystathionine  $\beta$ -lyase. Alternatively however, malodour precursor substrate biotransforming bacteria may possess a novel enzyme which is able to convert dipeptide malodour precursor substrate into its constituent thioalcohol in a single-step process. This may be particularly true of physiological substrates, as there is no direct empirical evidence for the involvement of cystathionine  $\beta$ -lyase in Cys-Gly-3M3SH biotransformation.

To assess which enzyme(s) is/are involved in intracellular S-Benzyl-L-cysteinylglycine catabolism in *E. coli*, substrate biotransformation assays were performed using Keio Collection strains mutated in genes with known C-S-  $\beta$ -lyase activity. *E. coli* possesses two known C-S-  $\beta$ -lyase encoding genes, *malY* and *metC*, as discussed in section 1.5.3.

Mutants of both *malY* and *metC* showed no significant decrease in benzyl-mercaptan production compared to wild-type in an S-Benzyl-L-cysteinylglycine biotransformation assay (Fig. 5.2B). This implies that neither MalY or MetC alone are essential for S-Benzyl-L-cysteinylglycine biotransformation. This surprising result led to further examination of relevant literature to identify other *E. coli* genes with characterised C-S-  $\beta$ -lyase activity, which revealed *tnaA* as a possible candidate. In *E. coli*, TnaA has a biological role in tryptophan catabolism, enabling the bacterium to utilise L-tryptophan as a carbon or nitrogen source (Phillips *et al.*, 2003). TnaA has also been shown to possess C-S-  $\beta$ -lyase activity against S-Benzyl-L-cysteine (Awano *et al.*, 2003, Awano *et al.*, 2005). A *tnaA*

mutant,  $\Delta tnaA$ , was completely incapable of biotransforming S-Benzyl-L-cysteinylglycine, demonstrating that TnaA is an essential protein for S-Benzyl-L-cysteinylglycine catabolism in *E. coli*, although the requirement for an initial dipeptidase step in the biotransformation reaction remains to be determined.

In summary, it has been established that *C. jeikeium* cystathionine  $\beta$ -lyase is able to biotransform the model malodour precursor substrate S-Benzyl-L-cysteine but not S-Benzyl-L-cysteinylglycine or the physiological malodour precursor substrate Cys-Gly-3M3SH. In *E. coli*, S-Benzyl-L-cysteinylglycine catabolism is dependent upon TnaA and not the commonly recognised C-S-  $\beta$ -lyase proteins MalY or MetC. Given the relative similarities in structure between L-tryptophan and S-Benzyl-L-cysteine, with both containing a bulky aromatic ring, the fact that TnaA is able to catabolise both molecules is unsurprising, although given the abundance of proteins with C-S-  $\beta$ -lyase activity that *E. coli* possesses, it is remarkable that TnaA is the only protein involved in S-Benzyl-L-cysteine catabolism.

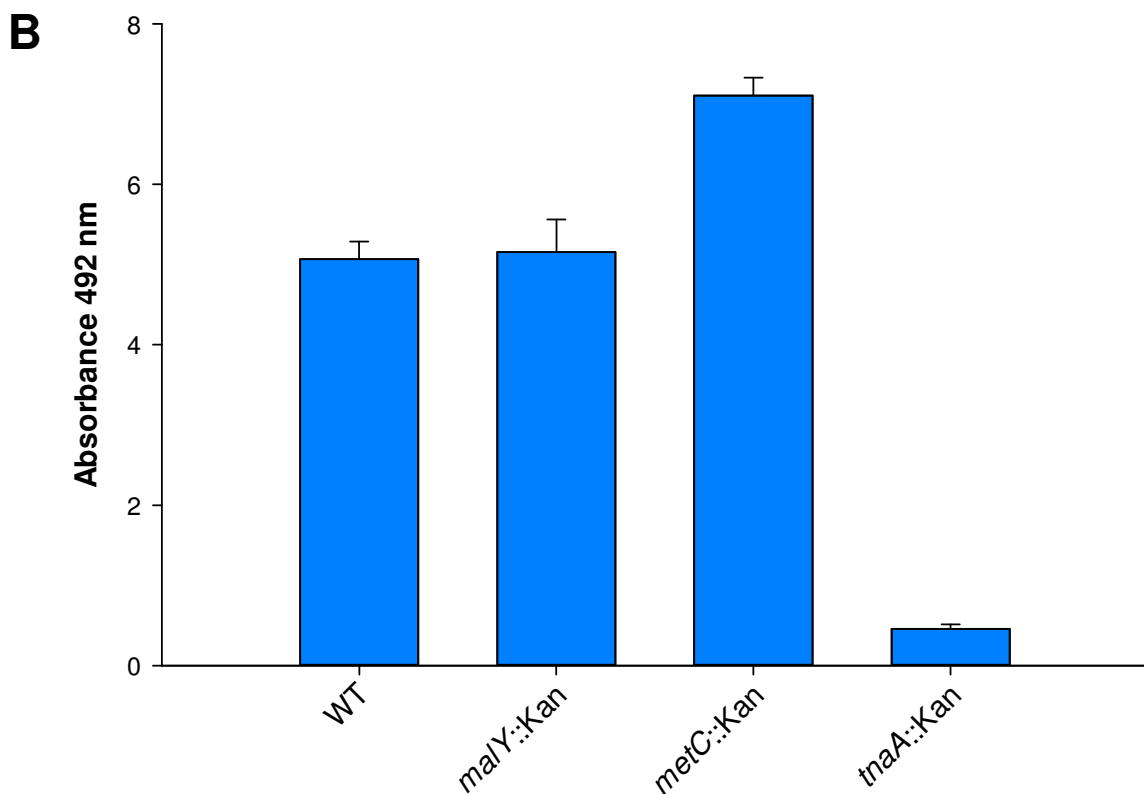
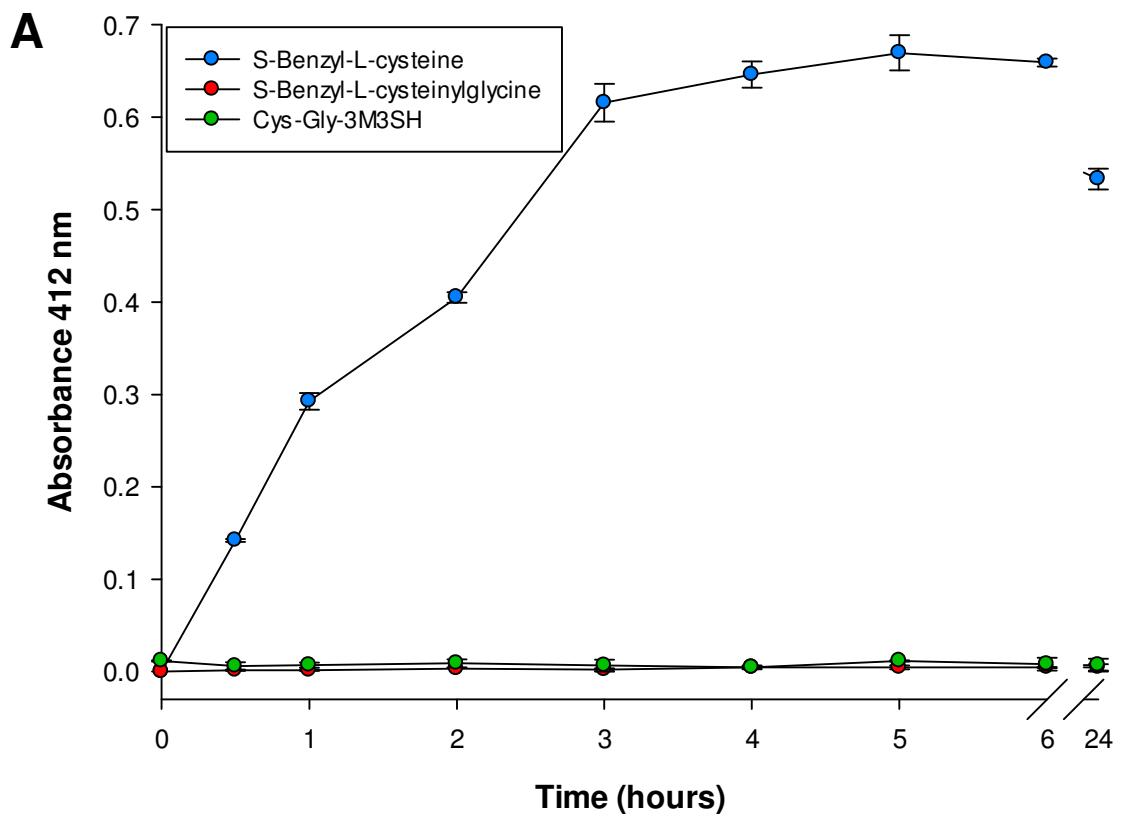


**Figure 5.2. (A)** Biotransformation of S-Benzyl-L-cysteine and S-Benzyl-L-cysteinylglycine by purified C-S-  $\beta$ -lyase from *C. jeikeium* K411. Thioalcohol yield ( $A_{412}$ ) was quantified using DTNB. ‘Enzyme only’ refers to purified C-S-  $\beta$ -lyase incubated in the absence of substrate. Error bars represent standard deviation of two technical replicates. **(B)** Biotransformation of S-Benzyl-L-cysteinylglycine by *E. coli* C-S-  $\beta$ -lyase mutants. Thioalcohol yield ( $A_{492}$ ) was quantified using MTS/PMS following 4 h incubation. Error bars represent standard deviation of three biological replicates.

### 5.3 Transport and biotransformation of S-Benzyl-L-cysteinylglycine by TD-Pep *E. coli*

Following the discovery that TnaA is an essential enzyme in malodour precursor biotransformation, analysis of putative malodour precursor transporters in *E. coli* was undertaken. Given that the backbone structure of the S-Benzyl-L-cysteinylglycine is dipeptide-based, it was predicted that it would be transported by a peptide transporter. To identify which transport system(s) *E. coli* uses to transport malodour precursors, the TD-Pep strains were screened for S-Benzyl-L-cysteinylglycine biotransformation ability.

A reduction in benzyl-mercaptan yield of approximately 70% was observed for  $\Delta$ DB5 (Fig. 5.3). This was almost exclusively attributable to the mutation in *dtpB*, as  $\Delta$ *dtpB* exhibited approximately 60% reduction in benzyl-mercaptan yield. No significant decrease in benzyl-mercaptan yield relative to wild-type was observed for  $\Delta$ DB1 ( $\Delta$ *dppC*  $\Delta$ *oppC*),  $\Delta$ *dtpA*,  $\Delta$ *dtpC* or  $\Delta$ *dtpD*, demonstrating that these transporters are not involved in S-Benzyl-L-cysteinylglycine uptake. Two other strains that were assessed in the screen were Keio Collection strains *cstA::kan* and *sapC::kan*. *sapC* encodes a transport system for antimicrobial peptides whereas *cstA* is a peptide symporter expressed during carbon starvation (see section 1.5.2). Neither *sapC::kan* nor *cstA::kan* showed any reduction in benzyl-mercaptan yield and are therefore not involved in S-Benzyl-L-cysteinylglycine uptake.

It was concluded that DtpB is the principal S-Benzyl-L-cysteinylglycine transporter, which represents a novel phenotype for this Dtp transporter in *E. coli*. The absence of a significant cumulative effect of mutating multiple Dtp transporters ( $\Delta$ DB5) on S-Benzyl-L-cysteinylglycine biotransformation suggests that DtpB may be more specialised in terms of substrate specificity than other Dtp transporters.

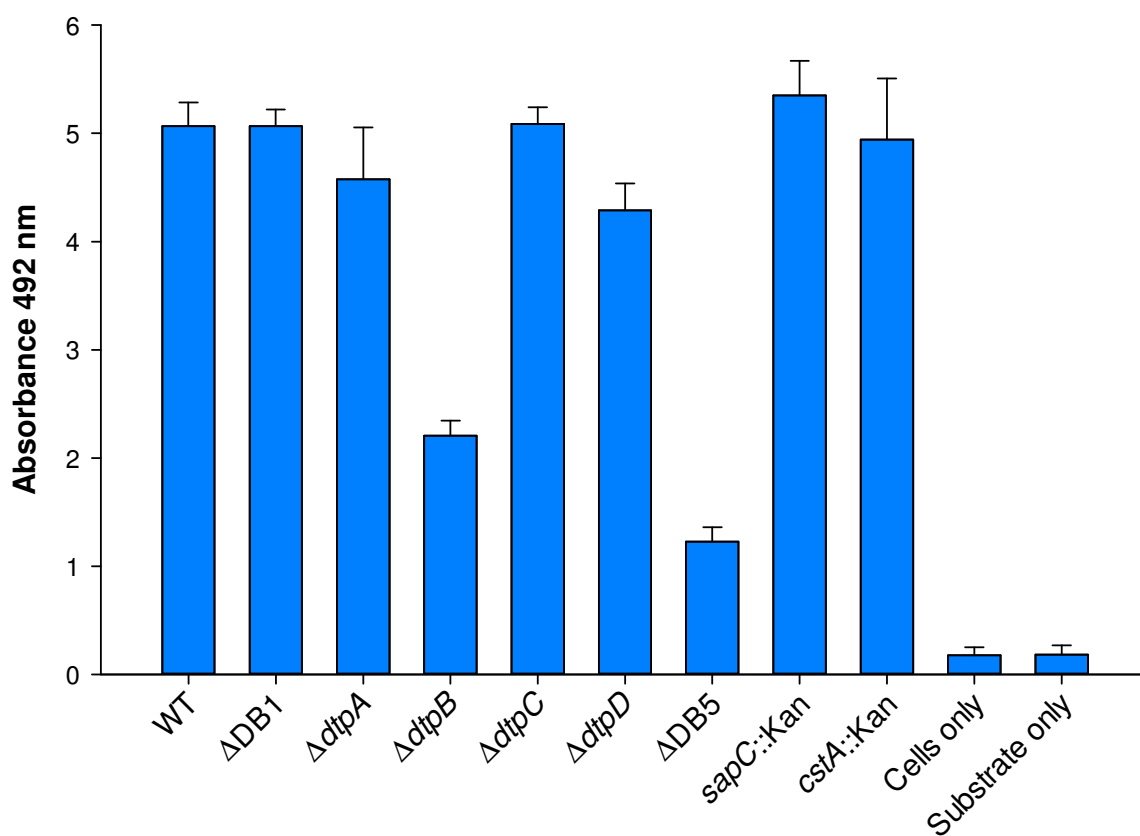


**Figure 5.3.** Biotransformation of S-Benzyl-L-cysteinylglycine by TD-Pep *E. coli*. Thioalcohol yield ( $A_{492}$ ) was quantified for each strain using MTS/PMS following 4 h incubation. ‘Substrate only’ and ‘cells only’ refer to reactions incubated in the absence of S-Benzyl-L-cysteinylglycine or bacterial cells respectively. Error bars represent standard deviation of three biological replicates.

## 5.4 Cloning, overexpression and functional complementation of *dtpA*, *dtpB*, *dtpC* and *dtpD*

To confirm the role of DtpB in malodour precursor transport and to verify that this role is unique to DtpB and no other Dtp transporter, *dtpA*, *dtpB*, *dtpC* and *dtpD* from *E. coli* were cloned into a high copy number inducible expression vector pBADcLIC2005 (Fig. 5.4.1A) (Geertsma & Poolman, 2007). pBADcLIC2005 is a ligation-independent cloning (LIC) vector and is routinely used for protein overexpression in *E. coli*. It contains an *araBAD* arabinose-inducible promoter and generates proteins with a C-terminal decahistidine tag. This vector was chosen as it was anticipated that Dtp transporter overexpression would give a stronger overall signal in malodour precursor biotransformation assays than using a low copy number complementation vector, assuming that homologous protein overexpression was not toxic to the bacterium. There was also the added benefit that pBADcLIC2005 produces His-tagged proteins which would be useful for downstream purification analysis, if required. All four *dtp* genes were cloned into pBADcLIC2005 by ligation independent cloning (see section 2.2.10.3). Resulting constructs were checked by Sanger sequencing and named pDtpA, pDtpB, pDtpC and pDtpD respectively. The isogenic background strain, *E. coli* K-12 BW25113 was transformed with each plasmid to create strains WT pDtpA, WT pDtpB, WT pDtpC and WT pDtpD.

To confirm that DtpB is responsible for S-Benzyl-L-cysteinyglycine transport in *E. coli* substrate biotransformation assays were carried out using WT pDtpA, WT pDtpB, WT pDtpC and WT pDtpD. Cultures containing plasmid were induced overnight to ensure that high levels of Dtp protein were present at the beginning of the assay. High benzyl-mercaptan yield was observed for WT pDtpB, following 10 min incubation (Fig. 5.4.1B). No significant differences in benzyl-mercaptan yield were observed for strains overexpressing DtpA, DtpC or DtpD, relative to wild-type. This confirms that DtpB is solely responsible for uptake of S-Benzyl-L-cysteinyglycine in *E. coli*. Given the high benzyl-mercaptan yield following only 10 min incubation (wild-type takes > 1 h to reach a similar benzyl-mercaptan yield; see Fig. 5.1A), it can be suggested that native *dtpB* expression in *E. coli* is low.

The benzyl-mercaptan yield from S-Benzyl-L-cysteinyglycine biotransformation by WT pDtpB increased as the *araBAD* promoter was titrated with increasing concentrations of L-arabinose (Fig. 5.4.2A). Maximum benzyl-mercaptan yield was achieved using an overnight induction L-arabinose concentration of 0.1%. This was however coupled with a decrease in total cell yield (data not shown), suggesting that excessive overexpression of

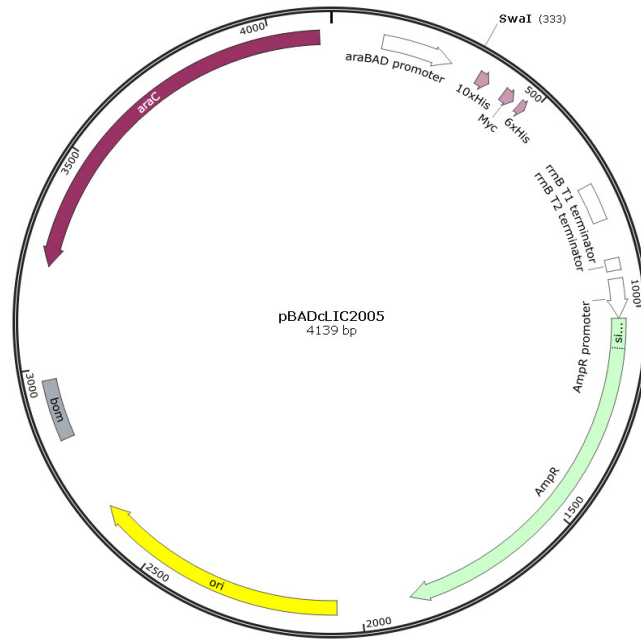
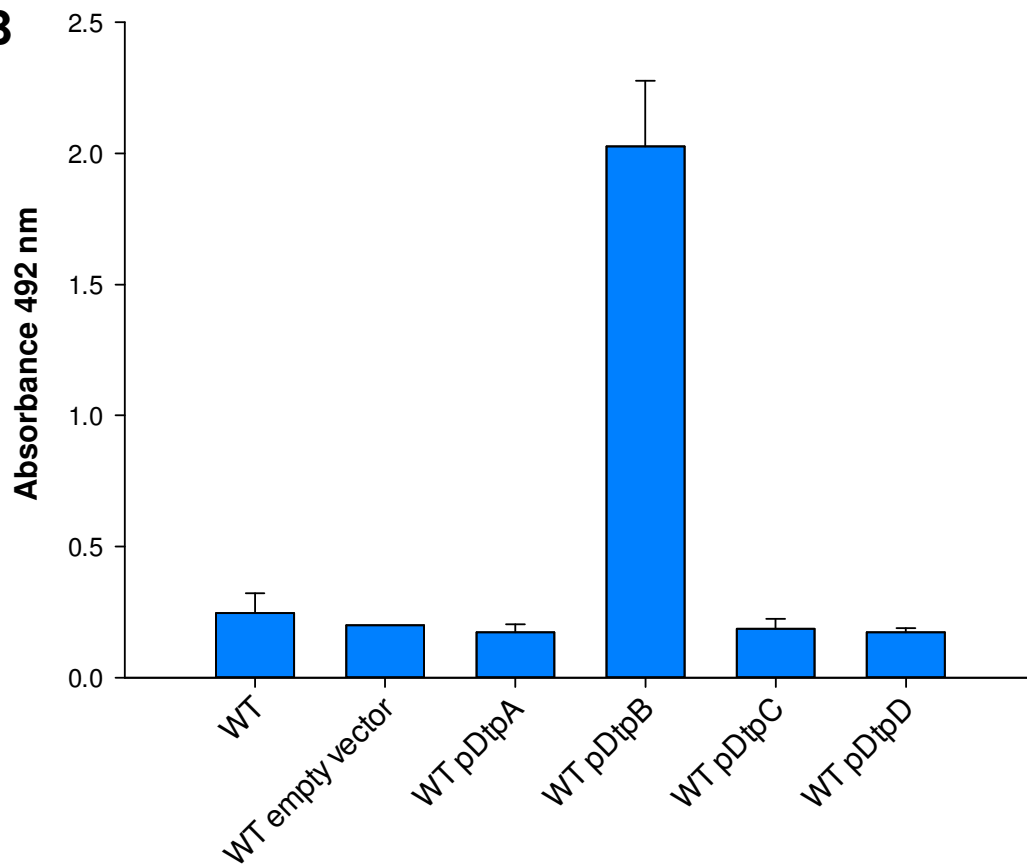
DtpB is toxic to the bacterium. For this reason, all subsequent experiments used an overnight L-arabinose induction concentration of 0.0001%, which correlated with high benzyl-mercaptan yield (Fig. 5.4.2A) and high cell yield (data not shown).

To further characterise S-Benzyl-L-cysteinylglycine biotransformation in *E. coli*, analysis of additional mutant strains was carried out. It was observed that S-Benzyl-L-cysteinylglycine biotransformation in  $\Delta tnaA$  cannot be rescued by overexpression of DtpB (Fig. 5.4.2B), confirming that substrate uptake and biotransformation are independent processes. It was also shown that CCCP was able to inhibit S-Benzyl-L-cysteinylglycine biotransformation in WT pDtpB, confirming that a proton gradient is required to transport the substrate into the cytoplasm of *E. coli*.

Whole cell lysate was prepared from WT pDtpB and used in S-Benzyl-L-cysteinylglycine biotransformation assays in parallel with WT pDtpB whole cells to assess the effect of peptide competitor molecules on substrate biotransformation. It was predicted that the peptide competitors would prevent either transport or intracellular catabolism of S-Benzyl-L-cysteinylglycine and this assay would discriminate between these two possibilities. Almost identical yields of benzyl-mercaptan were produced in whole cells and whole cell lysate in the absence of any competitor molecule (Fig. 5.4.3). This confirmed that enzymes required to biotransform S-Benzyl-L-cysteinylglycine were captured in the cell lysate preparation and remained functional throughout the assay. When dipeptide competitor molecules were added, Ala-Tyr failed to inhibit benzyl-mercaptan production in whole cells, but inhibited production by whole cell lysate by approximately 72%. This suggests that Ala-Tyr inhibits the enzymatic catabolism of S-Benzyl-L-cysteinylglycine but does not affect uptake via DtpB. In contrast, both Ala-Ala and Tyr-Ala strongly inhibited benzyl-mercaptan production in both whole cell and whole cell lysate assays, suggesting that these dipeptides are substrates for the S-Benzyl-L-cysteinylglycine catabolic enzyme(s) and potentially DtpB. No significant effect on S-Benzyl-L-cysteinylglycine biotransformation was observed following addition of either Gly-Gly or Gly-Gly-Gly, confirming that DtpB and the S-Benzyl-L-cysteinylglycine catabolic enzymes are not completely promiscuous in terms of substrate specificity.

In summary, following cloning and overexpression of all four *E. coli* Dtp peptide symporters, it has been demonstrated that S-Benzyl-L-cysteinylglycine is transported solely by DtpB, which represents a novel substrate for this transporter. Overexpression of DtpB allows for rapid and efficient uptake and biotransformation of S-Benzyl-L-cysteinylglycine, suggesting that *dtpB* is expressed at low intrinsic levels in *E. coli* and the

rate of substrate biotransformation is limited at the level of transport. As expected, S-Benzyl-L-cysteinylglycine uptake via overexpressed DtpB can be blocked by CCCP but also Ala-Ala and Tyr-Ala, suggesting that these two dipeptides are also DtpB substrates. Some dipeptides, including Ala-Ala, Ala-Tyr and Tyr-Ala, also block the catabolic enzymes required to biotransform S-Benzyl-L-cysteinylglycine, providing a cautionary note that not all inhibitors of this process act to prevent substrate biotransformation at the level of transport.

**A****B**

**Figure 5.4.1. (A)** Plasmid map of pBADcLIC2005. Decahistidine tag (10xHis), origin of replication (ori) and LIC insertion site (SwaI) are marked. Plasmid map was created using SnapGene Viewer 2.2.2. **(B)** Biotransformation of S-Benzyl-L-cysteinylglycine by Dtp protein-overexpressing *E. coli*. Cultures containing strains harbouring plasmids were pre-induced with 0.0001% L-arabinose overnight. 'WT empty vector' refers to wild-type *E. coli* expressing pBADcLIC2005 with no gene insertion. Thioalcohol yield ( $A_{492}$ ) was quantified using MTS/PMS after 10 min incubation. Error bars represent standard deviation of three biological replicates.

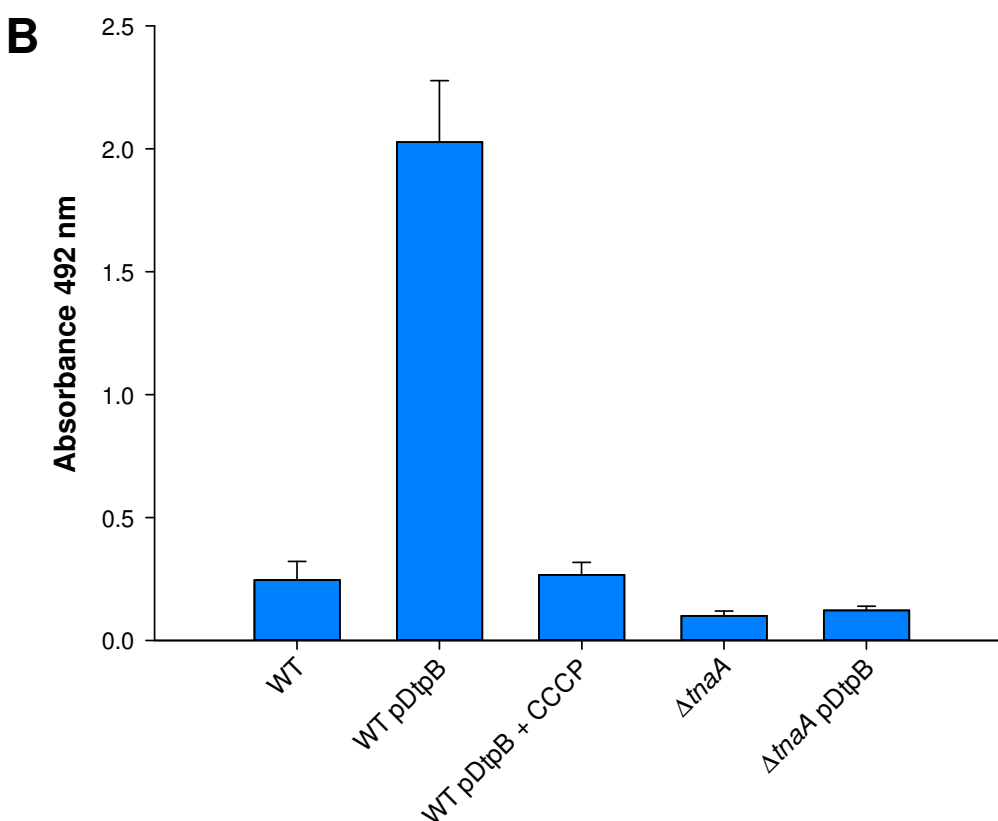
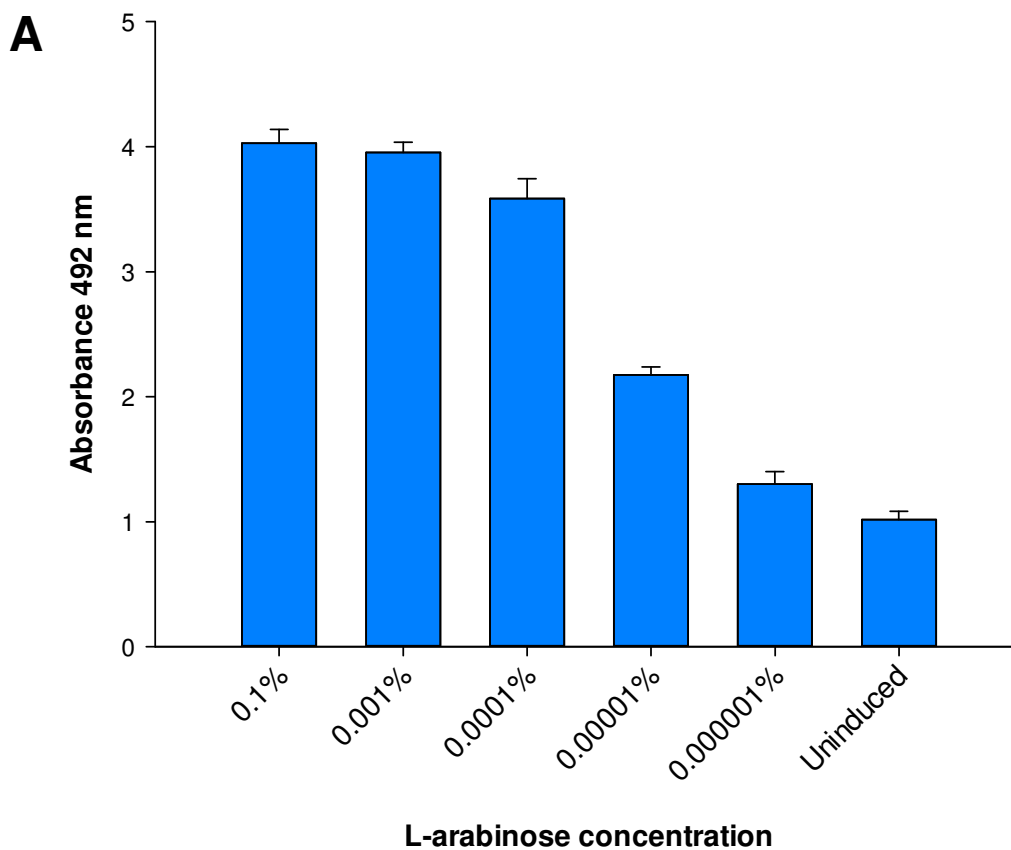


**Figure 5.4.2. (A)** Biotransformation of S-Benzyl-L-cysteinylglycine by *E. coli* WT pDtpB with decreasing levels of overnight L-arabinose induction. **(B)** Biotransformation of S-Benzyl-L-cysteinylglycine by *E. coli* WT, WT pDtpB, WT pDtpB,  $\Delta tnaA$  and  $\Delta tnaA$  pDtpB in the presence of 100  $\mu$ M CCCP. Thioalcohol yield ( $A_{492}$ ) was quantified using MTS/PMS after 30 min incubation (part A) or 10 min incubation (part B). Error bars represent standard deviation of three biological replicates.

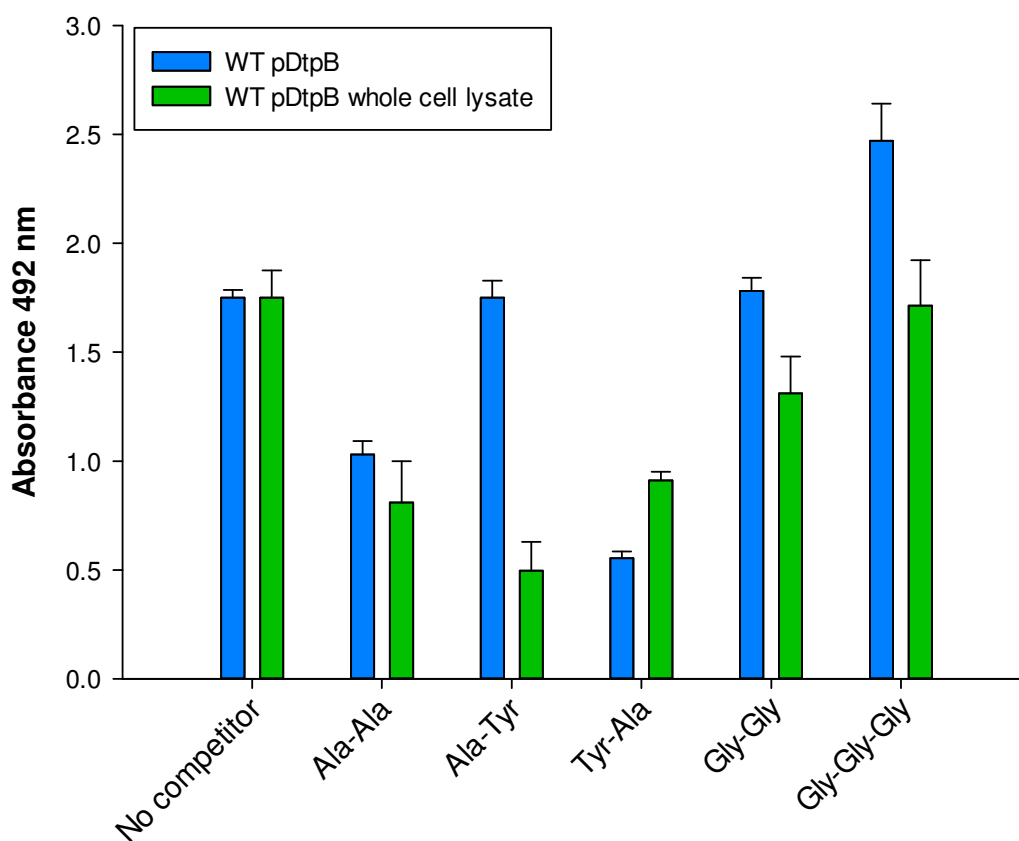


**Figure 5.4.3.** Biotransformation of S-Benzyl-L-cysteinylglycine by *E. coli* WT pDtpB and whole cell lysate prepared from WT pDtpB in the presence of 20 mM (10-fold excess) peptide competitor molecules. Thioalcohol yield ( $A_{492}$ ) was quantified using MTS/PMS after 10 min incubation. Error bars represent standard deviation of three biological replicates.

## 5.5 Overexpression of DtpB transforms *E. coli* into an efficient Cys-Gly-3M3SH biotransforming bacterium

It was previously stated that wild-type *E. coli* K-12 is a poor biotransformer of the physiological malodour precursor molecule Cys-Gly-3M3SH. If *E. coli* is to be a useful model organism for malodour production analysis, it is required to biotransform physiologically relevant malodour precursor molecules, particularly Cys-Gly-3M3SH. To assess whether overexpression of Dtp transport proteins could transform *E. coli* into a Cys-Gly-3M3SH biotransforming bacterium, biotransformation assays were carried out with Dtp-overexpressing strains.

WT pDtpB was able to efficiently convert Cys-Gly-3M3SH into 3M3SH following 5 h incubation (Fig, 5.5A). This phenotype was exclusive to WT pDtpB, as neither WT pDtpA, WT pDtpC nor WT pDtpD were able to biotransform Cys-Gly-3M3SH. The final 3M3SH yield obtained from WT pDtpB ( $A_{412} = 0.166$ ) is only 28% less than that obtained from *S. hominis* B10 over the same time period. Intracellular biotransformation of Cys-Gly-3M3SH is also dependent on TnaA, as  $\Delta tnaA$  overexpressing DtpB reaches only negligible 3M3SH yield (Fig. 5.5.B). This is surprising, given the structural dissimilarity between Cys-Gly-3M3SH and the biological substrate of TnaA, L-tryptophan. It was also observed that CCCP was able to inhibit Cys-Gly-3M3SH biotransformation in WT pDtpB, again, confirming that a proton gradient is required to transport the substrate into the cytoplasm of *E. coli*.

Overall, it was demonstrated here that *E. coli* K-12 could be converted into a Cys-Gly-3M3SH biotransforming strain by overexpression of DtpB and also shown that Cys-Gly-3M3SH biotransformation is dependent upon TnaA.

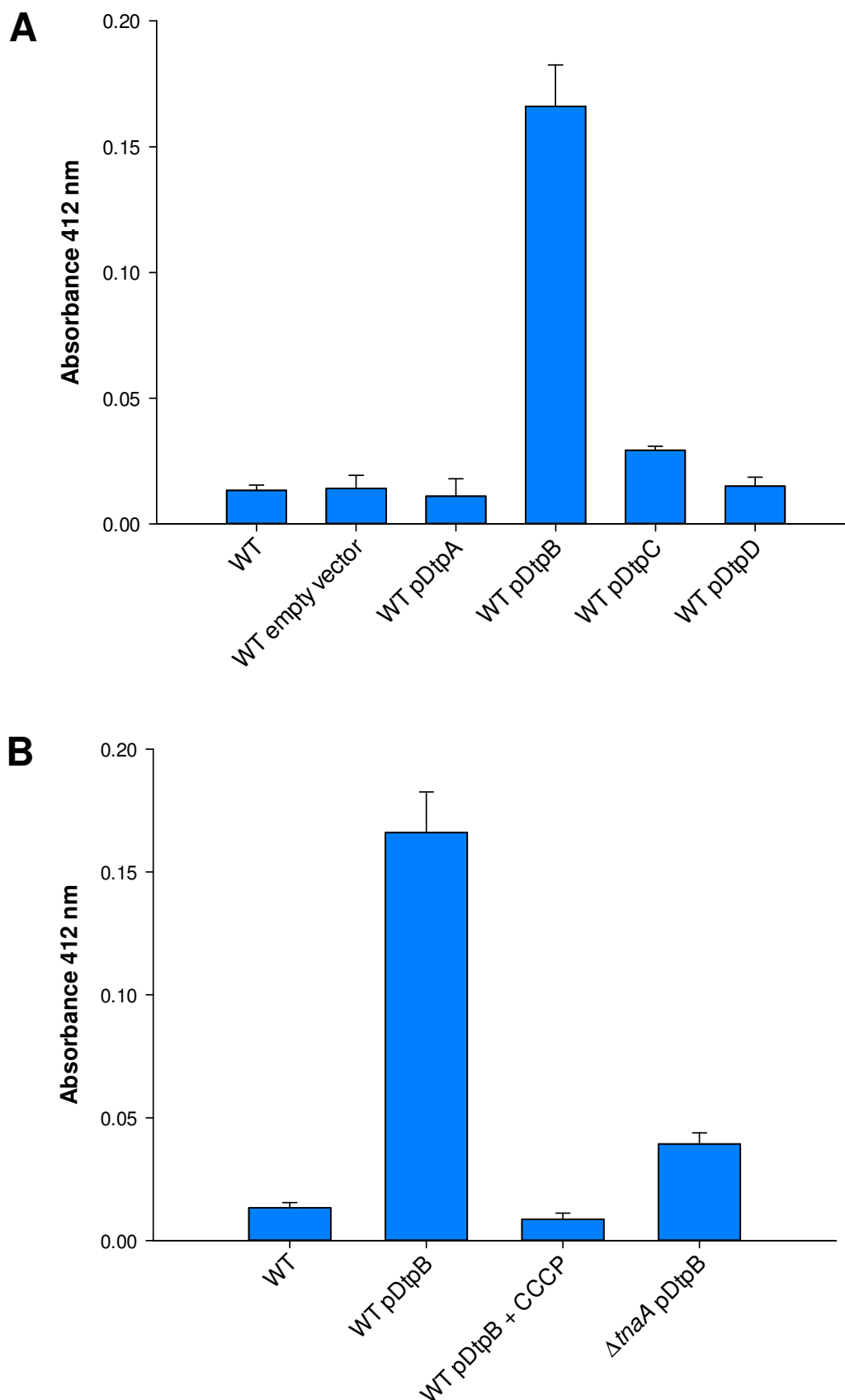


**Figure 5.5.** Biotransformation of Cys-Gly-3M3SH by **(A)** Dtp protein-overexpressing *E. coli* and **(B)** *E. coli* WT, WT pDtpB, WT pDtpB and  $\Delta$ tnaA pDtpB in the presence of 100  $\mu$ M CCCP. Thioalcohol yield ( $A_{412}$ ) was quantified using DTNB after 5 h incubation. Error bars represent standard deviation of three biological replicates.

## 5.6 Discussion

Through the work described in this chapter, it is possible to offer a model of malodour precursor biotransformation in *E. coli*, which is detailed in Fig. 5.6. The model suggests that Cys-Gly-malodour precursor molecules are transported by DtpB and intracellularly catabolised either solely by TnaA, or by a combination of a dipeptidase and TnaA, as discussed. The liberated thioalcohol is then excreted from the cell, likely via passive diffusion across the membrane into the periplasm and then ultimately to the extracellular environment.

It was demonstrated that *E. coli* is an efficient biotransformer of the model malodour precursor substrate S-Benzyl-L-cysteinylglycine. The TLC assay (Fig. 5.1B) shows that S-Benzyl-L-cysteinylglycine was completely depleted in the buffer medium between 2 and 3 h after incubation, although the time course of S-Benzyl-L-cysteinylglycine biotransformation shows that maximum benzyl-mercaptan yield is not reached until approximately 4.5 h. The prolonged time required to fully biotransform the substrate following uptake may be due to an overload of substrate inside the cell, as the cells may transport S-Benzyl-L-cysteinylglycine faster than they can catabolise it, effectively creating a substrate backlog which takes, in this case, 90 minutes to overcome. It was demonstrated that S-Benzyl-L-cysteinylglycine is transported by DtpB, with a *dtpB* knockout strain,  $\Delta dtpB$ , producing only 40% of the benzyl-mercaptan yield compared to wild-type (Fig. 5.3). The  $\Delta dtpB$  strain could be complemented when *dtpB* was overexpressed on a high copy number plasmid with an inducible promoter. Overexpression of *dtpB* converted *E. coli* into a highly efficient biotransformer not only of S-Benzyl-L-cysteinylglycine, but also the physiological malodour precursor substrate, Cys-Gly-3M3SH. This confirmed that in *E. coli*, dipeptide-based malodour precursor molecules are transported by a protein that recognises the dipeptide moiety of the molecule. It is interesting that DtpB should have such a unique function, which was not attributable to any other Dtp protein. This suggests a role for DtpB in uptake of unusual peptide-based molecules which may explain why no clear phenotype was observed for  $\Delta dtpB$  during the growth phenotype analyses outlined in chapter 4. However, DtpB has been shown to transport several simple, non-modified dipeptide molecules including the glycine containing dipeptides glycyaspartate (Gly-Asp), lysylglycine (Lys-Gly) and the non-hydrolysable glycy sarcosine (Gly-Sar) (Harder *et al.*, 2008). This suggests that the variety of substrates that DtpB is able to recognise and transport ranges from xenopeptide substrates such as S-Benzyl-L-cysteinylglycine and Cys-Gly-3M3SH to conventional dipeptides such as those cited by Harder.

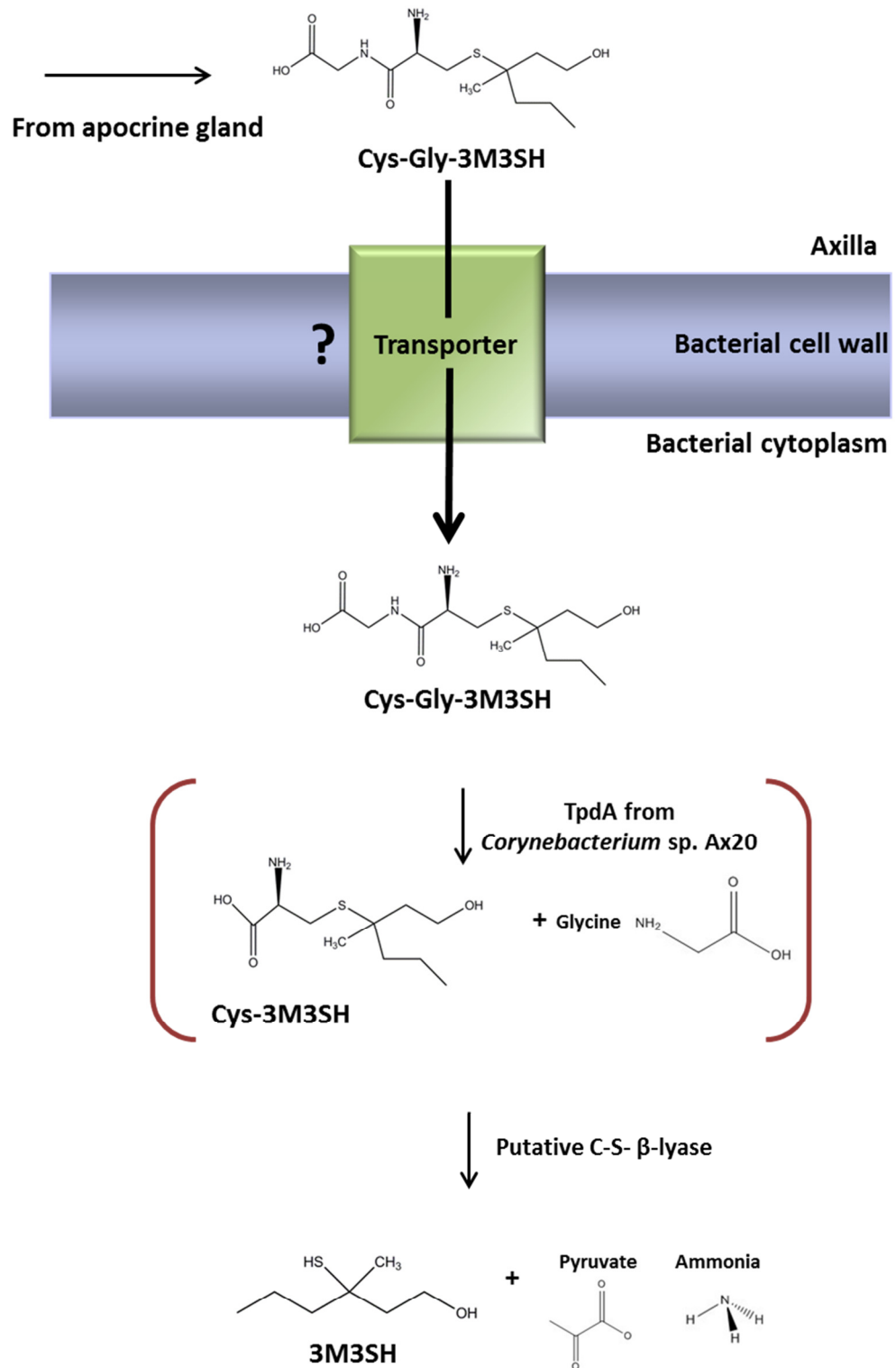


**Figure 5.6.** Proposed model of malodour precursor substrate biotransformation by *E. coli* K-12. Cys-Gly-malodour precursor (S-Benzyl-L-cysteinylglycine or Cys-Gly-3M3SH (shown here)) are transported into the cytoplasm via DtpB. A thiol precursor dipeptidase may initially act to cleave glycine from the substrate (displayed in red brackets), liberating Cys-malodour precursor prior to further catabolism by TnaA. Alternatively, TnaA is able to directly biotransform the Cys-Gly-malodour precursor into glycine, ammonia, pyruvate and thioalcohol. The thioalcohol molecule then diffuses across the membrane.

It may be the case that the Dtp proteins in *E. coli* (and other members of the Enterobacteriaceae) have evolved unique substrate specificities, each playing an individual role in specific peptide or peptide-based molecular transport, with some level of substrate specificity overlap, as discussed in chapter 4. This would allow the bacterium to transport a larger number of peptide-based molecules, increasing the overall pool of available growth substrates, potentially conferring a fitness advantage to an individual bacterium in a mixed bacterial population.

It is interesting to note that overexpression of DtpB conferred onto *E. coli* the ability to uptake and biotransform Cys-Gly-3M3SH, a process that wild-type *E. coli* is unable to carry out. Clearly, the inability of *E. coli* to catabolise Cys-Gly-3M3SH is limited at the level of transport and the bacterium possesses the necessary intracellular machinery to biotransform the substrate. This indirectly suggests that under growth in LB medium, constitutive expression of *ntpB* is low and that expression of this gene may be induced by substrates of the transporter. This would be consistent with the biological substrates of other transporters in *E. coli* which also activate expression of their cognate transporters, for example L-arabinose, which activates expression of the L-arabinose symporter *araE* (Daruwalla *et al.*, 1981).

When the mechanism of intracellular S-Benzyl-L-cysteinylglycine catabolism was analysed in more detail, it was surprising that mutants of MetC and MaY, the two characterised C-S-  $\beta$ -lyases of *E. coli* displayed no reduced S-Benzyl-L-cysteinylglycine catabolism, given that corynebacterial homologues of MetC are active against S-benzyl-containing substrates (James *et al.*, 2013). Further analysis revealed that S-Benzyl-L-cysteinylglycine biotransformation was dependent upon TnaA, the cellular tryptophanase of *E. coli*. TnaA not only degrades tryptophan, but is also one of the most important intracellular cysteine desulphydrase enzymes in the cell (Awano *et al.*, 2003), playing a role in intracellular L-cysteine degradation. Previous studies on TnaA revealed that it is also able to catalyse the breakdown of S-Benzyl-L-cysteine (Watanabe & Snell, 1977). Remarkably, the  $K_m$  of TnaA for S-Benzyl-L-cysteine is 4-fold lower (0.065 mM) than its natural substrate, L-tryptophan (0.3 mM) and both substrates share a similar  $k_{cat}$  ( $5.2 \pm 0.4 \text{ s}^{-1}$  for S-Benzyl-L-cysteine compared to  $6.8 \text{ s}^{-1}$  for L-tryptophan) (Phillips *et al.*, 1991). It is therefore unsurprising that TnaA is also required for intracellular biotransformation of S-Benzyl-L-cysteinylglycine, but perhaps more surprising that the same enzyme is required for catabolism of Cys-Gly-3M3SH. Given the disparity in structural similarity between the hydroxyalkyl groups of S-Benzyl-L-cysteinylglycine and Cys-Gly-3M3SH, it is surprising that both can be accommodated and correctly orientated in the active site of TnaA, although Watanabe & Snell (1977) demonstrated that TnaA catalyses the breakdown of a

wide spectrum of structurally dissimilar substrates. Structurally, TnaA is a homotetramer formed of two catalytic dimers with each individual domain consisting of a small and large subunit (London & Goldberg, 1972). The first crystal structure of the *E. coli* apoenzyme was solved by Ku *et al.* (2006) but to date, no holoenzyme structure is available so it is difficult to accurately propose how malodour precursor molecules would be orientated in the active site of the enzyme. However, structural data of the apoenzyme with L-tryptophan modelled into the active site (Ku *et al.*, 2006) combined with previous biochemical studies (Phillips *et al.*, 2002), suggests that the indole ring of L-tryptophan is coordinated by His463 from one subunit of the catalytic dimer and Tyr74 from the other. This proposal is based on reports that mutations in either of these residues leads to at least a 3000-fold reduction in tryptophanase activity (Phillips *et al.*, 2002). The  $\alpha$ -amino group of L-tryptophan is proposed to form an imine bond with the lysine-stabilised PLP molecule, a function that could feasibly be achieved by the  $\alpha$ -amino group of the Cys-Gly dipeptide moiety of the malodour precursor molecule. The proposed model of substrate orientation in the active site of TnaA is consistent with this enzyme possessing the ability to catalyse the biotransformation of S-Benzyl-L-cysteinylglycine. In this instance, the benzyl ring of this substrate would be orientated by His463 and Tyr74, although the importance of these catalytic residues for  $\beta$ -elimination reactions of non-physiological substrates such as S-ethyl-L-cysteine appears to be less important than for L-tryptophan (Phillips *et al.*, 2002). However, the observation that TnaA is required to biotransform Cys-Gly-3M3SH is puzzling as the orientation of the hydroxyalkyl moiety of this molecule in the active site of TnaA is difficult to determine. Nonetheless, given that TnaA is promiscuous in terms of substrate specificity, it may be that the structural flexibility of the enzyme, as demonstrated previously (Tsesin *et al.*, 2007), directly permits the orientation and subsequent catabolism of structurally diverse substrates within the active site.

While TnaA appears to be crucial for malodour precursor biotransformation in *E. coli*, it cannot be responsible for the same process in the high Cys-Gly-3M3SH biotransforming *Staphylococcus* species, as there is no TnaA orthologue in the *Staphylococcus* genus as a whole.

It also remains unclear whether, in *E. coli*, an initial dipeptidase step is required to liberate the Cys-conjugate of the dipeptide precursor molecule prior to catabolism by TnaA, or whether TnaA is able to facilitate the biotransformation of the complete dipeptide conjugate. These questions will remain unanswered until further biochemical studies are undertaken on TnaA using this newly identified class of substrates.

Several dipeptide molecules were shown to inhibit S-Benzyl-L-cysteinylglycine biotransformation in *E. coli* (Fig. 5.4.3). Ala-Ala and Tyr-Ala were particularly effective in whole cell and whole cell lysate assays but an additional dipeptide, Ala-Tyr, inhibited S-Benzyl-L-cysteinylglycine biotransformation only in whole cell lysate assays. In a similar vein to the competitor assays undertaken with *S. hominis* B10, it is unclear whether this inhibition is at the level of substrate transport or intracellular catabolism, although it appears that Ala-Tyr limits S-Benzyl-L-cysteinylglycine by inhibiting an important intracellular enzymatic process, as it was only effective in whole cell lysate assays. Competitive inhibition of TnaA by dipeptides has not been demonstrated, despite an abundance of amino acids and their structural analogues being able to efficiently prevent L-tryptophan catabolism to indole by this enzyme (Watanabe & Snell, 1977). This may suggest that dipeptides such as Ala-Tyr inhibit the dipeptidase enzyme which may catalyse a putative first step in S-Benzyl-L-cysteinylglycine biotransformation; cleavage of the glycine residue to liberate S-Benzyl-L-cysteine which is potentially the genuine substrate of TnaA.

Identification of the transport route along with insight into the intracellular catabolic capabilities of *E. coli* in terms of Cys-Gly-3M3SH biotransformation allows *E. coli* to be used as a model organism to study thioalcohol-based malodour. Previously, *C. jeikeium* has been used as a model *Corynebacterium* sp. (Troccaz *et al.*, 2009), owing mainly to its efficiency in biotransforming the model malodour substrate S-Benzyl-L-cysteine, as outlined in Fig. 5.2A. However, as previously discussed, *C. jeikeium* is unable to biotransform Cys-Gly-3M3SH, making it a poor model organism in this respect. Using *E. coli* as a model organism to study this process has an obvious benefit compared to staphylococcal or corynebacterial equivalents in that *E. coli* represents one of the most genetically well characterised and tractable bacterial species. This allows multiple gene deletions to be made in the host to indirectly study the role of the staphylococcal homologues in malodour precursor biotransformation. It also opens up the possibility to clone into *E. coli* staphylococcal genes with putative roles in malodour precursor biotransformation in order to test their activity directly. Without the discovery that overexpression of *dtpB* is an essential step in allowing *E. coli* to biotransform Cys-Gly-3M3SH, the concept of *E. coli* as a model host for this biochemical process could not have been proposed.

This work allows provides a proof-of-principle that a gene encoding a transport protein can be cloned into pBADcLIC2005 and overexpressed in *E. coli*, resulting in a gain-of-function, as seen here with Cys-Gly-3M3SH biotransformation by overexpression of *dtpB*. This principle can be taken forward by identifying putative Cys-Gly-3M3SH transporters from *S.*

*hominis* with a view to clone and overexpress them in wild-type *E. coli*. Any transporter that has intrinsic Cys-Gly-3M3SH transport ability will, in principal, convert *E. coli* into a Cys-Gly-3M3SH biotransformer.

## **Chapter 6**

# **Identification and characterisation of malodour precursor catabolic genes from *S. hominis***

## Introduction and aims

It was observed that when overexpressed in *E. coli*, the peptide symporter DtpB transforms this organism into an efficient biotransformer of Cys-Gly-3M3SH. This property can be exploited by cloning putative Cys-Gly-3M3SH transporters from the skin-isolated *S. hominis* B10 and recombinantly expressing these proteins in *E. coli*. It is foreseen that this will confer a gain-of-function phenotype, similar to that observed when DtpB is overexpressed. As no direct orthologue of DtpB is evident in *S. hominis*, an attempt will be made to identify the Cys-Gly-3M3SH transporter in this organism initially by *in silico* analysis. Following this, molecular cloning of the putative transporter gene(s) and recombinant expression in *E. coli* will be performed.

In *E. coli*, Cys-Gly-3M3SH is intracellularly catabolised, in part, by TnaA. This was directly demonstrated when a  $\Delta tnaA$  mutant failed to produce malodour (section 5.2). However, despite a C-S-  $\beta$ -lyase having been cloned and recombinantly expressed (Troccaz *et al.*, 2008), the intracellular enzymes involved in Cys-Gly-3M3SH biotransformation in *S. hominis* have not been identified. Therefore, as with identification of the Cys-Gly-3M3SH transporter, a similar approach will be taken to identify and characterise the putative C-S-  $\beta$ -lyase gene in *S. hominis*.

## Specific aims

- To carry out an *in silico* audit of molecular symporters in *S. hominis*.
- To clone genes from *S. hominis* that are putatively involved in Cys-Gly-3M3SH transport and use these constructs to complement Cys-Gly-3M3SH biotransformation deficient *E. coli* TD-Pep mutants.
- To identify and clone a putative Cys-Gly-3M3SH biotransforming C-S-  $\beta$ -lyase from *S. hominis* B10 and recombinantly express and functionally complement an *E. coli*  $\Delta tnaA$  strain.

## 6.1 Bioinformatic analysis of the secondary transporter (symporter) repertoire of *S. hominis* SK119 and identification of C-S- $\beta$ -lyase

In the model organism *E. coli*, Cys-Gly-3M3SH uptake is dependent upon the peptide symporter, DtpB. However, there is no clear orthologue of DtpB in *S. hominis*. For this reason, a list of all symport proteins of *S. hominis* SK119 was compiled in order to give a complete picture of molecular symport in this bacterium and to aid in identifying the Cys-Gly-3M3SH transporter, which, as in *E. coli*, was postulated to be a peptide transporter. *S. hominis* SK119 was used for the bioinformatic analysis as it represents a genome sequenced *S. hominis* strain, originally isolated from human skin (Tatusova *et al.*, 2014). Unfortunately, no genome sequence is available for the skin isolate *S. hominis* B10. Although SK119 was not characterised biochemically for Cys-Gly-3M3SH biotransformation activity, it is strongly hypothesised that this strain, as is the case with 90% of other *S. hominis* strains tested (see section 3.6), would have the molecular capacity to produce thioalcohol malodour.

51 annotated symporters were identified in *S. hominis* SK119 (Table 6.1). Within this list, there is a single annotated peptide symporter, STAHO0001\_1446 (NCBI: EEK12089.1) and another symporter, STAHO0001\_0415 (NCBI: EEK11635.1), which, following a more detailed substrate specificity analysis was also identified as a peptide transporter. The genome context of these two genes is shown in Fig. 6.1A. It was anticipated that, as in *E. coli*, the inability of a particular *Staphylococcus* species to biotransform Cys-Gly-3M3SH would be limited at the level of transport. If this hypothesis were correct, then bacteria that could biotransform Cys-Gly-3M3SH, *S. hominis*, *S. lugdunensis* and *S. haemolyticus* (plus potentially other staphylococci that were not included in the original screen) would possess a peptide transporter that was absent from non-Cys-Gly-3M3SH biotransforming staphylococci. Further analysis revealed that STAHO0001\_0415 is present only in *S. hominis* and *S. haemolyticus*, whereas STAHO0001\_1446 is present in all sequenced staphylococci and therefore likely to participate in general peptide uptake. Although the candidate Cys-Gly-3M3SH transporter STAHO0001\_0415 was not present in *S. lugdunensis*, it represented the most likely transporter of Cys-Gly-3M3SH and therefore became the focus of subsequent experimental analysis. STAHO0001\_1446 was also taken forward as a control.

The BioCyc Database Collection was also used to identify the putative C-S-  $\beta$ -lyase enzyme that was hypothesised to be involved in Cys-Gly-3M3SH catabolism in *S. hominis*. A single annotated C-S-  $\beta$ -lyase gene, STAHO0001\_2140, was identified through

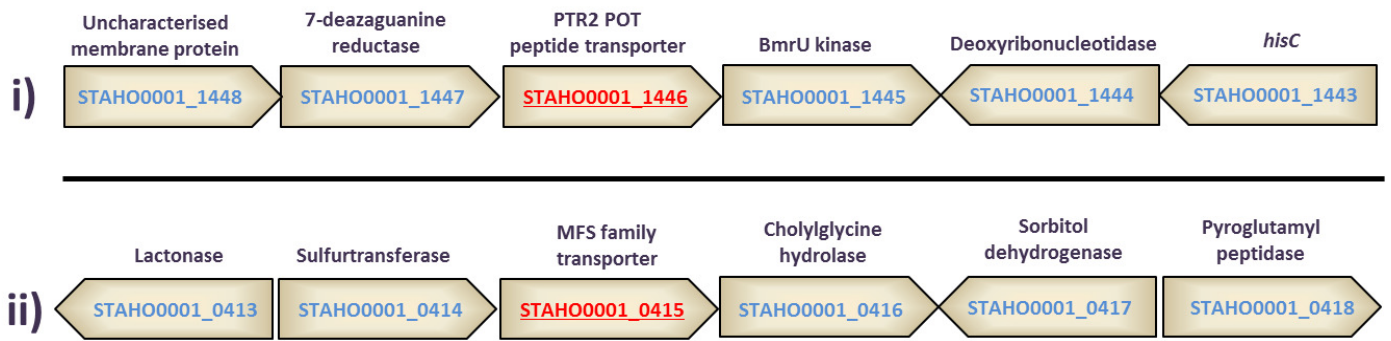
analysis of the *S. hominis* SK119 genome. The genome context of this gene is shown in Fig. 6.1B. With no prior knowledge of the relative activity of staphylococcal C-S-  $\beta$ -lyase proteins in terms of malodour precursor biotransformation, STAHO0001\_2140 represented an appropriate candidate to test for activity against Cys-Gly-3M3SH.

In summary, bioinformatics-based analysis identified two candidate Cys-Gly-3M3SH transporters in the model *S. hominis* strain SK119, along with a putative C-S-  $\beta$ -lyase gene with potential malodour precursor biotransformation activity. These three candidates were taken forward for experimental characterisation.

**Table 6.1.** Metabolite symporters of *S. hominis* SK119 as identified using BioCyc Database Collection. Genes identified in this analysis were annotated as either a 'permease' or 'transporter' and are encoded by a single chromosomal gene. STAHO0001\_XXXX is the BioCyc locus identifier and the EEK number represents the NCBI identifier. The two putative Cys-Gly-3M3SH transporters, STAHO0001\_0415 and STAHO0001\_1446 are highlighted in yellow.

<i>S. hominis</i> SK119 gene annotation	BioCyc annotation	<i>S. hominis</i> SK119 gene annotation	BioCyc annotation
<a href="#">STAHO0001_1373</a> <a href="#">EEK12616.1</a>	Transporter gate domain protein	<a href="#">STAHO0001_0295</a> <a href="#">EEK11670.1</a>	Permease of the drug/metabolite transporter
<a href="#">STAHO0001_2122</a> <a href="#">EEK13239.1</a>	Dicarboxylate/amino acid cation symporter	<a href="#">STAHO0001_0237</a> <a href="#">EEK12030.1</a>	Phosphate transporter family protein
<a href="#">STAHO0001_0415</a> <a href="#">EEK11635.1</a>	Transporter MFS family	<a href="#">STAHO0001_0070</a> <a href="#">EEK11134.1</a>	Sodium-dependent dicarboxylate transporter (SdcS)
<a href="#">STAHO0001_1838</a> <a href="#">EEK12893.1</a>	Transporter	<a href="#">STAHO0001_2105</a> <a href="#">EEK13231.1</a>	Sodium-dependent transporter
<a href="#">STAHO0001_0038</a> <a href="#">EEK11124.1</a>	YihY family protein	<a href="#">STAHO0001_1710</a> <a href="#">EEK11601.1</a>	Sugar transporter MFS protein
<a href="#">STAHO0001_1283</a> <a href="#">EEK12756.1</a>	MFS transporter	<a href="#">STAHO0001_0537</a> <a href="#">EEK11787.1</a>	Sugar transporter
<a href="#">STAHO0001_1164</a> <a href="#">EEK12868.1</a>	ABC-2-type transporter	<a href="#">STAHO0001_0404</a> <a href="#">EEK11671.1</a>	Urea transporter
<a href="#">STAHO0001_1103</a> <a href="#">EEK12783.1</a>	Amino acid permease	<a href="#">STAHO0001_2001</a> <a href="#">EEK12544.1</a>	Zinc transporter
<a href="#">STAHO0001_0108</a> <a href="#">EEK12905.1</a>	Ammonium transporter NrgA	<a href="#">STAHO0001_0562</a> <a href="#">EEK11672.1</a>	Permease
<a href="#">STAHO0001_0326</a> <a href="#">EEK11821.1</a>	Anaerobic C4 dicarboxylate transporter (Dcu family)	<a href="#">STAHO0001_0139</a> <a href="#">EEK11528.1</a>	ABC transport permease
<a href="#">STAHO0001_0528</a> <a href="#">EEK11634.1</a>	Anion transporter (DASS family)	<a href="#">STAHO0001_0305</a> <a href="#">EEK11917.1</a>	Amino acid permease family protein
<a href="#">STAHO0001_1162</a> <a href="#">EEK12570.1</a>	Cationic transporter (CorA-like) Metal ion transporter	<a href="#">STAHO0001_1732</a> <a href="#">EEK11622.1</a>	Fructose permease
<a href="#">STAHO0001_0325</a> <a href="#">EEK11857.1</a>	Choline-glycine-betaine transporter	<a href="#">STAHO0001_1203</a> <a href="#">EEK12671.1</a>	Glycolate permease Lactate permease
<a href="#">STAHO0001_1442</a> <a href="#">EEK12083.1</a>	Choline transporter ABC Transporter QAT family	<a href="#">STAHO0001_1808</a> <a href="#">EEK12231.1</a>	Lysine permease
<a href="#">STAHO0001_1446</a> <a href="#">EEK12089.1</a>	Di/Tripeptide transporter	<a href="#">STAHO0001_0666</a> <a href="#">EEK12071.1</a>	Lysine permease Amino acid permease
<a href="#">STAHO0001_1216</a> <a href="#">EEK12709.1</a>	Embr/QacA drug resistance transporter	<a href="#">STAHO0001_1243</a> <a href="#">EEK12785.1</a>	Proline permease
<a href="#">STAHO0001_1142</a> <a href="#">EEK12789.1</a>	Formate/Nitrite transporter	<a href="#">STAHO0001_1822</a> <a href="#">EEK12247.1</a>	Proline permease
<a href="#">STAHO0001_1073</a> <a href="#">EEK12679.1</a>	Glucarate transporter	<a href="#">STAHO0001_0517</a> <a href="#">EEK11627.1</a>	Amino acid permease
<a href="#">STAHO0001_1611</a> <a href="#">EEK12935.1</a>	Na/H antiporter	<a href="#">STAHO0001_1120</a> <a href="#">EEK12761.1</a>	Amino acid permease
<a href="#">STAHO0001_1610</a> <a href="#">EEK13096.1</a>	Magnesium transporter	<a href="#">STAHO0001_1616</a> <a href="#">EEK13050.1</a>	Glycolipid permease
<a href="#">STAHO0001_0493</a> <a href="#">EEK11850.1</a>	Myo-inositol transporter IoIT	<a href="#">STAHO0001_1208</a> <a href="#">EEK12711.1</a>	Hemin permease Efflux ABC transporter
<a href="#">STAHO0001_1101</a> <a href="#">EEK12757.1</a>	Chloramphenicol transporter	<a href="#">STAHO0001_0217</a> <a href="#">EEK12038.1</a>	Teichoic acid transporter
<a href="#">STAHO0001_1695</a> <a href="#">EEK13122.1</a>	Manganese transporter	<a href="#">STAHO0001_1027</a> <a href="#">EEK12335.1</a>	Uracil permease
<a href="#">STAHO0001_0894</a> <a href="#">EEK11441.1</a>	Hypothetical protein	<a href="#">STAHO0001_1295</a> <a href="#">EEK12818.1</a>	Xanthine/uracil permease
<a href="#">STAHO0001_1378</a> <a href="#">EEK12844.1</a>	Multidrug transporter	<a href="#">STAHO0001_2116</a> <a href="#">EEK13191.1</a>	Xanthine permease
		<a href="#">STAHO0001_1438</a> <a href="#">EEK12086.1</a>	Zinc/Iron permease

## A



## B



**Figure 6.1.** Genome context of **(A)** STAHO0001\_1446 (i) and STAHO0001\_0415 (ii) and **(B)** STAHO0001\_2140. The genome context was reproduced from the original BioCyc graphical representation at each respective locus. Not to scale.

## 6.2 Cloning, expression and characterisation of *S. hominis* B10 peptide transporters

*S. hominis* B10 was used as the parental strain for gene cloning as it represents a direct skin-isolated *S. hominis* strain. With no available genome sequence for *S. hominis* B10, degenerate primers were designed for each gene using the genome sequence of *S. hominis* SK119 as a template.

Both STAHO0001\_0415 and STAHO0001\_1446 were amplified successfully from *S. hominis* B10. These genes were cloned into pBADcLIC2005 and named pSH0415 and pSH1446, linking them to their specific *S. hominis* gene locus identifiers. Wild-type *E. coli* K-12 was transformed with pSH0415 and pSH1446. Malodour precursor biotransformation assays were repeated with these new strains to assess if a gain-of-function phenotype was conferred.

The ability of STAHO0001\_1446 and STAHO0001\_0415 to convert wild-type *E. coli* from a poor to an efficient biotransformer of S-Benzyl-L-cysteinylglycine was assessed. Overexpression of STAHO0001\_0415 improved the ability of *E. coli* to metabolise S-Benzyl-L-cysteinylglycine (Fig. 6.2A). However, there was no observable phenotype when STAHO0001\_1446 was overexpressed, suggesting that this protein is not involved in the transport of this molecule.

In contrast, when uptake of Cys-Gly-3M3SH was studied, no gain-of-function was attributable to overexpression of STAHO0001\_0415, confirming that, despite showing an affinity for S-Benzyl-L-cysteinylglycine, this transporter does not transport Cys-Gly-3M3SH. However, Cys-Gly-3M3SH biotransformation was dramatically improved when STAHO0001\_1446 was overexpressed (Fig. 6.2B), with cells producing a total 3M3SH yield 2-fold higher than when overexpressing *dtpB* following 4 h incubation, suggesting that STAHO0001\_1446 has a high affinity for Cys-Gly-3M3SH.

Although the cloned inserts were only sequenced following integration into pBADcLIC2005 and not directly following PCR amplification, the observed activity of both constructs against malodour precursor substrates implies that the cloned genes are expressed and functional in the *E. coli* system.

Overall, it was established that the protein product of the *S. hominis* B10 gene STAHO0001\_0415 is responsible for S-Benzyl-L-cysteinylglycine uptake, whereas STAHO0001\_1446 is responsible for uptake of the physiological malodour precursor Cys-Gly-3M3SH. All sequenced staphylococci have an orthologue of STAHO0001\_1446, suggesting that all species are able to uptake Cys-Gly-3M3SH. Logically, this suggests that the ability to biotransform Cys-Gly-3M3SH in staphylococci is limited not by transport of the substrate into the cell, but at the level of intracellular substrate biotransformation.

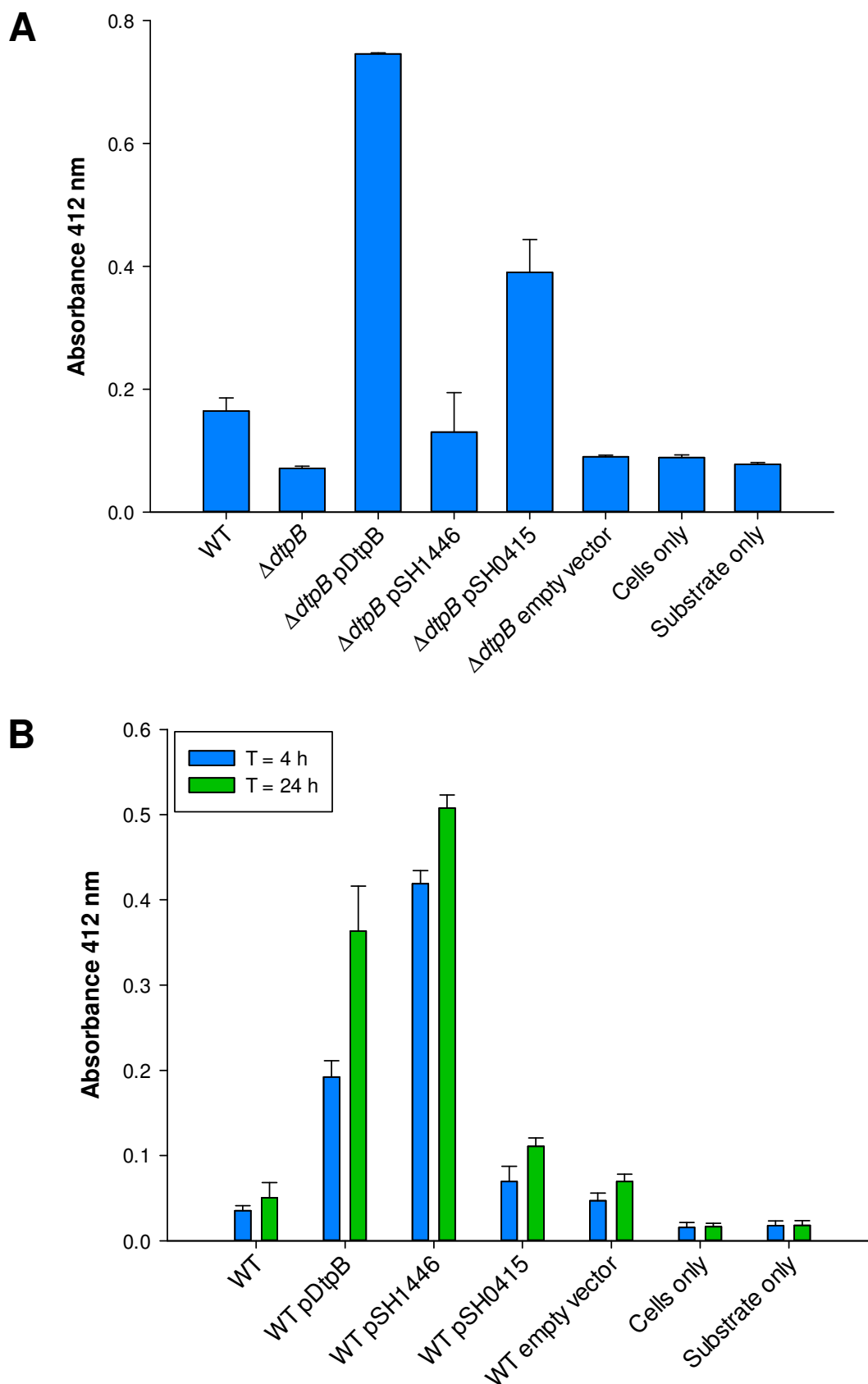


**Figure 6.2.** Biotransformation of **(A)** S-Benzyl-L-cysteinylglycine and **(B)** Cys-Gly-3M3SH by *E. coli* overexpressing STAHO0001\_1446 (pSH1446) and STAHO0001\_0415 (pSH0415). *E. coli* overexpressing *dtpB* (pDtpB) is shown for reference. 'Empty vector' refers to *E. coli* expressing pBADcLIC2005 with no gene insertion. Cultures containing strains harbouring plasmids were pre-induced with 0.0001% L-arabinose overnight. Thioalcohol yield ( $A_{412}$ ) was quantified using DTNB after 30 min incubation for S-Benzyl-L-cysteinylglycine and 4 h (blue bars) and 24 h incubation (green bars) for Cys-Gly-3M3SH. Error bars represent standard deviation of three biological replicates.

### 6.3 Cloning, expression and characterisation of *S. hominis* B10 C-S- $\beta$ -lyase

Given that the ability to biotransform Cys-Gly-3M3SH in staphylococci is not limited by the ability to transport the substrate into the cell, but at the level of intracellular substrate biotransformation, characterisation of a C-S-  $\beta$ -lyase protein identified originally in *S. hominis* SK119 was carried out.

STAH00001\_2140, the candidate C-S-  $\beta$ -lyase from *S. hominis* SK119, was amplified from *S. hominis* B10 and cloned into pBADcLIC2005. *E. coli* strain  $\Delta tnaA$  was transformed with the resulting plasmid, pSH2140, and malodour precursor biotransformation assays were repeated using model malodour substrates with the new strain to assess for complementation of TnaA.

The ability of STAH00001\_2140 to functionally complement  $\Delta tnaA$  was assessed by S-Benzyl-L-cysteine and S-Benzyl-L-cysteinylglycine biotransformation assays. It was observed that STAH00001\_2140 could complement the *tnaA* mutation in S-Benzyl-L-cysteine biotransformation assays (Fig. 6.3A) but not in S-Benzyl-L-cysteinylglycine assays (Fig. 6.3B). While STAH00001\_2140 cannot catabolise S-Benzyl-L-cysteinylglycine, logically, it suggests that TnaA does have this ability. Therefore, TnaA may either have intrinsic dipeptidase activity, or have the ability to catalyse a  $\beta$ -elimination reaction directly from S-Benzyl-L-cysteinylglycine, liberating benzyl-mercaptan without the requirement to first cleave glycine. The previously suggested hypothesis that an additional enzyme is required to liberate S-Benzyl-L-cysteine from S-Benzyl-L-cysteinylglycine prior to liberation of benzyl-mercaptan by TnaA in *E. coli* appears unlikely.

In summary, when expressed in *E. coli*  $\Delta tnaA$ , STAH00001\_2140 is unable to biotransform S-Benzyl-L-cysteinylglycine, suggesting that TnaA can directly biotransform this substrate. This also suggests that STAH00001\_2140 is not responsible for biotransformation of the physiological malodour precursor Cys-Gly-3M3SH and a different protein(s) with C-S-  $\beta$ -lyase activity are likely to carry out this reaction in *S. hominis*. It was not possible to assess biotransformation of Cys-Gly-3M3SH by STAH00001\_2140, as biotransformation of this substrate in *E. coli* requires overexpression of DtpB (Fig. 5.5A), a feature that could not be achieved in *E. coli*  $\Delta tnaA$  due to plasmid incompatibility issues.

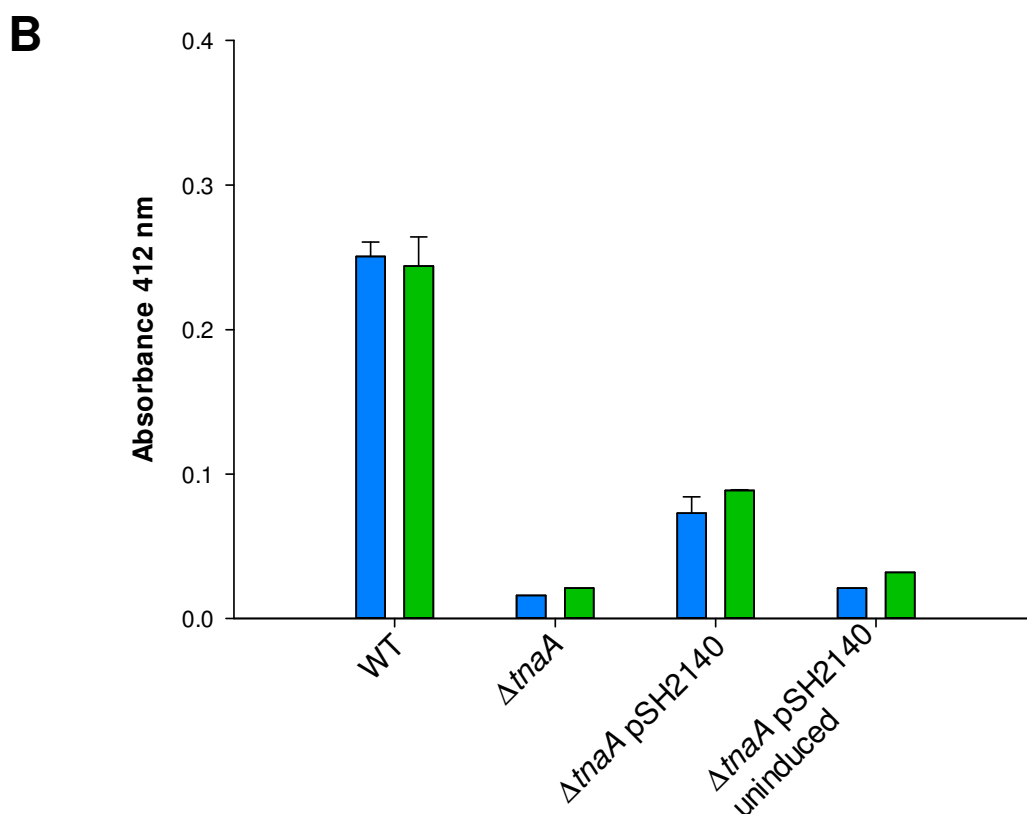
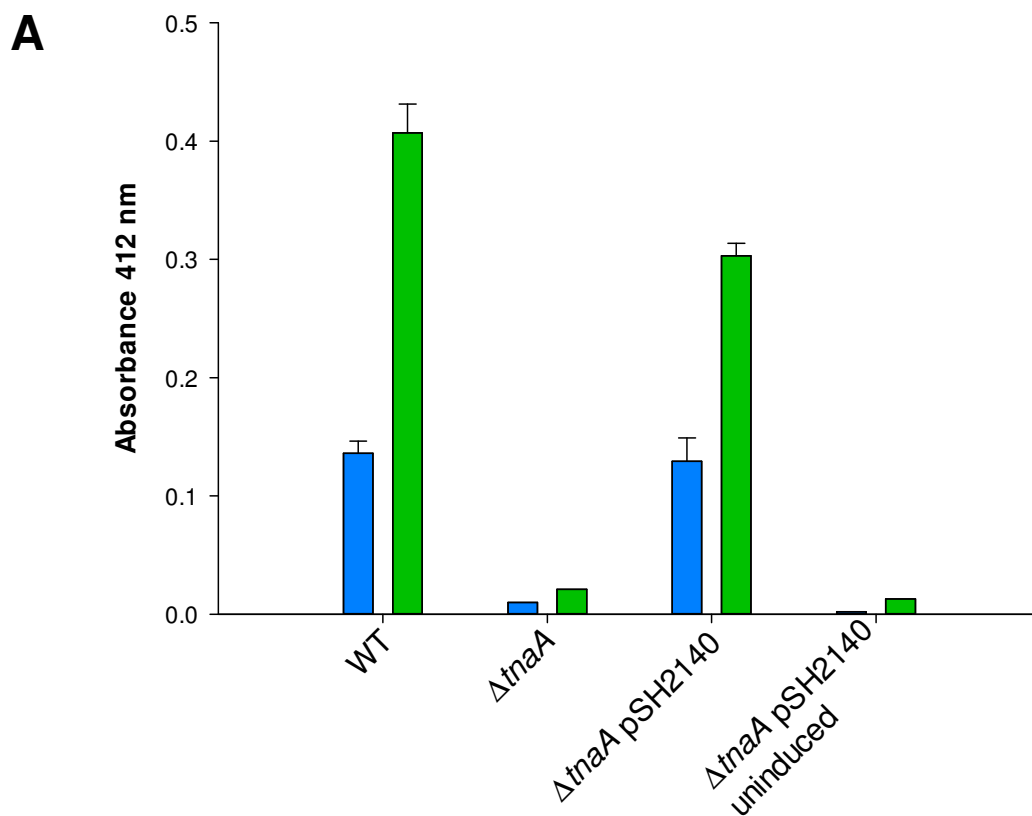


**Figure 6.3.** Biotransformation of **(A)** S-Benzyl-L-cysteine and **(B)** S-Benzyl-L-cysteinylglycine by  $\Delta tnaA$  *E. coli* expressing STAHO0001\_2140. Cultures containing strains harbouring plasmids were pre-induced with 0.0001% L-arabinose overnight. Thioalcohol yield ( $A_{412}$ ) was quantified using DTNB after 2 h incubation (blue bars) and 4 h incubation (green bars). Error bars represent standard deviation of three biological replicates.

## 6.4 Bioinformatic-based analysis of malodour precursor catabolic genes in staphylococci

Following preliminary characterisation of STAHO0001\_2140, which implied that this protein could not directly biotransform the model dipeptide malodour substrate S-Benzyl-L-cysteinylglycine, an attempt was made to identify the gene(s) responsible for malodour precursor biotransformation. Due to time constraints, a bioinformatic-based characterisation was the only feasible option available. The protein sequence of the characterised C-S-  $\beta$ -lyase from *C. jeikeium* K411 was used as a BLAST template to search for homologous proteins in staphylococci, particularly *S. hominis*, *S. haemolyticus* and *S. lugdunensis*.

The sequences of candidate staphylococcal C-S- lyase proteins were compiled and the phylogenetic relationship between these proteins is displayed in Fig. 6.4.1. The majority of staphylococci have three C-S- lyase-type proteins, one of which from each species forms a clade of proteins orthologous to the partially characterised protein STAHO0001\_2140. Of the other two clades of C-S- lyase-type proteins, one was homologous to the MetC family (see section 1.5.3) and the other was annotated as a cystathionine gamma-lyase/synthase. Interestingly however, an additional protein (forming a fourth C-S- lyase-type protein clade) was identified in *S. hominis* C80 (EFS20384.1), *S. hominis* SK119 (EEK11697.1), *S. lugdunensis* HKU-09-01 (YP\_003470502.1) and *S. haemolyticus* JCSC1435 (YP\_252136.1), and also in other strains of these three species (not shown). These four proteins are all annotated as aminotransferases, although this arbitrary annotation is likely to be incorrect as it is common for experimentally characterised C-S-  $\beta$ -lyase proteins to be incorrectly annotated as aminotransferases in the first instance such as PatB from *B. subtilis*, for example (Auger *et al.*, 2005). When EEK11697.1 was used as a BLAST query, it was clear that this protein shares no orthology with any other protein across the bacterial kingdom (Fig. 6.4.2A). The closest non- *S. hominis*, *S. lugdunensis* or *S. haemolyticus* match is from *Eubacterium acidaminophilum*, an obligate anaerobic amino-acid degrading bacterium originally isolated from black mud samples (Zindel *et al.*, 1988). Multiple protein domains are present in EEK11697.1. The majority relate to aminotransferase activity, for example AAT\_like, Aminotran\_1\_2 and Aminotran\_3 domains were all detected, along with two C-S- lyase activity domains such as MalY and C-S-lyase\_PatB (Fig. 6.4.2B).

The genome context of the protein is similar in all 3 species, although in *S. hominis* SK119 and *S. haemolyticus* JCSC1435, the putative Cys-Gly-3M3SH biotransforming enzyme is

located in an operon with a small, 135 amino acid-long hypothetical protein. This small protein is absent from the genome of *S. lugdunensis* HKU-09-01, suggesting that it is not essential for Cys-Gly-3M3SH biotransformation, assuming that these genome sequenced strains are all efficient biotransformers of Cys-Gly-3M3SH. When this hypothetical protein is used as a BLAST query, there appear to be no orthologues in any organism apart from *S. hominis* and *S. haemolyticus* (data not shown). The only functional domain present is annotated as COG2128, which is functionally unassigned. The closest matching protein with an annotated function is WP\_0100947466.1 from *Ornithinibacillus scapharcae*, which is annotated as an alkylhydroperoxidase. Without access to the specific genome-sequenced *Staphylococcus* isolates it is difficult to make strong predictions regarding the role of the putative alkylhydroperoxidase in Cys-Gly-3M3SH biotransformation, if any, particularly as it is not present in *S. lugdunensis*.

Overall, through bioinformatic-based analysis, a putative Cys-Gly-3M3SH biotransforming protein has been identified in *S. hominis*, *S. lugdunensis* and *S. haemolyticus*. This protein appears to be unique to these three organisms as no orthologous protein was identified in any other bacteria. This suggests that these proteins likely play a unique role in the cell, possibly in Cys-Gly-3M3SH biotransformation.

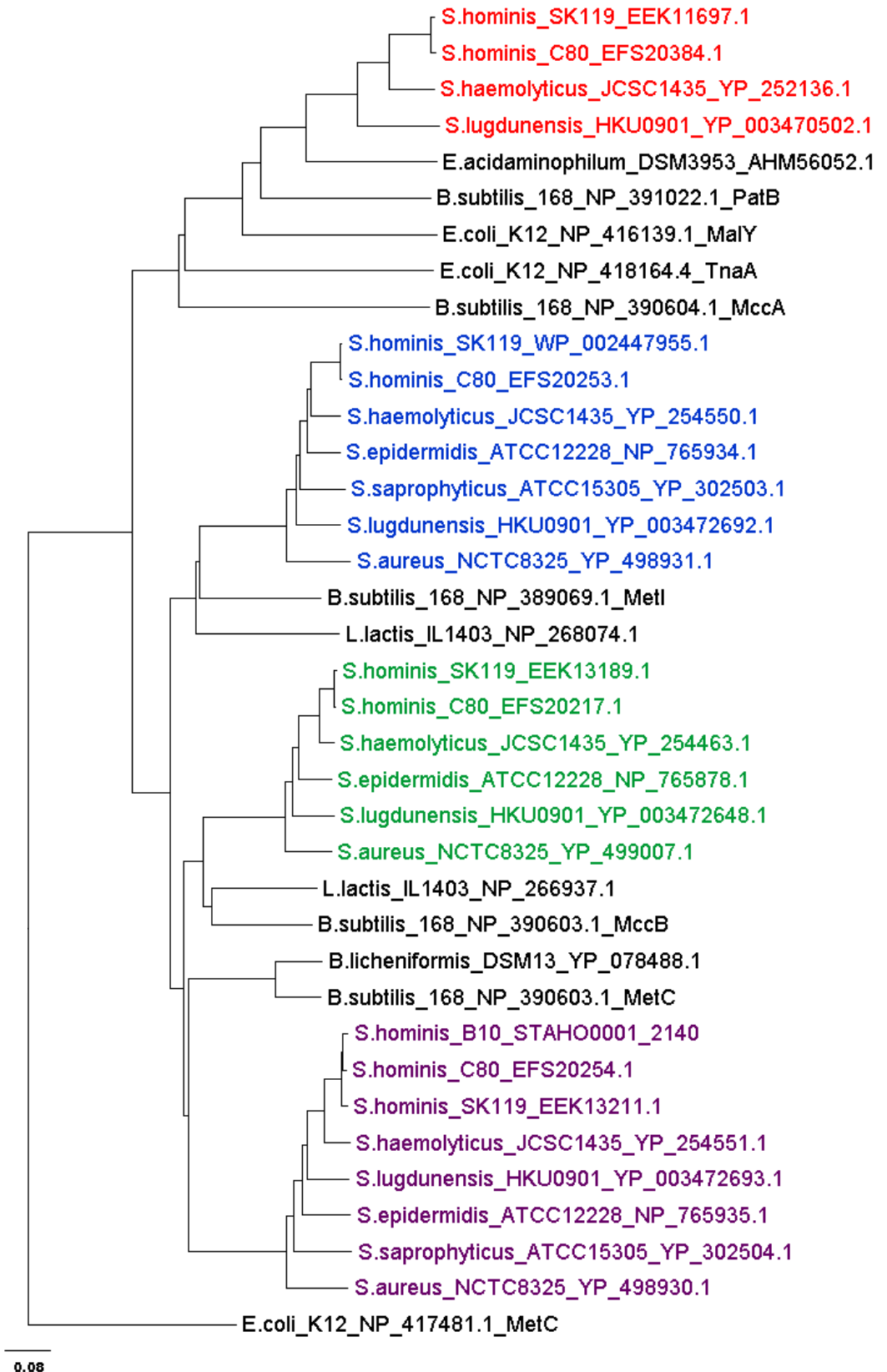


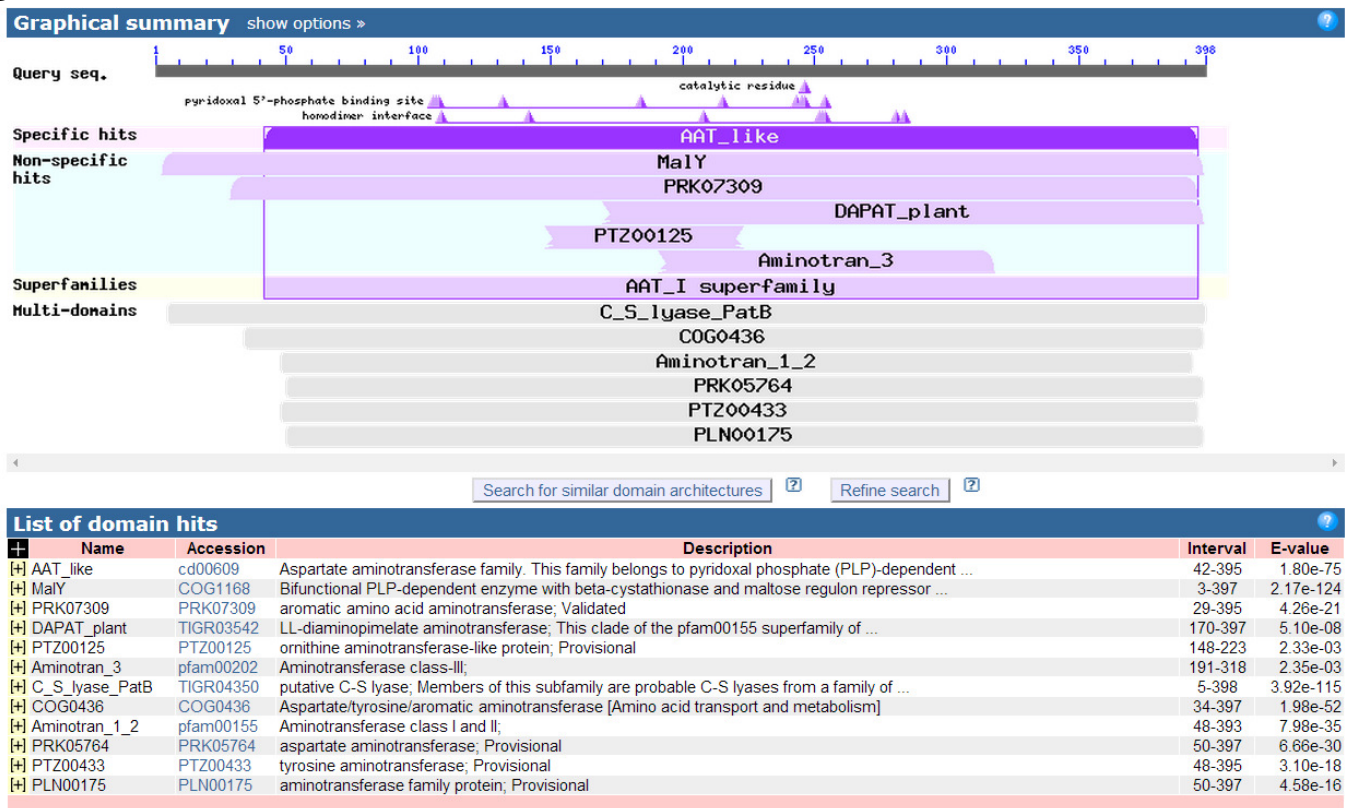
**Figure 6.4.1.** Rooted phylogenetic tree showing the relationship between C-S- lyase type proteins in staphylococci. Clades of orthologous staphylococci proteins are coloured individually with the unique clade of putative Cys-Gly-3M3SH biotransforming proteins coloured red. Examples of experimentally characterised C-S- lyase proteins from *E. coli*, *Bacillus* spp. and *L. lactis* are included for reference. Multiple sequence alignment and phylogenetic tree building was carried out using ClustalX2.

**A**

Sequences producing significant alignments:

Select: [All](#) [None](#) Selected:0

	Description	Max score	Total score	Query cover	E value	Ident	Accession
<input type="checkbox"/>	<a href="#">aminotransferase [Staphylococcus hominis]</a>	830	830	100%	0.0	100%	<a href="#">WP_002449246.1</a>
<input type="checkbox"/>	<a href="#">aminotransferase [Staphylococcus hominis]</a>	818	818	100%	0.0	98%	<a href="#">WP_002488459.1</a>
<input type="checkbox"/>	<a href="#">aminotransferase [Staphylococcus hominis]</a>	805	805	100%	0.0	97%	<a href="#">WP_017174763.1</a>
<input type="checkbox"/>	<a href="#">aminotransferase [Staphylococcus sp. MDS7B]</a>	798	798	98%	0.0	97%	<a href="#">WP_019835080.1</a>
<input type="checkbox"/>	<a href="#">aminotransferase [Staphylococcus hominis]</a>	729	729	89%	0.0	99%	<a href="#">WP_002454642.1</a>
<input type="checkbox"/>	<a href="#">aminotransferase [Staphylococcus haemolyticus]</a>	718	718	100%	0.0	84%	<a href="#">WP_016930549.1</a>
<input type="checkbox"/>	<a href="#">aminotransferase [Staphylococcus haemolyticus]</a>	639	639	89%	0.0	84%	<a href="#">WP_011274550.1</a>
<input type="checkbox"/>	<a href="#">aminotransferase [Staphylococcus lugdunensis]</a>	619	619	100%	0.0	72%	<a href="#">WP_002479040.1</a>
<input type="checkbox"/>	<a href="#">aminotransferase [Staphylococcus lugdunensis]</a>	619	619	100%	0.0	72%	<a href="#">WP_002492387.1</a>
<input type="checkbox"/>	<a href="#">putative C-S lyase [Staphylococcus lugdunensis VCU150]</a>	619	619	100%	0.0	72%	<a href="#">KAK58237.1</a>
<input type="checkbox"/>	<a href="#">aminotransferase [Staphylococcus lugdunensis]</a>	608	608	100%	0.0	71%	<a href="#">WP_002460749.1</a>
<input type="checkbox"/>	<a href="#">aminotransferase [Eubacterium acidaminophilum]</a>	462	462	98%	4e-158	54%	<a href="#">WP_025435087.1</a>
<input type="checkbox"/>	<a href="#">aminotransferase [Paenibacillus sp. 1-49]</a>	454	454	99%	8e-155	53%	<a href="#">WP_025684200.1</a>
<input type="checkbox"/>	<a href="#">aminotransferase [Clostridium carboxidivorans]</a>	452	452	99%	3e-154	54%	<a href="#">WP_007064372.1</a>
<input type="checkbox"/>	MULTISPECIES: <a href="#">aminotransferase [Paenibacillus]</a>	451	451	100%	2e-153	52%	<a href="#">WP_024631194.1</a>
<input type="checkbox"/>	<a href="#">aminotransferase [Clostridium scatologenes]</a>	450	450	100%	2e-153	54%	<a href="#">WP_029160267.1</a>

**B**

**Figure 6.4.2. (A)** BLAST search using the protein sequence of EEK11697.1 as a query searching for homologous proteins in the bacterial kingdom **(B)** Identification of multiple functional domains of the protein EEK11697.1 via the NCBI domain analysis database.

## 6.5 Discussion

In this chapter, two putative Cys-Gly-3M3SH transporters, STAHO0001\_1446 and STAHO0001\_0415 were identified based on analysis of the *S. hominis* SK119 genome. Only peptide transporters were studied as it had been previously demonstrated that in *E. coli*, a dedicated peptide transporter was responsible for uptake of Cys-Gly-3M3SH. Neither STAHO0001\_1446 nor STAHO0001\_0415 had been experimentally characterised and little is known about peptide transport in general in *S. hominis*, presumably due to the clinical insignificance of this species in relation to the important clinical pathogen, *S. aureus*. Overexpressed STAHO0001\_1446 from *S. hominis* B10 transformed wild-type *E. coli* into an efficient biotransformer of Cys-Gly-3M3SH, demonstrating that the physiological malodour precursor substrate is transported with high capacity by this protein. Given that it was demonstrated in chapter 5 that the *E. coli* PTR family transporter DtpB was responsible for Cys-Gly-3M3SH, it is unsurprising that STAHO0001\_1446 is also member of the same transporter family. An orthologue of STAHO0001\_1446 is present in all sequenced *Staphylococcus* spp. and consequently it can be hypothesised that all staphylococci have the ability to transport Cys-Gly-3M3SH across the cell membrane, but only a limited number such as those identified here as *S. hominis*, *S. haemolyticus* and *S. lugdunensis* possess the necessary intracellular enzymes required to biotransform the substrate into thioalcohol product. Knowledge of peptide transport in staphylococci is mainly limited to analyses of *S. aureus*. Perry & Abraham (1979) used a competitive inhibition assay to show that a wide range of di- and tripeptides are taken up by this organism, although the authors acknowledge that multiple peptide transport systems are likely to exist and so the exact route for general peptide uptake in *S. aureus* remained uncertain. A subsequent study by Perry (1980) similarly identified several di- and tripeptide substrates for *S. aureus* that were able to reduce the bactericidal effects of the peptide antibiotic bacilysin, with Ala-Ala-Ala being particularly effective among the chosen library of competitors. Interestingly, blocking either the N- or C-terminus of Ala-Ala-Ala with an acetyl methyl group, respectively, resulted in significant loss of antagonistic effect, suggesting that the general peptide transport system of *S. aureus* requires unsubstituted carboxy- and amino-termini to facilitate substrate entry into the cell. This structural requirement of peptide substrates is similar to that of the high affinity *dpp* and *opp* peptide transport systems of *E. coli*, both of which require the presence of an unsubstituted  $\alpha$ -amino group (Payne, 1971), and for *dpp*, the presence of an unsubstituted terminal carboxyl-group (Payne, 1968). It was later demonstrated that *S. aureus* NCTC8325 possesses four Opp-like proteins that are able to transport peptides ranging in size from 3 to 8 amino acids in length (Hiron *et al.*, 2007). Interestingly however, dipeptide transport in this organism is driven solely by DtpT, the *S. aureus*

orthologue of *S. hominis* STAHO0001\_1446. With most staphylococci possessing an orthologue of STAHO0001\_1446, it is likely that in staphylococci, dipeptide transport is driven solely by this transporter. Logically, this suggests that the substrate specificity of this transporter must be relatively wide-ranging as staphylococci do not appear to possess an alternative route for dipeptide uptake. Hiron *et al.* (2007) also demonstrated that DtpT of *S. aureus* NCTC8325 is solely responsible for the uptake of several tripeptides, including Gly-Gly-Gln and Lys-Gly-Gly, suggesting that transport of the dipeptide malodour precursor substrate Cys-Gly-3M3SH would not be excluded from the binding cavity of DtpT based on size, as confirmed here when STAHO0001\_1446 was shown to actively transport this substrate when overexpressed in *E. coli*.

In terms of intracellular catabolism of Cys-Gly-3M3SH, it was demonstrated by Emter & Natsch (2008) that *Corynebacterium* sp. Ax20 possesses a novel dipeptidase (TpdA) that is able to cleave the glycine residue from Cys-Gly-3M3SH to liberate Cys-3M3SH. The group further demonstrated that liberated Cys-3M3SH is a substrate for the  $\beta$ -lyase of the same organism, confirming that *in vitro*, *Corynebacterium* sp. Ax20 employs a two-enzyme Cys-Gly-3M3SH biotransformation process to liberate 3M3SH. Orthologues of *tpdA* are not widespread among the bacterial kingdom and there are no clear orthologues in staphylococci. Therefore, *S. hominis*, *S. haemolyticus* and *S. lugdunensis* must employ a different enzyme or enzymes in order to biotransform malodour precursor molecules. In disagreement with the observation by Emter & Natsch, it was demonstrated here that recombinant C-S-  $\beta$ -lyase from *S. hominis* B10 (STAHO0001\_2140) was only able to fully complement  $\Delta tnaA$  in biotransformation of S-Benzyl-L-cysteine and not S-Benzyl-L-cysteinylglycine (Fig. 6.3). This indirectly suggests that in contrast to *Corynebacterium* sp. Ax20, wild-type *E. coli*, employs only a single enzyme, TnaA, for biotransformation of dipeptide malodour precursor molecules such as S-Benzyl-L-cysteinylglycine. This proposal corresponds to observations made by Starckenmann *et al.* (2005), on studies relating to the high Cys-Gly-3M3SH biotransforming bacterium, *S. haemolyticus*. Starckenmann postulates that a single enzyme is responsible for Cys-Gly-3M3SH biotransformation in *S. haemolyticus*. In the 2005 study, it was demonstrated that *S. haemolyticus* is able to accomplish Cys-Gly-3M3SH biotransformation (75% product yield) more efficiently than biotransformation of the smaller malodour precursor molecule, Cys-3M3SH (25% product yield). This result suggested to Starckenmann that *S. haemolyticus* possesses a novel enzyme that is able to directly catabolise Cys-Gly-3M3SH. This is because dual-step biotransformation of Cys- and Cys-Gly-3M3SH should yield an equivalent amount of 3M3SH in both cases as the C-S-  $\beta$ -lyase step is dependent upon the initial dipeptidase step. This is an attractive hypothesis, however, a simpler explanation relates to differences in the transport rate of Cys-Gly-3M3SH, which is

actively transported into the cell by STAHO0001\_1446 (in *S. hominis*), compared to Cys-3M3SH which, being a smaller molecule, is more likely to passively diffuse into the cell. This would lead to a slower biotransformation rate of Cys-3M3SH and lower thioalcohol yield, possibly explaining why Starckenmann observed lower 3M3SH yield from *S. haemolyticus* biotransformation of Cys-3M3SH compared to Cys-Gly-3M3SH.

Following on from this initial observation by Starckenmann, Troccaz *et al.* (2008), cloned the putative Cys-Gly-3M3SH C-S- $\beta$ -lyase from *S. haemolyticus*, expressed the recombinant enzyme and characterised its biochemical activity against common C-S- $\beta$ -lyase substrates along with malodour precursor molecules. Curiously, the recombinant enzyme showed little activity against Cys-Gly-3M3SH (0.01% activity) or Cys-3M3SH (0.22% activity), relative to activity against the natural C-S- $\beta$ -lyase substrates, L-cystathionine. It therefore appears that a different enzyme is responsible for biotransformation of Cys-Gly-3M3SH in *S. haemolyticus*, possibly the orthologue of the *S. hominis* gene STAHO0001\_0481, as identified in Fig. 6.4.1.

STAHO0001\_0481 from *S. hominis* SK119 represents a gene encoding a novel enzyme in the respect that an orthologue can only be identified in those other bacteria able to biotransform Cys-Gly-3M3SH: *S. haemolyticus* and *S. lugdunensis*. Both *S. hominis* STAHO0001\_0481 and *E. coli* TnaA are part of the AAT\_I (aspartate aminotransferase fold type I) superfamily, suggesting that although they share little sequence similarity at the amino acid level, there is some common domain architecture between the two proteins, which may lead to overlapping functionalities in terms of malodour precursor biotransformation.

In summary, a *S. hominis* peptide transporter, STAHO0001\_1446, has been identified, experimentally characterised and shown to transport the physiological malodour precursor molecule, Cys-Gly-3M3SH. A strong bioinformatics-based hypothesis has also been proposed which suggests that once internalised by STAHO0001\_1446, Cys-Gly-3M3SH is catabolised by a novel aminotransferase-like protein, STAHO0001\_0481, which is only present in those staphylococci that show strong Cys-Gly-3M3SH biotransformation activity (*S. hominis*, *S. lugdunensis* and *S. haemolyticus*). These findings represent novel insights into the molecular mechanism of thioalcohol-based malodour by members of the axillary microbiota and open up the possibility of employing novel strategies to directly target specific proteins involved in catabolism of such precursor substrates in order to reduce the formation of axillary malodour.

# **Summary and future directions**

In this study, *E. coli* was used as a model organism to study thioalcohol-conjugated malodour precursor biotransformation. A series of peptide transporter-deficient (TD-Pep) *E. coli* strains were created and phenotypically characterised. This revealed an interesting pattern of substrate recognition for the lesser-studied PTR-family transporters, DtpA, DtpB, DtpC and DtpD. Strong phenotypic growth defects were observed when multiple PTR transporters were mutated and the strains subsequently grown on peptide-containing media, suggesting that the overall contribution of these transporters to growth on peptides is likely to be more important than previously suggested. A strong phenotype was particularly apparent when  $\Delta dtpA \Delta dtpB \Delta dtpC \Delta dtpD$  ( $\Delta DB5$ ) was grown on Ala-Ala as the sole source of nitrogen, suggesting that multiple PTR proteins are able to recognise and transport this simple dipeptide substrate. Additionally, dipeptide-conjugated malodour precursor compounds were also transported by the PTR transporter DtpB which represents a novel phenotype for a member of this family. It also suggests that the substrate specificity of PTR transporters, particularly DtpB, is dynamic and able to accommodate structurally diverse molecules. This observation potentially re-opens the possibility of designing novel antimicrobials that are specifically targeted for uptake by these proteins, rather than following the earlier proposal of targeting such compounds to the Dpp and Opp systems (Ames *et al.*, 1973, Diddens *et al.*, 1976). Although to do this, a comprehensive analysis of the entire substrate specificity of the PTR transporters would have to be carried out, perhaps by designing a high-throughput substrate screening method.

The more widely characterised ABC peptide transporters Opp and Dpp were also studied and the findings generally supported previous literature suggesting that Opp is a general oligopeptide transporter (Hiles *et al.*, 1987, Naider & Becker, 1975). The ability of both Opp and Dpp to transport dipeptides was also reinforced when a double mutant,  $\Delta dppC \Delta oppC$  ( $\Delta DB1$ ) displayed a weaker growth rate on Ala-Phe as the sole source of nitrogen, compared to either single mutant strain alone. No phenotype was observed for *dpp* or *opp* mutants when required to transport dipeptide-conjugated malodour precursor molecules, again reinforcing the importance of *E. coli* Dtp transporters.

Specifically regarding the biochemical basis of axillary malodour, this project has assessed, in detail, the relative contribution of multiple axillary-isolated bacterial species to thioalcohol-based malodour. Whole cell Cys-Gly-3M3SH biotransformation assays revealed that three *Staphylococcus* species, *S. hominis*, *S. lugdunensis* and *S. haemolyticus* were the most active biotransformers of this substrate and generated a significantly greater thioalcohol yield than other *Staphylococcus* spp. or any corynebacteria. This discovery casts doubt on to previous observations that

corynebacteria, particularly *C. tuberculostearicum*, contribute to thioalcohol-based malodour (Jackman & Noble, 1983, Taylor *et al.*, 2003, James *et al.*, 2013), given that in this study, 8 out of 8 *C. tuberculostearicum* isolates were unable to generate 3M3SH. These findings also raise questions about the overall contribution of the genus *Corynebacterium* to typical axillary malodour, given that the most prevalent *Corynebacterium* spp. within the axillary microbiota, *C. tuberculostearicum* and *C. mucifaciens* (Taylor *et al.*, 2003) are not involved in either thioalcohol- or VFA-associated malodour (James *et al.*, 2013), the two major axillary odour pathways. It is possible that a *Corynebacterium*-dense axilla is associated with but not causal to the high-odour axilla phenotype. This mis-association could be ubiquitous for several reasons. Firstly, the relative abundance of different *Staphylococcus* species in a malodorous axilla has never been investigated, so it is possible that high corynebacterial numbers drive up the relative proportion of thioalcohol-producing staphylococci such as *S. hominis*, *S. lugdunensis* and *S. haemolyticus*. This would effectively lead to a case of mistaken identity, whereby corynebacteria are wrongly linked to malodour. Conversely, in a staphylococcal dominated axilla, where the most prevalent species is likely to be *S. epidermidis* (Kloos & Musselwhite, 1975), the *S. hominis*, *S. lugdunensis* and *S. haemolyticus* population may be much lower resulting in a non-malodour phenotype. This would lead to what is observed in literature, whereby the genus *Staphylococcus* is not correlated with axillary malodour (Taylor *et al.*, 2003). It is also feasible but unlikely that corynebacteria are able to biotransform a yet to be identified malodour molecule with particularly high olfactory impact. Clearly there is a requirement to quantify the axillary microbiota at the species level. With the advent of high-throughput DNA sequencing it would be feasible to adopt a metagenomic approach to sequence and delineate the relative abundance of individual bacterial species across a statistically significant number of axillae. It would also be interesting to note any evolutionary-associated patterns, for example, do individuals that are unable to secrete Cys-Gly-3M3SH due to the *ABCC11* mutation (Martin *et al.*, 2010) carry a lower percentage of *S. hominis* than individuals with a functional *ABCC11* allele? Similarly, is there a relationship between the abundance of *S. hominis* in the axilla and the amount of 3M3SH produced?

Also in this work, the biochemical basis of Cys-Gly-3M3SH biotransformation in *S. hominis* has been characterised, with uptake of the molecule in this bacterium mediated by a general staphylococcal transport protein, STAHO0001\_1446. This transporter, a member of the PTR family, is present in all sequenced staphylococci. The partially-characterised orthologue in *S. aureus* participates in general peptide uptake (Perry, 1980). Evidently, the substrate specificity of STAHO0001\_1446 is dynamic enough to bind and transport dipeptide analogues and, similar to most characterised peptide transporters,

likely recognises the peptide backbone of the molecule rather than the side chain. It would be interesting to elucidate whether STAHO0001\_1446 has evolved to specifically recognise and transport Cys-Gly-3M3SH, or whether Cys-Gly-3M3SH transport can be mediated by STAHO0001\_1446 orthologues from a parent strain that does not biotransform Cys-Gly-3M3SH, such as *S. aureus*. This would be a relatively simple experiment to carry out and would only require cloning of the orthologous *S. aureus* gene and expression in *E. coli* followed by a Cys-Gly-3M3SH biotransformation assay to assess functional complementation. It would be appealing to determine whether STAHO0001\_1446 is also able to recognise and transport the minor thioalcohol-conjugated precursor, Cys-3M3SH. Despite being present in apocrine secretions at relatively low abundance compared to Cys-Gly-3M3SH (Emter & Natsch, 2008), the bacterium would certainly benefit if the same transporter could import both molecules, although this is unlikely to be the case given the absence of a peptide bond in Cys-3M3SH.

In addition to characterising the transport mechanism of Cys-Gly-3M3SH in physiologically relevant bacteria, a hypothesis was proposed describing the most likely route of intracellular substrate catabolism. It was suggested that the ability to biotransform Cys-Gly-3M3SH was limited at the level of intracellular catabolism, given that all staphylococci, in theory, have the ability to transport this molecule. Using *in silico* analysis, a unique aminotransferase-like protein with C-S-  $\beta$ -lyase activity was identified and is only present in those *Staphylococcus* species able to biotransform Cys-Gly-3M3SH. Following this observation, the immediate experimental objective would be to clone this gene from *S. hominis* and assess its ability to convert a non-Cys-Gly-3M3SH biotransforming *Staphylococcus* sp. into a thioalcohol producing strain. This could be achieved using a *Staphylococcus/E. coli* shuttle vector and would categorically demonstrate that Cys-Gly-3M3SH biotransformation is limited by an inability of most *Staphylococcus* spp. to intracellularly catabolise the substrate.

The effectiveness of using model substrates to characterise important physiological processes was questioned when it was demonstrated that the pattern of biotransformation of the model thioalcohol-conjugated dipeptide substrate S-Benzyl-L-cysteinylglycine by individual bacterial species was completely different to that of the physiological substrate Cys-Gly-3M3SH. From the bioinformatic-based analysis, this difference likely stems from the specific enzymes involved in the biotransformation of these substrates. S-Benzyl-L-cysteinylglycine is likely metabolised by a general cystathionase-type C-S-  $\beta$ -lyase whereas Cys-Gly-3M3SH is hypothesised to be broken down by the unique bacterial lyase only present in *S. hominis*, *S. lugdunensis* and *S. haemolyticus*. For this reason, general

C-S-  $\beta$ -lyase activity can no longer be used a sufficient measure of Cys-Gly-3M3SH biotransformation ability.

Human body odour has been subjectively described for centuries but with significant technological advancement over the previous decades, the microbial, molecular and biochemical origins of body odour are becoming apparent. Historically, body odour is likely to have served as a specific and necessary olfactory cue but as modern society evolved it became an unpleasant and undesirable facet of human evolution. This work provides significant molecular and biochemical evidence for the route to thioalcohol-based odour in the human axilla.

## Abbreviations

3M2H	( <i>E</i> )-3-methyl-2-hexenoic acid
3M3SH	3-methyl-3-sulfanylhexanol
A <sub>xxx</sub>	Optical absorbance at stated wavelength of light
ABC	ATP-binding cassette
AHAS	Acetohydroxy acid synthase
Amp	Ampicillin
ASOB1	Apocrine Secretion Odor-Binding protein 1
ASOB2	Apocrine Secretion Odor-Binding protein 2
BLAST	Basic Local Alignment Search Tool
Cam	Chloramphenicol
CCCP	Carbonyl cyanide <i>m</i> -chlorophenyl hydrazone
Cys-Gly-3M3SH	( <i>S</i> )-(1-(2-hydroxyethyl)-1-methylbutyl)-L-cysteinylglycine
C-S- $\beta$ -lyase	Carbon-sulphur (usually cystathionine)- $\beta$ -lyase
dATP	Deoxyadenosine triphosphate
dCTP	Deoxycytosine triphosphate
dGTP	Deoxyguanosine triphosphate
dH <sub>2</sub> O	Distilled water
DTNB	5,5'-dithiobis-(2-nitrobenzoic acid)
dTTP	Deoxythymidine triphosphate
DHT	5 $\alpha$ -dihydrotestosterone
GC-MS	Gas chromatography-mass spectrometry
HMHA	3-hydroxy-3-methylhexanoic acid
HPLC	High-performance liquid chromatography
HPLC/GC	High-performance liquid chromatography coupled to gas chromatography
LIC	Ligation-independent cloning
LB	Luria-Bertani
LC-MS	Liquid chromatography-mass spectrometry

MHC	Major histocompatibility complex
MTS	(3-(4,5-dimethylthiazol-2-yl)-5-(3-carboxymethoxyphenyl)-2-(4-sulfophenyl)-2H-tetrazolium)
NCBI	National Center for Biotechnology Information
NTB	2-nitro-5-thiobenzoate
OBP	Odorant binding protein
OD	Optical density
POT	Proton-dependent oligopeptide transporter
ppb	Parts per billion
PCR	Polymerase chain reaction
PMS	Phenazine methosulfate
Psi	Parts per square inch
Rpm	Revolutions per minute
SOC	Super optimal broth with catabolite repression
TD Pep	Peptide transporter-deficient <i>E. coli</i>
TLC	Thin layer chromatography
TSAT	Tryptone soy broth with tween (agar)
TSBT	Tryptone soy broth with tween
MRM	Minimal recovery medium
sp.	Species (singular)
spp.	Species (plural)
WT	Wild-type
w/v	Weight to volume ratio
VFA	Volatile fatty acid
v/v	Volume to volume ratio

## Reference list

- Abramson, J., Smirnova, I., Kasho, V., Verner, G., Kaback, H. R. & Iwata, S. (2003) Structure and Mechanism of the Lactose Permease of *Escherichia coli*. *Science*, 301, 610-5.
- Adelman, S., Taylor, C. R. & Heglund, N. C. (1975) Sweating on Paws and Palms: What Is Its Function? *Am J Physiol*, 229, 1400-2.
- Adibi, S. A. (1971) Intestinal Transport of Dipeptides in Man: Relative Importance of Hydrolysis and Intact Absorption. *J Clin Invest*, 50, 2266-75.
- Aly, R. & Maibach, H. I. (1977) Aerobic Microbial Flora of Intertriginous Skin. *Appl Env Micro* 33, 97-100.
- Ames, B. N., Ames, G. F., Young, J. D., Tsuchiya, D. & Lecocq, J. (1973) Illicit Transport: The Oligopeptide Permease. *Proc Natl Acad Sci U S A*, 70, 456-8.
- Amoore, J. E., Pelosi, P. A. O. L., Forrester, L. J. (1977). Specific Anosmias to 5 $\alpha$ -androst-16-en-3-one and  $\omega$ -Pentadecalactone: The Urinous and Musky Primary Odors. *J Chem Senses*, 2, 401-25.
- Andrews, J. C., Blevins, T. C. & Short, S. A. (1986) Regulation of Peptide Transport in *Escherichia coli*: Induction of the Trp-Linked Operon Encoding the Oligopeptide Permease. *J Bacteriol*, 165, 428-33.
- Asahina, M., Suzuki, A., Mori, M., Kanekane, T. & Hattori, T. (2003) Emotional Sweating Response in a Patient with Bilateral Amygdala Damage. *Int J Psychophysiol*, 47, 87-93.
- Auger, S., Gomez, M. P., Danchin, A. & Martin-Verstraete, I. (2005) The Patb Protein of *Bacillus subtilis* Is a C-S-Lyase. *Biochimie*, 87, 231-8.
- Austin, C. & Ellis, J. (2003) Microbial Pathways Leading to Steroidal Malodour in the Axilla. *J Steroid Biochem Mol Biol*, 87, 105-10.
- Awano, N., Wada, M., Kohdoh, A., Oikawa, T., Takagi, H. & Nakamori, S. (2003) Effect of Cysteine Desulfhydrase Gene Disruption on L-Cysteine Overproduction in *Escherichia coli*. *Appl Microbiol Biotechnol*, 62, 239-43.
- Awano, N., Wada, M., Mori, H., Nakamori, S. & Takagi, H. (2005) Identification and Functional Analysis of *Escherichia coli* Cysteine Desulfhydrases. *Appl Environ Microbiol*, 71, 4149-52.
- Baba, T., Ara, T., Hasegawa, M., Takai, Y., Okumura, Y., Baba, M., Datsenko, K. A., Tomita, M., Wanner, B. L. & Mori, H. (2006) Construction of *Escherichia coli* K-12 in-Frame, Single-Gene Knockout Mutants: The Keio Collection. *Mol Syst Biol*, 2,
- Baev, M. V., Baev, D., Radek, A. J. & Campbell, J. W. (2006a) Growth of *Escherichia coli* MG1655 on LB Medium: Monitoring Utilization of Amino Acids, Peptides, and Nucleotides with Transcriptional Microarrays. *Appl Microbiol Biotechnol*, 71, 317-22.
- Baev, M. V., Baev, D., Radek, A. J. & Campbell, J. W. (2006b) Growth of *Escherichia coli* MG1655 on LB Medium: Determining Metabolic Strategy with Transcriptional Microarrays. *Appl Microbiol Biotechnol*, 71, 323-8.

- Banowski, B., Bockmühl, D. & Scholtyssek, R. (2007) Inhibitors of *Staphylococcus Hominis* in Deodorants and Antiperspirants. US Patent EP1738803 A1.
- Barak, Z. & Gilbarg, C. (1975) Specialized Peptide Transport System in *Escherichia coli*. *J Bacteriol*, 122, 1200-7.
- Barzantny, H., Brune, I. & Tauch, A. (2011) Molecular Basis of Human Body Odour Formation: Insights Deduced from Corynebacterial Genome Sequences. *Int J Cosmetic Sci*, 34, 2-11.
- Biegel, A., Knutter, I., Hartrodt, B., Gebauer, S., Theis, S., Luckner, P., Kottra, G., Rastetter, M., Zebisch, K., Thondorf, I., Daniel, H., Neubert, K. & Brandsch, M. (2006) The Renal Type H<sup>+</sup>/Peptide Symporter Pept2: Structure-Affinity Relationships. *Amino Acids*, 31, 137-56.
- Blattner, F. R., Plunkett, G., 3rd, Bloch, C. A., Perna, N. T., Burland, V., Riley, M., Collado-Vides, J., Glasner, J. D., Rode, C. K., Mayhew, G. F., Gregor, J., Davis, N. W., Kirkpatrick, H. A., Goeden, M. A., Rose, D. J., Mau, B. & Shao, Y. (1997) The Complete Genome Sequence of *Escherichia coli* K-12. *Science*, 277, 1453-62.
- Bojar, R. A. & Holland, K. T. (2004) Acne and Propionibacterium Acnes. *Clin Dermatol*, 22, 375-9.
- Boutelier, A. (1959) The Role of Sebum in the Defense Mechanisms of the Cutaneous Organ is Essentially of a Physical Nature. Contribution to the Study of the Physiology of the Skin: The Skin as Organ of Defense. *Bull Soc Fr Dermatol Syphiligr*, 5, 806-7
- Bouvier, J., Bordes, P., Romeo, Y., Fourcans, A., Bouvier, I. & Gutierrez, C. (2000) Characterization of OpuA, a Glycine-Betaine Uptake System of *Lactococcus lactis*. *J Mol Microbiol Biotechnol*, 2, 199-205.
- Brooksbank, B. W. L., Brown, R. & Gustafsson, J. A. (1974). The Detection of 5 $\alpha$ -androst-16-en-3 $\alpha$ -ol in Human Male Axillary Sweat. *Experientia* 30: 864-65.
- Busch, W. & Saier, M. H., Jr. (2002) The Transporter Classification (Tc) System. *Crit Rev Biochem Mol Biol*, 37, 287-337.
- Callewaert, C., Kerckhof, F. M., Granitsiotis, M. S., Van Gele, M., Van De Wiele, T. & Boon, N. (2013) Characterization of *Staphylococcus* and *Corynebacterium* Clusters in the Human Axillary Region. *PLoS One*, 8, e70538.
- Casagrande, F., Harder, D., Schenk, A., Meury, M., Ucurum, Z., Engel, A., Weitz, D., Daniel, H. & Fotiadis, D. (2009) Projection Structure of DtpD (YbgH), a Prokaryotic Member of the Peptide Transporter Family. *J Mol Biol*, 394, 708-17.
- Cernoch, J. M. & Porter, R. H. (1985) Recognition of Maternal Axillary Odors by Infants. *Child Dev*, 56, 1593-8.
- Cherepanov, P. P. & Wackernagel, W. (1995) Gene Disruption in *Escherichia coli*: Tcr and Kmr Cassettes with the Option of Flp-Catalyzed Excision of the Antibiotic-Resistance Determinant. *Gene*, 158, 9-14.
- Claus R. & Alsing W. (1976). Occurrence of 5 $\alpha$ -androst-16-en-3-one, a Boar Pheromone, in Man and its Relationship to Testosterone. *J Endocr*, 68, 483-4.
- Clausen, T., Schlegel, A., Peist, R., Schneider, E., Steegborn, C., Chang, Y. S., Haase, A., Bourenkov, G. P., Bartunik, H. D. & Boos, W. (2000) X-Ray Structure of MalY from *Escherichia coli*: A Pyridoxal 5'-Phosphate-Dependent Enzyme Acting as a Modulator in Mal Gene Expression. *EMBO J*, 19, 831-42.

- Cohn, J. R. & Emmett, E. A. (1978) The Excretion of Trace Metals in Human Sweat. *Ann Clin Lab Sci*, 8, 270-5.
- Costello, E. K., Lauber, C. L., Hamady, M., Fierer, N., Gordon, J. I. & Knight, R. (2009) Bacterial Community Variation in Human Body Habitats Across Space and Time. *Science*, 326, 1694-7.
- Cowan, S. T. (1968) A Dictionary of Medical Taxonomic Usage. Oliver & Boyd, Edinburgh.
- Cummins, C. S. (1962) Chemical Composition and Antigenic Structure of Cell Walls of *Corynebacterium*, *Mycobacterium*, *Nocardia*, *Actinomyces* and *Arthrobacter*. *J Gen Microbiol*, 28, 35-50.
- Dal Prá, V., Bisol, L. B., Paraboni, M. L. R. & Siqueira, L. O. (2013). Evaluation of Endothelial Adaptation and Parameters of Oxidative Stress in Patients After Hemodialysis Sessions. *J Appl Pharm Sci*, 3, 39-44.
- Daniel, H., Spanier, B., Kottra, G. & Weitz, D. (2006) From Bacteria to Man: Archaic Proton-Dependent Peptide Transporters at Work. *Physiology (Bethesda)*, 21, 93-102.
- Daruwalla, K. R., Paxton, A. T. & Henderson, P. J. (1981) Energization of the Transport Systems for Arabinose and Comparison with Galactose Transport in *Escherichia coli*. *Biochem J*, 200, 611-27.
- Datsenko, K. A. & Wanner, B. L. (2000) One-Step Inactivation of Chromosomal Genes in *Escherichia coli* K-12 Using PCR Products. *Proc Natl Acad Sci U S A*, 97, 6640-5.
- De Felice, M., Guardiola, J., Lamberti, A. & Iaccarino, M. (1973) *Escherichia coli* K-12 Mutants Altered in the Transport Systems for Oligo- and Dipeptides. *J Bacteriol*, 116, 751-56.
- Detmers, F. J., Lanfermeijer, F. C. & Poolman, B. (2001) Peptides and ATP Binding Cassette Peptide Transporters. *Res Microbiol*, 152, 245-58.
- Diddens, H., Zahner, H., Kraas, E., Gohring, W. & Jung, G. (1976) On the Transport of Tripeptide Antibiotics in Bacteria. *Eur J Biochem*, 66, 11-23.
- Doki, S., Kato, H. E., Solcan, N., Iwaki, M., Koyama, M., Hattori, M., Iwase, N., Tsukazaki, T., Sugita, Y., Kandori, H., Newstead, S., Ishitani, R. & Nureki, O. (2013) Structural Basis for Dynamic Mechanism of Proton-Coupled Symport by the Peptide Transporter POT. *Proc Natl Acad Sci U S A*, 110, 11343-8.
- Dubey, A. K., Baker, C. S., Suzuki, K., Jones, A. D., Pandit, P., Romeo, T. & Babitzke, P. (2003) CsrA Regulates Translation of the *Escherichia coli* Carbon Starvation Gene, *cstA*, by Blocking Ribosome Access to the *cstA* Transcript. *J Bacteriol*, 185, 4450-60.
- Dunten, P. & Mowbray, S. L. (1995) Crystal Structure of the Dipeptide Binding Protein from *Escherichia coli* Involved in Active Transport and Chemotaxis. *Protein Science : A Publication of the Protein Society*, 4, 2327-34.
- Dunten, P. W., Harris, J. H., Feiz, V. & Mowbray, S. L. (1993) Crystallization and Preliminary X-Ray Analysis of the Periplasmic Dipeptide Binding Protein from *Escherichia coli*. *J Mol Biol*, 231, 145-7.
- Egert, M., Schmidt, I., Höhne, H.-M., Lachnit, T., Schmitz, R. A. & Breves, R. (2011) rRNA-Based Profiling of Bacteria in the Axilla of Healthy Males Suggests Right-Left Asymmetry in Bacterial Activity. *FEMS Microbiol Ecol*, 77, 146-53.

- Ellman, G. L. (1958) A Colorimetric Method for Determining Low Concentrations of Mercaptans. *Arch Biochem Biophys*, 74, 443-50.
- Emter, R. & Natsch, A. (2008) The Sequential Action of a Dipeptidase and a B-Lyase Is Required for the Release of the Human Body Odorant 3-Methyl-3-Sulfanylhexan-1-ol from a Secreted Cys-Gly-(S) Conjugate by corynebacteria. *J Biol Chem*, 283, 20645-52.
- Ernst, H. A., Pham, A., Hald, H., Kastrup, J. S., Rahman, M. & Mirza, O. (2009) Ligand Binding Analyses of the Putative Peptide Transporter YjdL from *E. coli* Display a Significant Selectivity Towards Dipeptides. *Biochem Biophys Res Commun*, 389, 112-6.
- Fei, Y. J., Liu, W., Prasad, P. D., Kekuda, R., Oblak, T. G., Ganapathy, V. & Leibach, F. H. (1997) Identification of the Histidyl Residue Obligatory for the Catalytic Activity of the Human H<sup>+</sup>/Peptide Cotransporters Pept1 and Pept2. *Biochem*, 36, 452-60.
- Feurer, C., Clermont, D., Bimet, F., Candrea, A., Jackson, M., Glaser, P., Bizet, C. & Dauga, C. (2004) Taxonomic Characterization of Nine Strains Isolated from Clinical and Environmental Specimens, and Proposal of *Corynebacterium tuberculostearicum* sp. Nov. *Int J Syst Evol Microbiol*, 54, 1055-61.
- Flower, D. R. (1996) The Lipocalin Protein Family: Structure and Function. *Biochem J*, 318 ( Pt 1), 1-14.
- Folk, G. E., Jr. & Semken, H. A., Jr. (1991) The Evolution of Sweat Glands. *Int J Biometeorol*, 35, 180-6.
- Furness, G., Sambury, S. & Evangelista, A. T. (1979) *Corynebacterium pseudogenitalium* sp. Nov. Commensals of the Human Male and Female Urogenital Tracts. *Invest Urol*, 16, 292-5.
- Gallik, S. (2013). Histology of Skin Appendages. *Histology OLM 4.0*, Available: [http://stevegallik.org/histologyolm\\_Ch13\\_P06.html](http://stevegallik.org/histologyolm_Ch13_P06.html) [Accessed: 03/09/2014].
- Geertsma, E. R. & Poolman, B. (2007) High-Throughput Cloning and Expression in Recalcitrant Bacteria. *Nat Meth*, 4, 705-7.
- Gibson, M. M., Price, M. & Higgins, C. F. (1984) Genetic Characterization and Molecular Cloning of the Tripeptide Permease (*tpp*) Genes of *Salmonella typhimurium*. *J Bacteriol*, 160, 122-30.
- Glover, I. D., Denny, R. C., Nguti, N. D., Mcsweeney, S. M., Kinder, S. H., Thompson, A. W., Dodson, E. J., Wilkinson, A. J. & Tame, J. R. (1995) Structure Determination of OppA at 2.3 Å Resolution Using Multiple-Wavelength Anomalous Dispersion Methods. *Acta Crystallogr D Biol Crystallogr*, 51, 39-47.
- Goodwin, C. J., Holt, S. J., Downes, S. & Marshall, N. J. (1995) Microculture Tetrazolium Assays: A Comparison between Two New Tetrazolium Salts, Xtt and Mts. *J Immunol Methods*, 179, 95-103.
- Gordon, S. G., Smith, K., Rabinowitz, J. L. & Vagelos, P. R. (1973) Studies of Trans-3-Methyl-2-Hexenoic Acid in Normal and Schizophrenic Humans. *J Lipid Res*, 14, 495-503.
- Gower, D. B. (1972)  $\Delta^{16}$ -unsaturated C19 Steroids: a Review of Their Chemistry, Biochemistry and Possible Physiological Role. *J Steroid Biochem*, 3, 45-103.
- Gower, D. B., Holland, K. T., Mallet, A. I., Rennie, P. J. & Watkins, W. J. (1994) Comparison of 16-Androstene Steroid Concentrations in Sterile Apocrine Sweat

and Axillary Secretions: Interconversions of 16-Androstenes by the Axillary Microflora - a Mechanism for Axillary Odour Production in Man? *J Steroid Biochem Mol Biol*, 48, 409-18.

- Gower, D. B., Nixon, A., Jackman, P. J. & Mallett, A. I. (1986) Transformation of Steroids by Axillary Coryneform Bacteria. *Int J Cosmet Sci*, 8, 149-58.
- Gower, D. B., Nixon, A., & Mallet, I. (1988) The Significance of Odorous Steroids in Axillary Odour, In: *Perfumery: The Psychology and Biology of Fragrance*, Chapman and Hall, London, p. 47.
- Grant-Preece, P. A., Pardon, K. H., Capone, D. L., Cordente, A. G., Sefton, M. A., Jeffery, D. W. & Elsey, G. M. (2010) Synthesis of Wine Thiol Conjugates and Labeled Analogues: Fermentation of the Glutathione Conjugate of 3-Mercaptohexan-1-ol Yields the Corresponding Cysteine Conjugate and Free Thiol. *J Agric Food Chem*, 58, 1383-9.
- Guettou, F., Quistgaard, E. M., Tresaugues, L., Moberg, P., Jegerschold, C., Zhu, L., Jong, A. J., Nordlund, P. & Low, C. (2013) Structural Insights into Substrate Recognition in Proton-Dependent Oligopeptide Transporters. *EMBO Rep*, 14, 804-10.
- Guyer, C. A., Morgan, D. G. & Staros, J. V. (1986) Binding Specificity of the Periplasmic Oligopeptide-Binding Protein from *Escherichia coli*. *J Bacteriol*, 168, 775-9.
- Hagen, A. (1901) Die Sexuelle Oosphresologie.
- Hagting, A., Kunji, E. R., Leenhouts, K. J., Poolman, B. & Konings, W. N. (1994) The Di- and Tripeptide Transport Protein of *Lactococcus lactis*. A New Type of Bacterial Peptide Transporter. *J Biol Chem*, 269, 11391-9.
- Hagting, A., Vd Velde, J., Poolman, B. & Konings, W. N. (1997) Membrane Topology of the Di- and Tripeptide Transport Protein of *Lactococcus lactis*. *Biochem*, 36, 6777-85.
- Harder, D., Stolz, J., Casagrande, F., Obrdlik, P., Weitz, D., Fotiadis, D. & Daniel, H. (2008) DtpB (YhiP) and DtpA (TppA, YdgR) Are Prototypical Proton-Dependent Peptide Transporters of *Escherichia coli*. *FEBS J*, 275, 3290-8.
- Harker, M., Carvell, A. M., Marti, V. P., Riazanskaia, S., Kelso, H., Taylor, D., Grimshaw, S., Arnold, D. S., Zillmer, R., Shaw, J., Kirk, J. M., Alcasid, Z. M., Gonzales-Tanon, S., Chan, G. P., Rosing, E. A. & Smith, A. M. (2014) Functional Characterisation of a SNP in the ABCC11 Allele - Effects on Axillary Skin Metabolism, Odour Generation and Associated Behaviours. *J Dermatol Sci*, 73, 23-30.
- Hasegawa, Y., Yabuki, M. & Matsukane, M. (2004) Identification of New Odoriferous Compounds in Human Axillary Sweat. *Chem Biodivers*, 1, 2042-50.
- Higgins, C. F. (2001) ABC Transporters: Physiology, Structure and Mechanism - an Overview. *Res Microbiol*, 152, 205-210.
- Higgins, C. F., Hiles, I. D., Salmond, G. P., Gill, D. R., Downie, J. A., Evans, I. J., Holland, I. B., Gray, L., Buckel, S. D., Bell, A. W. & Et Al. (1986) A Family of Related ATP-Binding Subunits Coupled to Many Distinct Biological Processes in Bacteria. *Nature*, 323, 448-50.
- Hiles, I. D., Gallagher, M. P., Jamieson, D. J. & Higgins, C. F. (1987) Molecular Characterization of the Oligopeptide Permease of *Salmonella typhimurium*. *J Mol Biol*, 195, 125-42.

- Hirokawa, T., Okamoto, H., Gosyo, Y., Tsuda, T. & Timerbaev, A. R. (2007) Simultaneous Monitoring of Inorganic Cations, Amines and Amino Acids in Human Sweat by Capillary Electrophoresis. *Anal Chim Acta*, 581, 83-8.
- Hiron, A., Borezee-Durant, E., Piard, J. C. & Juillard, V. (2007) Only One of Four Oligopeptide Transport Systems Mediates Nitrogen Nutrition in *Staphylococcus aureus*. *J Bacteriol*, 189, 5119-29.
- Holzle, E. (2002) Pathophysiology of Sweating. *Curr. Probl. Dermatol.* 30, 10–22.
- Hurley, H. J. (1953) The Distribution of Cholinesterases in Human Skin, with Special Reference to Eccrine and Apocrine Sweat Glands. *J Invest Dermatol*, 21, 139-47.
- Jackman, P. J. H. & Noble, W. C. (1983) Normal Axillary Skin in Various Populations. *Clin Exp Dermatol*, 8, 259-68.
- James, A. G., Austin, C. J., Cox, D. S., Taylor, D. & Calvert, R. (2013) Microbiological and Biochemical Origins of Human Axillary Odour. *FEMS Microbiol Ecol*, 83, 527-40.
- James, A. G., Hyliands, D. & Johnston, H. (2004) Generation of Volatile Fatty Acids by Axillary Bacteria<sup>1</sup>. *Int J Cosmetic Sci*, 26, 149-56.
- Jensen, J. M., Simonsen, F. C., Mastali, A., Hald, H., Lillebro, I., Diness, F., Olsen, L. & Mirza, O. (2012) Biophysical Characterization of the Proton-Coupled Oligopeptide Transporter *yjdL*. *Peptides*, 38, 89-93.
- Kaback, H. R., Reeves, J. P., Short, S. A. & Lombardi, F. J. (1974) Mechanisms of Active Transport in Isolated Bacterial Membrane Vesicles. 18. The Mechanism of Action of Carbonylcyanide M-Chlorophenylhydrazone. *Arch Biochem Biophys*, 160, 215-22.
- Kalinowski, J., Bathe, B., Bartels, D., Bischoff, N., Bott, M., Burkovski, A., Dusch, N., Eggeling, L., Eikmanns, B. J., Gaigalat, L., Goesmann, A., Hartmann, M., Huthmacher, K., Kramer, R., Linke, B., Mchardy, A. C., Meyer, F., Mockel, B., Pfeifferle, W., Puhler, A., Rey, D. A., Ruckert, C., Rupp, O., Sahm, H., Wendisch, V. F., Wiegrabe, I. & Tauch, A. (2003) The Complete *Corynebacterium glutamicum* ATCC 13032 Genome Sequence and Its Impact on the Production of L-Aspartate-Derived Amino Acids and Vitamins. *J Biotechnol*, 104, 5-25.
- Kawahata, A. (1950) Studies on the Function of Human Sweat Organs. *J Mie Med College* 1, 25-41.
- Kelly, J. (2013) PhD Thesis. University of Liverpool
- Kloos, W. & Schleifer, K. (1975) Isolation and Characterization of Staphylococci from Human Skin. *Int J Syst Bacteriol*, 25, 62-79.
- Kloos, W. E. & Musselwhite, M. S. (1975) Distribution and Persistence of *Staphylococcus* and *Micrococcus* Species and Other Aerobic Bacteria on Human Skin. *Appl Microbiol*, 30, 381-5.
- Ku, S. Y., Yip, P. & Howell, P. L. (2006) Structure of *Escherichia coli* Tryptophanase. *Acta Crystallogr D Biol Crystallogr*, 62, 814-23.
- Kuno, Y. (1965) The Mechanism of Human Sweat Secretion. *Proc 23rd Int'l Congr Physiol Sei*, Excerpta Medica International Congress Series 87, 3.
- Kurosumi, K., Shibasaki, S. & Ito, T. (1984) Cytology of the Secretion in Mammalian Sweat Glands. *Int Rev Cytol*, 87, 253-329.

- Laycock, T. (1840) The Special Relations of the Reproductive Organs, In: *A Treatise on the Nervous Diseases of Women*, Longman, London p. 20.
- Leavitt, R. I. & Umbarger, H. E. (1962) Isoleucine and Valine Metabolism in *Escherichia coli*. Xi. Valine Inhibition of the Growth of *Escherichia coli* Strain K-12. *J Bacteriol*, 83, 624-30.
- Lederberg, J. & Tatum, E. L. (1946) Gene Recombination in *Escherichia coli*. *Nature*, 158, 558.
- Leyden, J. J., Mcginley, K. J., Holzle, E., Labows, J. N. & Kligman, A. M. (1981) The Microbiology of the Human Axilla and Its Relationship to Axillary Odor. *J Invest Dermatol*, 77, 413-6.
- Linton, K. J. & Higgins, C. F. (1998) The *Escherichia coli* ATP-Binding Cassette (ABC) Proteins. *Mol Microbiol*, 28, 5-13.
- London, J. & Goldberg, M. E. (1972) The Tryptophanase from *Escherichia coli* K-12. I. Purification, Physical Properties, and Quaternary Structure. *J Biol Chem*, 247, 1566-70.
- Lyon, S. B., O'Neal, C., Van der Lee, H. & Rogers, B. (1991) to Gillette Co., US Pat. 5213791 (*Chem Abstr*, 115, 499001).
- Mader, U., Schmeisky, A. G., Florez, L. A. & Stulke, J. (2011). *SubtWiki - A Comprehensive Community Resource for the Model Organism Bacillus subtilis*
- Madigan & Martinko, (2006) Periplasmic Binding Proteins and the ABC System, In: Brock Biology of Microorganisms. *Pearson Education Ltd*, London, p. 74.
- Maqbool, A., Levdikov, V. M., Blagova, E., Herve, M., Horler, R. S. P., Wilkinson, A. J. & Thomas, G. H. (2011). *J Biol Chem*, 286, 31512-21.
- Marples, R. R. & Williamson, P. (1969) Effects of Systemic Demethylchlorotetracycline in Human Cutaneous Microflora. *Appl Microbiol*, 18, 228-34.
- Martin, A., Saathoff, M., Kuhn, F., Max, H., Terstegen, L. & Natsch, A. (2009) A Functional ABCC11 Allele Is Essential in the Biochemical Formation of Human Axillary Odor. *J Invest Dermatol*, 130, 529-40.
- Matsunaga, E. (1962) The Dimorphism in Human Normal Cerumen. *Ann Hum Genet*, 25, 273-86.
- Meagher, S., Penn, D. J. & Potts, W. K. (2000) Male-Male Competition Magnifies Inbreeding Depression in Wild House Mice. *Proc Natl Acad Sci U S A*, 97, 3324-9.
- Meredith, D., Boyd, C. A., Bronk, J. R., Bailey, P. D., Morgan, K. M., Collier, I. D. & Temple, C. S. (1998) 4-Aminomethylbenzoic Acid Is a Non-Translocated Competitive Inhibitor of the Epithelial Peptide Transporter Pept1. *J Physiol*, 512 ( Pt 3), 629-34.
- Miller, C. G. & Schwartz, G. (1978) Peptidase-Deficient Mutants of *Escherichia coli*. *J Bacteriol*, 135, 603-11.
- Montagna, W & Parakkal, P. F. (1974) The Structure and Function of Skin. *New York: Academic Press*.
- Morley, J. S., Payne, J. W. & Hennessey, T. D. (1983) Antibacterial Activity and Uptake into *Escherichia coli* of Backbone-Modified Analogues of Small Peptides. *J Gen Microbiol*, 129, 3701-8.

- Mosher, H. H. (1933) Simultaneous Study of Constituents of Urine and Perspiration. *J Biol Chem*, 99, 781–90.
- Mullins, K., Faloon, F., Scharf, S., Saiki, R., Horn, G. & Erlich, H. (1986) Specific Enzymatic Amplification of DNA in vitro: The Polymerase Chain Reaction. *Cold Spring Harb Symp Quant Biol*, 51 (pt 1), 263-73.
- Naider, F. & Becker, J. M. (1975) Multiplicity of Oligopeptide Transport Systems in *Escherichia coli*. *J Bacteriol*, 122, 1208-15.
- Naruse, S., Ishiguro, H., Suzuki, Y., Fujiki, K., Ko, S. B., Mizuno, N., Takemura, T., Yamamoto, A., Yoshikawa, T., Jin, C., Suzuki, R., Kitagawa, M., Tsuda, T., Kondo, T. & Hayakawa, T. (2004) A Finger Sweat Chloride Test for the Detection of a High-Risk Group of Chronic Pancreatitis. *Pancreas*, 28, 80-5.
- Natsch, A., Gfeller, H., Gygax, P., Schmid, J. & Acuna, G. (2003) A Specific Bacterial Aminoacylase Cleaves Odorant Precursors Secreted in the Human Axilla. *J Biol Chem*, 278, 5718-27.
- Natsch, A., Schmid, J. & Flachsmann, F. (2004) Identification of Odoriferous Sulfanylalkanols in Human Axilla Secretions and Their Formation through Cleavage of Cysteine Precursors by a C-S Lyase Isolated from Axilla Bacteria. *Chem Biodivers*, 1, 1058-72.
- Natsch, A., Derrer, S., Flachsmann, F. & Schmid, J. (2006) A Broad Diversity of Volatile Carboxylic Acids, Released by a Bacterial Aminoacylase from Axilla Secretions, as Candidate Molecules for the Determination of Human-Body Odor Type. *Chem Biodivers*, 3, 1-20.
- Natsch, A. & Granier, T. (2014) Glutamine Derivatives as Deodorants. WIPO Patent WO2012056014 A1.
- Newstead, S., Drew, D., Cameron, A. D., Postis, V. L., Xia, X., Fowler, P. W., Ingram, J. C., Carpenter, E. P., Sansom, M. S., Mcpherson, M. J., Baldwin, S. A. & Iwata, S. (2011) Crystal Structure of a Prokaryotic Homologue of the Mammalian Oligopeptide-Proton Symporters, Pept1 and Pept2. *EMBO J*, 30, 417-26.
- Newstead, S. (2014) Molecular Insights into Proton Coupled Peptide Transport in the PTR Family of Oligopeptide Transporters. *Biochim Biophys Acta*, In Press.
- Nixon, A., Mallet, A. I., Jackman, P. J. & Gower, D. B. (1986) Testosterone Metabolism by Isolated Human Axillary *Corynebacterium* spp.: A Gas-Chromatographic Mass-Spectrometric Study. *J Steroid Biochem*, 24, 887-92.
- Olson, E. R., Duniyak, D. S., Jurss, L. M. & Poorman, R. A. (1991) Identification and Characterization of *dppA*, an *Escherichia coli* Gene Encoding a Periplasmic Dipeptide Transport Protein. *J. Bacteriol*, 173, 234-44.
- Parra-Lopez, C., Baer, M. T. & Groisman, E. A. (1993) Molecular Genetic Analysis of a Locus Required for Resistance to Antimicrobial Peptides in *Salmonella typhimurium*. *EMBO J*, 12, 4053-62.
- Patterson, M. J., Galloway, S. D. & Nimmo, M. A. (2000) Variations in Regional Sweat Composition in Normal Human Males. *Exp Physiol*, 85, 869-75.
- Pao S. S., Paulsen I.T. & Saier Jr M. H. (1998) Major Facilitator Superfamily. *Microbiol Molec Biol Rev*, 62, 1–34.
- Paulsen, I. T. & Skurray, R. A. (1994) The POT Family of Transport Proteins. *Trends Biochem Sci*, 19, 404.

- Payne, J. W. & Gilvarg, C. (1968) Size Restriction on Peptide Utilisation in *Escherichia coli*. *J Bacteriol*, 243, 6291-9.
- Payne, J. W. (1971) The Utilization of Prolyl Peptides by *Escherichia coli*. *Biochem J*, 123, 255-60.
- Payne, J. W., Morley, J. S., Armitage, P. & Payne, G. M. (1984) Transport and Hydrolysis of Antibacterial Peptide Analogues in *Escherichia coli*: Backbone-Modified Aminoxy Peptides. *J Gen Microbiol*, 130, 2253-65.
- Perego, M., Higgins, C. F., Pearce, S. R., Gallagher, M. P. & Hoch, J. A. (1991) The Oligopeptide Transport System of *Bacillus subtilis* Plays a Role in the Initiation of Sporulation. *Mol Microbiol*, 5, 173-85.
- Perry, D. (1980) Peptide Transport in *Staphylococcus aureus*. *J Gen Microbiol*, 124, 425-8.
- Perry, D. & Abraham, E. P. (1979) Transport and Metabolism of Bacilysin and Other Peptides by Suspensions of *Staphylococcus aureus*. *J Gen Microbiol*, 115, 213-21.
- Petersen, L. J. (1999) Interstitial Lactate Levels in Human Skin at Rest and During an Oral Glucose Load: A Microdialysis Study. *Clin Physiol*, 19, 246-50.
- Phillips, R. S., Demidkina, T. V. & Faleev, N. G. (2003) Structure and Mechanism of Tryptophan Indole-Lyase and Tyrosine Phenol-Lyase. *Biochim Biophys Acta*, 1647, 167-72.
- Phillips, R. S., Johnson, N. & Kamath, A. V. (2002) Formation in Vitro of Hybrid Dimers of H463F and Y74F Mutant *Escherichia coli* Tryptophan Indole-Lyase Rescues Activity with L-Tryptophan. *Biochem*, 41, 4012-9.
- Phillips, R. S., Richter, I., Gollnick, P., Brzovic, P. & Dunn, M. F. (1991) Replacement of Lysine 269 by Arginine in *Escherichia coli* Tryptophan Indole-Lyase Affects the Formation and Breakdown of Quinonoid Complexes. *J Biol Chem*, 266, 18642-8.
- Pitcher, D. G. (1983) Deoxyribonucleic Acid Base Composition of *Corynebacterium diphtheriae* and Other corynebacteria with Cell Wall Type Iv. *FEMS Microbiol Lett*, 16, 291-5.
- Prabhala, B. K., Aduri, N. G., Jensen, J. M., Ernst, H. A., Iram, N., Rahman, M. & Mirza, O. (2014) New Insights into the Substrate Specificities of Proton-Coupled Oligopeptide Transporters from *E. coli* by a pH Sensitive Assay. *FEBS Lett*, 588, 560-5.
- Riegel, P., Ruimy, R., De Briel, D., Prevost, G., Jehl, F., Christen, R. & Monteil, H. (1995) Taxonomy of *Corynebacterium diphtheriae* and Related Taxa, with Recognition of *Corynebacterium ulcerans* sp. Nov. Nom. Rev. *FEMS Microbiol Lett*, 126, 271-6.
- Rikowski, A. and Grammer, K. (1999) Human Body Odour, Symmetry and Attractiveness *Proc R Soc London Ser B* 266, 869-74.
- Riley, M., Abe, T., Arnaud, M. B., Berlyn, M. K., Blattner, F. R., Chaudhuri, R. R., Glasner, J. D., Horiuchi, T., Keseler, I. M., Kosuge, T., Mori, H., Perna, N. T., Plunkett, G., 3rd, Rudd, K. E., Serres, M. H., Thomas, G. H., Thomson, N. R., Wishart, D. & Wanner, B. L. (2006) *Escherichia coli* K-12: A Cooperatively Developed Annotation Snapshot. *Nucleic Acids Res*, 34, 1-9.
- Robertshaw, D. (1985) Sweat and Heat Exchange in Man and Other Mammals. *J Hum Evol* 14, 63-73.

- Rowbury, R. J. & Woods, D. D. (1964) Repression by Methionine of Cystathionase Formation in *Escherichia coli*. *J Gen Microbiol*, 35, 145-58.
- Russell, M. J. (1976) Human Olfactory Communication. *Nature*, 260, 520-2.
- Saier, M. H., Jr. (2000a) A Functional-Phylogenetic Classification System for Transmembrane Solute Transporters. *Microbiol Mol Biol Rev*, 64, 354-411.
- Saier, M. H., Jr. (2000b) Families of Transmembrane Sugar Transport Proteins. *Mol Microbiol*, 35, 699-710.
- Santiago, L. Y., Nowak, R. W., Peter Rubin, J. & Marra, K. G. (2006) Peptide-Surface Modification of Poly(Caprolactone) with Laminin-Derived Sequences for Adipose-Derived Stem Cell Applications. *Biomater*, 27, 2962-9.
- Sato, A. K., Viswanathan, M., Kent, R. B. & Wood, C. R. (2006) Therapeutic Peptides: Technological Advances Driving Peptides into Development. *Curr Opin Biotechnol*, 17, 638-42.
- Schiefferdecker, P. (1922). Die hautdrüsen des menschen und der saugetierte, ihre biologische und rassenatomische bedeutung, sowie die muscularis sexualis. *Zoologica* 72, 1.
- Schitteck, B., Hipfel, R., Sauer, B., Bauer, J., Kalbacher, H., Stevanovic, S., Schirle, M., Schroeder, K., Blin, N., Meier, F., Rassner, G. & Garbe, C. (2001) Dermcidin: A Novel Human Antibiotic Peptide Secreted by Sweat Glands. *Nat Immunol*, 2, 1133-7.
- Schroeder, K., Jularic, M., Horsburgh, S. M., Hirschhausen, N., Neumann, C., Bertling, A., Schulte, A., Foster, S., Kehrel, B. E., Peters, G. & Heilmann, C. (2009) Molecular Characterization of a Novel Staphylococcus Aureus Surface Protein (SasC) Involved in Cell Aggregation and Biofilm Accumulation. *PLoS One*, 4, e7567.
- Schultz, J. E. & Matin, A. (1991) Molecular and Functional Characterization of a Carbon Starvation Gene of *Escherichia coli*. *J Mol Biol*, 218, 129-40.
- Sezonov, G., Joseleau-Petit, D. & D'ari, R. (2007) *Escherichia coli* Physiology in Luria-Bertani Broth. *J Bacteriol*, 189, 8746-9.
- Shehadeh, N. H. & Kligman, A. M. (1963) The Bacteria Responsible for Axillary Odor II. *J Invest Dermatol* 41, 3.
- Shelley, W. B. & Hurley, H. J., Jr. (1975) Studies on Topical Antiperspirant Control of Axillary Hyperhidrosis. *Acta Derm Venereol*, 55, 241-60.
- Shelley, W. B., Hurley, H. J. & Nichols, A. C. (1953) Axillary Odor: Experimental Study of the Role of Bacteria, Apocrine Sweat, and Deodorants. *AMA Arch Derm Syphilol*, 68, 430-46.
- Smith, K., Thompson, G. F. & Koster, H. D. (1969) Sweat in Schizophrenic Patients: Identification of the Odorous Substance. *Science*, 166, 398-9.
- Smith, M. W. & Payne, J. W. (1990) Simultaneous Exploitation of Different Peptide Permeases by Combinations of Synthetic Peptide Smugglers Can Lead to Enhanced Antibacterial Activity. *FEMS Microbiol Lett*, 58, 311-6.
- Smith, M. W. & Payne, J. W. (1992) Expression of Periplasmic Binding Proteins for Peptide Transport Is Subject to Negative Regulation by Phosphate Limitation in *Escherichia coli*. *FEMS Microbiol Lett*, 100, 183-90.

- Smith, M. W., Tyreman, D. R., Payne, G. M., Marshall, N. J. & Payne, J. W. (1999) Substrate Specificity of the Periplasmic Dipeptide-Binding Protein from *Escherichia coli*: Experimental Basis for the Design of Peptide Prodrugs. *Microbiol*, 145, 2891-901.
- Solcan, N., Kwok, J., Fowler, P. W., Cameron, A. D., Drew, D., Iwata, S. & Newstead, S. (2012) Alternating Access Mechanism in the POT Family of Oligopeptide Transporters. *Embo J*, 31, 3411-21.
- Song, Y., Liu, C. & Finegold, S. M. (2007) Development of a Flow Chart for Identification of Gram-Positive Anaerobic Cocci in the Clinical Laboratory. *J Clin Microbiol*, 45, 512-6.
- Spielman, A. I., Zeng, X. N., Leyden, J. J. & Preti, G. (1995) Proteinaceous Precursors of Human Axillary Odor: Isolation of Two Novel Odor-Binding Proteins. *Experientia*, 51, 40-7.
- Starkenmann, C., Niclass, Y., Troccaz, M. & Clark, A. J. (2005) Identification of the Precursor of (S)-3-Methyl-3-Sulfanylhexan-1-ol, the Sulfury Malodour of Human Axilla Sweat. *Chem Biodivers*, 2, 705-16.
- Staskawicz, B. J. & Panopoulos, N. J. (1980) Phaseolotoxin Transport in *Escherichia coli* and *Salmonella typhimurium* Via the Oligopeptide Permease. *J Bacteriol*, 142, 474-9.
- Steiner, H. Y., Naider, F. & Becker, J. M. (1995) The PTR Family: A New Group of Peptide Transporters. *Mol Microbiol*, 16, 825-34.
- Stoddart, D. M. (1991) The Apocrine Glands, In: *The Scented Ape*, Cambridge University Press, p. 60-61.
- Suzuki, H., Kamatani, S., Kim, E.-S. & Kumagai, H. (2001) Aminopeptidases a, B, and N and Dipeptidase D Are the Four Cysteinyglycinases of *Escherichia coli* K-12. *J Bacteriol*, 183, 1489-90.
- Tatusova T., Ciufu S., Fedorov B., O'Neill K. & Tolstoy I. (2014) RefSeq Microbial Genomes Database: New Representation and Annotation Strategy. *Nucleic Acids Res.* 1;42(1):D553-9. Available from: [http://www.ncbi.nlm.nih.gov/genome/2014?genome\\_assembly\\_id=171977](http://www.ncbi.nlm.nih.gov/genome/2014?genome_assembly_id=171977)
- Tauch, A., Kaiser, O., Hain, T., Goesmann, A., Weisshaar, B., Albersmeier, A., Bekel, T., Bischoff, N., Brune, I., Chakraborty, T., Kalinowski, J., Meyer, F., Rupp, O., Schneiker, S., Viehoveer, P. & Puhler, A. (2005) Complete Genome Sequence and Analysis of the Multiresistant Nosocomial Pathogen *Corynebacterium jeikeium* K411, a Lipid-Requiring Bacterium of the Human Skin Flora. *J Bacteriol*, 187, 4671-82.
- Taylor, D., Daulby, A., Grimshaw, S., James, G., Mercer, J. & Vaziri, S. (2003) Characterization of the Microflora of the Human Axilla. *Int J of Cosmet Sci*, 25, 137-45.
- Tegoni, M., Pelosi, P., Vincent, F., Spinelli, S., Campanacci, V., Grolli, S., Ramoni, R. & Cambillau, C. (2000) Mammalian Odorant Binding Proteins. *Biochim Biophys Acta*, 1482, 229-40.
- Terada, T., Irie, M., Okuda, M. & Inui, K. (2004) Genetic Variant Arg57His in Human H<sup>+</sup>/Peptide Cotransporter 2 Causes a Complete Loss of Transport Function. *Biochem Biophys Res Commun*, 316, 416-20.

- Thierry, A., Maillard, M. B. & Yvon, M. (2002) Conversion of L-Leucine to Isovaleric Acid by *Propionibacterium freudenreichii* T1 34 and Itgp23. *Appl Environ Microbiol*, 68, 608-15.
- Thornhill R & Gangestad S. W. (1999). The Scent of Symmetry: a Human Sex Pheromone That Signals Fitness? *Evol Hum Behav* 20, 175-201.
- Tominaga, T., Peyrot des Gachons, C. & Dubourdieu, D. (1998) A New Type of Flavor Precursors in *Vitis vinifera* L. cv. Sauvignon Blanc: S-Cysteine Conjugates. *J Agric Food Chem* 46, 5215-9.
- Tominaga, T. & Dubourdieu, D. (2000) Identification of Cysteinylated Aroma Precursors of Certain Volatile Thiols in Passion Fruit Juice. *J Agric Food Chem*, 48, 2874-6.
- Tritz, G. J. (1987). In: *Escherichia coli* and *Salmonella typhimurium*: cellular and molecular biology. *American Society for Microbiology*, Washington, D.C.
- Troccaz, M., Starkenmann, C., Niclass, Y., Van De Waal, M. & Clark, A. J. (2004) 3-Methyl-3-Sulfanyhexan-1-ol as a Major Descriptor for the Human Axilla-Sweat Odour Profile. *Chem Biodivers*, 1, 1022-35.
- Troccaz, M., Benattia, F., Borchard, G. & Clark, A. J. (2008) Properties of Recombinant *Staphylococcus haemolyticus* Cystathionine Beta-Lyase (MetC) and Its Potential Role in the Generation of Volatile Thiols in Axillary Malodor. *Chem Biodivers*, 5, 2372-85.
- Troccaz, M., Borchard, G., Vuilleumier, C., Raviot-Derrien, S., Niclass, Y., Beccucci, S. & Starkenmann, C. (2009) Gender-Specific Differences between the Concentrations of Nonvolatile (R)/(S)-3-Methyl-3-Sulfanyhexan-1-ol and (R)/(S)-3-Hydroxy-3-Methyl-Hexanoic Acid Odor Precursors in Axillary Secretions. *Chem Sens*, 34, 203-210.
- Tsesin, N., Kogan, A., Gdalevsky, G. Y., Himanen, J. P., Cohen-Luria, R., Parola, A. H., Goldgur, Y. & Almog, O. (2007) The Structure of Apo Tryptophanase from *Escherichia coli* Reveals a Wide-Open Conformation. *Acta Crystallogr D Biol Crystallogr*, 63, 969-74.
- Tue, C. J., Bojar, R. A. & Holland, K. T. (1998) The Adhesion of Cutaneous Micro-Organisms to Human Skin Lipids. *Dermatol*, 196, 71-2.
- Uchiyama, T., Kulkarni, A. A., Davies, D. L. & Lee, V. H. (2003) Biophysical Evidence for His57 as a Proton-Binding Site in the Mammalian Intestinal Transporter hPepT1. *Pharm Res*, 20, 1911-6.
- Urbanowski, M. L., Stauffer, L. T. & Stauffer, G. V. (2000) The Gcvb Gene Encodes a Small Untranslated Rna Involved in Expression of the Dipeptide and Oligopeptide Transport Systems in *Escherichia coli*. *Mol Microbiol*, 37, 856-68.
- van Heyningen, R. E. (1952) A Comparison of Arm-bag and Body Aweat. *J Physiol* 116, 395-403.
- Van Horn, J. D. (2003) A Protocol for the Determination of Free Thiols. *University of Missouri-Kansas City*, Available: <http://v.web.umkc.edu/vanhornj/freethiol.htm> [Accessed: 03/09/2014].
- Vermeulen, C., Gijs, L. & Collin, S. (2005) Sensorial Contribution and Formation Pathways of Thiols in Foods: A Review. *Food Rev Int* 21, 69-137.

- Vonder Haar, R. A. & Umbarger, H. E. (1972) Isoleucine and Valine Metabolism in *Escherichia coli*. XIX. Inhibition of Isoleucine Biosynthesis by Glycyl-Leucine. *J Bacteriol*, 112, 142-7.
- Watanabe, T. & Snell, E. E. (1977) The Interaction of *Escherichia coli* Tryptophanase with Various Amino and Their Analogs. Active Site Mapping. *J Biochem*, 82, 733-45.
- Wedekind, C., Seebeck, T., Bettens, F. & Paepke, A. J. (1995) MHC-Dependent Mate Preferences in Humans. *Proc Biol Sci*, 260, 245-9.
- Wedekind, C. & Penn, D. (2000) Mhc Genes, Body Odours, and Odour Preferences. *Nephrol Dial Transplant*, 15, 1269-71.
- Weiner, J. S. & Hellmann, K. (1959) The Sweat Glands. *Biol Rev*, 35, 141-79.
- Weitz, D., Harder, D., Casagrande, F., Fotiadis, D., Obrdlik, P., Kelety, B. & Daniel, H. (2007) Functional and Structural Characterization of a Prokaryotic Peptide Transporter with Features Similar to Mammalian PepT1. *J Biol Chem*, 282, 2832-9.
- Westall, R. G. (1953) The Amino Acids and Other Ampholytes of Urine. 2. The Isolation of a New Sulphur-Containing Amino Acid from Cat Urine. *Biochem J*, 55, 244-8.
- Wilke, K., Martin, A., Terstegen, L. & Biel, S. S. (2007) A Short History of Sweat Gland Biology. *Int J Cosmet Sci*, 29, 169-79.
- Zdych, E., Peist, R., Reidl, J. & Boos, W. (1995) MalY of *Escherichia coli* Is an Enzyme with the Activity of a Beta C-S Lyase (Cystathionase). *J Bacteriol*, 177, 5035-9.
- Zeng, X. N., Leyden, J. J., lawley, H. J., Sawano, K., Nohara, I. & Preti, G. (1991). Analysis of Characteristic Odors from Human Male Axillae. *J Chem Ecol*, 17, 1469-92.
- Zeng, C., Spielman, A. I., Vowels, B. R., Leyden, J. J., Biemann, K. & Preti, G. (1996) A Human Axillary Odorant Is Carried by Apolipoprotein D. *Proc Natl Acad Sci U S A*, 93, 6626-30.
- Zhang, J., Reddy, J., Buckland, B. & Greasham, R. (2003) Toward Consistent and Productive Complex Media for Industrial Fermentations: Studies on Yeast Extract for a Recombinant Yeast Fermentation Process. *Biotechnol Bioeng*, 82, 640-52.
- Zimmer, D. P., Soupene, E., Lee, H. L., Wendisch, V. F., Khodursky, A. B., Peter, B. J., Bender, R. A. & Kustu, S. (2000) Nitrogen Regulatory Protein C-Controlled Genes of *Escherichia coli*: Scavenging as a Defense against Nitrogen Limitation. *Proc Natl Acad Sci U S A*, 97, 14674-9.
- Zindel, U., Freudenberg, W., Reith, M., Andreesen, R., Schnell, J. & Widdel, L. (1988) *Eubacterium acidaminophilum* sp. nov., a Versatile Amino Acid-Degrading Anaerobe Producing or Utilizing H<sub>2</sub> or Formate. *Arch Microbiol*, 150, 254-66.